The University Of Sheffield.

The Nature and Use of Trimlines for Analysing 3-Dimensional Glacier Change in Rugged Terrain

Camilla Mary Rootes

Department of Geography
University of Sheffield

PhD Thesis

Submitted in accordance with the requirements
for the degree of Doctor of Philosophy

June 2018

Abstract

Reconstructions of former ice sheets and glaciers provide important palaeoglaciological information about their behaviour in response to climate changes. It is also possible to use such reconstructions to test and refine numerical glacial models, improving understanding of both palaeo and modern ice masses. The geomorphological evidence base for palaeoglacial reconstructions is often fragmentary, requiring interpolation across spatial gaps and estimation of ice thickness. These elements of subjectivity limit the robustness and reproducibility of reconstructions and this is particularly so in the rugged terrain of mountainous regions, where ice margins interact strongly with topography. This thesis aims to improve understanding of the geomorphological signature of ice margins in rugged terrain, in order to increase accuracy and confidence in producing empirical palaeoglacial reconstructions.

An empirically-based method for improving interpolation between ice marginal landforms was investigated using characteristics of modern glacier-topography relationships. Despite much early promise in a pilot study, collection of sufficient data to underpin the method became too cumbersome, due to excessive measurement sensitivity in GIS analysis, and was abandoned for the purpose of this thesis. It is suggested that this avenue could be usefully continued with machine learning approaches.

Glacial trimlines were then investigated because they assist both ice margin interpolation and constraint of palaeo ice thickness but have been under-utilised. A literature review on trimline characteristics and analysis of glacial trimlines in Svalbard led to a new classification scheme for their identification and interpretation, insights into controls on their formation and preservation, and examples of best practice for their mapping from remotely sensed imagery. As a proof of concept, glacial trimlines were combined with modelling to produce 3-dimensional reconstructions of the Little Ice Age geometry and volume of 15 glaciers in central western Spitsbergen, Svalbard. Glacier reduction to their modern size was found to be highly varied and related to topographic controls.

The findings and recommendations of this research should be built on, in order to expand the use of glacial trimlines in palaeoglacial reconstructions and in the study of the impact of topography on glacier fluctuations.

Acknowledgements

Firstly, I would like to thank my supervisor Prof. Chris Clark for the advice, encouragement and guidance he provided over the course of this PhD. Hopefully this relationship has been in some way reciprocal – Chris certainly has a better idea of the varied uses for Microsoft Powerpoint than before we began to work together!

I would also like to thank the academic and support staff in the Department of Geography at Sheffield for their advice and assistance. Discussions with Jeremy Ely, Darrel Swift, and Felix Ng have been particularly insightful and Richard Hayes generously provided access to some of his own data. Assistance from staff at UNIS and the Norwegian Polar Institute helped greatly with my data collection, both in the field and remotely sensed, with the feedback on my initial trimline mapping from Ólafur Ingólfsson, Helena Alexanderson, Mona Henriksen being especially useful. Heïdi Sevestre is also thanked for sharing the relevant parts of her Svalbard surge-type glacier inventory with me, prior to its publication.

I have received significant support in the use of the GlaRe toolbox from Ramón Pellitero, whose guidance and endless troubleshooting made the production of my Little Ice Age glacier reconstructions possible. Various contributors on the ESRI Geonet forums are also thanked for their advice and technical support.

I would also like to acknowledge financial support from the University of Sheffield Faculty of Social Sciences, whose scholarship funded the first three years of this research.

Finally, I would like to thank my friends and family for their continued support throughout my PhD studies. Particularly, my fiancé Dom for being a huge emotional help, as well as providing assistance with mathematics and spreadsheets, and my parents for their on-going love and for patiently listening to me complain about my thesis on many occasions.

Table of Contents

Tables and Figures

Tables

Figures

Chapter 1

Introduction

1.1 Reconstructing palaeo ice margins in rugged terrain

The study of past ice masses, known as palaeoglaciology, has a long history and is concerned with understanding the extent, behaviour and fluctuations of ice masses in response to changes in climate. Since the time of Louis Agassiz in the 1840s, this field has utilised the landforms left behind during previous glaciations to reconstruct ice margins (e.g. Figure 1.1; Geikie 1878; Charlesworth 1921; Charlesworth 1955; Sissons 1974; Ives 1978; Thorp 1986; Landvik *et al.* 1998; Ballantyne *et al.* 2006; Hughes *et al.* 2011; Lukas *et al.* 2012; Way *et al.* 2015; Barth *et al*. 2016; Sugden *et al*. 2017).

The former ice margins, ice thickness and surface morphology of palaeo ice masses can be reconstructed to provide us with a wealth of information about the ice itself and glaciological properties, such as the position of the palaeo Equilibrium Line Altitude (ELA). These palaeoglacial reconstructions can also inform our knowledge of the local environment and climate at the time of the reconstructed ice mass, particularly through reconstruction of the precipitation required to sustain the ice mass (Carr *et al.* 2010; Golledge 2010; Benn and Ballantyne 2005). Palaeoglacial studies can also shed light on the behaviour of modern glaciers and ice sheets. In particular, reconstructions of palaeo ice sheets have developed our understanding of the ice-bed interface in modern ice masses (Bingham *et al.* 2010) and, by studying the fluctuations of past ice sheets, significant improvements can be made in our ability to predict the response of Greenland and West Antarctica to on-going anthropogenic climate warming.

For much of the history of palaeoglaciology the reconstructions produced have been primarily 2-dimensional (2D) outlines of palaeo ice masses. Whilst these 2D reconstructions have been useful, 3-dimensional (3D) reconstructions are increasingly favoured (e.g. Clark *et al.* 2012; Hannesdóttir *et al.* 2015; Sugden *et al.* 2017), whereby both the horizontal and vertical extent of ice masses are reconstructed permitting calculation of the ice volume and computation of the changes in ice thickness and volume between different glacial events or time periods. Reconstructing this vertical dimension is important for extracting information about the local climate and provides a much more detailed understanding of the response

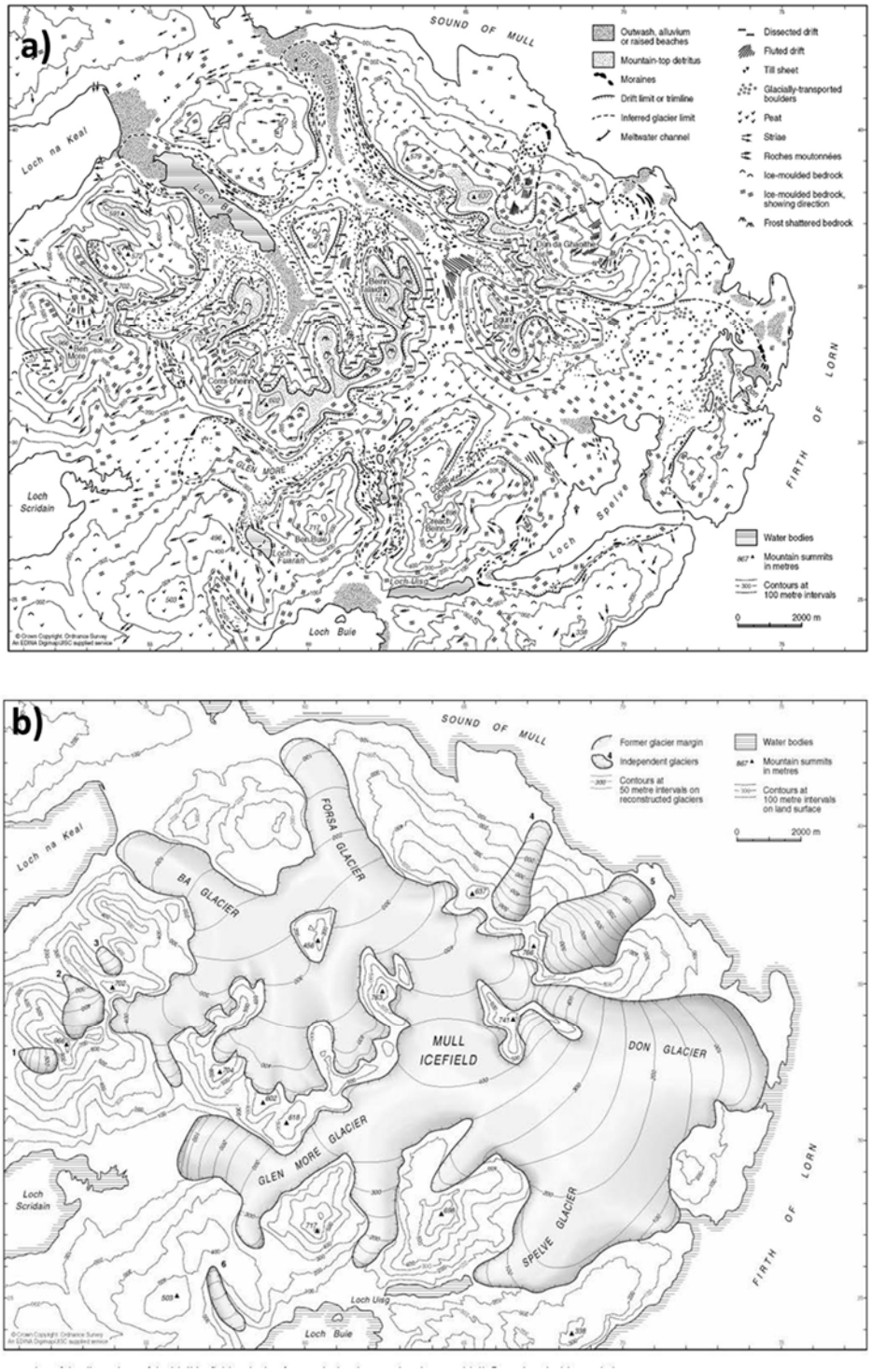

Figure 1.1 – This example of a 3-dimensional palaeoglacial reconstruction is taken from Ballantyne (2002, pp.761-762) and shows the extent of the former Mull Icefield in Scotland during the Younger Dryas glacial event. A detailed map of the glacial geomorphological evidence associated with the former ice field (a) was used to produce the 3D reconstruction (b).

of ice masses to climate changes. Additionally, 3D palaeoglacial reconstructions are much more useful for testing and refining numerical glacial models, which usually compute ice thickness values either along flow lines or at points distributed across the former glacier.

Numerical glacial models apply a simplification of ice internal physics, sometimes coupled with a simplification of the oceans and atmosphere, to determine how the ice mass will react to a given climate change or 'forcing' (Benn and Evans 2010; Rowan 2012). Such models have become important tools for palaeoglaciology, glaciology and climate science. Large ice masses, such as the ice sheets of Greenland and Antarctica, can respond relatively quickly, over a few months or years, to some forcings but much more slowly to others, over decades, millennia or tens of thousands of years. Therefore, it is essential that numerical glacial models are thoroughly tested across a range of timescales, to ensure that they utilise representations of the ice physics that yield accurate results for a variety of climate forcings. In order to test numerical glacial models, the model's output for a given glacial event or climate forcing can be compared with ice thickness and ice area (i.e. 3D) palaeoglacial reconstructions of the same event, based on the empirical geomorphological evidence (e.g. Patton *et al.* 2013a/b). For this reason, it is important that 3D palaeoglacial reconstructions are produced wherever possible and that these reconstructions are robust and produced with a sound and reproducible basis in the glacial geomorphological record.

1.1.1 Producing reconstructions from the glacial geomorphological record

In order to produce palaeo ice margin reconstructions, four key problems must be overcome (Figure 1.2; Figure 1.3): 1) interpreting the landforms to identify those that are ice marginal; 2) establishing synchroneity between landforms; 3) connecting landforms spatially to produce continuous ice margins across gaps in the geomorphological record; and 4) ensuring that the resulting reconstruction is glaciologically plausible, particularly when connecting landforms over large gaps in the geomorphological record. If a 3D reconstruction is desired then defining plausible palaeo ice thicknesses and ice surface morphologies are additional issues, especially given that very few landforms empirically record the thickness of the ice.

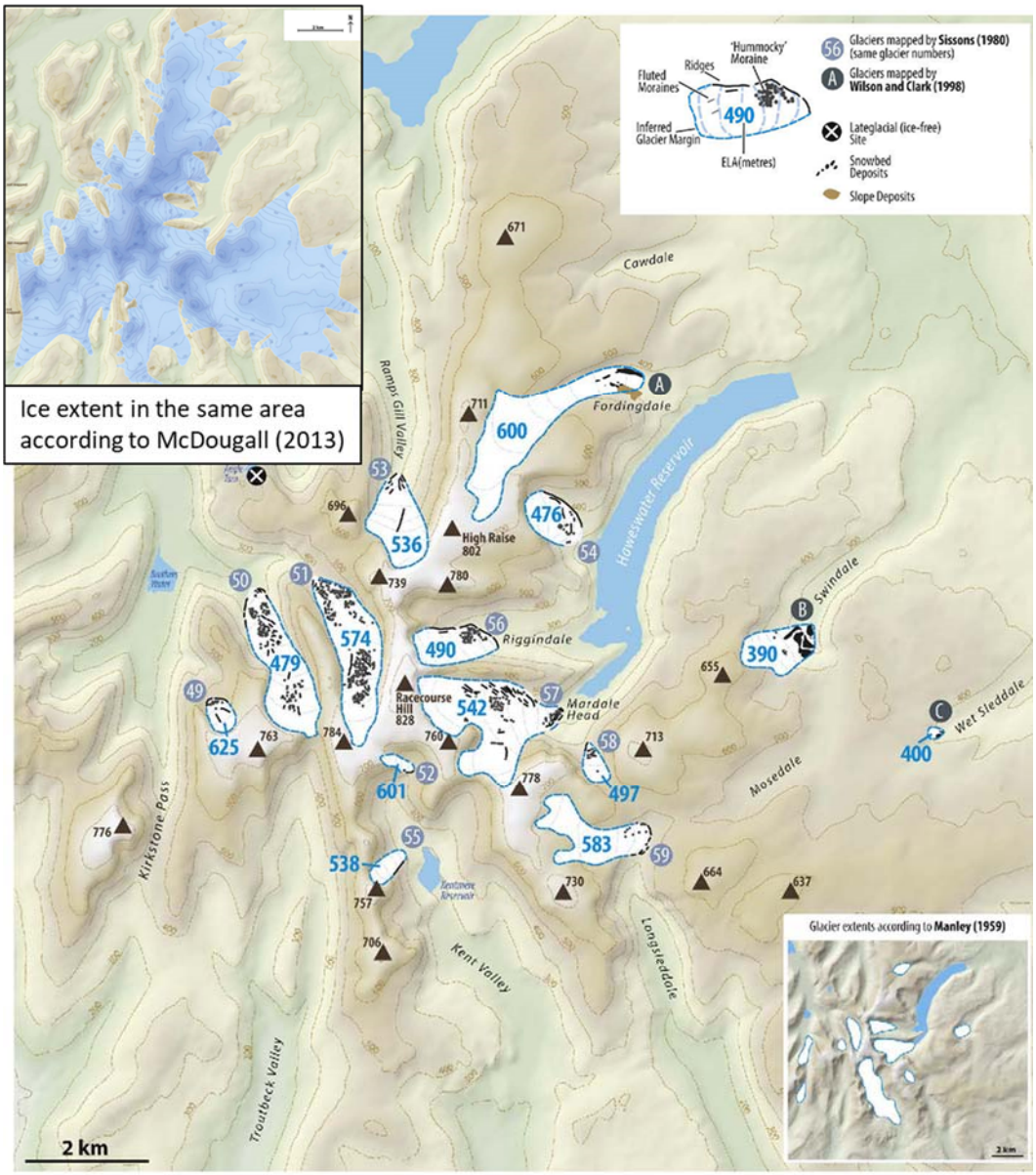

Figure 1.2 – This example, modified from McDougall (2013, pp.51 & 56), shows three conflicting reconstructions of the same area in the English Lake District during the Younger Dryas glacial event, all based on the same geomorphological evidence. It is clear from this example that various interpretations of the glacial geomorphological evidence, different assumptions guiding interpolation, and differing age estimates for landforms have led to problems with the robustness and reproducibility of these reconstructions.

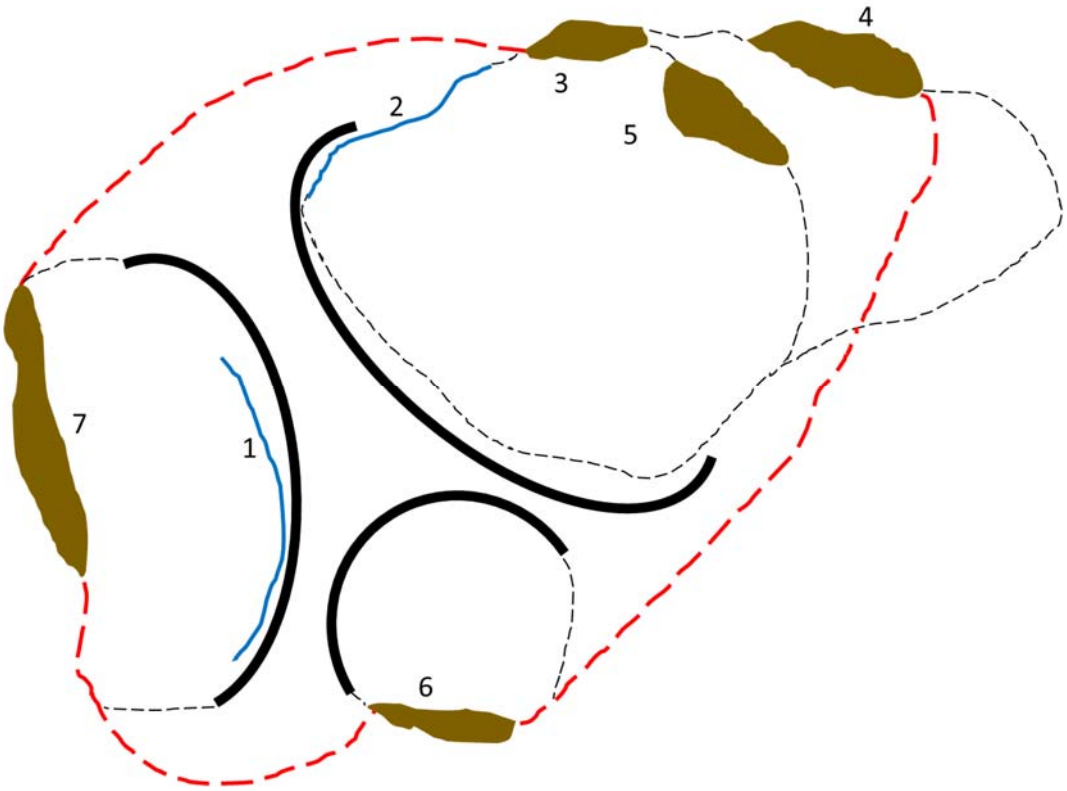

Figure 1.3 – This schematic illustrates the four key issues in the production of palaeoglacial reconstructions, which can lead to situations where the most likely reconstruction is not clear (e.g. Figure 1.2). The black curves represent three cirques cut into a summit, with a geomorphological record comprising glacial trimlines (blue lines) and moraines (brown) that can be interpreted to produce multiple possible ice margin reconstructions. These comprise either an ice cap (dashed red line) or separate cirque glaciers (dashed black lines), one of which has a retreat position. The first issue to be overcome is the interpretation of the landforms, with the trimline marked 1 being a particular problem because it could mark the upper surface of the ice in its cirque but could also represent a subglacial thermal boundary, implying that ice cover may have submerged the ridge (i.e. supporting the dashed red line reconstruction). The second issue is establishing synchroneity, which can appear obvious (e.g. trimline 2 and moraine 3 appear synchronous) but can be difficult to determine, particularly between valleys/ cirques (e.g. is moraine 3 synchronous with moraine 4 or 5 in its own cirque? What about with moraines 6 and 7 in the other cirques?). The third issue surrounds interpolation between landforms, for example if we believe moraine 4 and trimline 2 are synchronous and ice marginal, where do we draw the continuous ice margin across the gap between them? Once we have decided on possible ice margin positions, the fourth issue is to determine if our ice margin is glaciologically plausible. For example, it is not clear whether it is more glaciologically plausible have three distinct cirque glaciers (dashed black lines), or if we should link all three cirques together (dashed red line). These four problems are compounded by rugged terrain and also by consideration of the ice thickness, which can help to resolve landform interpretations and synchronicity but can also add additional uncertainty where empirical constraint over the ice thickness is poor.

When glacial features have been identified and mapped, the landforms or elements are commonly classified according to their position relative to the palaeo ice mass (e.g. 'subglacial', 'proglacial', 'ice marginal' etc). Where the geomorphological record is multitemporal or palimpsest, the inversion method of Kleman and Borgström (1996) is generally used to interpret the evidence and produce reconstructions that separate features into their various timeslices. This initial interpretation of the geomorphological evidence is made more difficult where the processes of formation for any of the glacial landforms present are not clearly understood. A particular problem surrounds the interpretation of glacial trimlines, which are breaks or transitions between contrasting zones on valley slopes that have historically been considered to mark the upper limit of a former glaciation and are an important constraint on palaeo ice thickness (e.g. Thorp 1981; McCarroll *et al.* 1995; Ballantyne *et al.* 1998a/b; Stone and Ballantyne 2006). Recent research in Britain and Ireland has challenged this interpretation and suggested that these features can also form subglacially, representing former thermal divides between areas of cold-based and warm-based ice, but no consensus has been reached on the relative proportion of subglacial and ice marginal trimlines or on the best method for differentiating between them (see Chapter 3; Ballantyne 2010; Fabel *et al.* 2012; McCarroll 2016). Therefore, the use of glacial trimlines in reconstructions has become much more uncertain – should they be generally assumed to be ice marginal or is this assumption no longer justifiable and, if so, in what settings does the assumption still hold? Comparatively, other types of glacial landform, such as moraines, are much better understood and their location relative to the palaeo ice mass can be interpreted more confidently (e.g. Barr and Lovell 2014; Lukas 2012; Lukas *et al.* 2012; Anderson *et al.* 2012; Kirkbride and Winkler 2012). Disparities in the amount of research into different types of landform creates problems both with establishing synchroneity and with interpolation between disparate features. For example, poor understanding of landform formation and preservation can be a problem for relative dating methods and can make it difficult to identify and accurately map glacial landforms, contributing to gaps in the landform record that require bridging using interpolation.

Having interpreted the geomorphological record and identified the landforms most likely to be ice marginal, the establishment of synchroneity is required in order to group landforms into timeslices. Relative dating methods are commonly used to establish synchroneity, for example subglacial landforms may be grouped into 'flow sets' using spatial patterns in their orientation, superposition, and cross-cutting relationships (Clark 1993). These relative dating methods may be supplemented by consideration of the stratigraphy or by use of absolute

dating. Environmental dating techniques use samples taken in the field to identify the absolute rather than relative age of landforms in time (e.g. cosmogenic nuclide dating of trimlines in Ireland, Ballantyne and Stone 2015; radiocarbon, cosmogenic nuclide, and optically stimulated luminescence dating of landforms in Bolivia, May *et al.* 2011). Advances in these methods have greatly improved the time constraints in glacier and ice sheet reconstruction, but the number of actual dates available are typically so low that much interpolation and relative age estimation is still required (Hughes *et al.* 2011). Additionally, it may not always be possible to establish synchroneity or to separate different glacial events using absolute dating due to the frequently large uncertainties in the dates produced, particularly for older glacial events or where samples are poor quality or sparsely distributed spatially.

When synchronous landforms have been identified, it is usually the case that there are spatial gaps between them and these can vary significantly in size and number, depending on the extent and quality of the geomorphological record. In order to produce a continuous reconstruction of the palaeo ice margin for any given timeslice, these gaps need to be bridged and the synchronous landforms connected together. This process of interpolation is most often carried out by eye, with the experience of the researcher and their understanding of typical ice margin morphologies producing a reconstruction that is necessarily subjective and can be difficult to reproduce (e.g. Figure 1.2; Sissons 1974; Clark *et al.* 2012). The subjectivity of interpolation introduces a degree of uncertainty into 3D palaeoglacial reconstructions, potentially leading to misleading results when these reconstructions are used to tune or test numerical glacial models. Advances in the mapping and identification of glacial geomorphological evidence, particularly developments in remote sensing (Clark 1997; Smith and Pain 2009), have expanded the coverage and detail of the geomorphological record but gaps between landforms remain common and subjective interpolation is still required to bridge these. Conflict over the correct interpretation of landforms can also increase the need for interpolation, particularly when there are difficulties separating subglacial and ice marginal landforms or where establishment of synchroneity has been problematic.

In some situations, relatively small gaps in the geomorphological record may be interpolated across with reasonable confidence (e.g. trimline 2 and moraine 3 in Figure 1.3). However, relatively large gaps or a lack of landforms in crucial areas of the former ice mass can require assumptions about the morphology of ice margins to be made in order for interpolation to

be used (e.g. joining together the cirques in Figure 1.3). The use of interpolation in this way could potentially lead to glaciologically implausible reconstructions due to the lack of a sound empirical basis for large sections of the ice margin. However, there is currently no standardised method for interpolation and little discussion or testing of the assumptions used to guide this process (see Chapter 2; Sissons 1974; Clark *et al.* 2012). A particular problem is the reconstruction of the accumulation area of palaeo ice masses in rugged terrain, where the poorly-understood glacial trimlines are often the only landform recording former positions of the ice margin. This can lead to difficulties producing robust reconstructions of the accumulation area, which can make it challenging to determine palaeo confluence across topographic ridges (e.g. can we assume that the ice submerged the ridge between the cirques in Figure 1.3?).

Difficulties in reconstructing the accumulation area of palaeo ice masses can also cause problems in the use of palaeoglacial reconstructions to infer estimates of the local palaeo climate. Reconstructing climate variables from 3D palaeoglacial reconstructions primarily uses methods based in consideration of the glacier's hypsometry and/or in the ratio between the accumulation and ablation areas (Pellitero *et al.* 2015). Where reconstruction of the accumulation area ice margin is based on limited empirical evidence and large areas have been interpolated, there will be higher uncertainty in any subsequent palaeo climate reconstruction. Similarly where the palaeo ice thickness is poorly constrained by empirical evidence, uncertainty can be introduced into 3D palaeoglacial reconstructions and associated palaeo climate reconstructions. Glacial trimlines are, therefore, important landforms for resolving both palaeo ice margins and ice thickness, particularly in the accumulation area where they are one of the few useful landforms that exist (Thorp 1986; Kelly *et al.* 2004; Ackert *et al.* 2011). The generally poor understanding of glacial trimlines is currently limiting the confidence and robustness of ice thickness constraints in 3D palaeoglacial reconstructions, particularly because these landforms are difficult to interpret and often under-used in favour of other better understood landforms. Without good use of the geomorphological record to constrain ice thickness, ice surface contours may have to be added to reconstructions by eye or ice thickness values may need to be estimated using numerical glacial models, introducing an issue of circularity if the resulting 3D reconstruction is then used to test other numerical models.

Overall, producing palaeoglacial reconstructions, particularly 3D reconstructions, from glacial geomorphological evidence is rarely straightforward and is particularly difficult in

rugged terrain, where the complex topography interacts with the ice physics and climate forcings to create particularly varied glacial behaviours and responses. The production of robust and reproducible 3D palaeoglacial reconstructions is an area of importance for understanding past glacial events and especially for tuning numerical models to improve forecasts of the responses of modern ice masses to anthropogenic climate change. This thesis aims to improve 3D palaeoglacial reconstructions in rugged terrain using a detailed study of glacial trimlines and by considering a new method for interpolation to reduce uncertainty and increase reproducibility.

1.2 Thesis aims and structure

1.2.1 Overall aim

The overall aim of this thesis is to improve understanding of the geomorphological signature of ice margins in rugged terrain, in order to increase the accuracy and confidence of empirical palaeoglacial reconstructions.

1.2.2 Objectives

Given the problems with empirical palaeoglacial reconstructions identified in Figure 1.3 and outlined above, the specific objectives are:

1. To improve the reconstruction of ice margins from fragmentary evidence by producing a framework for interpolation based in empirical research.

2. To expand understanding of the formation and preservation of glacial trimlines – an under-researched landform that is crucial for reconstructing ice thickness and producing empirically-based 3D palaeoglacial reconstructions.

3. To produce a new classification system for glacial trimlines to aid in their correlation and interpretation.

4. To identify and map glacial trimlines in a case study location, demonstrating best practice.

5. To trial the results of the above analyses in the production of 3D palaeoglacial reconstructions for a set of Little Ice Age glaciers in Svalbard. Comparison of these

reconstructions with the modern ice extent will be used to analyse the responses of the glaciers to the intervening climate change.

6. To make recommendations for the identification, mapping and interpretation of trimlines in rugged terrain as well as for their usage in palaeoglacial reconstructions.

These objectives aim to reduce uncertainty in 3D palaeoglacial reconstructions by improving the reproducibility of interpolation and by developing a deeper understanding of glacial trimlines, along with providing tools to encourage better use of these features. These outputs aim to increase the accuracy of ice margin and ice thickness reconstructions in rugged terrain, increasing the confidence with which 3D palaeoglacial reconstructions can be used to test and refine numerical modelling.

1.2.3 Structure of this thesis

This thesis will begin by discussing methods for interpolation in areas with a fragmentary glacial geomorphological record (Chapter 2). Also in this chapter will be a summary of the research conducted into reducing subjectivity in interpolation, along with the outputs of this work. A detailed review of the use of glacial trimlines within the existing literature is used to develop a new classification system for these features in Chapter 3. Application of this classification system to the mapping and identification of trimlines in a case study area in Svalbard is used to explore the processes of trimline formation and preservation (Chapter 4). From this wider case study area, a select group of glaciers are reconstructed in 3D from their Little Ice Age (LIA) glacial trimlines utilising a new method, which is detailed in Chapter 5. The resulting 3D reconstructions are compared with the modern glaciers to determine the responses of these glaciers to the post-LIA climate change in Svalbard (Chapter 6). Finally, the results and outputs of this thesis are summarised in Chapter 7 and their implications for 3D palaeoglacial reconstructions are discussed, producing several suggestions for further research.

Chapter 2

Exploring the interpolation of palaeo ice margins from fragmentary evidence in rugged terrain

2.1 Introduction

The process of interpolation is used to bridge gaps between fragmentary glacial geomorphological evidence, in order to produce continuous ice margin reconstructions. This 'joining of the dots' is fundamental to all empirical palaeoglacial reconstructions due to the incomplete nature of the geomorphological record and because of the difficulties surrounding the interpretation and correlation of glacial landforms (Chapter 1). However, it is not often obvious how to connect between ice marginal landforms, particularly across relatively large gaps, and complex interactions between ice masses and topography make this process especially challenging in rugged terrain. This can lead to multiple possible ice margin positions being produced from the same geomorphological evidence, causing problems establishing the most glaciologically plausible option, which reduces the robustness and reproducibility of the resulting reconstruction (Figure 2.1).

Despite its critical role in the production of palaeoglacial reconstructions, interpolation has received little discussion in the published literature, with relatively very few papers even mentioning that the process has taken place or describing their methods of interpolation. Those papers that do mention interpolation tend to have linked together glacial landforms 'by eye', meaning that the researchers drew-in what they felt to be a plausible ice margin across any gaps in the geomorphological record (e.g. Lukas and Bradwell 2010; Larsen *et al.* 2014; Hughes 2018; Figure 2.2). This subjective process is governed by assumptions about 'typical' ice margin morphologies, guided by the researcher's understanding of the interactions between ice and topography. As J.B. Sissons (1974) put it, the drawing of ice margins (i.e. 'by eye' interpolation) is:

"constrained by the field evidence, by ground configuration, and by the form the glacier surface could reasonably be expected to have possessed in particular situations."
Sissons (1974, pp.106)

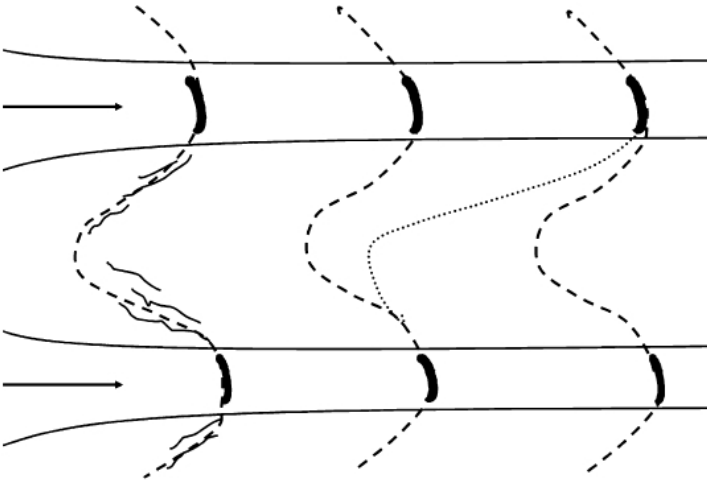

Figure 2.1 – This schematic demonstrates the subjective nature of interpolation between spatially disparate features in the geomorphological record. Two parallel trunk valleys are shown (thin black lines with arrows indicating ice flow direction), which contain a series of moraines (thick black lines) and some lateral meltwater channels (thin wiggly lines). Several possible ice margin reconstructions are shown (dashed lines), all of which have been produced by interpolating between the glacial landforms in the two valleys. In some cases, the position of the palaeo ice margin is fairly obvious (e.g. between the first set of moraines and meltwater channels on the left side of the schematic) and reasonably high confidence can then be placed in the resulting reconstruction. However, where the interpolation is more subjective and less well constrained by the geomorphological record, it is harder to be sure of the most glaciologically plausible reconstruction without the collection of further empirical evidence or the use of environmental dating. Reproduced from Clark *et al.* (2012, p.123).

Scrutiny of reconstructions of the former British-Irish Ice Sheet (BIIS) during the Last Glacial Maximum (LGM) and Younger Dryas (YD) glacial events yielded just one paper that stated anything about the assumptions guiding their interpolation, which was the above paper by Sissons (1974). This example does not give much detail about the specifics of the assumptions used and it is unclear exactly what assumptions about glaciology would be most appropriate for use in interpolation. Despite this, many papers mention that they have used interpolation and/or feature some visual identification of the interpolated areas of their ice margins (e.g. Figure 2.2; Clark *et al.* 2012; Larsen *et al.* 2014; Darvill *et al.* 2015; Hughes 2018). Perhaps different researchers use different assumptions, potentially creating conflicting reconstructions, problems with their reproducibility, and making it hard to produce a quantifiable uncertainty for the position of palaeo ice margins.

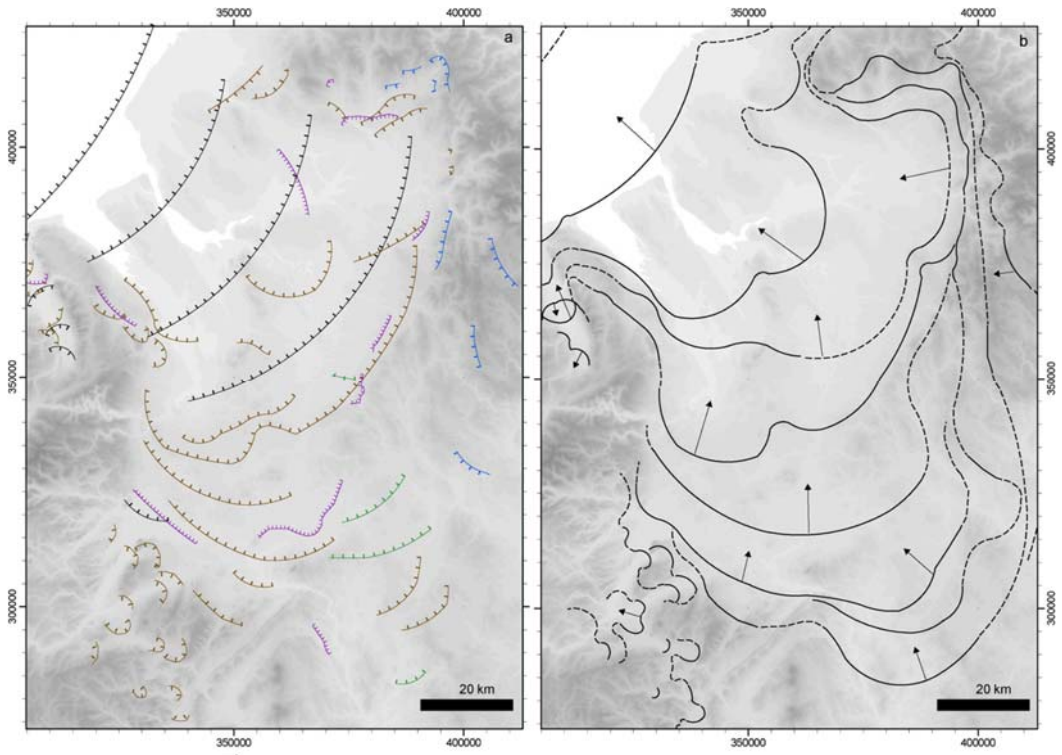

Figure 2.2 – An example of complex interpolation producing a pattern of ice margin retreat with clearly marked distinctions between the areas constrained by the geomorphological record and the interpolated sections of the reconstruction. a) shows a range of geomorphological features that have been interpreted to indicate the marked former ice margin positions (colours correspond to the type of geomorphological feature, which is not relevant here). b) the finished reconstruction of ice margin retreat produced from the interpretation of the geomorphological evidence shown in a), with solid lines corresponding with the location of empirical evidence and dashed lines indicating areas of interpolation. Reproduced from Clark *et al.* (2012, pp.122).

The lack of transparency in the assumptions used to guide 'by eye' interpolation can lead to multiple conflicting reconstructions based on the same geomorphological evidence. This has sometimes been the case (e.g. Figure 1.2 in Chapter 1) but there has actually been a surprising level of agreement between researchers and most reconstructions of the same location and timeslice are broadly comparable, with only minor discrepancies (e.g. Figure 2.3). This suggests that most researchers are utilising the same or very similar assumptions to guide their interpolation and that an experienced researcher is generally good at identifying the most likely position of a palaeo ice margin in a given topography. It should, therefore, be possible to tease out these assumptions in order to better define the process of interpolation and produce a more robust and standardised interpolation method,

increasing the reliability and reproducibility of palaeoglacial reconstructions. This chapter will explore a possible avenue for improving interpolation and suggest options for future research into this area.

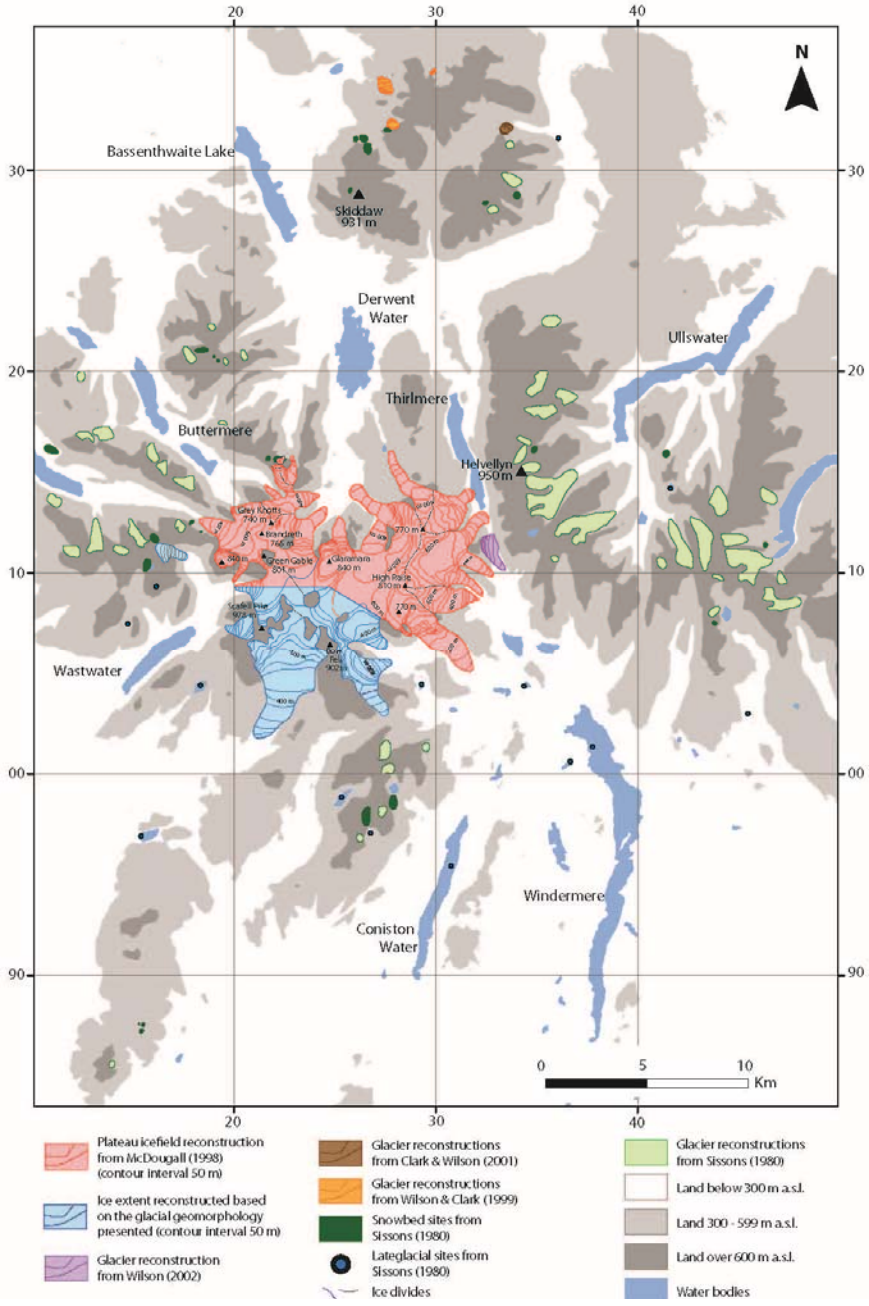

Figure 2.3 – In this example multiple reconstructions of the Younger Dryas in the English Lake District from several authors have been synthesised and significant agreement has been found, particularly in the joining of the blue (Brown *et al.* 2013) and red (McDougall 1998) sections of the plateau ice field. This demonstrates that interpolation can produce complementary palaeoglacial reconstructions of the same or adjacent areas, indicating that different researchers must be utilising a very similar set of assumptions to guide their 'by eye' interpolation. Reproduced from Brown *et al.* (2013, pp.1039).

2.2 Approaches investigated to improve interpolation

Consideration of the process of 'by eye' interpolation led to the idea that researchers' possess some unstated understanding of the glaciology governing the relationship between the ice margin position and the topography, particularly the slopes of the valley. For example, in Figure 2.4a a researcher (R. Hayes) was able to easily draw-in possible glaciers using just the topography and no geomorphological evidence. When a numerical glacial model was given the same topography, it produced an extremely similar set of glaciers (Figure 2.4b). This suggests that the mathematical simplification of the interactions between the ice physics and the topography used by the numerical model were similar to the innate assumptions used by the researcher. However, simply using a numerical glacial model to produce plausible ice margins creates an issue of circularity if the resulting reconstruction is intended to be used to test similar models. Therefore, an alternative method is required to guide interpolation, without resorting to numerical modelling, in order to evaluate numerical modelling independently.

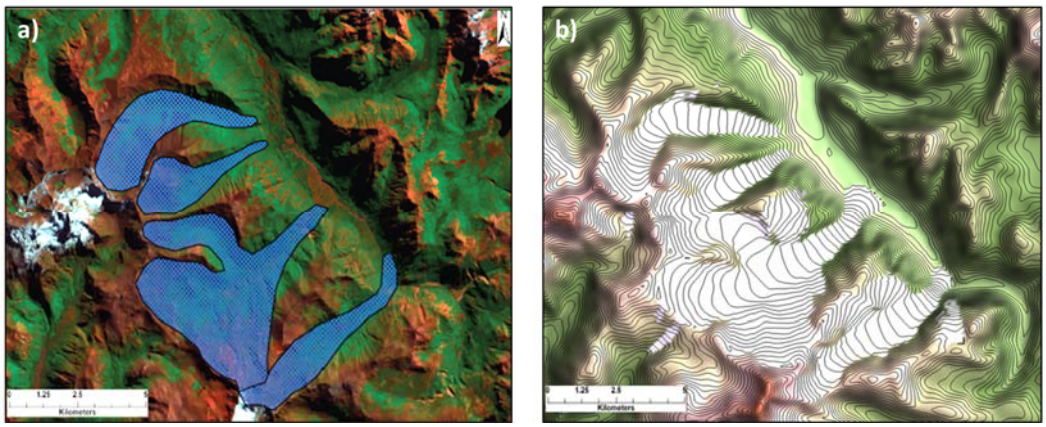

Figure 2.4 – a) shows R. Hayes' hand-drawn glaciers, produced only by considering the topography and attempting to draw a reasonable set of distinct valley glaciers. b) shows the results of running a numerical glacial model over the same topography, producing a broadly similar set of valley glaciers (modelling conducted by D. Egholm in conjunction with R. Hayes using a model presented in Egholm *et al.* 2011). The similarities between the modelled and hand-drawn glaciers suggests that both are based on similar underlying assumptions about the interaction between ice and topography. Reproduced with permission from R. Hayes (Lat. 36.893606°, Long. 1.147231°).

Further consideration of the ways in which researchers draw ice margins along the side of valleys suggested that investigation of the interaction between the ice margin and the topographic slope on which it sits might lead to a way of refining 'by eye' interpolation. If both researchers and numerical glacial models use assumptions about the interaction between the topography and ice physics to determine the most likely position for the ice margin, it would be logical to consider the interaction between ice margins and topography in order to pick apart this process and identify the key assumptions. Therefore, it was decided to investigate the 'external' contour angle formed between the ice margin and the topographic contours (Figure 2.5). The variations of this external contour angle along the side of a glacier provide a relatively simple measure of the interaction between the ice and the topography, allowing comparison of this interaction between multiple glaciers.

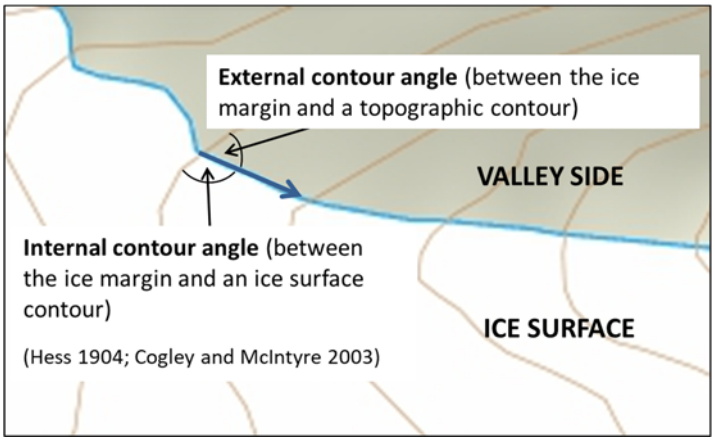

Figure 2.5 – The ice surface and valley side are separated by the ice margin (blue line with a blue arrow representing ice flow direction), which meets the topographic and ice surface contours to form two contour angles. The internal contour angle forms between the ice margin and ice surface contours and has been relatively well studied compared with the external contour angle, which forms between the topographic contours and the ice margin.

The study of the morphology of ice surface contours and consideration of the interaction of the ice margin and the topographic contours has received some previous research. In particular, ice surface contours have also been previously used to identify the position of the Equilibrium Line Altitude (ELA e.g. Hess 1904; Cogley and McIntyre 2003). Hess (1904) utilised the pattern of ice surface contours to identify the 'Hess altitude', where the ice surface contour is closest to being straight (i.e. the internal contour angle is close to 90^{o}), which Hess proposed should be roughly equal to the ELA. Recently, this method for estimating the ELA from ice surface contours has fallen out of favour as more accurate and more easily

measured approximations for the ELA have been developed (Cogley and McIntyre 2003). However, Hess also discussed the relationship between the topographic contours and the ice margin, positing this as a potential alternative to using ice surface contours to identify the ELA (Figure 2.6). In his discussion, Hess notes that there is a clear distinction around the ELA in the angle at which topographic contours meet the ice margin (i.e. the external contour angle). This angle is very sharp in the ablation area, with an abrupt change of angle as the contour crosses the ice margin, but much gentler in the accumulation area, with the topographic contours continuing almost unchanged across the ice margin (Figure 2.6; see translation of Hess' discussion from the original German in the Appendix to Cogley and McIntyre 2003).

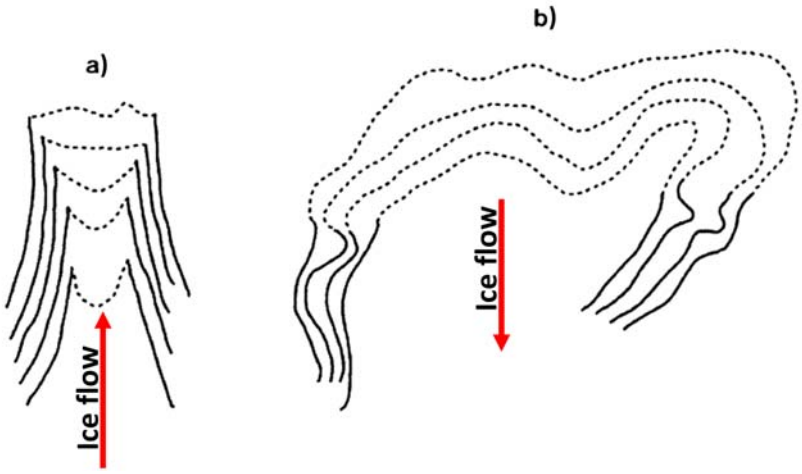

Figure 2.6 – A modification of Hess' original figure explaining the difference in the angle at which topographic contours meet the ice margin in the ablation area (a) compared to the accumulation area (b). The contours are solid on land (i.e. topographic contours) and dashed on the glacier ice (i.e. ice surface contours). Hess suggested that consideration of the area where these angles (i.e. the external contour angles) change from one pattern to the other could be used as an alternative to the Hess altitude for identifying the position of the ELA. Reproduced from Cogley and McIntyre's (2003, Appendix) translation of Hess' original discussion (Hess 1904).

Given the relationships between the ice margin and both internal and external contour angles, described by Hess (1904), it was hypothesised that both types of contour angle will vary systematically along a glacier margin from snout to headwall (Figure 2.7). There is already a long history of using the pattern of internal contour angles to add a 3-dimensional element to palaeoglacial reconstructions by drawing-in estimated ice surface contours (e.g. Sissons 1974; Hughes 2002). If this assumption is justifiable, there should be a reliable trend in the internal contour angle, between the ice surface contour and the ice margin (Figure 2.7b). According to Hess (1904), a similar trend in the external contour angle, between the

topographic contours and the ice margin, might also be expected and this trend could potentially be used as a tool to guide interpolation (Figure 2.7c).

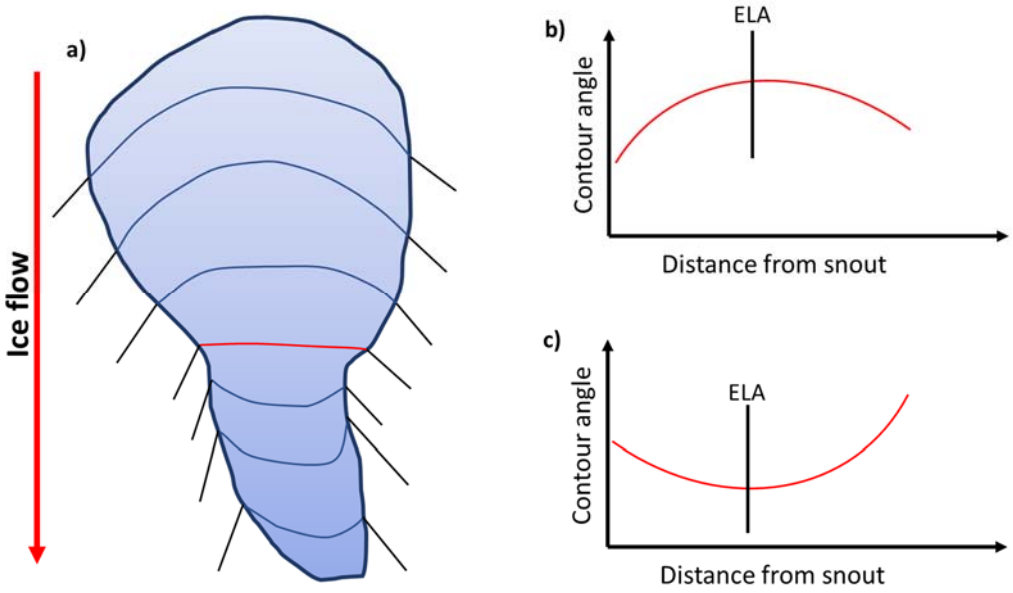

Figure 2.7 – a) This schematic shows the pattern of varying internal and external contour angles expected along the margins of a glacier, based on the theories of Hess (1904). The ice surface contours are coloured blue, with the Hess altitude marked in red, and the topographic contours are show in black. From this schematic, sketched graphs of the anticipated trends in internal (b) and external (c) contour angles are shown.

Using a trend describing the systematic variation in the external contour angles upglacier (i.e. Figure 2.7c but empirically derived from a large sample of modern glaciers), it should be possible to automate ice margin interpolation given the valley topography and a single piece of geomorphological evidence (e.g. Figure 2.8). This could be done by starting from the location of the geomorphological evidence and systematically varying the angles at which the ice margin meets each topographic contour, so that they fit the external contour angle trend. Use of this method could reduce uncertainty and improve the reproducibility of interpolation, as well as ensuring a continuous ice margin reconstruction that should be glaciologically plausible. Furthermore, it could potentially be possible to quantify a measure of uncertainty in existing reconstructed ice margins by comparing the trend in their external contour angles with the measured trend. The key to making these improvements to 'by eye' interpolation will be the identification of a robust trend in external contour angles based on a large sample of glaciers in a wide range of glaciological, climatic, geological, and topographic settings.

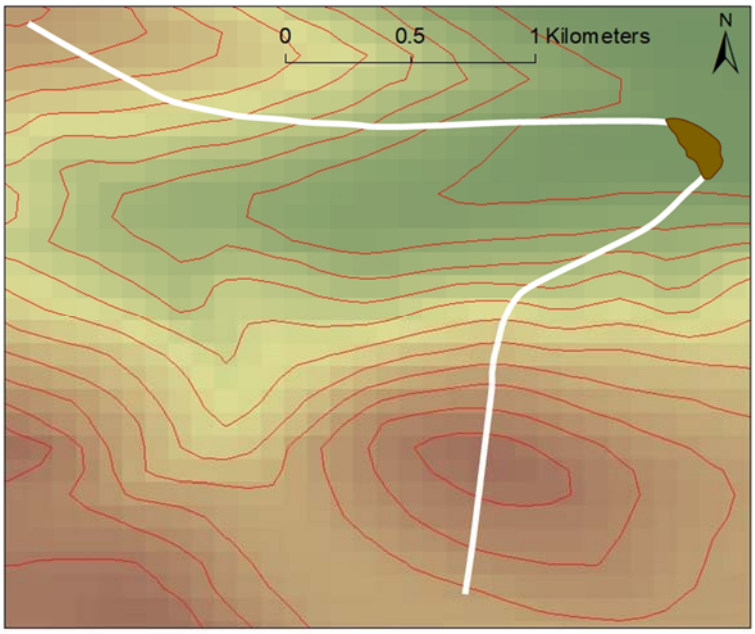

Figure 2.8 – In this example an ice-free topography is shown with 50 m topographic contours (red lines) and a moraine in the bottom of the valley (brown polygon), from which a set of ice margins (white lines) have been drawn using interpolation informed by external contour angles. To draw the ice margin the external contour angle at each contour was matched to the trend of expected contour angles in Figure 2.7c. Due to the differences in topography along the two sides of the valley, this method produces two distinct ice margins that are not mirror images of each other but are both based in the same external contour angle trend extrapolated from the position of the moraine. In theory, this method should be possible wherever an ice marginal landform can be found to provide an initial empirical constraint on the ice margin and should be both glaciologically plausible and reproducible, providing that a sufficiently robust trend in external contour angles is used. It may even be possible to automate the method by defining a start point (e.g. the end of the moraine in this example) and supplying an external contour angle trend to which the computer can then fit an ice margin, given the topography.

2.3 Measuring contour angles

Despite the previous research into the interactions between internal and external contour angles and the ELA (Hess 1904; Cogley and McIntyre 2003), there is no established method for measuring these angles and it was necessary to produce a new method. It was decided to explore methods for measuring only the external contour angle because these show the most promise for improving 'by eye' interpolation by using the method outlined in Figure 2.8.

2.3.1 By hand

An initial pilot study was carried out measuring external contour angles by hand, to determine if any clear trends in the contour angles upglacier were identifiable within a small sample of seven modern glaciers and seven reconstructed glaciers (Figure 2.9 and Figure 2.10). The inclusion of reconstructed glaciers enabled comparison with the modern glacier contour angle trends, to confirm if researchers are already producing ice margins with contour angles that are comparable to those found on similar existing glaciers.

The modern glaciers were chosen because they are all in rugged terrain but represent a wide range of glaciological, climatic, and geological settings. It was hoped that similarities and differences between the contour angle trends of these glaciers might identify the most fruitful settings to investigate further, as well as possibly suggesting if climate, glaciology or geology exerts a measurable control over the morphology of the ice margin. Additionally, all of the modern glaciers had high resolution topographic maps covering the entire glacier, which was essential to facilitate measurement of the contour angles by hand. For the Mer de Glace, topographic maps produced by the Institut Geographique National at a scale of 1:25,000 were used to measure the contour angles (Sheet 3630 OT). The Norwegian glaciers were all measured using images taken from online mapping resources, with the TopoSvalbard platform used for Scott Turnerbreen and Ayerbreen (http://toposvalbard.npolar.no/) and the Norgeskart platform used for Nigardsbreen and Fåbergstølsbreen (http://norgeskart.no/). Similarly, the contour angles of Múlajökull were measured from the National Land Survey of Iceland's online map viewer (http://kortasja.lmi.is/en/) and Fox Glacier was measured from an online topographic map that sources its data from Land Information New Zealand (http://www.topomap.co.nz/).

The reconstructed glaciers were chosen as a set of very similar glaciers from similar glaciological and climatic settings. All are Younger Dryas (YD) ice cap/ ice field outlet glaciers, in either North-West England or in Scotland, that have been reconstructed 'by eye' from the glacial geomorphological record, without the use of numerical glacial models. The aim for measuring the external contour angles of reconstructed glaciers was to compare them with the modern glaciers to see if the contour angle trends upglacier were similar, with the expectation that similar glaciers should have similar trends and that the trends between modern and reconstructed glaciers would generally be comparable. All of the reconstructed glaciers' external contour angles were measured from the maps of the reconstructions

presented in the original source papers (Benn and Ballantyne 2005; Lukas and Bradwell 2010; and Brown *et al.* 2013).

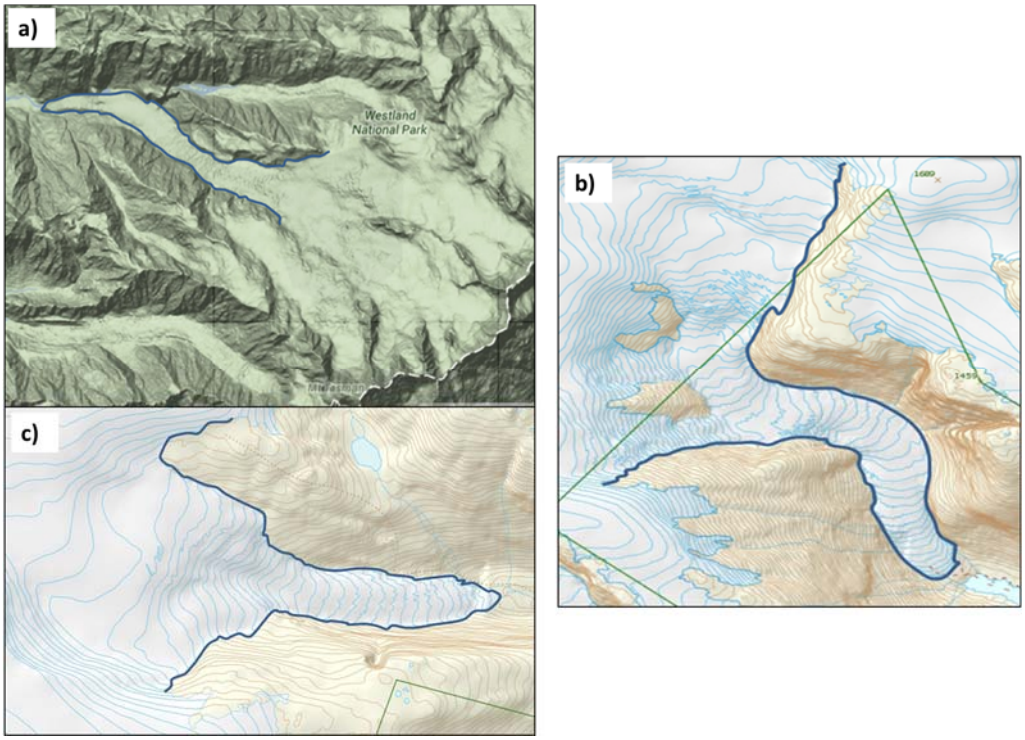

Figure 2.9 (2.9d, 2.9e, 2.9f & 2.9g on next page) **–** The modern glaciers used in the pilot study were chosen to represent a wide range of types, sizes and settings. For glaciers with a large and complex accumulation area, or for those that are ice cap outlets, only the confined area of the glacier was considered during the initial pilot study (outlined blue in the images). This minimised complications caused by complex ice margin morphologies in the accumulation areas and enabled both distinct valley glaciers and ice cap outlet glaciers to be considered together. The glacier area information covers the whole glacier, i.e. both the confined and unconfined areas, and was taken from the records in the Global Land Ice Measurements from Space (GLIMS) online data viewer (http://www.glims.org/maps/glims). The images of each glacier are taken from the sources listed in Section 2.3.1. The glaciers are: a) Fox Glacier in the Southern Alps, New Zealand; b) Nigardsbreen, an outlet of Jostedalsbreen, Norway; c) Fåbergstølsbreen, an outlet of Jostedalsbreen, Norway; d) Mer de Glace in the European Alps, France; e) Scott Turnerbreen in Svalbard, Norway; f) Ayerbreen in Svalbard, Norway; g) Múlajökull, an outlet of Hofsjökull, Iceland.


d)
Glacier des Grands
Glacier du Tacul

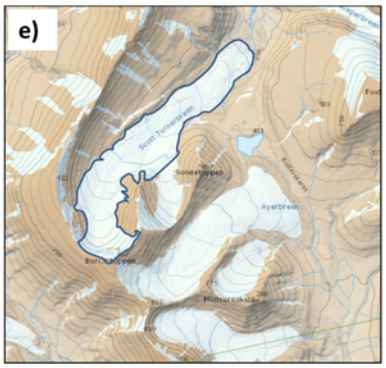
e)

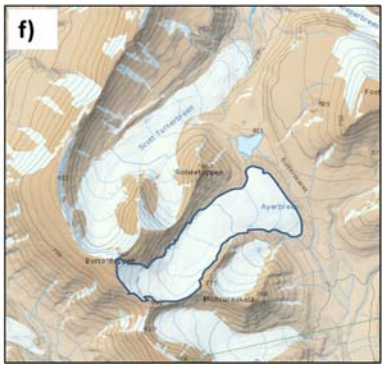
f)

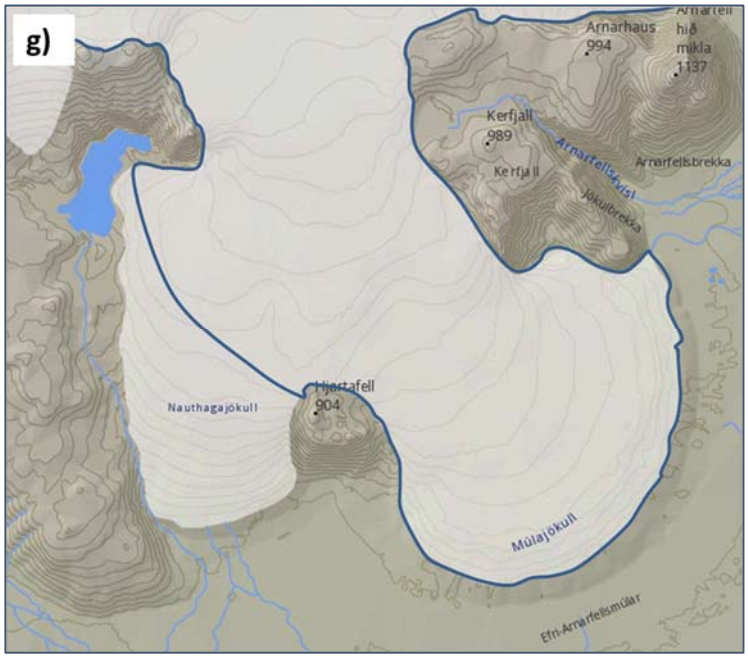
g)
Arnarhaus
994
Arnarfell hið mikla
1137
Kerfjall
989
Kerfjall
Arnarfellsbrekka
Jökulbrekka
Hjartafell
904
Nauthagajökull
Múlajökull
Efri-Arnarfellsmúlar

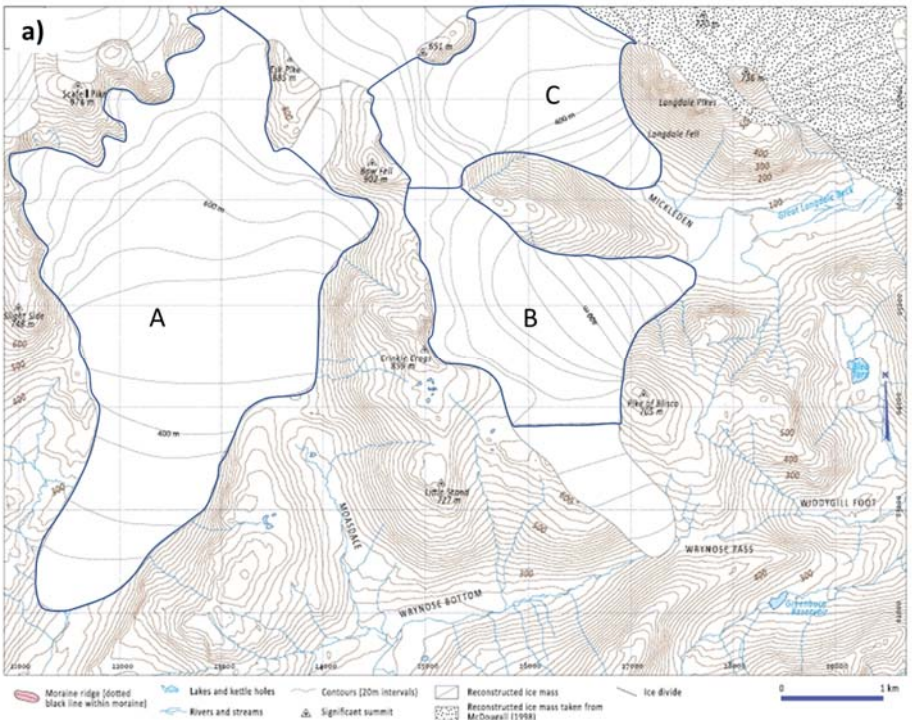

Figure 2.10 (2.10c on next page) **–** The reconstructed glaciers chosen for the pilot study were selected because of their similar morphologies and due to the similarities in their climatic and glaciological settings. The images of the glaciers are taken from the relevant papers. a) Glaciers A, B & C are three ice field outlet glaciers in the English Lake District, reconstructed by Brown *et al.* (2013). b) Glaciers D & E are two ice cap outlets in the Central Scottish Highlands, reconstructed by Benn and Ballantyne (2005). c) Glacier F & G are two ice cap outlets in the north-west Scottish Highlands, reconstructed by Lukas and Bradwell (2010).

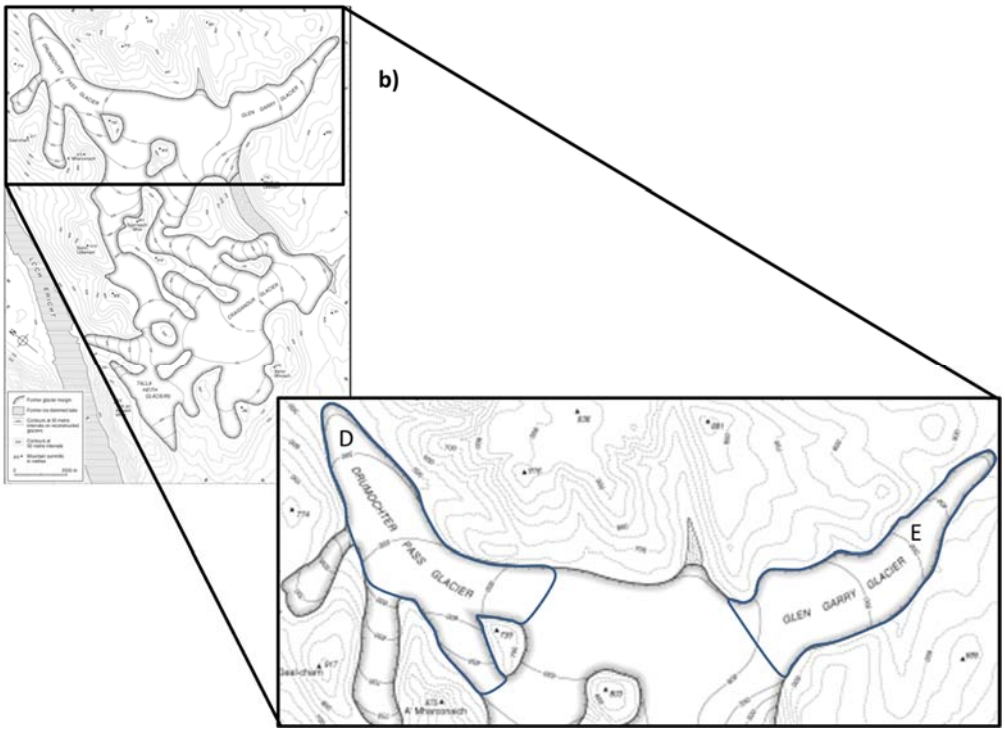

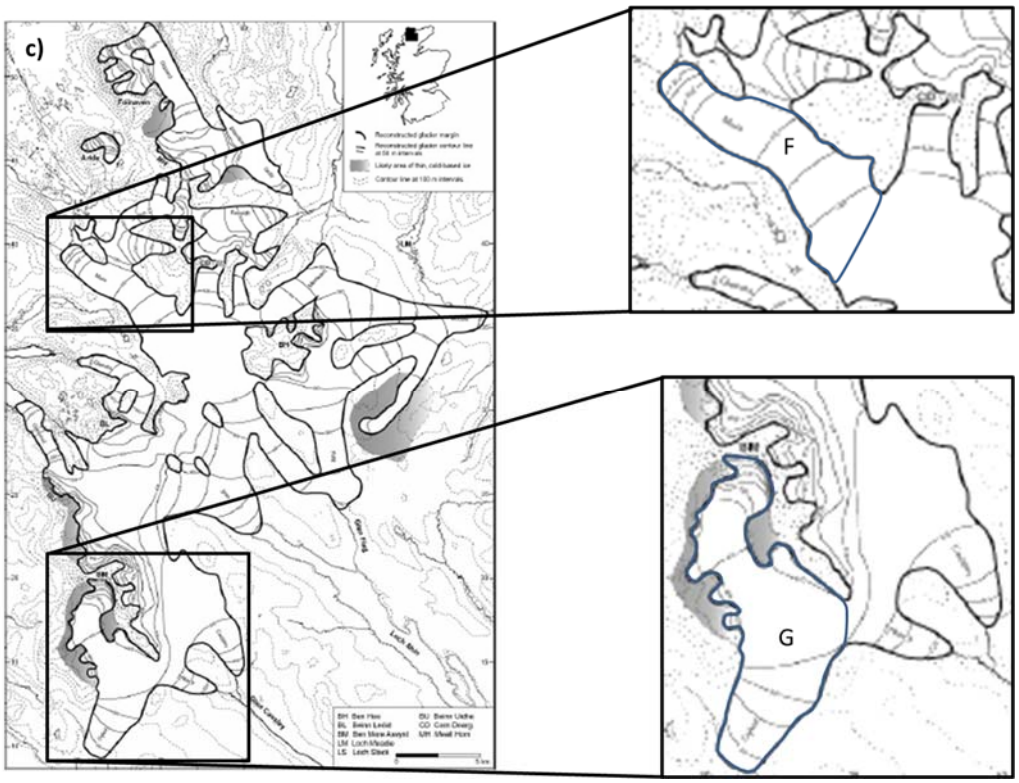

Having selected a sample of glaciers and acquired the topographic maps required, the measurement of external contour angles was conducted by hand using a protractor and print-outs of the relevant maps. The 'by hand' method for measuring external contour angles proved difficult to carry out reliably and with good accuracy, as well as being very slow. It was, therefore, decided that an automated or semi-automated method for measuring contour angles would be required if the results of the pilot study merited further investigation or expansion.

The external contour angles measured for the modern glaciers were graphed, so that they could be visually analysed (e.g. Figure 2.11). This revealed discernible trendlines that were usually consistent with the hypothesised trend (i.e. Figure 2.7c). However, all of the modern glaciers produced a reasonably high degree of variability in their external contour angles, which was generally centred around the snout (e.g. Figure 2.11a). The reason for this concentration of variable external contour angles most likely reflects the complex ice margin morphology around the snouts of the glaciers, where there are usually lots of small-scale variations in the ice margin morphology. Further variability found higher up the glaciers is harder to explain but may also reflect relatively small-scale variations in the ice margin. However, this seems unlikely given that there is often more variability and a less distinct

trend for one margin of a glacier than for the other (e.g. compare Figures 2.11b and 2.11c). This suggests that larger-scale topographic differences between the two margins could be causing a significant change in the morphology of one margin but not the other, which is reflected in different patterns of external contour angles.

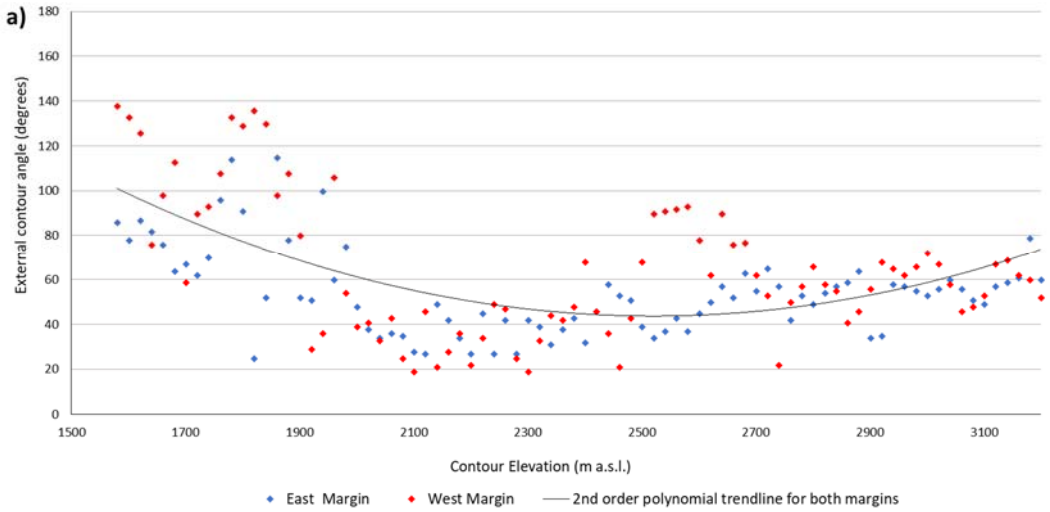

Figure 2.11 (2.11b and 2.11c on next page) **–** An example of the data produced by the manual measurement of external contour angles, in this case the data is from the Mer de Glace. a) includes the data from both margins of the glacier, which have been used to produce a 2nd order polynomial trendline that is a reasonably good fit for the data ($r^2 = 0.34$) and matches the expected trend shown in Figure 2.7c. When the two margins of the glacier are separated, a more complex picture emerges with both margins featuring areas of more variable external contour angles that coincide with topographic features. b) shows the data for the west margin of the glacier, which has a lot of variability surrounding the glacier snout and around the Séracs du Géant ice fall at around the 2500 m contour elevation. c) shows the data for the east margin, which also has a lot of variability surrounding the snout but is markedly more uniform along the rest of the glacier. The difference between these margins may be because the west margin is also flowing around a topographic spur as it negotiates the ice fall, increasing the complexity of the ice margin morphology and leading to more varied external contour angles.

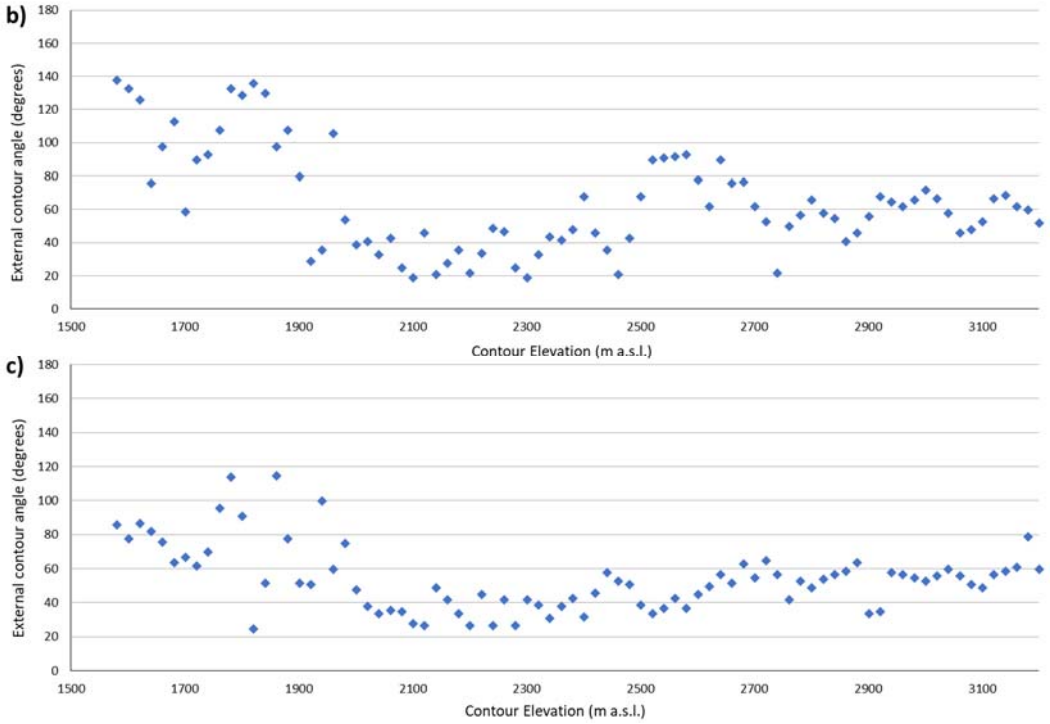

In order to determine the cause of the variability identified in the external contour angles of individual glacier margins, comparisons were made between the external contour angles and the topography for each glacier's two margins. This comparison led to the finding that the sections of the ice margin with the highest degree of variability usually coincided with larger-scale features of the valley topography, such as truncated spurs or bedrock steps (e.g. Figure 2.11b). This finding raises the potential for utilising external contour angles to explore the impact of larger topographic features on the ice margin morphology, with better quantification of this interaction possibly able to improve interpolation in rugged terrain. To confirm if a topographic signature can be extract from the external contour angles and to verify the primary control over the variability in external contour angles around the glacier snout, further investigation with a larger sample of glaciers would be required.

When multiple modern glaciers were compared together (Figure 2.12), normalised to adjust for different glacier lengths, it was clear that the majority of the glaciers studied had a trend that mirrored the trend shape expected (Figure 2.7c). However, not all glaciers produced the expected trend and Scott Turnerbreen (black) and Múlajökull (light blue) are clear exceptions, with very different trends and a significantly greater degree of variability in external contour angles than the other glaciers. Both Múlajökull (Johnson *et al.* 2010; Jonsson *et al.* 2014) and Scott Turnerbreen (Hodgkins *et al.* 1999) are known to be surge-

type glaciers, indicating that there may be distinctive trends in external contour angles for surge-type glaciers compared with other glacier types. This suggested that a larger sample of surge-type glaciers' external contour angles should be collected to investigate this relationship.

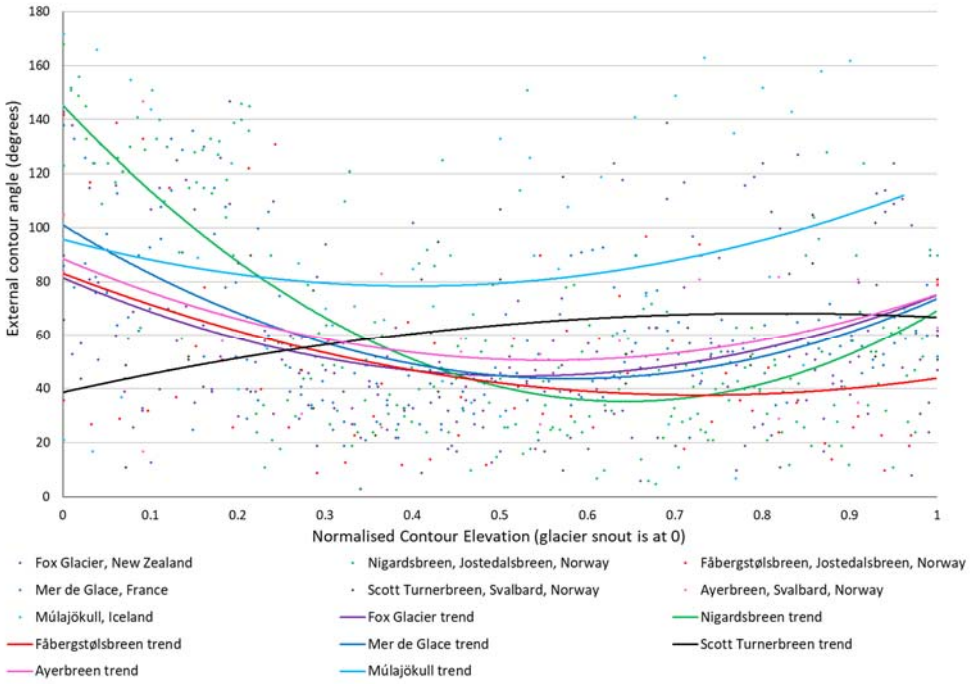

Figure 2.12 – All of the modern glacier external contour angle measurements are shown in this graph, normalised to a scale of 0-1 where the snout is at 0. Second order polynomial trends were found to be a good fit for the majority of glaciers (e.g. Figure 2.11a) and show that most glaciers do produce something similar to the expected external contour angle trend in Figure 2.7c, despite the variability caused by large-scale topography. Excluding the clear anomalies of Múlajökull and Scott Turnerbreen, the r^2 values for the trends shown range from 0.10 - 0.50 (mean of 0.25).

Compared to the modern glaciers, the reconstructed glaciers produced a much more standardised picture, with clearer external contour angle trends and generally lower levels of variability (Figure 2.13). In particular, there are no areas of particularly pronounced variability in the external contour angles, such as those seen around the snouts of the modern glaciers or associated with large-scale topographic features. Instead, the level of variability in the external contour angles measured for the reconstructed glaciers is much more uniform along the full length of the ice margins. This suggests that the variability here is more likely to be due to smaller-scale variations in the morphology of the ice margin or topography and implies that researchers may be subconsciously smoothing ice margins as they draw them, reducing the natural variability in external contour angles associated with larger features of the valley topography. However, the overall trend of all of the

reconstructed glaciers' external contour angles is generally similar to that of the modern glaciers (e.g. compare Figure 2.12 and Figure 2.13) and the reconstructed glaciers also produce the anticipated curve from Figure 2.7c. This suggests that researchers are generally drawing fairly accurate ice margins using 'by-eye' interpolation but it may be possible to improve and standardise this method by further developing the use of trends in external contour angles to constrain interpolation. In particular, the possible links found between external contour angles and larger-scale valley topography, such as truncated spurs, could potential allow for specific contour angle patterns to be identified that fit certain topographic features, enabling better constraint of ice margin morphologies associated with these landforms. This could increase confidence in the interpolation of ice margins in rugged terrain, where these topographic features are more common. Therefore, it was decided to pursue methods for automating the collection of contour angle measurements, so that a larger sample of modern glaciers could be considered, in the anticipation that clearer trends in external contour angles would emerge that could be used to improve interpolation by utilising the method similar to that shown in Figure 2.8.

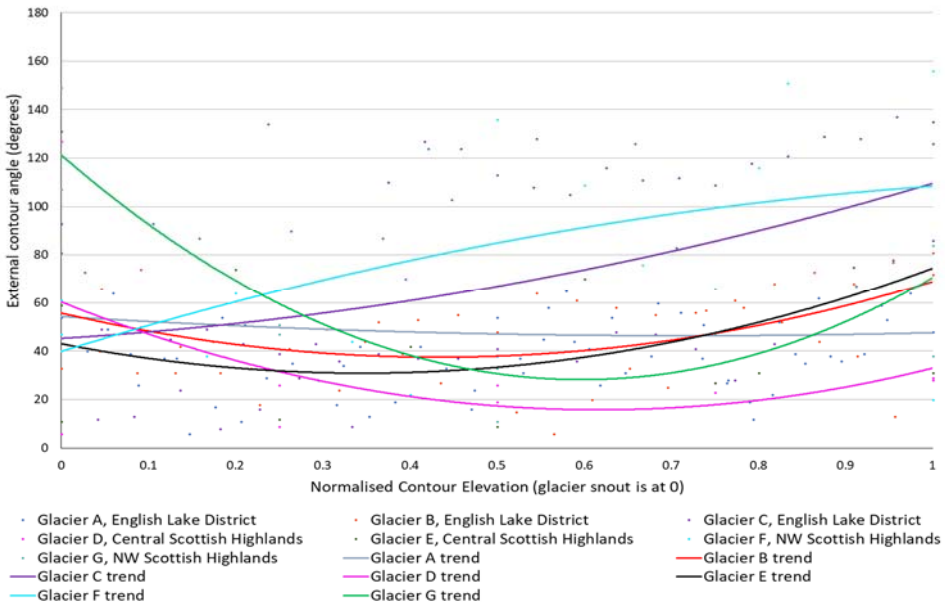

Figure 2.13 – Compared to the modern glacier external contour angle data (Figure 2.12), the reconstructed glaciers produced a more uniform picture. In particular, there is less variety in the contour angles measured and no clear links were found between the pattern of external contour angles for any given glacier and the larger-scale topographic features of the glacier's valley. This suggests that whilst 'by eye' interpolation clearly produces ice margins that roughly fit the expected trend for external contour angles, the missing influence of larger-scale topographic features suggests that consideration of external contour angles could improve the accuracy of interpolation, as well as standardising the process. It is interesting to note that, like the modern glaciers, the reconstructed glaciers did produce a couple of exceptions to the expected trend, which could perhaps indicate unusual glacial settings (e.g. surge-type glaciers).

2.3.2 Automating the measurement of contour angles

To build on the pilot study and produce a reliable method for interpolation based on trends in external contour angles, a large data set of contour angles for glaciers in a wide range of topographic, geological, glaciological, and climatic settings was required. A data set of the required size could not be feasibly or reliably collected by hand; therefore, an automated method of data collection was required.

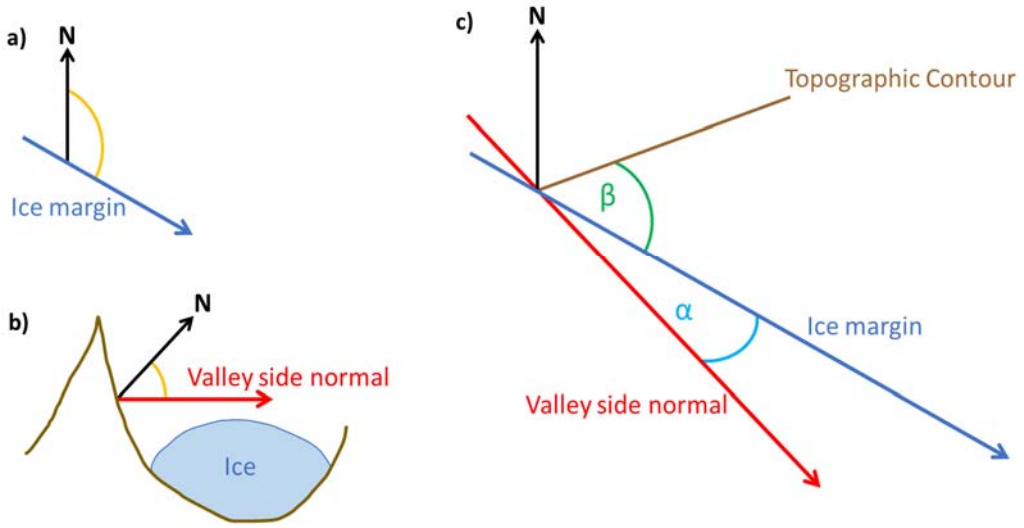

Figure 2.14 – These schematics show the mathematics used to compute the external contour angle automatically in ArcGIS 10.1. a) the orange curve shows the angle of ice margin orientation, computed in degrees from north (i.e. the angle of azimuth). b) shows a cross-section through the glacier valley with the angle of aspect between the valley side normal and north shown in orange. c) shows the final step to extract the external contour angle (β) using the angle between the valley side normal and the ice margin (α), which can be determined when the angles in a) and b) are known.

Investigation into possible methods for automatically collecting external contour angle data suggested the idea of computing the angle of orientation of the ice margin from north and comparing it to the valley side mean topographic aspect, which is also measured from north (Figure 2.14a and 2.14b). Using these two angles measured from north, it is possible to compute the angle between the ice margin and the valley side normal (α in Figure 2.14c). It is then possible to compute the external contour angle because the topographic contour must be perpendicular to the valley side normal, meaning that the external contour angle (β in Figure 2.14c) and α will sum to 90°. The disadvantage of this mathematical method for computing the external contour angle is that it is not possible to compute contour angles greater than 90°, despite external contour angles up to 180° being possible. However, the pilot study demonstrated that the majority (81%) of external contour angles measured were

equal to or below 90°, with larger angles largely confined to the snout and headwall of the glacier. As these areas are often relatively better constrained by the geomorphological record, particularly around the snout, it was still deemed worth pursuing this method of automated contour angle calculation.

Having determined a potential method for collecting external contour angles automatically, the method was applied to a set of morphologically simple glaciers (Figure 2.15). Application of the automated method to morphologically simple glaciers was needed to ensure that the method worked as expected and to give an opportunity to resolve any teething issues, before applying it to more complex ice margins. The following criteria were used to identify suitable glaciers for testing and refining the automated method:

1. The glacier must have a 'classic' valley glacier morphology, i.e. from just the snout position it would be likely that 'by eye' interpolation would cause a researcher to draw the rest of the glacier approximately as it is in reality.
2. The snout must be tongue-shaped and not a piedmont lobe, calving margin, on an ice fall etc.
3. The glacier must sit in a single U-shaped valley without obvious ice falls, topographic spurs or other large topographic variations.
4. There must be no tributaries or other complicating factors, for example not a surge-type glacier.
5. It must be a separate glacier, i.e. not a tributary itself or part of an ice field and not an ice sheet or ice cap outlet glacier.
6. Glacier area of c. 10-20km^2.
7. Located between 60° N to 56° S and preferably not at high altitude, to enable easy access to reliable Digital Elevation Models (DEMs) and to avoid problems with DEM distortion.

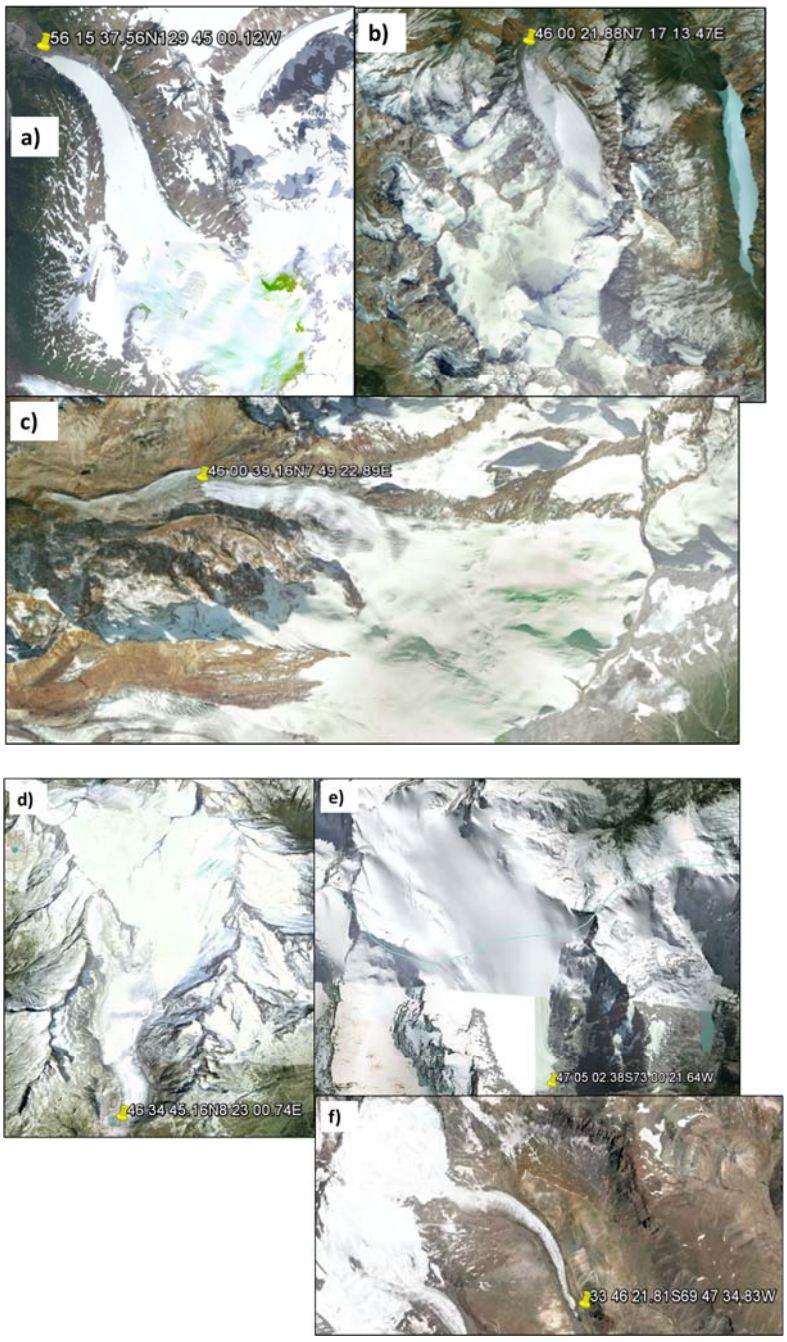

Figure 2.15 – These glaciers were chosen to test the automated contour angle data collection method because they have relatively simple morphologies and met the criteria in Section 2.3.2. The images of the glaciers were sourced from Google Earth, which also provided the coordinates of the glacier snouts. The glaciers were given study names as several are currently unnamed: a) British Columbia 1; b) European Alps 1; c) European Alps 2; d) European Alps 3; e) Andes 1; f) Andes 2.

To test the accuracy of the automated contour angle measurements, the external contour angles for each of the glaciers in Figure 2.15 were also measured by hand and compared to the automated measurements. For both the automated and manual measurements, outlines of each glacier were downloaded from the Randolph Glacier Inventory version 5.0 (https://www.glims.org/RGI/) and the topography was represented using DEMs collected by the Shuttle Radar Topography Mission (accessed from the United States Geological Survey https://dds.cr.usgs.gov/srtm/version2_1/).

Initially, the automated external contour angle collection method yielded reasonable results when compared with the manual measurements of the test glaciers, but the contour angles produced by the automated method had a much larger degree of variability. The manual method necessarily had to work at a lower resolution than the automated method and this may have produced a smoothing effect from the use of topographic contours and lower-resolution ice margin maps compared to DEMs and relatively high-resolution glacier outline polygons. Whilst the variability in external contour angles produced by the manual method seems to be primarily related to large-scale valley topography (Section 2.3.1), it appeared that the automated method was picking up much more of the smaller variations in the valley side and ice margin morphologies, introducing a high degree of variability and masking any underlying trend. Therefore, the decision was taken to try adding a degree of smoothing into the automated method to reduce the 'noise' from small-scale variations in the valley side topography and in the morphology of the ice margin. A series of tests of different smoothing methods were conducted and it was determined that the glacier outline required a degree of smoothing to optimise the method but that smoothing the DEM was not required. The ice margin was first generalised to 90 m tolerance, bringing its resolution in line with that of the DEM, before being smoothed using a B-spline smoothing curve via the ET GeoWizards 'polyline smoothing' tool with the minimum freedom setting of 3 and a smoothness of 20 (Figure 2.16).

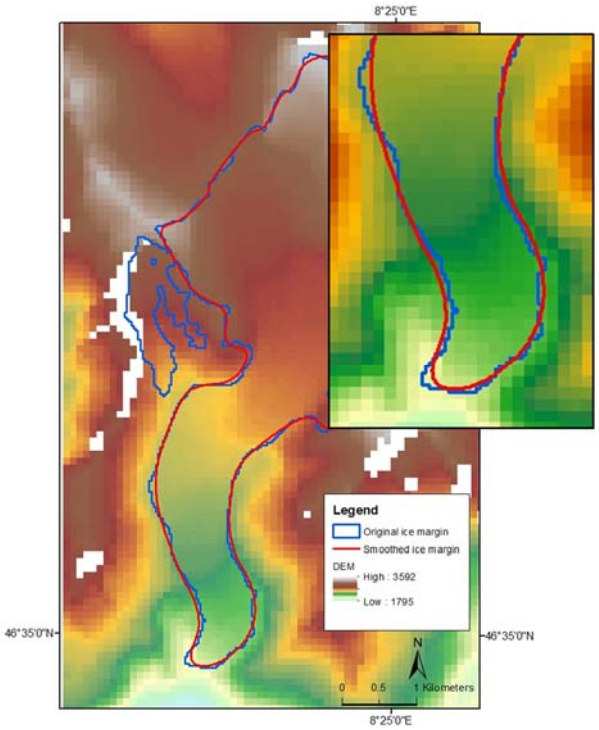

Figure 2.16 – The ice margin of the test glacier European Alps 3 is shown both before and after the smoothing process. The inset shows an enlargement of the ablation area of the glacier, showing how the smoothing process has preserved the general morphology of the ice margin but has greatly reduced the 'noise' of small-scale complexities. It was theorised that the highly detailed nature of the Randolph Glacier Inventory ice margin polygons was introducing additional variability into the external contour angles because the automated method was picking up on every minor change in ice margin orientation. Therefore, the smoothing process was designed to minimise orientation changes to only those essential to maintaining the overall form of the glacier.

The inclusion of ice margin smoothing was found to reduce the amount of variability in the data generated by the automated method. This improvement in the method enabled links between large-scale valley topography and external contours angles to be more easily identified, bringing the automated method into closer agreement with findings of the pilot study (e.g. Figure 2.17). This supported the notion that contour angles could be used to better constrain the likely morphology of the ice margin in rugged terrain, in order to improve 'by eye' interpolation.

Despite the improvements made to the automated method for measuring external contour angles, the data produced is still more variable than manual measurements. This makes it more difficult to determine reproducible trends and to identify the influence of topography. Further refinement of the automated method could potentially resolve this problem but

there were several other issues identified during the testing process that may additionally limit the usefulness of the method.

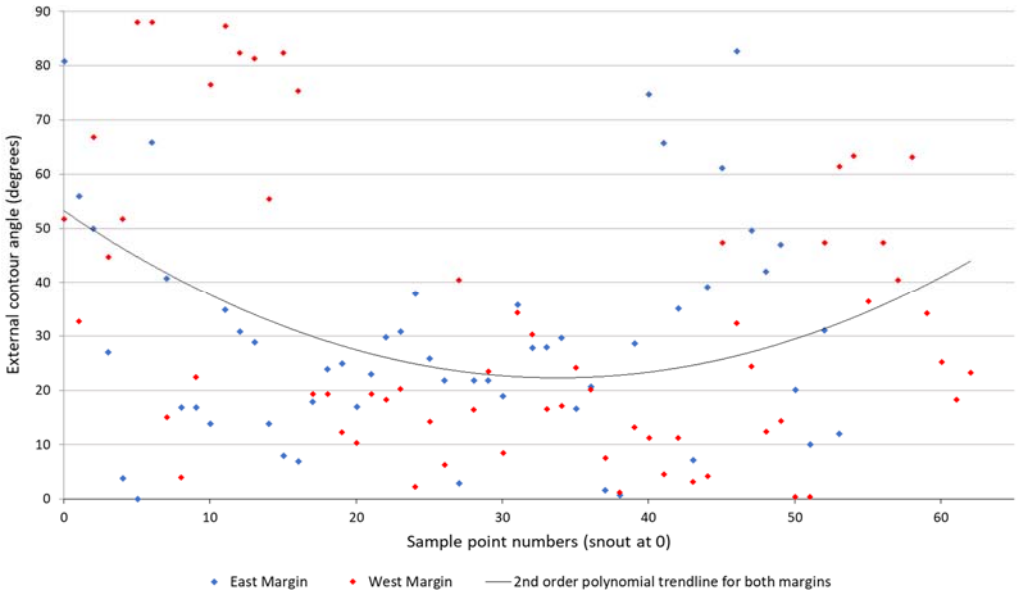

Figure 2.17 – The automatically measured external contour angles of European Alps 3 show a similar pattern of variability and a very similar overall trend to the manually measured modern glaciers in the pilot study (e.g. Figure 2.9a). This suggest that the automated method, including smoothing of the ice margin, does produce reasonable measurements of the external contour angles of a relatively simple glacier. However, there is still a somewhat greater degree of variability and the trendline is not as good a fit, indicating that the automated method requires further refinement to match the accuracy of manually measuring contour angles. Despite this, it is possible to identify the impact of a topographic spur that has produced a slight increase in the mean external contour angle of both margins around the location of sample point 30.

2.3.3 Problems with the automated method

The automated method for external contour angles measurement has practical issues because it is more truly a semi-automated method in its current form, with several steps that require manual processing in ArcGIS or Microsoft Excel™. These manual steps increase the time needed to measure the contour angles (currently taking an experienced user c. 1.5 hours per glacier) and introduces some subjectivity and potential for human error into the process. In particular, the choice of sampling intervals for ice margin orientation and valley side aspect have proved difficult to confidently define, despite extensive testing. This can lead to sampling that is too detailed, obscuring trends with excess data, or too coarse. Even with further testing, it is likely that these sampling intervals may need to vary between individual glaciers, depending on the size of the glacier and the complexity of the topography. If this is the case, then it will be difficult to significantly increase the speed at which external

contour angles can be measured, reducing the number of glaciers that can be practically investigated. As well as limiting the practicality of the automated method, these subjective sampling decisions introduce uncertainty into the measurements of external contour angles. At present this uncertainty is not well defined and, although not thought to be large, could be impacting on the results of analysing the external contour angles produced by the automated method.

The input data for the automated method also contains a degree of uncertainty. The resolution of the DEM is well defined at 90 m but the Randolph Glacier Inventory glacier outlines are more variable in their accuracy, with a stated mean uncertainty of around ± 5% (Pfeffer *et al.* 2015). Additionally, it has proved difficult to define exactly what impact the smoothing process has on the resolution of the input glacier margins but it is likely to have decreased the resolution and increased the potential uncertainty.

The mathematical limitations of the method do not allow external contour angles greater than 90^{o} to be measured, despite angles larger than this being identified during the pilot study (Section 2.3.1). The omission of larger angles reduces the usefulness of the method, particularly in the snout and headwall areas of the glacier where angles greater than 90^{o} are more common. However, the majority of external contour angles measured during the pilot study were below 90^{o}, so this issue is not likely to have a large impact.

Despite the reduction of variability in the measured contour angles achieved by using smoothing processes applied to the ice margin, the automated method is still highly sensitive to relatively small changes in the valley topography and ice margin morphology. This produces a relatively high level of 'noise' in the data produced by the method (e.g. compare Figure 2.17 and Figure 2.11a), making it challenging to interpret the data and to produce meaningful results that could then be used to improve interpolation. A fairly high level of variability was also identified in the manual measurements used in the pilot study, suggesting that resorting to manual measurement would not entirely solve the problem.

Therefore, the conclusion drawn from the investigations presented in the chapter is that external contour angles appear to be too variable within and between glaciers to be used to constrain interpolation and that this level of variability appears to be strongly related to sampling choices in the methods of contour angle measurement. This implies that if a way could be identified to further improve the automated method and reduce its sensitivity, this could potentially lead to more usable data and enable external contour angles to be used to

guide interpolation. However, despite various attempts to refine the automated method, it has so far not proved possible to further reduce the sensitivity sufficiently. Therefore, the decision was taken to cease work on improving interpolation via external contour angles. The current state of the automated method is that it is too slow to investigate a large enough number of glaciers as well as being too sensitive and subjective to yield meaningful results, particularly because of the noise produced by the method's sensitivity to minor changes in the ice margin and valley side topography.

2.4 Where next for contour angles?

Despite the decision not to continue developing the automated method for external contour angle measurement, the use of contour angles to improve interpolation is still thought to be a potentially fruitful avenue of research. The pilot study and some of the data produced by the automated method support the notion that external contour angles can be used to identifying the impact on the position of the ice margin of major changes in the valley topography (e.g. Figure 2.11a and Figure 2.17). Therefore, better methods for collecting external contour angle data are worthy of further consideration. The timeframe of the research for this thesis did not enable further exploration of this topic but on-going improvements in Geographic Information Systems (GIS) and general computing power may make this research more viable in future. In particular, recent developments in machine learning are promising and this sort of software could potentially be trained to identify optimal choice of variables for the collection of contour angle data for individual glaciers, such as sampling distances for the ice margin orientation. Investigation of this approach, as well as exploration of other methods for improving the robustness and reproducibility 'by eye' interpolation, is commended to other researchers.

The uncertainty that 'by eye' interpolation introduces into palaeoglacial reconstructions remains unresolved, so it is more important than ever to improve the use of the glacial geomorphological record to reduce the need for subjective interpolation. Therefore, the remainder of this thesis will concentrate on developing a better understanding of glacial trimlines, which are a currently under-utilised but potentially very important landform that proves a rare constraint on palaeo ice thickness.

Chapter 3

Using trimlines to identify former ice margins and the nature of trimline expression

3.1 Introduction

Glacial trimlines are breaks or transitions between contrasting zones on the slopes of glacierised or glaciated valleys (Figure 3.1). Along with other indicators of previous ice margin positions, glacial trimlines are used in the production of palaeoglacial reconstructions and are particularly important constraints over both the ice margin position and the ice thickness (Ballantyne 2010).

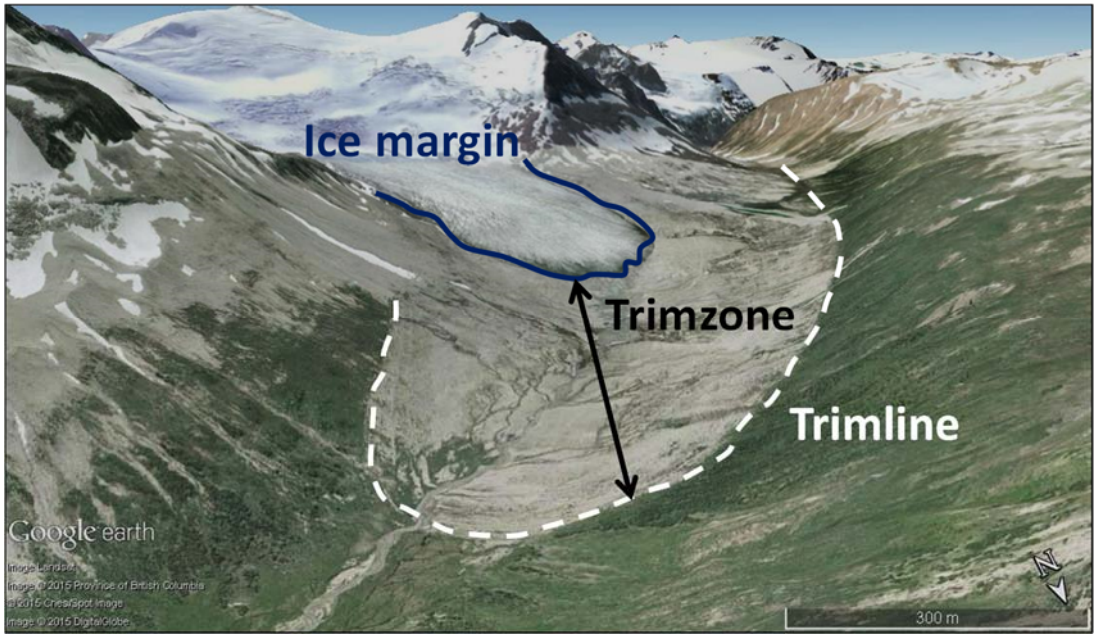

Figure 3.1 – Example of a glacial trimline (white) associated with an unnamed glacier flowing down from Icemaker Mountain in British Columbia, Canada. This trimline is an example of a vegetation contrast that records both the lateral and frontal ice margin positions at the time of trimline formation. The largely vegetation-free area between the modern ice margin (blue) and the trimline (white) is termed the 'trimzone' (black). (Annotated from Google Earth; imagery from Landsat)

Glacial trimlines located on lateral ice margins record the ice surface elevation at the time of their formation, enabling the production of 3-dimensional (3D) reconstructions (Ballantyne 2010). For areas of historic glacier retreat, trimlines may be compared with the modern ice surface to determine the surface elevation change, or 'down-wasting', since the date of trimline formation (Navarro *et al.* 2005; Kohler *et al.* 2007). From calculations of down-wasting it is possible to compute the volume of ice lost and, where a series of previous ice margin positions are known, rates of ice loss can be computed (Glasser *et al.* 2011). Comparison of these data with climate records allows the glacier's response time to specific climate forcings to be determined (e.g. Harrison *et al.* 2007; Csatho *et al.* 2008; Glasser *et al.* 2011). These outputs from the study of glacial trimlines are particularly important for understanding and predicting the likely response rates and ice loss patterns that may be expected over the next century due to global climate warming (Ackert *et al.* 2011; Kuchar *et al.* 2012).

A similar process can be applied to the glacial trimlines of Quaternary ice masses to determine the maximum ice surface elevation of glaciation and hence compute the total ice volume and sea level contribution of that glaciation (Ballantyne and Hall 2008). In Quaternary settings trimlines are particularly important because they are commonly found in areas where other glacial features are not preserved, especially in the accumulation area of palaeo ice masses (Thorp 1986; Ackert *et al.* 2011). However, care must be taken when interpreting glacial trimlines associated with large glaciations because these features may represent a thermal boundary beneath an ice sheet, rather than an ice margin position (Ballantyne 2010). By providing information about palaeo ice margin positions and patterns of thermal regime, glacial trimlines are a vital component of empirical glacial reconstructions. These reconstructions are a key testing ground for numerical ice sheet models, which are used to simulate modern ice sheets in order to predict the responses of Greenland and Antarctica to on-going climate change (Kuchar *et al.* 2012).

Despite the important applications of glacial trimlines they have mostly been reported on a case-by-case basis, with little systematic exploration of their formation, distribution, expression and morphology. The overall lack of knowledge about glacial trimlines and conflicting opinions surrounding their interpretation is limiting the potential for these features to be used productively in palaeoglacial reconstructions.

3.1.1 Aim and structure of this review

The aim of this literature review is to document the state of the art in the field of glacial trimline research and to identify issues in the interpretation of glacial trimlines, in order to highlight areas for further study. An initial discussion of the terminology of glacial trimline research (Section 3.2) will be followed by a brief history of the field (Section 3.3). More detail will then be given regarding the methods used to study Quaternary and historic trimlines (Section 3.4) and the applications for trimlines and trimline-based reconstructions (Section 3.5). On-going debates and issues raised by previous trimlines research will be identified in Section 3.6. Several significant gaps exist in the literature, which will be discussed in Section 3.7. Section 3.8 presents a new terminology to improve the clarity of future discussion of glacial trimlines and help to reduce confusion in the field of trimline research. Finally, a summary and suggestions for further study will be given (Section 3.9).

3.2 Trimline terminology

The terms used to refer to glacial trimlines have been neither consistent nor clear in the literature. In particular, several terms have developed a double-meaning and been used both to describe the expression of a type of trimline and to imply a particular interpretation. This section will describe the established terminology and highlight areas of conflict and confusion.

3.2.1 What is a trimline?

This question is more complex than it may first appear due to the range of different glaciogenic features that have been termed 'trimlines', or that overlap with glacial trimlines in terms of expression or usage. For example, differences in the vegetation density on glacierised valley sides have been termed 'trimlines' (e.g. Wolken *et al.* 2005; Harrison *et al.* 2007; Kelley *et al.* 2012; Figure 3.1). Similarly, distinctions between zones of glacial erosion compared to adjacent areas of periglacial weathering in settings of Quaternary glaciation have also been called 'trimlines' (e.g. McCarroll *et al.* 1995; Ballantyne *et al.* 1998b; Rae *et al.* 2004; McCarroll 2016). Clearly these breaks or contrasts in surface characteristics have formed in very different ways but both arise from some sort of 'trimming' and can be interpreted as former ice margin positions. However, lateral moraines on the sides of glaciated valleys also mark ice margin positions and have been used in reconstructions in the same way as the previous two examples (e.g. Csatho *et al.* 2008; Hannesdóttir *et al.* 2015;

Kjeldsen *et al.* 2015). Are lateral moraines also a kind of 'trimline'? At the moment there is no clear answer to this question in the literature, with different authors including different sets of glaciogenic features under the umbrella term of 'trimline'. This creates confusion in the use of the term and problems in defining what is and is not a 'trimline'.

Additionally, it is possible to view 'trimlines' as either a linear feature or a transition area between two slope zones with differing characteristics, sometimes termed a 'trimzone' (Figure 3.1; e.g. Csatho *et al.* 2005; Forman *et al.* 2007; Csatho *et al.* 2008 Figure 3.2). Previous trimlines research has also used discussed 'weathering zones' (e.g. Ives 1976; Ives *et al.* 1976; Ives 1978; Ballantyne *et al.* 1998a; Clark, P.U. *et al.* 2003; Sugden *et al.* 2005; Goehring *et al.* 2008) and 'erosional zones' (e.g. Hättestrand and Stroeven 2002; Nesje *et al.* 2007; Fu *et al.* 2013). It is notable that, although there are several exceptions (e.g. Ballantyne *et al.* 1998a in Britain; Sugden *et al.* 2005 in Antarctica; Fu *et al.* 2013 in Tibet), there appears to be a preference for using zonal terminology in North American (e.g. Ives 1976; Ives *et al.* 1976; Ives 1978; Clark, P.U. *et al.* 2003) and Scandinavian trimline research (e.g. Hättestrand and Stroeven 2002; Nesje *et al.* 2007; Goehring *et al.* 2008). Outside of these areas, trimlines are more commonly referred to in a linear sense as lines, limits, boundaries or similar (Table 3.1). The use of different terminology in different places is a further confusing factor that is complicating the discussion of glacial trimlines.

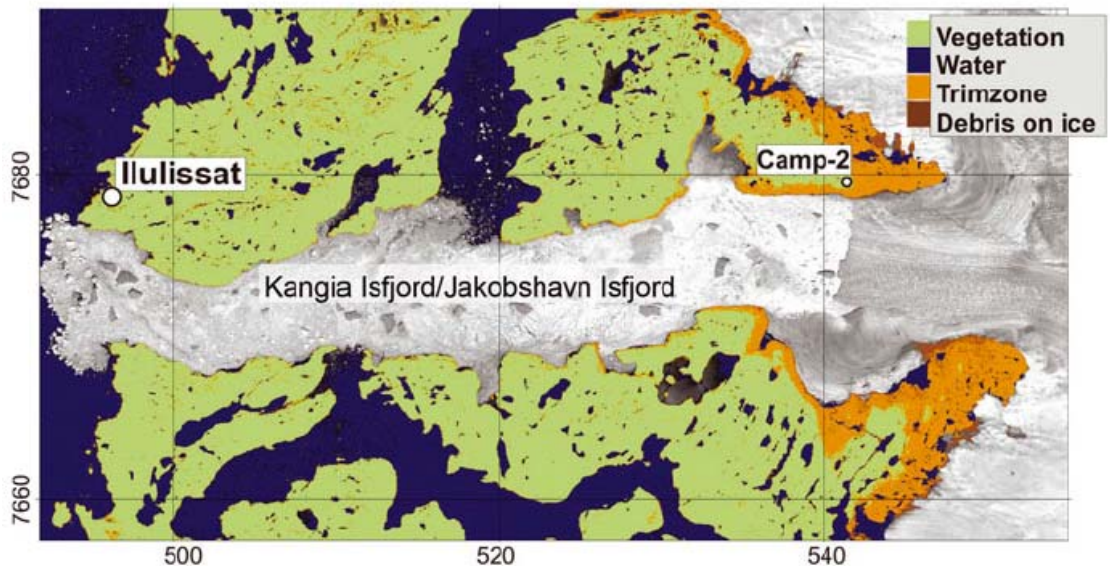

Figure 3.2 – The trimzone surrounding Jakobshavn Isfjord in western Greenland. Csatho *et al.* (2008) identified the trimzone using analysis of the spectral reflectance of different landsurfaces. In this case the trimzone is differentiated by a reduced lichen density compared to the surrounding area. They dated the outer edge of the trimzone, which could be considered to be a trimline, to the Little Ice Age. (Csatho *et al.* 2008, pp.135)

Trimlines have generally been held to be features of the lateral ice margin. However, it is not uncommon for these features to extend into the snout area of a glacier (e.g. Figure 3.1). In these situations, the term 'trimline moraines' has been used (Ó Cofaigh *et al.* 2003). However, this term is not in common usage and most authors do not make a distinction between lateral and frontal trimlines. A lack of research into frontal trimlines means that it is not possible to say whether these features should be considered separately from lateral trimlines.

Given the lack of consensus about what the term 'trimline' refers to, it is surprisingly uncommon to find an explicit definition of 'trimline' in the literature. The majority of papers discussing glacial trimlines simply use the term without either giving a definition or referring to a previous definition; presumably most authors believe that the meaning of the term is clear. However, the above discussion suggests that the meaning of the term 'trimline' can vary significantly.

Efforts to identify the origin of the term have proved inconclusive and no coining definition has been discovered. 'Trimline' appears to have been an established part of the research lexicon by the start of the 1950s (Lawrence 1950a/b; Mathews 1951; Heusser *et al.* 1954). Lawrence provides an early definition, describing 'forest trimlines' as "the line representing the maximum position attained by the ice front, where the forest was sheared off [trimmed] by the ice" (1950a, pp.243). During the 1950s the term 'trimline' was quickly adopted in other areas, such as Patagonia (Nicols and Miller 1951), and went on to become the dominant term for these features over the following decades (Table 3.1).

3.2.2 Trimline manifestations

Glacial trimlines can be expressed by a variety of means, which are not mutually exclusive within a single trimline or group of trimlines. Some terms previously employed in the literature have included description of trimline expression (Table 3.1). Examples include terms such as 'vegetation trimline' (e.g. Wolken *et al.* 2005; Harrison *et al.* 2007; Kelley *et al.* 2012; Figure 3.1) and 'weathering limit' (e.g. Ballantyne and Harris 1994; Rae *et al.* 2004; Evans *et al.* 2005; Boulton and Hagdorn 2006; Ballantyne *et al.* 2009). Despite the use of descriptive terms for some trimline expressions, the majority of trimline expressions have no established terminology.

Within trimline research, the term 'periglacial trimline' is in particularly widespread usage for describing a distinction between an area of glacial erosion and one of periglacial

weathering (Ballantyne and Harris 1994; Figure 3.3). This term implies an interpretation that 'periglacial trimlines' should be considered to represent a palaeo ice margin position (e.g. Figure 3.3; Ballantyne *et al.* 1997; Hughes 2002; Evans *et al.* 2005; Ballantyne *et al.* 2009; Ballantyne 2010; Ballantyne *et al.* 2011; Fabel *et al.* 2012). Application of cosmogenic nuclide dating has challenged this interpretation but the term 'periglacial trimline' has continued to be used and can now refer to both trimlines interpreted as palaeo ice margins and as palaeo thermal divides (Ballantyne 2010; McCarroll 2016; Figure 3.13). This confusing usage of 'periglacial trimline' has led to a decline in popularity and a rise in alternatives like 'erosional trimline' (e.g. Kaplan *et al.* 2001; Ballantyne 2007) and 'thermal trimline' (Benn and Evans 2010, pp.620).

Terms like 'periglacial trimline', 'erosional trimline' and 'thermal trimline' indicate a suggested interpretation, rather than solely describing the trimline expression. Similar interpretative terms, such as 'glacier limit' (Sissons 1974) and 'subglacial zone' (Hättestrand and Stroeven 2002), also suggest either an ice marginal or subglacial interpretation for the formation of the trimline feature. Other terms, such as 'ice sheet trimline' (Ballantyne *et al.* 1998a) or 'palaeo-trimline' (Hubbard *et al.* 2009), suggest that the trimline is linked to a particular style of glaciation or glacial period. Still other terms indicate an interpretation of the significance of a trimline feature within a given study area. For example, Nesje *et al.* (2007) use the term 'regional trimline' to describe the average trimline altitude across their study area. The layers of interpretation within trimline terminology can make terms difficult to use accurately and can be misleading to the reader.

In summary, there are several useful terms that describe a particular trimline expression but many forms of trimline expression do not have an appropriate descriptive term. This may be artificially focusing research on to the types of trimline that are already well described in the literature. Additionally, there is a lack of standardisation within trimline terminologies, with different terms used at different times and in different places. Many of the most common terms for glacial trimlines imply a degree of interpretation, rather than remaining solely descriptive. This fact is often not made clear and leads to confusing and sometimes conflicting usage of the established terminology. Trimline research would be improved by the application of a simplified and standardised terminology that has specific descriptive terms for all observable means of trimline expression and a clear distinction between descriptive and interpretative terms.

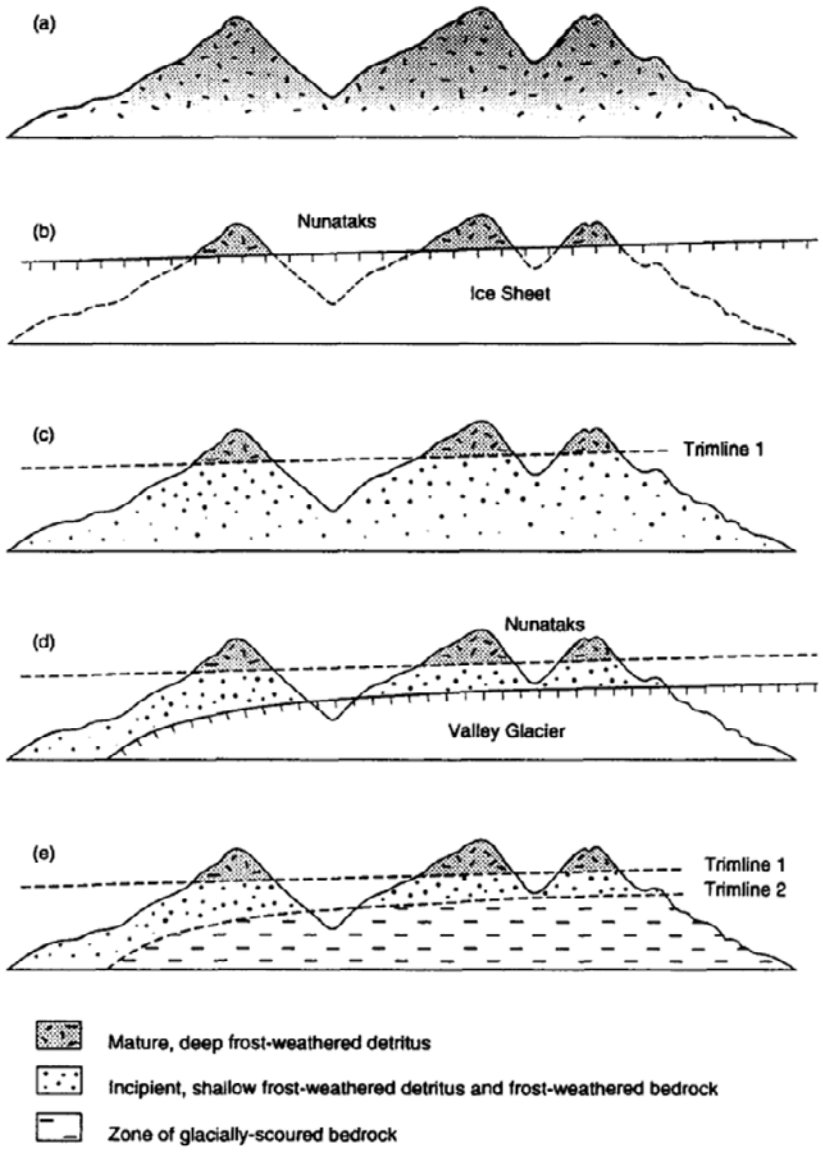

Figure 3.3 – A theory for the formation of 'periglacial trimlines', which are expressed as a contrast between evidence of intense frost weathering and adjacent areas of glacial scouring. a) The initial state of the mountains with a positive correlation between degree of frost weathering and altitude. b) Glacial advance 'trims' the frost weathering detritus, preserving it only on exposed nunataks. c) Retreat of the ice forms a periglacial trimline, expressed as a weathering contrast and erosional imprint limit. d) A smaller glacial readvance once again trims the weathering detritus. e) A second periglacial trimline marks the ice margin position of the readvance. At this stage there are three weathering zones separated by two trimlines, a situation that is observable across large areas of north-west Scotland (Ballantyne *et al.* 1997) and in the Torngat Mountains, Canada (Ives *et al.* 1976). (Ballantyne and Harris 1994, pp.182)

Table 3.1 (next page)– Terminologies used in the literature to refer to trimline features or zones. The wide range of terminology and the number of terms that lack a formal definition is hampering discussion of glacial trimlines and limiting the progress of research.

Term group	Term	Definition	Papers using this term
Generic linear	trimline	Glasser *et al.* (2005) provide a rare definition: "Sub-horizontal lines on valley sides separating areas of non-vegetated and vegetated land or areas covered by different types of vegetation" (pp.266). More often this term is undefined. Generally, a more specific term is used initially before resorting to just 'trimline' for the core of the paper. Commonly more specific terms are returned to in the discussion and conclusion. Also, it is quite common for a paragraph to start with a more specific term and then transition to using just 'trimline'.	Lawrence (1950a); Lawrence (1950b); Nicols and Miller (1951); Heusser *et al.* (1954); Thorp (1981); Thorp (1986); Nesje *et al.* (1987); Nesje *et al.* (1988); Thomsen and Winding (1988); Huber (1989); Reed (1989); Ballantyne (1990); Lawson (1990); Nesje and Dahl, S.-O. (1990); Orombelli *et al.* (1990); MacCarroll and Nesje (1993); Kleman (1994); Ballantyne (1994a/b); Ballantyne and Harris (1994); Locke (1995); McCarroll *et al.* (1995); Brook *et al.* (1996); Dahl, S.-O. *et al.* (1996a/b); Ballantyne (1997); Ballantyne *et al.* (1997); Lowe and Walker (1997); Ballantyne (1998); Ballantyne *et al.* (1998a/b); Florineth (1998); Florineth and Schluchter (1998); Lamb and Ballantyne (1998); Stone *et al.* (1998); Armienti and Baroni (1999); McCarroll and Ballantyne (2000); Ballantyne and Hallam (2001); Kaplan *et al.* (2001); Walden and Ballantyne (2002); Traczyk and Migoñ (2003); Clark, C.D. *et al.* (2004); Cockburn and Summerfield (2004); Kelly *et al.* (2004); McKinzey *et al.* (2004); Rae *et al.* (2004); Reuther *et al.* (2004); Csatho *et al.* (2005); Evans *et al.* (2005); Fiebig *et al.* (2005); Glasser *et al.* (2005); Wolken *et al.* (2005); van der Veen and Csatho (2005); Boulton and Hagdorn (2006); Fjellanger *et al.* (2006); Gosse *et al.* (2006); Hubbard *et al.* (2006); Linge *et al.* (2006); Stone and Ballantyne (2006); Ackert *et al.* (2007); Ballantyne (2007); Ballantyne *et al.* (2007); Forman *et al.* (2007); Goodfellow (2007); Harrison *et al.* (2007); Nesje *et al.* (2007); Reuther *et al.* (2007); Ballantyne *et al.* (2008); Ballantyne and Hall (2008); Baroni *et al.* (2008); Brooks *et al.* (2008); Castho *et al.* (2008); Fretwell *et al.* (2008); Glasser *et al.* (2008); Goehring *et al.* (2008); Hormes *et al.* (2008); Van der Beek and Bourbon (2008); Ballantyne *et al.* (2009); Ballantyne (2010); Benn and Evans (2010); Benn and Hulton (2010); Möller *et al.* (2010); Ackert *et al.* (2011); Ballantyne *et al.* (2011); Glasser *et al.* (2011); McCormack *et al.* (2011); Glasser *et al.* (2012); Fabel *et al.* (2012); Kelley *et al.* (2012); Kuchar *et al.* (2012); Gourronc *et al.* (2014); Lee *et al.* (2014); Loibl *et al.* (2014); Nixon and England (2014); White and Fink (2014); Ballantyne and Stone (2015); Hannesdóttir *et al.* (2015); Kjeldsen *et al.* (2015); Barth *et al.* (2016); Bickerdike *et al.* (2016); Evans (2016); McCarroll (2016); Edwards *et al.* (2017); Deswal *et al.* (2017); Sugden *et al.* (2017); Clark, C.D. *et al.* (2018); Pearce *et al.* (2018)
	trim-line	Undefined, presumably the same meaning as 'trimline'.	Chiverrell and Thomas (2010)

Generic linear	trim line	Indirectly defined by Cockburn and Summerfield (2004, pp.18): "Geomorphic indicators of previous ice levels range from clearly defined trim lines to more equivocal weathering limits which may reflect other zones of process transition, such as postglacial differential weathering or englacial boundaries between wet-based eroding ice and noneroding frozen-bed ice"	Cockburn and Summerfield (2004)
	glacial trimline	Undefined. Can be used to refer to an erosional feature that is presumed to approximate the palaeo ice margin (Kelly *et al.* 2004 p.61).	Kelly *et al.* (2004); Sugden *et al.* (2005); Nesje *et al.* (2007); Hormes *et al.* (2008); Oberholzer *et al.* (2008); Van der Beek and Bourbon (2008); Gourronc *et al.* (2014); Larsen *et al.* (2014); Lee *et al.* (2014); Makos and Niychoruk (2011); Makos *et al.* (2013); Zasadni and Kłapyta (2014); Wirsig *et al.* (2016a/b); Sugden *et al.* (2017)
Generic zonal	trimzone/ trimline zone	Terms used interchangeably to refer to the area between the trimline and the modern ice margin.	Thomsen and Winding (1988); Reed (1989); Csatho *et al.* (2005); Csaho *et al.* (2008); Forman *et al.* (2007); Zasadni and Kłapyta (2014); Wirsig *et al.* (2016a);
Ice mass	glacier trimline	Undefined. Presumed to mean a trimline that is associated with a glacier.	Csatho *et al.* (2005); van der Veen and Csatho (2005)
	ice sheet trimline/ ice-sheet trimline	Undefined. Seems to refer to a trimline formed at the margin of a palaeo ice sheet (see Ballantyne *et al.* 1998b, pp.65).	Lawson (1990); Ballantyne (1994b); McCarroll *et al.* (1995); Ballantyne (1997); Ballantyne *et al.* (1997); Ballantyne (1998); Ballantyne *et al.* (1998a/b); Lamb and Ballantyne (1998)
	ice-cap trimlines	Undefined. Likely to be very similar to 'ice sheet trimlines' but relating strictly to palaeo ice caps.	Wolken *et al.* (2005)

Age	palaeo-trimline	Undefined. Presumably refers to trimlines associated with Quaternary ice masses despite the fact that all trimlines are palaeo in that they are not active features.	Hubbard *et al.* (2009)
Study area significance	regional trimline	Undefined. Used by Nesje *et al.* (2007, pp.234) to describe the average trimline altitude across their study area.	Nesje *et al.* (2007)
Ice marginal interpretation	ice-marginal trimline	Undefined but used to distinguish the feature in question from englacial/ subglacial thermal boundaries (Nesje *et al.* 2007, pp.228).	Nesje *et al.* (2007)
	periglacial trimline	Defined as marking "the maximum level to which glacier ice has eroded or 'trimmed' a pre-existing zone of frost-weathered rock or debris on mountain slopes" (Ballantyne and Harris 1994, p.182. Re-stated by Ballantyne *et al.* (1997, pp.227; 2011, pp.3834)) and Ballantyne (2010, pp.524)). See list of identifying features in Benn and Evans (2010, pp.620)	Reed (1989); Ballantyne (1990); Ballantyne (1994a); Ballantyne and Harris (1994); Bennett (1994); McCarroll *et al.* (1995); Dahl, S.-O. *et al.* (1996a/b); Ballantyne (1997); Ballantyne *et al.* (1997); Ballantyne (1998); Ballantyne *et al.* (1998b); Lamb and Ballantyne (1998); Stone *et al.* (1998); Ballantyne (1999a/b); McCarroll and Ballantyne (2000); Ballantyne and Hallam (2001); Hughes (2002); Walden and Ballantyne (2002); Rae *et al.* (2004); Evans *et al.* (2005); Sugden *et al.* (2005); Ballantyne *et al.* (2006); Ballantyne *et al.* (2006); Stone and Ballantyne (2006); Ballantyne (2007); Ballantyne *et al.* (2007); Nesje *et al.* (2007); Ballantyne *et al.* (2009); Ballantyne (2010); Benn and Evans (2010, pp.619-620); Ballantyne *et al.* (2011); Fabel *et al.* (2012); Bickerdike *et al.* (2016); Evans (2016); McCarroll (2016); Wirsig *et al.* (2016b)

Ice marginal interpretation	glacier limit/ glacial limit/ limit of glaciation	Undefined. Presumed to refer to the location of the palaeo ice margin as recorded by a trimline.	Sissons (1974); Grant (1977); Traczyk and Migoñ (2003); Reuther *et al.* (2004); Gosse *et al.* (2006); Reuther *et al.* (2007); Benn and Evans (2010, pp.619); Hughes *et al.* (2012)
	ice sheet limit	Undefined. Used to refer to both the lateral and vertical dimensions of the palaeo ice sheet.	Brook *et al.* (1996); Fretwell *et al.* (2008)
	periglacial zone	Undefined. Used to refer to areas with evidence of periglacial weathering.	Ballantyne (1998)
Subglacial or thermal interpretation	englacial trimline	Defined as "marking the approximate upper boundary of warm-based ice" (Ballantyne 2010, pp.525).	Ballantyne (2010)
	subglacial zone	Undefined but used to describe areas with subglacial landforms. Often used alongside 'nonglacial zone', which describes the area with weathering or periglacial landforms.	Hattestrand and Stroeven (2002)
	thermal trimline	Defined as representing a "thermal boundary between cold-based and wet-based ice below an ice sheet, rather than a former ice surface" (Benn and Evans 2010, pp.620).	Benn and Evans (2010, pp.620); Zasadni and Kłapyta (2014)

Type of trimline expression	vegetation trimline	Defined as "light-toned, barely vegetated terrains displaying abrupt outer margins extend back to modern glaciers and ice caps" by Wolken *et al.* (2005, pp.343).	Knight *et al.* (1987); Wolken *et al.* (2005); Harrison *et al.* (2007); Benn and Evans (2010, pp.619); Kelley *et al.* (2012)
	forest trimline	Early equivalent to 'vegetation trimline'. Defined by Lawrence (1950a, pp.243) “the line representing the maximum position attained by the ice front, where the forest was sheared off by the ice”	Lawrence (1950a); Lawrence (1950b); Mathews (1951); Nicols and Miller (1951)
	lichen trimline	Undefined, likely to be similar to 'vegetation trimline' but expressed solely through a contrast in lichen cover.	Mahaney (1987); Mahaney (1991)
	vegetation-free zone/ lichen-free zone	Undefined. Used by Wolken *et al.* (2005) to describe the areas within their vegetation trimlines.	Wolken *et al.* (2005)

Type of trimline expression	weathering trimline/ limit/ boundary/ contrast	Defined by Boulton and Hagdorn (2006, pp.3361) as being "where glacially eroded surfaces at lower elevations gave way to weathered rock surfaces and ‘‘frost debris’’ at higher elevations" and by Ballantyne and Harris (1994, pp.182) as "the boundaries between [weathering] zones". Used interchangeably with 'periglacial trimline' by Ballantyne *et al.* (1997; 2009).	Ballantyne *et al.* (1987); Nesje *et al.* (1987); Ballantyne (1990); Nesje and Dahl, S.-O. (1990); Ballantyne (1994a); McCarroll *et al.* (1995); Brook *et al.* (1996); Ballantyne *et al.* (1997); Ballantyne *et al.* (1998b); Lamb and Ballantyne (1998); Stone *et al.* (1998); Walden and Ballantyne (2002); Cockburn and Summerfield (2004); Marquette *et al.* (2004); Rae *et al.* (2004); Evans *et al.* (2005); Ballantyne *et al.* (2006); Boulton and Hagdorn (2006); Fjellanger *et al.* (2006); Ballantyne *et al.* (2009)
	weathering zone/ frost-weathered zone/ zone of frost-weathering / weathered zone	Defined by Ballantyne (1994a, pp.182): "A related concept is that of weathering zones: as successive trimlines delimit altitudinal zones that have been exposed to weathering processes for different lengths of time, then the degree of rock weathering and soil development should be more advanced in the zone above any trimline than in the zone below." Also, by Clark, P.U. *et al.* (2003, pp.617) as "units of the land surface that are identified by distinct weathering features".	Løken (1962) [in French]; Boyer and Pheasant (1974); Ives (1975); Ives (1976); Ives *et al.* (1976); Grant (1977); Ives (1978); Dyke (1979); Reed (1989); Nesje and Dahl, S.-O. (1990); Ballantyne (1994a); Kleman (1994); MacCarroll *et al.* (1995); Ballantyne (1997); Ballantyne *et al.* (1997); Ballantyne (1998); Ballantyne *et al.* (1998a/b); Briner *et al.* (2003); Clark, P.U. *et al.* (2003); Rae *et al.* (2004); Sugden *et al.* (2005); Fjellanger *et al.* (2006); Gosse *et al.* (2006); Goodfellow (2007); Goehring *et al.* (2008)

Type of trimline expression	weathering surface	Undefined. Meaning appears to be similar to 'weathering zone'.	Kverndal and Sollid (1993)
	blockfield boundary/ block-field boundary	The margin of a periglacial blockfied. Defined by Goehring *et al.* (2008, pp.333): "represents an englacial thermal boundary between frozen bed nonerosive ice above and a wet-bed region below that was progressively more erosive with increasing ice thickness."	Dahl, R. (1966b); Brook *et al.* (1996); Goehring *et al.* (2008)
	erosional trimline/ limit/ boundary	Undefined but generally used interchangeable with 'periglacial trimline' or 'trimline'.	Nesje and Dahl, S.-O. (1990); Orombelli *et al.* (1990); Ballantyne (1998); Ballantyne *et al.* (1998a/b); Kaplan *et al.* (2001); Walden and Ballantyne (2002); Ballantyne (2007); Oberholzer *et al.* (2008); Möller *et al.* (2010); Sugden *et al.* (2017)
	erosional zone/ zone of glacial erosion/ scoured zone/ limit of effective glacial erosion	Undefined. Used to refer to areas with clear evidence of flowing warm-based ice.	Ballantyne (1997); Ballantyne *et al.* (1998a/b); Hattestrand and Stroeven (2002); Linge *et al.* (2006); Goodfellow (2007); Nesje *et al.* (2007); Fu *et al.* (2013)

Type of trimline expression	ice-scoured trimline	Undefined. Presumably similar to an erosional trimline.	Harrison *et al.* (2007)
	trimline moraine	Pictorially defined as a terminal or lateral-frontal moraine system that outlines the former ice margin position (Benn and Evans 2010, pp.513)	O'Cofaigh *et al.* (2003); Benn and Evans (2010, pp.513)
	boulder limit/ limit of glacial erratics	Undefined. Used to describe the upper bound of glacial erratic distributions. Suggested to indicate a thermal or ice flow boundary	Mackintosh *et al.* (2007)

3.2.3 Quaternary and historic trimlines

For the purpose of this literature review, trimlines will be referred to as either Quaternary or historic. 'Quaternary' trimlines are associated with the glaciations of the Quaternary geological period prior to the Little Ice Age, i.e. these are trimlines associated with glacial events for which we have no written historical record. Conversely, 'historic' trimlines were formed by more recent glaciations, particularly glacial retreat from the Little Ice Age readvance and in response to the on-going modern climate change.

This distinction between Quaternary and historic trimlines is made because of significant differences in the methods used to research trimlines of different ages. Additionally, there are differences in the expression of historic and Quaternary trimlines as well as differences in the applications of historic trimline research compared to Quaternary.

3.3 History of trimline research

Prior to the 1950s, trimline features were being utilised in palaeoglacial reconstructions without any specific term applied to describe them. J. Geikie (1873; 1878) appears to have originated the use of trimline features for palaeoglacial reconstructions in his work on Harris and South Uist in Scotland. Geikie described clear contrasts between glacial erosion in lowland areas compared with summit-top frost weathering and used the altitude of these contrasts to determine the ice thickness of the regional glaciation. However he did not refer to these contrasts by any specific term, indicating that the term 'trimline' was not in use until after this date. A typical example of Geikie's description of the weathering contrasts, in this case on the mountain Hecla on the island of South Uist, makes it clear that these features would now be termed 'trimlines'.

"Nothing can be more distinct than the line of demarcation between its sharp, jagged, peaked summit and its rounded, softly outlined shoulders, with their *moutonnée* surface."

(J. Geikie 1878, pp.851)

The first clear usage of the term 'trimline' appears in North American studies of vegetation trimlines in the early 1950s (Section 3.2.1; Lawrence 1950a/b; Mathews 1951; Heusser *et al.* 1954). These studies used dendrochronology to date changes in vegetation cover and reconstruct former ice limits, a process that was originally developed to identify palaeo nunataks (Ives 1974). Interest in palaeo nunataks was initially linked to the identification of

biological refugia in an attempt to explain how species were able to rapidly re-colonise after Quaternary glaciations (Ives 1974). The development of radiocarbon dating challenged the thinking that a glacial event would leave a *tabula rasa* because post-glacial specimens of plants and animals were found to be older than could be possible if they had migrated into the glaciated area from outside the former ice limits (Ives 1974). Therefore a new theory arose in the 1940s-1950s, which suggested that plants and animals must have survived glacial periods on exposed ground within the ice limits, i.e. on nunataks, in order to have re-colonised the glaciated areas so rapidly after deglaciation (Ives 1974). This idea of species surviving on isolated ice-free nunataks is called the 'glacial refugia' hypothesis (Ives 1974).

In order to test this theory, it was necessary to find evidence of nunataks associated with Quaternary glaciations. Consideration of the biogeography of previously glaciated areas in Canada led researchers to notice abrupt changes in vegetation cover and to link these to former ice margin positions (Ives 1974; e.g. Figure 3.1). Attempts to date palaeo ice margins and link them to specific glacial events led to the dendrochronology studies of the early 1950s (Lawrence 1950a/b; Mathews 1951; Heusser *et al.* 1954).

In Britain and Scandinavia, trimline research took a slightly different path, focused more on identifying weathering contrasts and the limits of glacial erosion (Figure 3.3; McCarroll *et al.* 1995; Kleman and Stroeven 1997; Ballantyne *et al.* 1997; Ballantyne *et al.* 1998b; Lamb and Ballantyne 1998; Stone *et al.* 1998; Hättestrand and Stroeven 2002; Stroeven *et al.* 2002; Rae *et al.* 2004; Evans *et al.* 2005; Nesje *et al.* 2007; Goehring *et al.* 2008; Ballantyne *et al.* 2009). There was a lack of clear vegetation trimlines in these areas, so the identification of palaeo nunataks used the distribution of streamlined glacial landforms compared to evidence of periglacial weathering, particularly tors (e.g. Linton 1949; Linton 1950; Dahl, E. 1955; Linton 1955). The identification of thick periglacial deposits on mountain summits, particularly in Scotland (Ballantyne 1998), was also suggested to be diagnostic of palaeo nunataks. This led to the emergence of the term 'periglacial trimline' in British trimlines research and the use of these features to reconstruct palaeo ice thickness, after Geikie's early example (Figure 3.3; Ballantyne and Harris 1994).

In Scandinavia, trimline interpretation was influenced by Sugden's work on identifying landscapes of differing glacial erosion and linking these to palaeo thermal regime (summarised in Sugden and John 1976). Researchers applied these ideas in Scandinavia (e.g. Kaitanen, 1969; Kleman and Borgström 1990; Kleman and Stroeven 1997) to identify areas of glacial erosion, indicating warm-based ice, and places where pre-glacial landscapes were

preserved under cold-based ice. Kleman has been a significant contributor to the development of these ideas through his work in northwest Sweden (Kleman and Borgström 1990; Kleman 1992; Kleman and Stroeven 1997). In particular, Kleman has contributed conceptual papers on the preservation of pre-glacial landforms beneath overriding ice cover (Kleman 1994) and on the distribution of regions of cold- and warm-based ice within ice sheets (Kleman and Glasser 2007). With his colleague Borgström, Kleman developed the glacial inversion method, a framework which underpins the reconstruction of ice masses in areas of complex palimpsest geomorphology (Kleman and Borgström 1996; Kleman *et al.* 1997). Recognition of trimlines within the geomorphology of Scandinavia and new understandings of the role of thermal regime in producing these palimpsest landscapes led to the suggestion that trimlines are not always ice marginal landforms but can indicate a boundary between areas of warm- and cold-based ice beneath a former ice sheet.

This Scandinavian research ignited a debate regarding the thickness of the British-Irish Ice Sheet (BIIS) and the origin of 'periglacial trimlines' (Ballantyne 2010). These features had been interpreted as ice marginal by assessing the relative degree of periglacial weathering above and below the trimlines (detail of the methods used in Section 3.4). However, the conclusions of Scandinavian research suggested that a thermal origin may be possible for BIIS trimlines. Alongside the development of cosmogenic nuclide dating, this re-opened debate into the formation of BIIS trimlines and has led to the identification of both thermal and ice marginal trimlines in the British Isles (see fuller discussion in Section 3.6).

3.3.1 Focus of trimline research

Thus far trimline research has focused predominantly on vegetation trimlines and on contrasts in glacial erosion compared to periglacial weathering. This narrow focus does not include the full range of possible modes of trimline expression. However other less 'traditional' types of glacial trimline have been used to produce 3D ice surface reconstructions and ice thickness estimates. In particular there has also been extensive work on characterising lateral moraines (e.g. Lukas *et al.* 2012), which have not generally come under the 'trimline' umbrella but that can be used in similar ways and are often found alongside trimlines (e.g. Ives 1976; Clark, P.U. *et al.* 2003; Glasser *et al.* 2005; 2008; Hormes *et al.* 2008).

Quaternary trimline research has been primarily focused on the BIIS (e.g. Ballantyne *et al.* 1997; Ballantyne *et al.* 1998a; Rae *et al.* 2004; Ballantyne *et al.* 2009; Ballantyne 2010; Ballantyne *et al.* 2011; Fabel *et al.* 2012; Ballantyne and Stone 2015), in Scandinavia (e.g.

Hättestrand and Stroeven 2002; Stroeven *et al.* 2002) and in North America (e.g. Ives 1976; Ives 1977; Ives 1978; Kaplan *et al.* 2001; Clark, P.U. *et al.* 2003). However, Quaternary trimlines have also been identified and studied in other locations (Figure 3.4a; Table 3.2). The temporal focus of Quaternary trimline research has been on the deglaciation from the Last Glacial Maximum (LGM c. 21 ka BP) (e.g. Ives 1976; Ballantyne 1997; Florineth and Schluchter 1998; Kaplan *et al.* 2001; Kelly *et al.* 2004; Sugden *et al.* 2005; Ballantyne *et al.* 2006; Hubbard *et al.* 2006; Stone and Ballantyne 2006; Nesje *et al.* 2007; Glasser *et al.* 2008). In North America (Figure 3.4c) and in Europe (Figure 3.4d) there has also been significant interest in reconstructing Younger Dryas (c. 13 ka - 11 ka BP) ice limits from trimlines (e.g. Thorp 1981; Thorp 1986; Bennet 1994; Ballantyne 2007). This focus on the LGM and the Younger Dryas is common to all empirical Quaternary reconstructions – the landform record is simply better preserved for these more recent glacial events compared to more ancient Quaternary glaciations. However, in some locations older trimlines are preserved and have been used to reconstruct glacial fluctuations over much longer time periods. Examples of older trimlines have primarily been found in areas of rugged terrain in West Antarctica, such as the Ohio Range, where the glaciations of the last 200 ka have been dated from trimlines and erratics (Ackert *et al.* 2011), and in the Ellsworth Mountains, where a glacial trimline has been dated to at least 2 million years ago and could be as old as c. 14 million years (Sugden *et al.* 2017).

Research into historic trimlines has been spatially focused in the Americas and in Greenland (Figure 3.4b; Table 3.2). Temporally, the focus of historical research has been on reconstructing the extent of the Little Ice Age readvance (LIA 1700-1930 AD) (e.g. McKinzey *et al.* 2004; Glasser *et al.* 2005; Wolken *et al.* 2005; Forman *et al.* 2007; Csatho *et al.* 2008; Glasser *et al.* 2011). No papers have specifically considered the very recent trimlines exposed by the rapid glacial retreat recorded in some areas over the past 50-100 years, although it is possible to observe these features through observation of recent and historic photographs of glaciers (e.g. Figure 3.9).

Overall, the majority of trimline research has been located in North America, Scandinavia and Britain/ Ireland. However, it is clear from Figure 3.4 that trimlines are extremely widespread and appear to be common features in most glacierised (Figure 3.4b) and glaciated landscapes (Figure 3.4a). There is a tight temporal focus of trimlines research on the Late Quaternary and there has been relatively limited consideration of historic trimlines, excepting the LIA in North America and Greenland (Table 3.2).

Given the focus on a narrow range of places, types of trimline expression and time periods, both Quaternary and historic trimlines are probably being under-utilised at present. An expansion in the spatial and temporal focus of trimlines research could enable these features to make more significant contributions to reconstructions of palaeo ice fluctuations globally. Additionally, recent discovery of possible glacial trimlines on Mars (Gourronc *et al.* 2014) raises the possibility of expanding the use of these landforms into extra-terrestrial settings.

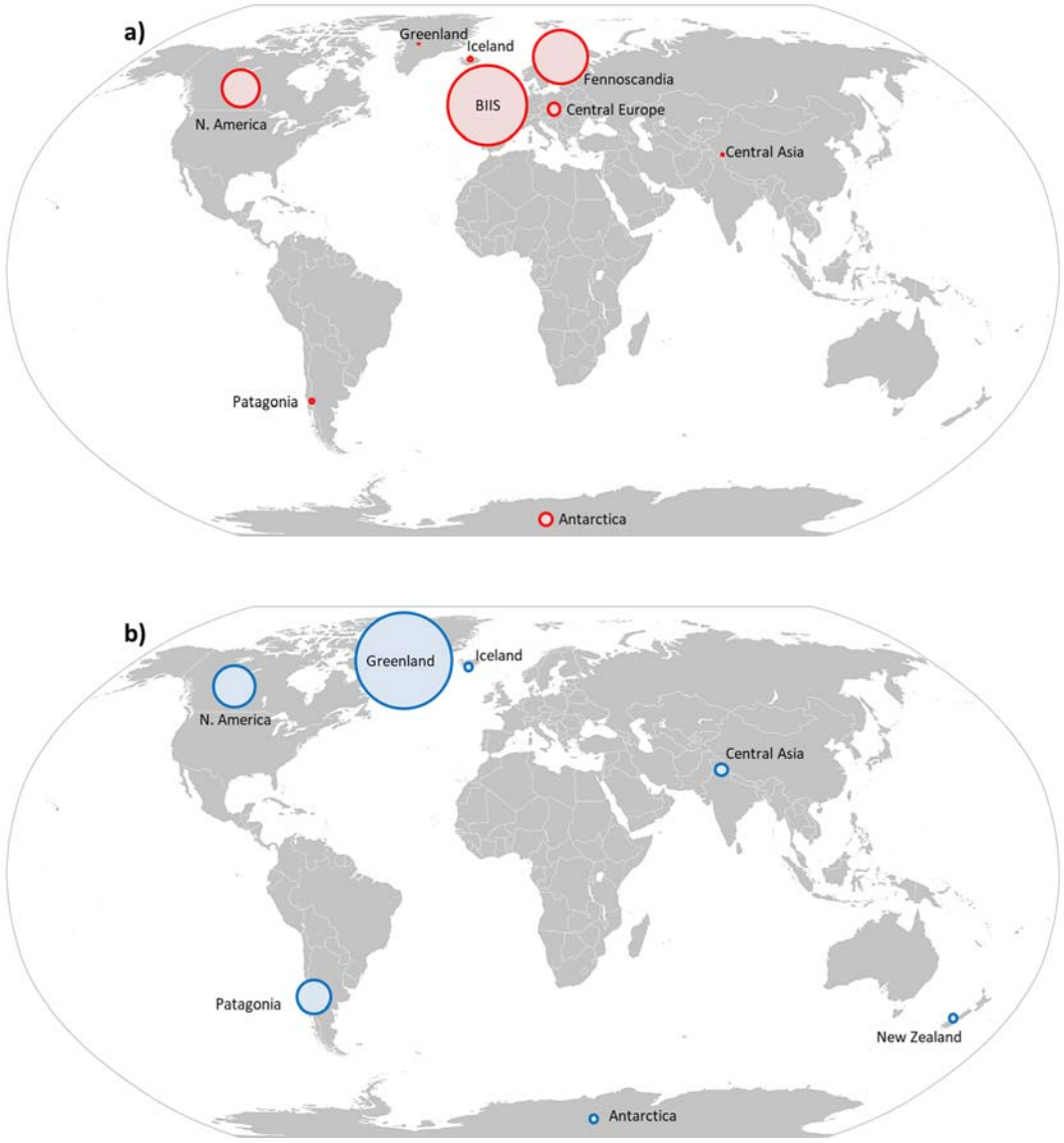

Figure 3.4 (next page for 3.4c and 3.4d) – Maps of the distribution of trimline research, with Quaternary studies in red and historic in blue. The size of the circles relates to the percentage of published studies located in each area. The global distribution of Quaternary (a) and historic (b) studies show that trimlines can be found in a wide range of glacial environments and are not limited to specific glaciological, climatic or geological conditions. From the global maps it is also clear that trimline research has been highly clustered, with higher paper densities in North America (c) and Europe (d) than other locations. Due to the global distribution of trimlines, this clustering suggests a bias towards locations that are easily accessible and generally well-researched. The regional distribution of trimline research in North America (c) shows a clustering around mountainous areas of on-going glaciation or at

the fringes of the former Laurentide and Cordilleran Ice Sheets. In Europe (d) research has similarly been focused in rugged terrain but trimlines have also been found in the central areas of former ice sheets, for example associated with the Fennoscandian Ice Sheet in Northern Sweden and Northern Norway. However there has been no research into Historic trimlines in Europe, despite clearly visible Little Ice Age trimlines associated with many glaciers in Scandinavia and the Alps (e.g. Figure 3.9). A full breakdown of the locations of trimline studies can be found in Table 3.2. Background map from Wikipedia Commons (file name: BlankMap-World6.svg).

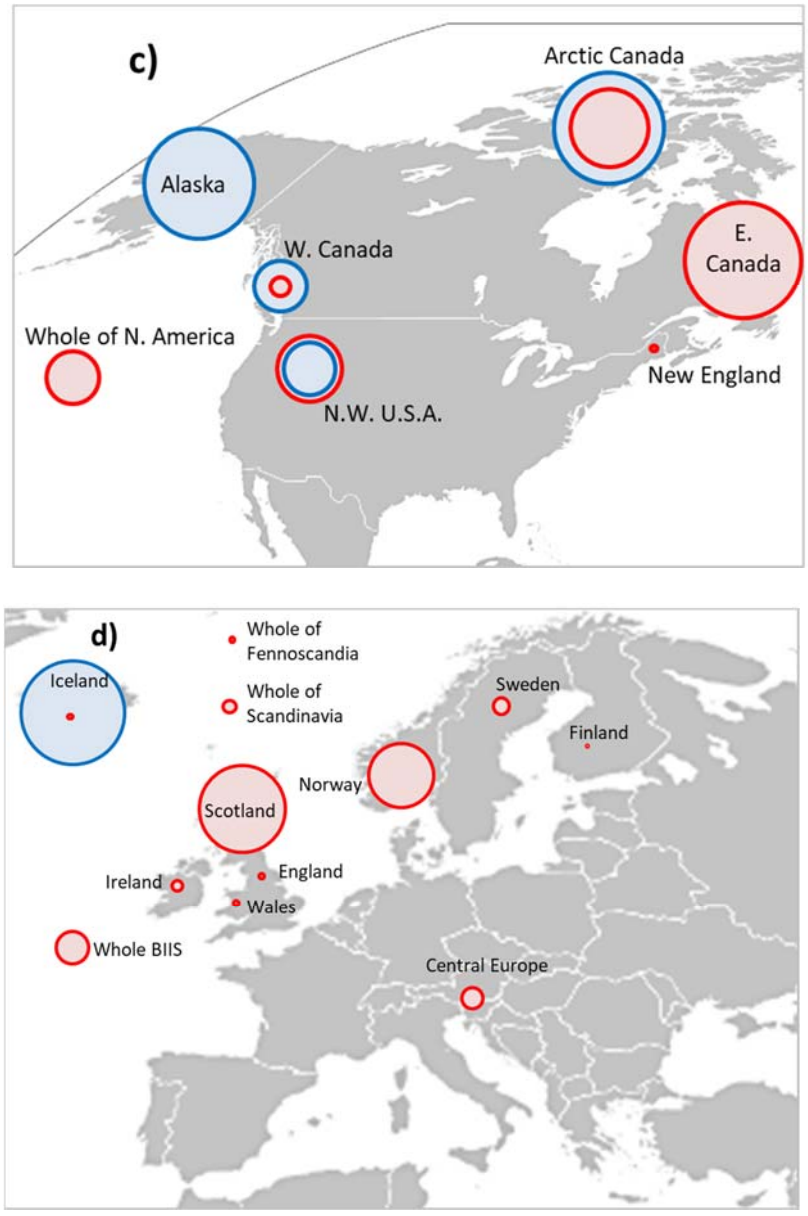

Table 3.2 (next page) – Full list of the papers used to produce this literature review, grouped by study location. Both Quaternary or older (black) and historic (red) papers are listed. From this table, and the maps in Figure 3.4, it is clear that there has been significant clustering of trimlines studies in certain locations. It is also obvious from this table that the majority of trimlines papers are solely Quaternary studies. This is particularly true because many of the highlighted historic papers also include some study of Quaternary glaciations, which is rarely true in reverse.

Region	Location	Sub-location	Paper count	References
Britain and Ireland	British Isles		21	Geikie (1874); Linton (1949); Boulton *et al.* (1977); Bowen *et al.* (1986); Nesje and Sjerup (1988); Lambeck (1993); Ballantyne (1994b); Lambeck (1995); Migoñ and Goudie (2001); Bowen *et al.* (2002); Clark, C.D. *et al.* (2004); Evans *et al.* (2005); Boulton & Hagdorn (2006); Fretwell *et al.* (2008); Hubbard *et al.* (2009); Ballantyne (2010); Chiverrell & Thomas (2010); Clark, C.D. *et al.* (2012); Kuchar *et al.* (2012); Bickerdike *et al.* (2016); Clark, C.D. *et al.* (2018)
	Ireland	All	1	Ballantyne & Stone (2015)
		North-West	1	Ballantyne *et al.* (2007)
		West	2	Ballantyne *et al.* (2008); Edwards *et al.* (2017)
		South-West	2	Ballantyne *et al.* (2011); Barth *et al.* (2016)
		East; including the Wicklow Mountains	1	Ballantyne *et al.* (2006)
	Scotland	All	6	Sissons (1967); Ballantyne (1984); Boulton *et al.* (1991); Bennett (1994); Ballantyne (1997); Ballantyne (1998)
		Grampians	5	Stevens and Wilson (1970); Sissons (1974); Thorp (1981); Thorp (1986); Thorp (1987)
		Cairngorms	4	Sugden (1968); Sugden (1970); Ballantyne (1994b); Phillips *et al.* (2006)
		North-West; including Wester Ross	16	Gordon (1979); Ballantyne (1987); Reed (1989); Lawson (1990); McCarroll *et al.* (1995); Ballantyne *et al.* (1997); Ballantyne *et al.* (1998a/b); Stone *et al.* (1998); Ballantyne (1999a/b); Walden and Ballantyne (2002); Ballantyne & Hall (2008); Phillips *et al.* (2008); McCormack *et al.* (2011); Fabel *et al.* (2012)
		North-East	5	Godard (1965); Romans *et al.* (1966); Hall (1985); Hall and Sugden (1987); Glasser (1995)
		Southern	1	Ragg and Bibby (1966)
		Outer Hebrides	6	Geikie (1873); Geikie (1878); Ballantyne and Hallam (2001); Ballantyne *et al.* (2006); Stone and Ballantyne (2006); Ballantyne (2007)
		Inner Hebrides	7	Anderson and Dunham (1966); Ballantyne (1989); Ballantyne (1990); Ballantyne (1994); Dahl, S.-O. *et al.* (1996); Ballantyne *et al.* (1997); Stone *et al.* (1998)

Britain and Ireland	Wales	All	2	Jansson and Glasser (2005); Glasser *et al.* (2012)
		Snowdonia	2	McCarroll and Ballantyne (2000); Hughes (2002)
	England	Dartmoor	1	Linton (1955)
		Lake District	3	Lamb and Ballantyne (1998); Ballantyne *et al.* (2009); Hughes *et al.* (2012)
Central Europe	The Alps	All	1	Wirsig *et al.* (2016b)
		Swiss	5	Florineth (1998); Florineth & Schluchter (1998); Kelly *et al.* (2002); Kelly *et al.* (2004); Wirsig *et al.* (2016a)
		French	3	Mahaney (1987); Mahaney (1991); van der Beek & Bourbon (2008)
		Italian	1	Hormes *et al.* (2008)
		Eastern	1	Fiebig *et al.* (2005)
	The Carpathians		5	Reuther *et al.* (2004); Reuther *et al.* (2007); Makos and Nitychoruk (2011); Makos *et al.* (2013); Zasadni & Kłapyta (2014)
	The Sudetes		1	Traczyk and Migoñ (2003)
Fennoscandia	All		2	Kleman *et al.* (1999); Fabel *et al.* (2002)
	Scandinavia		7	Wråk (1905); Linton (1949); Dahl, E. (1955); Dahl, E. (1961); Kleman (1994); Stroeven and Kleman (1999); Linge *et al.* (2006)
	Norway	All	9	Blytt (1876); Reusch (190); Ahlmann (1919); Nordhagen (1936); Gjærevoll (1963); Nordhagen (1963); Gjessing (1967); Mangerud (1973)
		North	10	Sørensen (1949); Grønlie (1953); Dahl, R. (1966a/b); Kverndal and Sollid (1993); Rea *et al.* (1996b); Whalley *et al.* (1997); Whalley *et al.* (2004); Fjellanger *et al.* (2006); Nesje *et al.* (2007)
		South	6	Nesje *et al.* (1988); Nesje (1989); Nesje and Dahl, S.-O. (1990); Nesje *et al.* (1994); Lidmar-Bergström *et al.* (2000); Goehring *et al.* (2008)
		Central	2	Sollid and Sørbel (1979); Sollid and Reite (1983)
		Western	8	Dahl, E. (1948); Mangerud *et al.* (1979); Sollid and Sørbel (1979); Roaldset (1982); Nesje *et al.* (1987); Rye *et al.* (1987); McCarroll and Nesje (1993); Brook *et al.* (1996)
		Svalbard	1	Henriksen *et al.* (2014)

Fennoscandia	Sweden	North-West	6	Sernander (1896); Lagerbäck (1988a/b); Kleman (1992); Kleman and Stroeven (1997); Clarhäll and Kleman (1999)
		North-East	2	Hättestrand and Stroeven (2002); Stroeven *et al.* (2002)
		Southern	1	Kleman and Borgström (1990)
	Finland	Lapland	1	Kaitanen (1969)
	NW Russia	Around the White Sea	1	Larsen *et al.* (2014)
North Atlantic	Faroe Islands		1	Walden and Ballantyne (2002)
	Iceland	All	2	Norddahl (1991); Hubbard *et al.* (2006)
		North	2	Norddahl (1983); Brynjólfsson *et al.* (2014)
		Vatnajökull	1	Hannesdóttir *et al.* (2015)
	Greenland	All	5	Gjærevoll and Ryvarden (1978); Weidick (1955); Sugden (1974); Ó Cofaigh *et al.* (2003); Kjeldsen *et al.* (2015)
		West or South-West	5	Weidick (1968); Weidick (1969); Weidick (1992); Kelley *et al.* (2012); Pearce *et al.* (2018)
		Jakobshavn	5	Knight *et al.* (1987); Thomsen and Winding (1988); Csatho *et al.* (2005); van der Veen and Csatho (2005); Csatho *et al.* (2008)
		Kangerlussuaq	1	Forman *et al.* (2007)
Asia	Tibet		2	Fu *et al.* (2013); Loibl *et al.* (2014)
	Tian Shan		1	Li and Li (2014)
	Altai-Sayan		1	Blomdin *et al.* (2016)
	NW India		2	Lee *et al.* (2014); Deswal *et al.* (2017)
New Zealand	South Island	Frans Josef Glacier	1	McKinzey *et al.* (2004)
South America	Patagonia	All	2	Glasser *et al.* (2008); Glasser *et al.* (2011)
		North	2	Glasser *et al.* (2005); Harrison *et al.* (2007)
		South	1	Nicols and Miller (1951)
	Tierra del Fuego		1	Möller *et al.* (2010)

North America	All		6	Ives (1978); Sugden (1977); Sugden (1978); Dyke and Prest (1987); Kleman (1994); Briner *et al.* (2006b)
	Arctic Canada	All	1	Ó Cofaigh *et al.* (2003)
		Baffin Island	9	Boyer and Pheasant (1974); Ives (1975); Ives (1977); Sugden and Watts (1977); Dyke (1979); Bierman *et al.* (1999); Kaplan *et al.* (2001); Briner *et al.* (2005); Briner *et al.* (2006a)
		Queen Elizabeth Islands	2	Wolken *et al.* (2005); Nixon and England (2014)
	Eastern Canada	Torngat/ Ungava	8	Ives (1957); Ives (1958a); Ives (1976); Ives *et al.* (1976); Clark, P.U (1988); Clark, P.U (1991); Clark, P.U *et al.* (2003); Marquette et al (2004)
		Newfoundland	2	Grant (1977); Gosse *et al.* (2006)
		Labrador/ Québec	4	Leiber (1861); Ives (1958b); Løken (1962); Jansson (2005)
	Western Canada	Keewatin & NW Territories	2	Aylesworth and Shilts (1989a); Aylesworth and Shilts (1989b)
		British Columbia	1	Mathews (1951)
	Northern USA	Pacific North-West	1	Lawrence (1950a)
		New England	1	Bierman *et al.* (2015)
		Alaska	2	Heusser *et al.* (1954); Lawrence (1950b)
		Minnesota	1	Bierman *et al.* (1999)
		Washington	1	Briner and Swanson (1998)
		Wyoming	1	Anderson (2002)
		Montana	1	Locke (1995)
		Utah	1	Munroe (2006)
		Yellowstone	1	Pierce (1979)
		Yosemite	1	Huber (1989)

Antarctica	West	All	1	Pollard and DeConto (2009)
		Peninsula	2	Bentley *et al.* (2006); Carrivick *et al.* (2012)
		Marie Byrd Land; including the Ohio Range	3	Sugden *et al.* (2005); Ackert *et al.* (2007); Ackert *et al.* (2011)
		Ellsworth Mountains	1	Sugden *et al.* (2017)
	East	Enderby Land	1	White and Fink (2014)
		Victoria Land	4	Orombelli *et al.* (1990); Armienti and Baroni (1999); French and Guglielmin (2002); Baroni *et al.* (2008);
		Mac. Robertson Land	1	Mackintosh *et al.* (2007)
		McMurdo Dry Valleys	3	Bruno *et al.* (1997); Stroeven and Kleman (1999); Oberholzer *et al.* (2008)
Conceptual/ Review/ Methods	[i.e. papers with no specific location]		14	Linton (1950); Ives (1974); Boulton (1979); Dahl, E. (1987); Sugden (1989); Dahl, E. (1992); Brunsden (1993); Kleman (1994); Cockburn & Summerfield (2004); Goodfellow (2007); Kleman & Glasser (2007); Benn and Hulton (2010); Evans (2016); McCarroll (2016)
Extra-terrestrial	Mars	Valles Marineris	1	Gourronc *et al.* (2014)

3.4 Methods of trimline research

Early research mapped and identified trimline features via extensive fieldwork (e.g. Geikie 1873; 1878). However, it was immediately clear that trimlines are often more visible from a distance, a fact that Geikie (1878) noted in his description of Hebridean trimlines. Despite these observations, it was not until the 1980s that trimlines were mapped from secondary data. The key paper that defined a method for identifying and mapping trimlines from aerial imagery was Thorp (1981), who used glacial trimlines in his reconstruction of an ice cap on Rannoch Moor in Scotland. Thorp's method describes best practice for using a combination of aerial photographs and field mapping to identify trimlines separating areas of glacial erosion in the valleys from areas of periglacial weathering on mountain summits and high moors (Figure 3.5). The greater visibility of many trimlines in remotely sensed images compared to the field makes Thorp's usage of aerial imagery a significant breakthrough. The 1981 paper set the precedent for mapping trimlines using a combination of aerial imagery and fieldwork observations and also established a method for linking trimlines across different mountains (Figure 3.5b). Further papers by Thorp (1986, 1987) developed this method and expanded on his original study area.

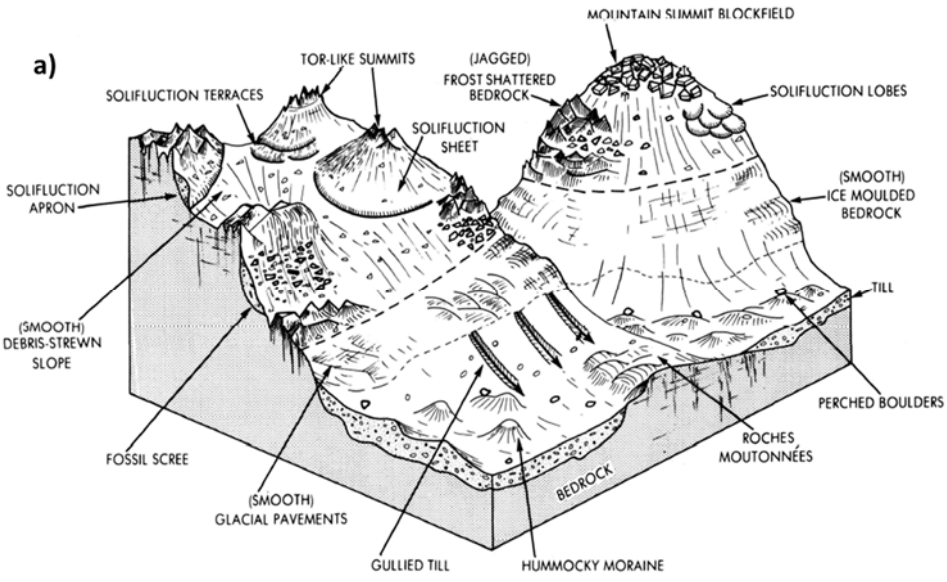

Figure 3.5 (3.5b on next page) – Thorp's method for identifying trimlines relies on mapping zones of glacial erosion and contrasting zones of frost weathering and periglacial slope processes. He found that clear trimline features were visible on spurs in his study area but that the boundary between the two landsurface zones was more diffuse on the majority of valley slopes. Therefore, he used aerial imagery and fieldwork to map the lower limit of frost weathering and the upper limit of glacial erosion, giving an upper and lower bound for the trimline location. a) This schematic diagram illustrates the key features that Thorp used to identify the two landsurface zones and the dotted lines represent the upper and lower bounds of trimline elevation (Thorp 1981, pp.57). b) Once the upper and lower bounds had

been identified, Thorp was able to calculate the mean elevation of the trimline on each mountain or spur. By comparing mean trimline elevations between mountains, he was able to draw in the mean trimline and determine the morphology of the former ice surface as well as the ice thickness (Thorp 1986, pp.94).

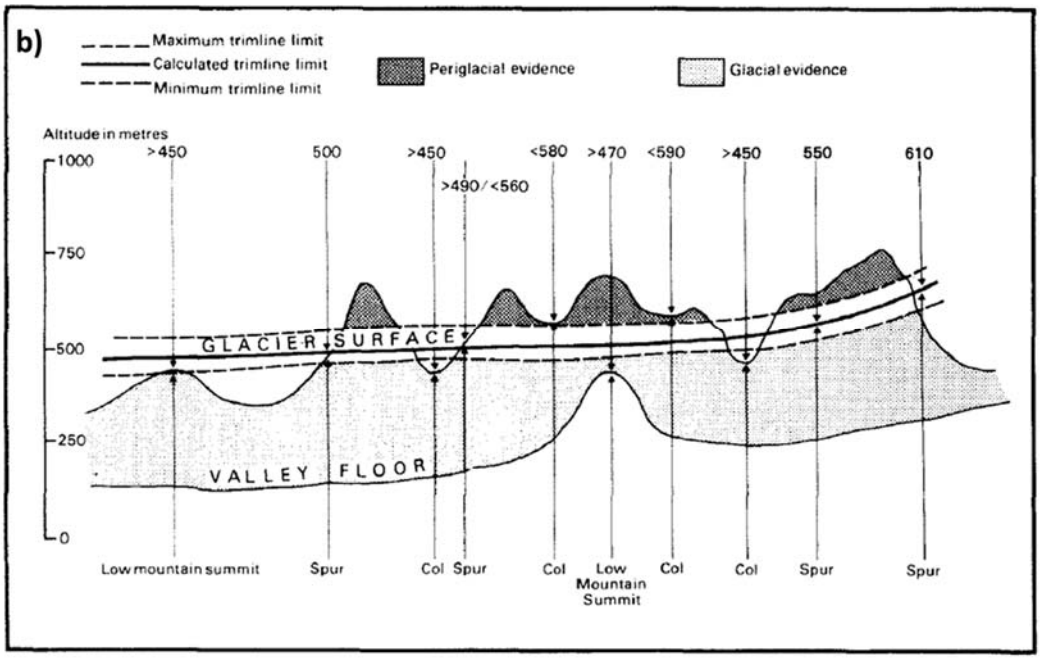

Subsequently, several authors have applied Thorp's methods to other areas in Britain and Ireland (Table 3.2). In particular Ballantyne has produced a series of papers utilising trimlines in reconstructions of ice surface morphologies in Scotland (McCarroll *et al.* 1995; Dahl, S.-O. *et al.* 1996; Ballantyne 1997; Ballantyne *et al.* 1997; Ballantyne 1998; Ballantyne *et al.* 1998a/b; Stone *et al.* 1998; Stone and Ballantyne 2006; Ballantyne 2007; Ballantyne and Hallam 2001; Ballantyne and Hall 2008; Fabel *et al.* 2012), Ireland (Ballantyne *et al.* 2006; Ballantyne *et al.* 2007; Ballantyne *et al.* 2011; Ballantyne and Stone 2015), Wales (McCarroll and Ballantyne 2000) and the English Lake District (Lamb and Ballantyne 1998; Ballantyne *et al.* 2009).

Ballantyne's work is particularly significant because of both the number of papers utilising trimlines and due to his application of cosmogenic nuclide dating to trimline features (reviewed in Ballantyne 2010). This method dates the age at which a rock surface was exposed to extra-terrestrial radiation, for example by deglaciation, by analysing the isotopic make-up of a surface sample (Cockburn and Summerfield 2004). Brook *et al.* (1996) were the first to use cosmogenic nuclides to date weathering limits, using this information to

reconstruct Younger Dryas ice cover in Norway. The work of Brook *et al.* (1996) motivated Stone *et al.* (1998) to apply the cosmogenic nuclide method to validate trimline interpretations on the Isle of Skye and in the north-western Scottish Highlands. Various isotopes can be used for this kind of analysis but the most common are ^{10}Be (e.g. Figure 3.6; Stone *et al.* 1998; Ballantyne *et al.* 1998b; Stone and Ballantyne 2006; Ballantyne *et al.* 2011; Ballantyne and Stone 2015) and ^{36}Cl (Stone and Ballantyne 2006; Ballantyne *et al.* 2009).

Ballantyne built on Stone *et al.*'s work and used cosmogenic nuclides to study the formation of BIIS trimlines and determine if individual trimlines were formed at the ice margin or at englacial thermal boundaries (summarised in Ballantyne 2010). If BIIS trimlines were ice marginal it ought to be the case that the above trimline exposure age, which would be on a nunatak, should always be significantly older than the below trimline exposure age, which would have been under ice cover. Alternatively, if the trimlines were thermal then there would be no clear jump in exposure age across the trimline altitude (e.g. Figure 3.6). The use of cosmogenic nuclide dating has become pivotal in the interpretation of BIIS trimlines and dating studies by Ballantyne and by other researchers have identified examples of both ice marginal and thermal trimlines (see discussion in Section 3.6; e.g. Ballantyne *et al.* 1998b; Stone and Ballantyne 2006; Ballantyne *et al.* 2009; Ballantyne *et al.* 2011; McCormack *et al.* 2011; Fabel *et al.* 2012; Glasser *et al.* 2012; Ballantyne and Stone 2015).

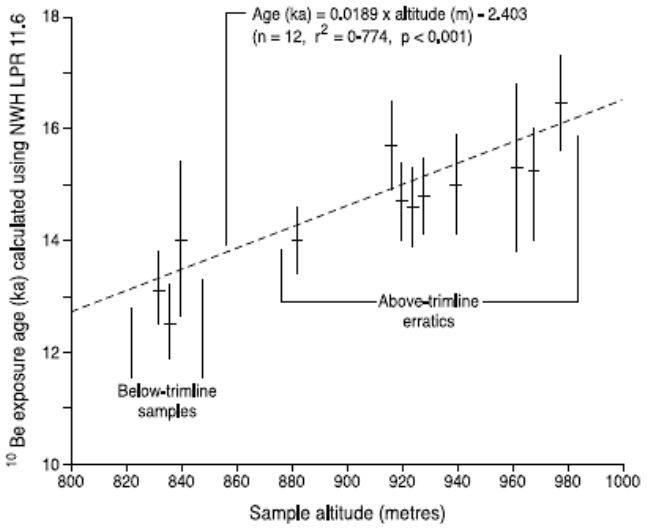

Figure 3.6 – Example of cosmogenic nuclide exposure ages from samples taken above and below a trimline, in this case in Wales, UK. In this study, Glasser *et al.* (2012) used the isotope ^{10}Be to confirm that there was no significant jump in exposure age across the trimline altitude because the linear trend of increasing exposure age with altitude is preserved. This allowed them to interpret the dated trimlines to have been formed at subglacial thermal boundaries and to rule out an ice marginal origin for these features. (Glasser *et al.* 2012, pp.97)

Absolute dating of trimlines via the cosmogenic nuclide method also allows much more accurate glaciation chronologies to be calculated and is vital for computing rates of ice thinning and volume change. Early work in Scandinavia followed by Stone *et al.*'s and later Ballantyne's application of this method to trimline interpretation demonstrated the usefulness of cosmogenic nuclide dating for trimline-based reconstructions, encouraging the adoption of this method in wider trimlines research (e.g. Kaplan *et al.* 2001; Stroeven *et al.* 2002; Clark, P.U. *et al.* 2003; Sugden *et al.* 2005; Ackert *et al.* 2007; Mckintosh *et al.* 2007; Nesje *et al.* 2007; McCormack *et al.* 2011; Glasser *et al.* 2012; Kelley *et al.* 2012; White and Fink 2014; Wirsig *et al.* 2016a).

Improvements in Geographic Information Science (GIS) have also led to progress in trimline research by enabling more advanced processing and increasing the speed of trimline mapping across large areas. An example is the work of Kelly *et al.* (2004), who reconstructed the LGM accumulation area ice surface in the Swiss Alps. They found that the majority of ice surface reconstructions were well-constrained by empirical evidence in the ablation area but that the accumulation area ice surface was generally estimated from ablation area landforms. To address uncertainty in the accumulation area ice surface, Kelly *et al.* mapped trimlines in the field and compared them to a digitisation of an existing reconstruction, using the trimlines to refine the accumulation area geometry. This method was only possible using modern GIS software to combine the previous reconstruction and the new trimline evidence into a single ice surface reconstruction. It is noteworthy that Kelly *et al.* had to assume that all the maximum glaciation landforms and trimlines in their study area were synchronous. This is an issue common to all regional trimline studies (see fuller discussion in Section 3.6). At present there is no certain way to determining synchronicity between trimlines, particularly in different valleys or on different massifs, although wider application of cosmogenic nuclide dating may help to combat this problem.

Lately, methods of trimline mapping have been developed beyond the aerial method of Thorp (1981; 1986) through the use of satellite imagery. Knight *et al.* (1987) showed that a multispectral classification of satellite imagery could be used to identify and map the changes in vegetation that mark the LIA trimzone in Greenland. This early use of satellite imagery demonstrated that trimlines research could expand beyond the valley or icefield scale, which it was previously restricted to due to the spatial limitations of fieldwork and aerial imagery. New methods, such as that of Knight *et al.* (1987), alongside improvements in the coverage and resolution of satellite imagery have enabled larger-scale trimline mapping. Increases in

the feasible scale of mapping studies has allowed for easier production of regional ice surface reconstructions, such as Glasser *et al.*'s (2005; 2008) reconstruction of the glacial history of Patagonia using data from the satellites Landsat 7 and ASTER. Larger-scale projects, such as Glasser *et al.*'s Patagonian work, are particularly significant for validating ice sheet models and refining predictions of future ice sheet behaviour.

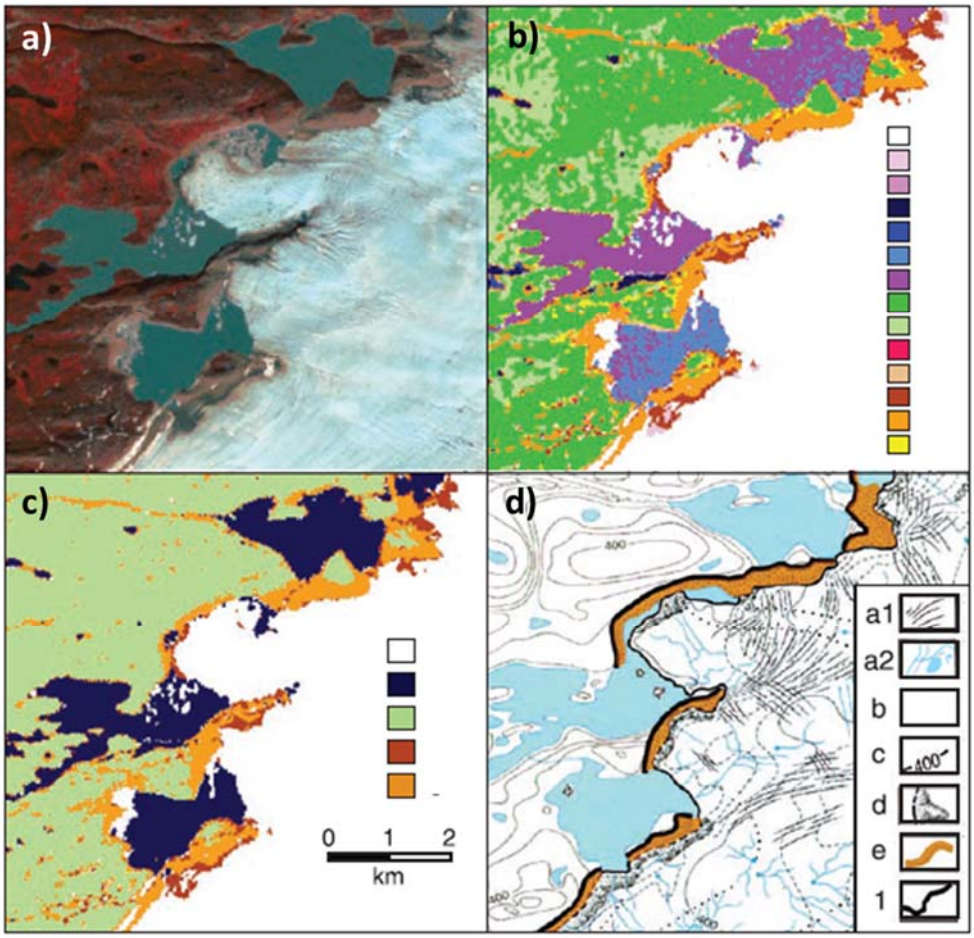

Figure 3.7 – This figure illustrates Csatho *et al.*'s method for mapping trimzones in west Greenland. a) Shows their input data: a pan-sharpened colour composite of Landsat ETM+ bands 2, 3, 4 and the panchromatic band. b) Their initial classification process divides the landsurface into 14 land-cover classes, based on the surface reflectance. c) Using fieldwork validation, they were able to simplify their classification to 5 major land-cover classes: (white) ice; (blue) water; (green) vegetated land; (brown) debris-covered ice; and (orange) the trimzone. d) They further validated their method by comparing the outputs with previous geomorphological mapping by Thomsen and Winding (1988): (a1) crevasses; (a2) ice surface meltwater features; (b) fjords and lakes; (c) land with elevation contours; (d) debris-covered ice; (e) trimline zone; (1) trimline. (Csatho *et al.* 2005, pp.60)

The desire to use trimlines in ice sheet scale studies and improvements in GIS processing led Csatho and colleagues to produce a semi-automated method for mapping vegetation trimlines over large spatial areas from satellite imagery (Figure 3.7; Csatho *et al.* 2005; van der Veen and Csatho 2005). Their method built on Knight *et al.*'s (1987) work and used multispectral imagery from the Landsat 7 satellite to characterise the spectral reflectance of different landsurfaces in the area around Jakobshavn Isfjord, west Greenland. This analysis enabled Csatho *et al.* to divide the landscape into spectral classes representing different landsurfaces (Figure 3.7b and 3.7c). They validated this classification system via fieldwork (Csatho *et al.* 2005) and by studying the spectral reflectance properties of Greenland lichens (van der Venn and Csatho 2005). From their classification of the landsurface they were able to map the LIA trimzone and associated trimline (Figure 3.2). Csatho *et al.* (2008) expanded on this initial study, utilising the same method but comparing the trimline altitude with recorded ice margin positions to determine rates of ice loss in the study area since the LIA. Despite the success of this study, the methods of Csatho and colleagues have not been widely adopted and have yet to be applied outside Greenland.

Kjeldsen *et al.* (2015) were likely inspired by the work of Csatho *et al.* (2008) to map LIA trimlines and moraines along the entire margin of the Greenland Ice Sheet (GrIS). Kjeldsen *et al.* used vertical stereo photogrammetric aerial imagery to map LIA trimlines in 3D and to compare them to the ice margin position at the time of the photographic survey (1978-1987 AD) (Figure 3.8a/3.8b). By extrapolating from the trimlines, they were able to compute the extent and spatial distribution of ice surface elevation and volume changes for the entire ice sheet between the peak of the LIA (assumed to be 1900 AD) and the aerial survey in 1978-1987 AD (Figure 3.8c).

Kjeldsen *et al.* (2015) was the first, and so far only, empirically based 3D reconstruction of the entire GrIS during the LIA. From their reconstruction, Kjeldsen *et al.* were able to determine the sea level contribution of the GrIS during the 20th Century with higher confidence than had previously been possible using modelled reconstructions. The historic contributions of Greenland and Antarctica to global sea levels are one of the largest uncertainties in the most recent Intergovernmental Panel on Climate Change report (IPCC 2014). Therefore, it is likely that the work of Kjeldsen *et al.* will be emulated in Antarctica as well as for other significant glacierised areas, such as Patagonia. The significant role of trimlines in the production of 3D reconstructions, which are vital for sea level contribution estimates, demonstrates the on-going relevance of research into these features.

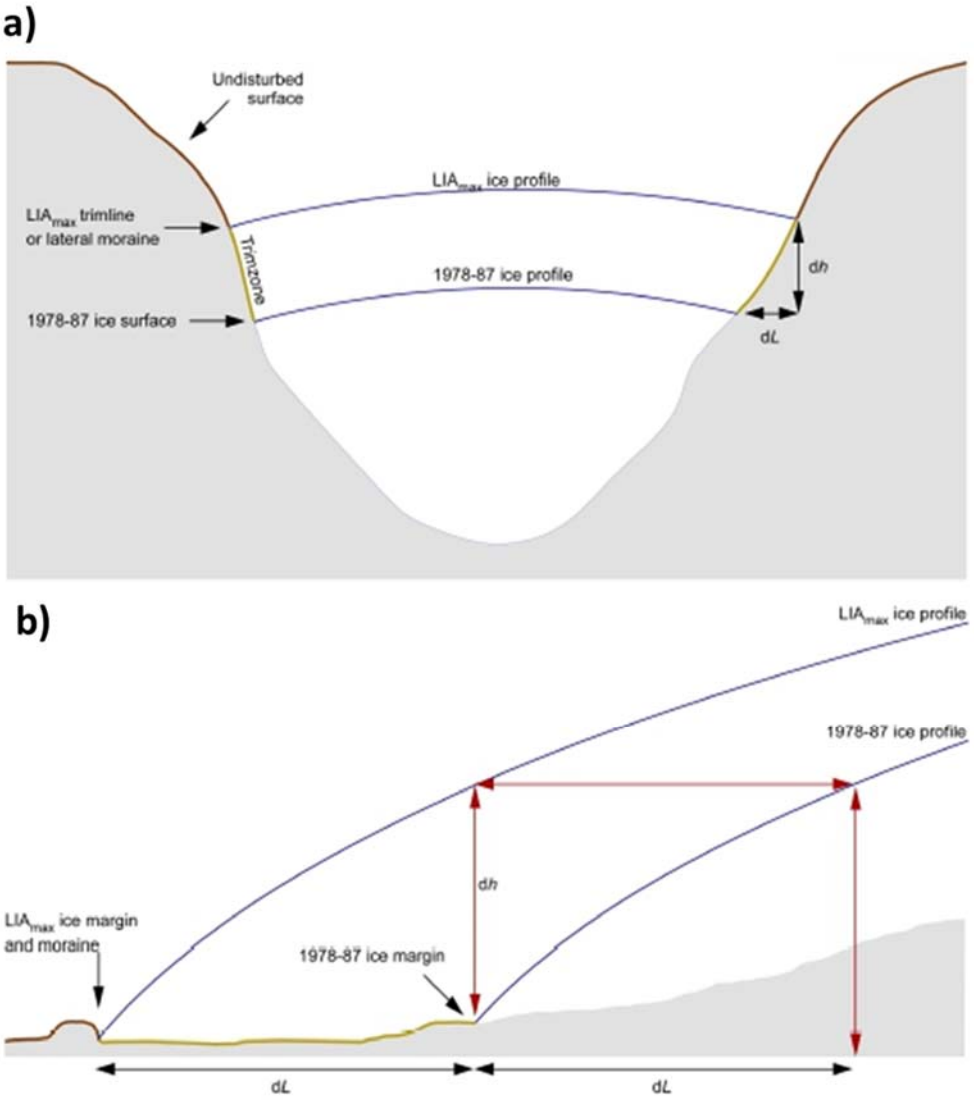

Figure 3.8 (3.8c on next page) **–** a) and b) show how Kjeldsen *et al.* (2015) determined the thinning of Greenland ice by comparing the modern ice margins (1978-1987), determined from aerial photographs, to 3D mapping of LIA trimlines. Note that they considered both lateral (a) and frontal (b) trimlines and that they used moraines in the same way as more 'traditional' trimlines (Kjeldsen *et al.* 2015, pp.408). c) Shows the elevation change computed from the comparison of the LIA trimlines and the 1978-1987 ice margin. From these point thinning measurements, Kjeldsen *et al.* were able to extrapolate across the entire ice sheet surface and compare the resulting thinning pattern to remotely sensed data and to modelling outputs (Kjeldsen *et al.* 2015, pp.409).

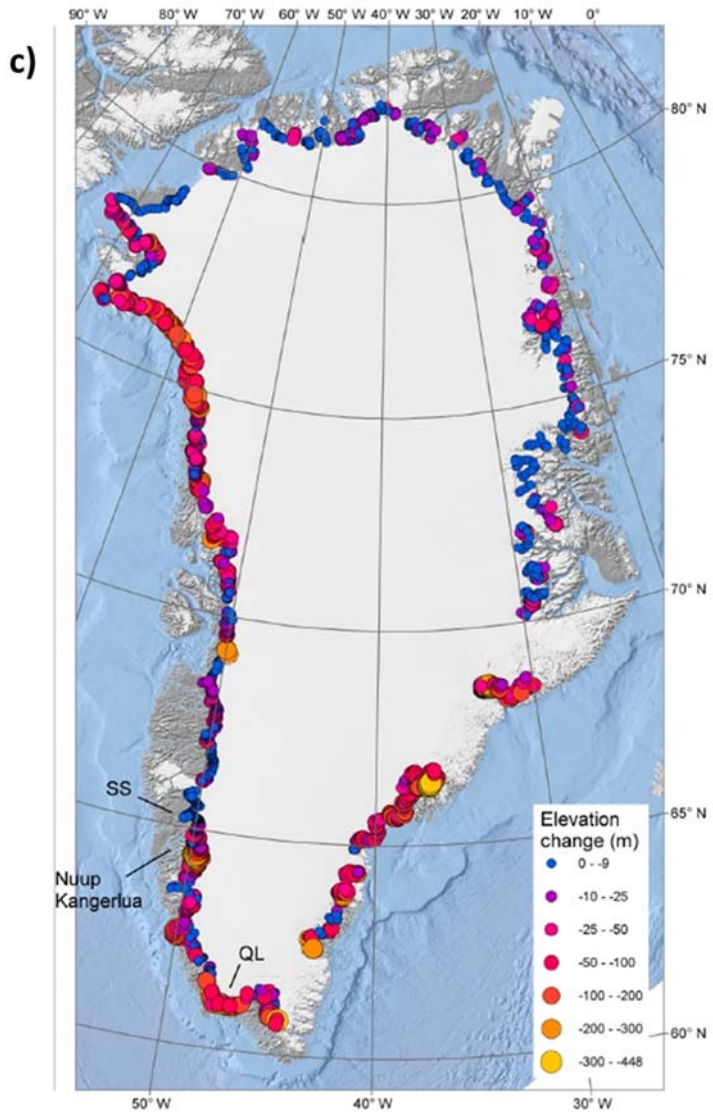

3.4.1 Comparing the methods of Quaternary and historic trimlines research

Both Quaternary and historic trimlines are generally mapped using analysis of remotely sensed imagery alongside fieldwork validation. However, there are significant differences in the application of these methods to Quaternary and historic trimlines as well as differences in the analysis and interpretation of these features.

In Quaternary trimline research more emphasis is placed on field observations and analyses compared to the greater significance of remotely sensed data in historical studies. Many Quaternary trimline studies have quantified the contrast in weathering across a trimline using Schmidt hammer measurements, bedrock joint depth analysis and by studying the soil composition above and below the trimline (e.g. McCarroll *et al.* 1995; Rae *et al.* 2004; Nesje *et al.* 2007; see summary of methods used in McCarroll 2016). The use of X-ray diffraction

clay-fraction mineralogy is particularly common in Quaternary settings, especially when trying to determine if a trimline is of ice marginal or thermal origin (e.g. McCarroll *et al.* 1995; Dahl, S.-O. *et al.* 1996; Ballantyne 1997; Lamb and Ballantyne 1998; Ballantyne *et al.* 1998b; Ballantyne 1998; McCarroll and Ballantyne 2000; Ballantyne and Hallam 2001; Rae *et al.* 2004; Ballantyne *et al.* 2006; Ballantyne *et al.* 2007; Nesje *et al.* 2007; Ballantyne *et al.* 2008; Ballantyne *et al.* 2011). This method considers the relative abundance of various clay minerals, particularly the weathering products gibbsite and kaolinite, in soils collected above and below the trimline (Ballantyne *et al.* 2008). Theoretically, a greater abundance of gibbsite and kaolinite above a trimline would suggest that the area above the trimline has been exposed to subaerial weathering for significantly longer than the area below the trimline – hence the trimline may be interpreted as ice marginal (Ballantyne *et al.* 2008). Despite finding some success, clay-fraction mineralogy and other methods of assessing the relative degree of weathering across a trimline have recently fallen out of favour due to the expansion of cosmogenic nuclide dating in Quaternary trimlines research (Ballantyne 2010). However, these methods are still in use and can provide additional information to aid the interpretation of Quaternary trimlines.

In historic settings the modern ice surface is often present and may act as a guide for reconstructing the morphology of the previous ice surface (Figure 3.9). Research into historic trimlines can also make use of additional data sources that are not available for Quaternary settings. For example, repeat aerial surveys and high-resolution satellite imagery of some glacierised areas can allow comparison of the modern ice margin to a series of trimlines and other recorded ice margin positions, which enables rates of down-wasting to be computed (e.g. Harrison *et al.* 2007; Csatho *et al.* 2008; Glasser *et al.* 2011).

As well as greater variety of remotely sensed data, historic glaciations can be recorded in paintings, sketches, historical documents and photographs (e.g. Figure 3.10). These secondary data can provide additional ice margin positions and can help to date trimlines and establish synchronicity between trimlines and other glacial features (e.g. compare Figure 3.9 and Figure 3.10). Validation studies have found these secondary data to be generally accurate representations of the former ice extent (e.g. in the Alps by Nussbaumer *et al.* 2007 and Zumbühl *et al.* 2008). Therefore, historic reconstructions in well-documented areas can be produced with higher confidence and with much more detail than is possible for Quaternary reconstructions, even when the trimline record is similarly preserved. However, the availability of secondary data may be contributing to the tight spatial focus of historic

trimlines research in well-documented areas (Figure 3.4b). Additionally, the greater difficulty collecting field data in glacierised areas may be limiting the choice of methods applied to historic trimline analysis and may also be causing research to focus on more accessible areas.

It is more common to find multiple trimlines associated with the same ice margin in historic settings compared to Quaternary. This is likely to be a function of the preservation potential of trimline features. For example, Forman *et al.* (2007) identified a clear LIA vegetation trimline associated with the ice margin in the Kangerlussuaq area of west Greenland but they also noticed several subtler changes in vegetation cover within the LIA trimzone. These features may well be trimlines linked to standstills during the post-LIA retreat of the ice margin. Another example of a subtle historic trimline can be seen in Figure 3.9, where there is a slight change in slope features roughly two-thirds of the way down from the 1820 trimline to the 2014 ice margin. These subtler trimlines probably do not have long-term preservation potential and may well not survive in Quaternary settings.

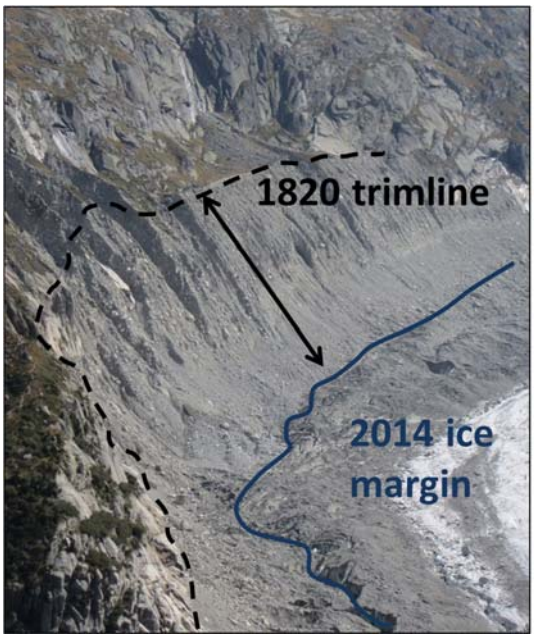

Figure 3.9 – Comparison between the 2014 ice margin (blue) and the 1820 trimline (black) on the Mer de Glace in the Mont Blanc area, France. The trimline is marked by a vegetation contrast as well as a discontinuity in the slope landforms, particularly gullies, alongside an erosional step and a fan. The date of the trimline is known from historical artwork (e.g. Figure 3.10) and written documents. From these two dated ice margin positions it is possible to calculate rates of down-wasting and volume loss since the Little Ice Age, which peaked in this area at around the time of trimline formation. An additional trimline feature can be distinguished two-thirds of the way down from the 1820 trimline to the 2014 ice margin, possibly marking a standstill during the post-Little Ice Age retreat. This subtler trimline is expressed as a discontinuity in the slope gullies and could possibly also be a glacial drift limit. (C.M. Rootes, October 2014)

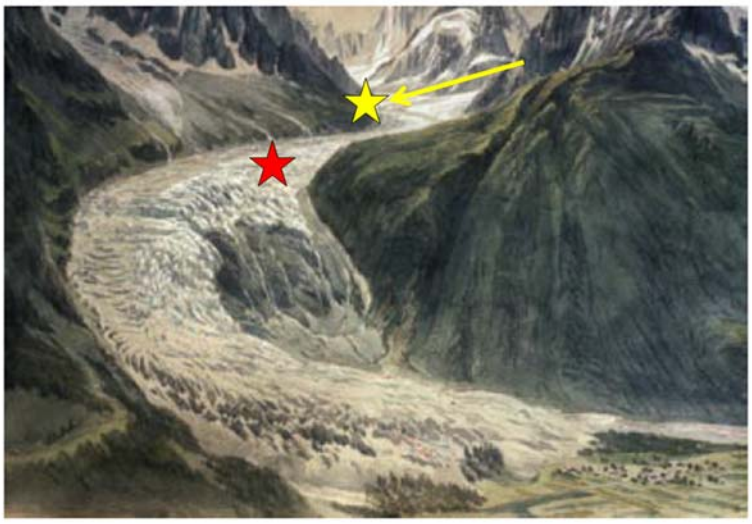

Figure 3.10 – Pencil and watercolour sketch of the Mer de Glace from la Flégère in 1823, by Samual Birmann (exert from: "à la Flégère. 1823"). The yellow star marks the approximate position of Figure 3.9 and the yellow arrow indicates the direction that the photograph was taken from. This sketch shows the ice margin roughly at the position of the 1820 trimline, confirming the date of this feature, and also shows the retreat of the glacier snout to the approximate 2014 snout position (red star). (Samual Birmann 1823; reproduced in Nussbaumer *et al.* 2007, pp.49)

3.5 Uses of trimlines

For all temporal periods and all geographic locations, the ability to produce 3D reconstructions using trimlines has been of particular significance (e.g. Figure 3.11). Estimates of palaeo ice thickness, derived from trimlines, allow ice volume change to be computed and have enabled the quantification of the sea level contribution of ice loss (e.g. Glasser *et al.* 2011; Kjeldsen *et al.* 2015; Edwards *et al.* 2017). Trimline studies are also utilised to test the outputs of numerical ice sheet models, a process used to validate and improve the models and hence predictions of future ice sheet behaviour (e.g. Dahl, S.-O. *et al.* 1996; Lamb and Ballantyne 1998; McCarroll and Ballantyne 2000; Ballantyne and Hallam 2001; Hubbard *et al.* 2006; Ackert *et al.* 2007; Figure 3.12).

The 3D reconstructions produced from Quaternary trimlines can be used to reconstruct palaeoclimate. Trimline distribution over large areas can reveal details of the surface morphology of the palaeo ice mass that may indicate particular palaeo wind patterns and precipitation gradients (Glasser *et al.* 2008). Reconstructions of palaeo precipitation gradients are particularly significant because there are very few other proxies for this climate variable. Palaeo equilibrium line altitude (ELA) can also be derived from 3D ice surface

reconstructions (e.g. Figure 3.11). The ELA is roughly equivalent to the snow line altitude and, as well as being a climate proxy in itself, is also useful for calculating palaeo mass balance and for studying the impact of glaciers on long-term landscape evolution, due to the links between ELA position and patterns of glacial erosion (Ballantyne 2007). Trimlines are particularly important for ELA reconstructions because they record ice thickness and are one of the only ice marginal features that can be found in the accumulation area, above the ELA (Thorp 1981; Kelly *et al.* 2004). An example of the use of trimlines in ELA reconstruction is van der Beek and Bourbon (2008). These authors used trimlines to reconstruct ice thickness and palaeo ELA in the French Alps, which enabled them to quantify the impact of glacial erosion on the topography of the region (Figure 3.11).

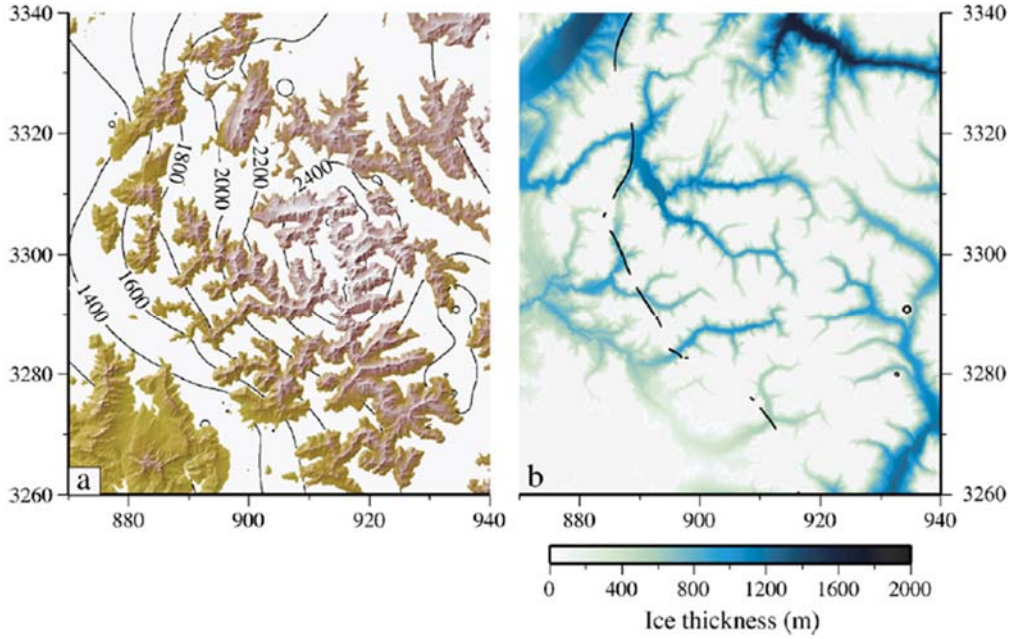

Figure 3.11 – a) Reconstructed ice surface (white) with elevation contours for the most extensive glaciation affecting the French Alps, produced by van der Beek and Bourbon (2008) from analysis of glacial trimlines. Nunataks are shown as topography and were identified because the landsurface exceeded the maximum trimline elevation. b) Reconstructed ice thickness, assuming that the modern topography is equivalent to the subglacial topography. The black dashed line indicates the inferred position of the equilibrium line altitude at the time of trimline formation. Eastings and northings in kilometres, according to the IGN Lambert-III grid. (van der Beek and Bourbon 2008, pp.60)

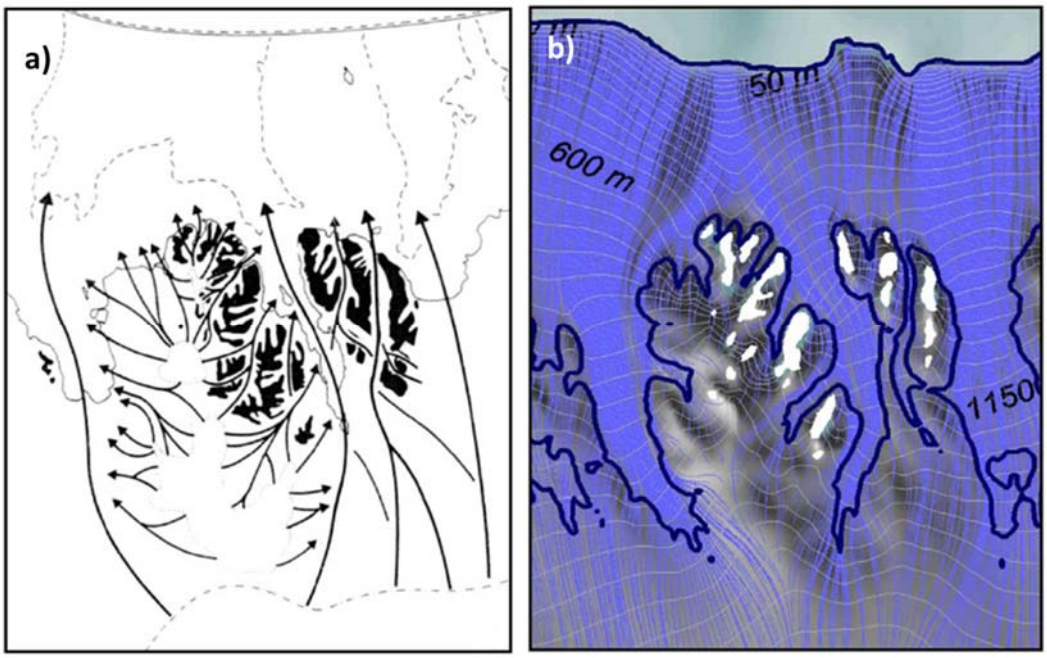

Figure 3.12 – Hubbard *et al.* (2006) modelled the last glacial maximum in Iceland and validated their reconstructed ice sheet against previous empirical reconstructions. a) Shows an exert from Norddahl's (1991) empirical reconstruction of ice flow patterns (arrows) and nunataks (shaded black), identified from trimlines, in the Tröllaskagi highlands. b) The outputs from Hubbard *et al.*'s model for the same area show a close match in the location of nunataks (white in the model) and of major ice flow pathways. This study is an example of the role of trimlines in validating ice sheet model outputs. Trimlines can also be utilised in testing modelled ice thickness, ice volume, ice surface morphology and rates of ice thickness and volume change. (Hubbard *et al.* 2006, pp.2292)

As well as being a proxy for palaeoclimate and ELA, reconstructions produced from Quaternary trimlines can be used to determine ice thickness and volume changes. The use of ice marginal trimlines to determine ice thickness has been termed the 'dipstick' method, in reference to engine oil dipsticks in cars (Mackintosh *et al.* 2007). For example, Mackintosh *et al.* (2007) looked for the upper limits of erratic distribution, which could be considered a type of trimline, on a transect of mountains in Mac. Robertson Land, East Antarctica. From the altitude of the trimlines they were able to determine the LGM ice thickness and, by comparing the trimlines to the modern ice surface, they were able to conclude that there has been little thinning in the study area since the LGM. This lack of significant ice loss allowed Mackintosh *et al.* (2007) to suggest a minimal contribution of East Antarctica to the deglacial sea level event Meltwater Pulse 1A.

'Dipstick' research in Antarctica is particularly significant because a longer landform record is preserved there than is typically found in mid-latitude settings. This allows for the

production of longer-term reconstructions, which can be compared to ice core climate records and to measurements of post-glacial isostatic adjustment. These comparisons enable better understandings to be developed of the interactions between the ice sheet, climate and sea level (Armienti and Baroni 1999; Ackert *et al.* 2007; Ackert *et al.* 2011; White and Fink 2014). An example is the work of Ackert *et al.* (2007), who make use of trimlines and erratic distributions to reconstruct ice surface elevation in the interior of West Antarctica, which they compared to climate records by dating ice margin positions using cosmogenic nuclide dating. From this analysis they were able to conclude that there was also no interior West Antarctic contribution to Meltwater Pulse 1A. Their study was developed further by Ackert *et al.* (2011), who revisited the area to take more dating samples and determine rates of ice surface elevation change, which they compared to the Dome Fuji Ice Core to produce a linked record of climate and ice thickness in West Antarctica over the last 200 ka.

Long-term linked ice thickness and climate studies are important for testing and empirically constraining ice sheet models, which may be run for hundreds of thousands of years in a single experiment. Ackert *et al.* (2011) compared their linked ice thickness and climate record to a numerical ice sheet model designed by Pollard and DeConto (2009). Ackert *et al.*'s independent test of the model outputs confirmed that the Pollard and DeConto's model reproduces the ice fluctuations recorded in the trimlines and erratics of the interior of West Antarctica. This study was particularly important because it is located in a crucial area for predicting the response of Antarctica to on-going climate change: the Ohio Range near to the on-set areas of the Siple Coast Ice Streams, which drain a significant area of West Antarctica.

In addition to ice marginal trimlines, research into the Quaternary trimlines of Scandinavia and the BIIS has identified examples of palaeo thermal boundaries, for example in the Caithness area of northern Scotland (Ballantyne and Hall 2008; Section 3.6). Thermal trimlines such as these are less applicable for reconstructing down-wasting and ice volume loss but instead provide useful information about the distribution of warm-based and cold-based ice at the base of the Quaternary ice sheet (Goodfellow 2007; Kleman and Glasser 2007; e.g. in Antarctica: Sugden *et al.* 2005; Baroni *et al.* 2008; in Tibet: Fu *et al.* 2013). This information can also be used to test numerical ice sheet models and can shed light on patterns of glacial erosion and ice flow pathways (e.g. Figure 3.12; Boulton and Hagdorn 2006).

As well as testing numerical models, Quaternary trimline reconstructions have also been used to validate satellite measurements. An example is the work of White and Fink (2014), who used cosmogenically dated trimlines in East Antarctica to reconstruct ice thickness and compared their results to the gravimetric measurements of the GRACE satellites. This comparison allowed them to validate the satellite data and to improve the outputs of isostatic adjustment models, which use the satellite's measurements as input data. Without the ice thickness information recorded in Quaternary trimlines, it would not be possible to carry out this kind of empirical validation of GRACE isostasy measurements.

Historic 3D reconstructions can be produced to a higher resolution, both spatially and temporally, than is possible for Quaternary reconstructions. The higher accuracy and resolution of historic reconstructions mean that they may be used with greater confidence for the same applications as Quaternary reconstructions. This includes testing numerical ice sheet models; although historic reconstructions may not cover a long enough time period to test models of lower temporal resolution or to constrain longer-term experiments.

It is more common to find multiple trimlines in historic settings and to have access to other records of previous ice margin positions, for example from aerial photography or artworks (e.g. Figure 3.10). Where multiple historic ice margin positions are dated, from a series of glacial trimlines or from documentary evidence, it is possible to calculate rates of down-wasting between ice margin positions (e.g. Kohler *et al.* 2007). The extent and rate of down-wasting can be compared with climate records to infer the response rate and retreat style of the glacier (e.g. Navarro *et al.* 2005; Kohler *et al.* 2007). Estimates of glacier response times are particularly significant for predicting local- and regional-scale changes to the cryosphere in response to on-going global climate warming (Raper and Braithwaite 2009). It is also possible to conduct comparison of historic volume change estimates with sea level measurements at high resolutions and to use this information to inform sea level forecasts (e.g. Nuth *et al.* 2007; Kjeldsen *et al.* 2015).

3.6 Debates and issues in trimline research

The use of trimlines in research surrounding the glacial refugia debate centred on the idea that these features represent a palaeo ice margin position (see Section 3.3). Only by making this assumption could trimlines be used to locate palaeo nunataks. This interpretation was

supported by field investigations on the relative degree of weathering above and below British, Irish and Scandinavian trimlines (Section 3.4.1; e.g. McCarroll *et al.* 1995; Dahl, S.-O. *et al.* 1996; Ballantyne 1997; Ballantyne *et al.* 1997/ 1998a/b; Ballantyne 1998; Lamb and Ballantyne 1998; Stone *et al.* 1998; McCarroll and Ballantyne 2000; Ballantyne and Hallam 2001; Rae *et al.* 2004; Ballantyne *et al.* 2006; Ballantyne *et al.* 2007; Nesje *et al.* 2007; Ballantyne *et al.* 2008; Ballantyne *et al.* 2011). These investigations were used to rule out alternative hypotheses of trimline formation, particularly that the trimlines represented changes in weathering conditions during deglaciation (Figure 3.13c; Ballantyne 1998).

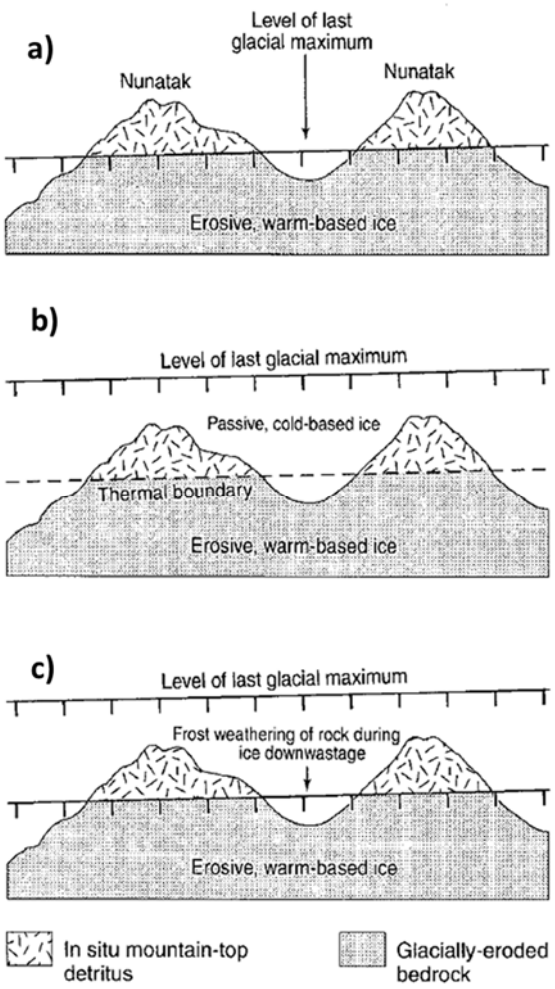

Figure 3.13 – Suggested formation scenarios for Scottish trimlines. a) The trimlines were formed at the margins of the ice sheet and demarcate palaeo nunataks (detailed schematic of this theory in Figure 3.4). b) Trimlines were formed at thermal boundaries between flowing warm-based ice in the valleys, which created a glacially scoured landsurface, and rigid cold-based ice on the mountain summits, which preserved the preglacial frost weathered landsurface. c) Trimlines were formed at the ice margin during standstills in deglaciation or due to changes in climate, and hence degree of weathering, during deglaciation. Field observations and analysis of Scottish trimlines suggest that c) is unlikely but distinguishing between a) and b) has proved much more difficult. (Ballantyne 1998, pp.329)

However, the relative degree of weathering across a trimline was insufficient evidence to discard a subglacial theory of trimline formation: that trimlines can form at the boundary between areas of erosive warm-based ice and areas of cold-based ice (Figure 3.13b; see Section 3.3). To rule out the subglacial formation of trimlines at thermal boundaries, researchers considered the morphology of the trimlines and tended to conclude in favour of an ice marginal origin. This conclusion was reached for three reasons: 1) the trimlines were deemed to be too sharp to be thermal; 2) the lack of an increase in trimline altitude on the stoss side of mountains compared to a decreased altitude, or 'pressure shadow', on the lee side, which would have indicated the high glacial velocities associated with warm-based ice; and 3) the regular decline of trimline altitudes along former flow lines was thought to be diagnostic of ice marginal formation (Ballantyne *et al.* 1997; Ballantyne *et al.* 1998a). The results of early cosmogenic nuclide dating studies were also supportive of the ice marginal hypothesis (e.g. Stone *et al.* 1998), although it was not possible to completely exclude a thermal origin.

The ice marginal interpretation of glacial trimlines found particular favour within the community of 'small BIIS' proponents, who concluded that the BIIS LGM did not extend out to the continental shelf break (Figure 3.14; e.g. Bowen *et al.* 1986; Bowen *et al.* 2002). This reconstruction required relatively thin ice cover in Scotland, which would mean that many mountains remained above the ice surface as nunataks (Stone *et al.* 1998). The abundance of trimlines in the west and north of Scotland was taken to support the 'small BIIS' reconstruction because these features were interpreted as ice marginal and therefore thought to indicate a large number of palaeo nunataks (e.g. Ballantyne *et al.* 1997; Ballantyne *et al.* 1998a; Lamb and Ballantyne 1998).

Early numerical modelling had suggested a larger BIIS, with fully submerged mountains in Scotland (e.g. Boulton *et al.* 1977), indicating that the trimlines of this area were of thermal origin. Later modelling utilised new understandings of the deformation of sediments beneath ice sheets, which was thought to provide lower basal resistance to flow and generate faster ice velocities. Increased flow rates in the new models yielded a thinner ice sheet and suggested the existence of nunataks, supporting the ice marginal interpretation of Scottish trimlines (Boulton *et al.* 1991; Lambeck 1993; Lambeck 1995). By the 1990s empirical and modelling studies had converged in support of the small BIIS theory and the interpretation of BIIS trimlines as ice marginal landforms (Ballantyne 2010).

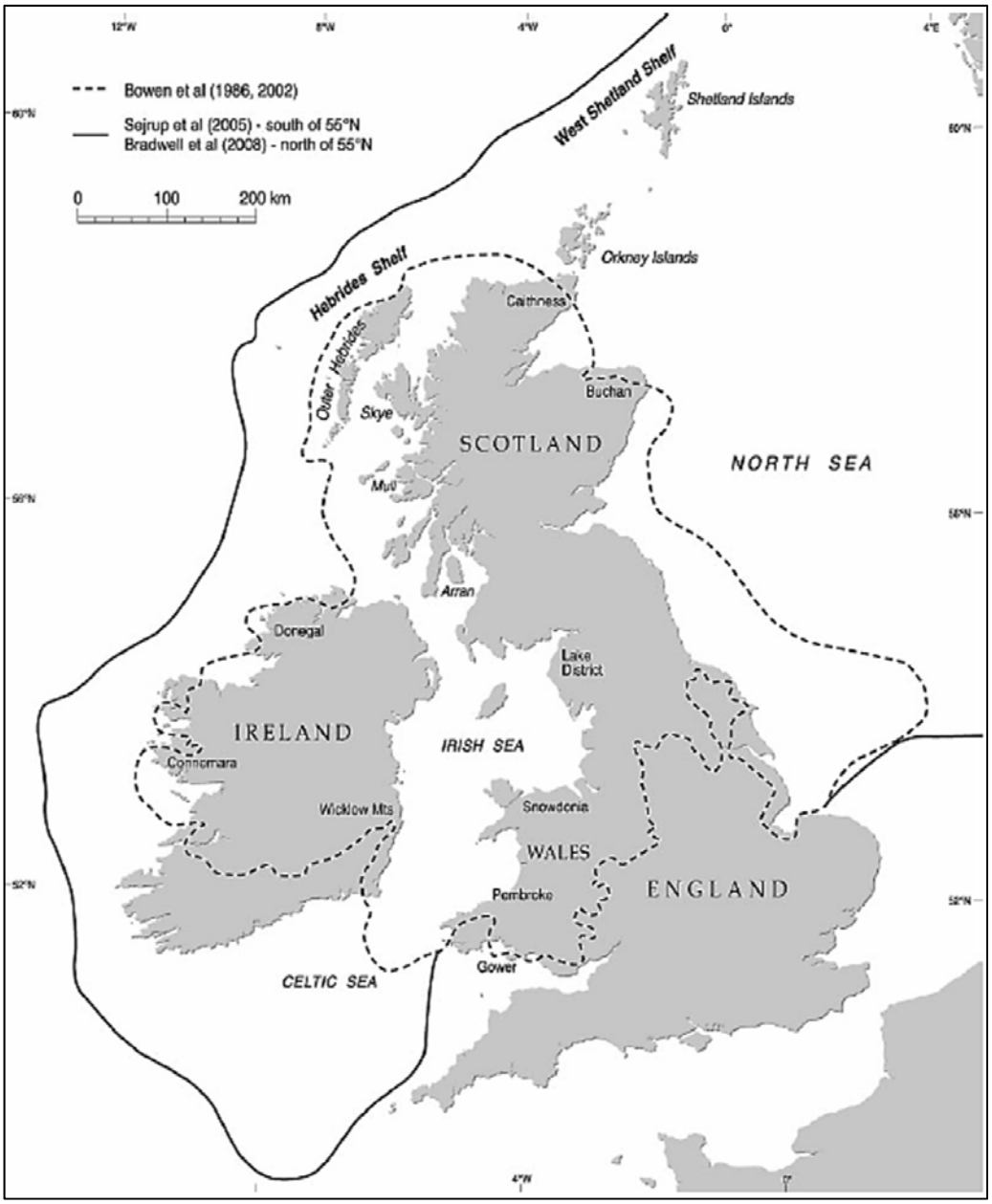

Figure 3.14 – The conflicting theories about the spatial extent of the BIIS during the last glacial maximum. The dashed line represents the ice extent of the 'small BIIS' hypothesis, drawn from the work of Bowen (1986; 2002). The glaciation of the 'large BIIS' theory is marked by the solid black line and is based on a synthesis of Sejrup *et al.* (2005) and Bradwell *et al.* (2008), produced by Ballantyne (2010). Comparison of the two theories demonstrates why the significantly larger ice sheet of the 'large BIIS' theory would require much thicker ice cover, particularly in the accumulation zones of northern and western Scotland. This thicker ice cover would probably prohibit the existence of palaeo nunataks in these regions. (Ballantyne 2010, pp.517)

Meanwhile, offshore geomorphological mapping and sedimentological studies were leading some authors to challenge the 'small BIIS' reconstruction and suggest that the last BIIS glaciation did reach the continental shelf break (Figure 3.14; e.g. Sejrup *et al.* 2005; Bradwell *et al.* 2008). This contrasting 'large BIIS' theory has been supported by a new phase of trimline dating that has favoured a thermal origin for many glacial trimlines, indicating a thicker and more spatially extensive ice sheet. Ballantyne and Hall (2008) demonstrate this shift in trimline interpretations with their reconstruction of the ice thickness in Caithness and east Sutherland, northern Scotland, using cosmogenically dated trimlines. Their dates and geomorphological evidence caused them to identify a thermal origin for their trimlines and to suggest that the presence of nunataks in the area during the LGM was unlikely. Other studies in north-west Scotland have also supported the 'large BIIS' reconstruction and identified examples of thermal trimlines (e.g. McCormack *et al.* 2011; Fabel *et al.* 2012).

Recent numerical modelling studies have also supported the 'large BIIS' theory (Boulton and Hagdorn 2006; Hubbard *et al.* 2009; Edwards *et al.* 2017). Both Boulton and Hagdorn (2006) and Hubbard *et al.* (2009) modelled the entire BIIS at the LGM and both studies considered the trimline evidence of western Scotland, as presented by Ballantyne *et al.* (1998a), to be of vital importance in constraining the accumulation area ice thickness. However, both noted that a thermal origin for these trimlines was possible and neither Boulton and Hagdorn nor Hubbard *et al.* were able to force their model to conform to the ice thickness estimates produced from Scottish trimlines by Ballantyne *et al.* (1998a). Therefore, both modelling studies concluded that Scottish trimlines in most mainland locations represented palaeo thermal boundaries and were not ice marginal features.

Application of cosmogenic dating to new study areas has led to the identification of thermal trimlines in other regions of the BIIS. For example, in Ireland (Ballantyne *et al.* 2008; Ballantyne *et al.* 2011; Stone and Ballantyne 2015), Wales (Glasser *et al.* 2012) and the Lake District (Ballantyne *et al.* 2009). The thermal theory is now recognised to have been the dominant process of trimline formation beneath central areas of the BIIS during the LGM (Ballantyne 2010). However, trimlines associated with the Younger Dryas in Britain and Ireland are still thought to be ice marginal features (e.g. Stone and Ballantyne 2006) and debate continues about the correct interpretation of some trimlines in areas of rugged terrain (McCarroll 2016; Clark, C.D. *et al.* 2018; e.g. Barth *et al.* 2016).

The example of the debate surrounding BIIS trimline interpretation illustrates that both ice marginal and thermal trimlines are possible and can exist within the same ice mass

(Ballantyne 2010). This indicates that trimlines in Quaternary settings can no longer be assumed to be ice marginal features. Outside the British Isles, there has been less extensive application of cosmogenic nuclide dating to Quaternary trimlines and there are few areas where trimline-based reconstructions and ice sheet modelling have been conducted in such close association. However, the conclusions of BIIS trimline research suggest that care must be taken when interpreting Quaternary trimlines associated with the accumulation areas of ice sheets or ice caps, where the thick ice can include areas of differing thermal regime.

Conversely for historic trimlines the assumption of ice marginal formation appears to hold true in most cases (e.g. Figure 3.9; Kelley *et al.* 2012). The reason for this may be to do with the relative preservation potentials of thermal trimlines compared to ice marginal trimlines, or it may be due to the lack of modern examples of recently deglaciated areas where differing thermal regimes are adjacent to each other. Perhaps some historic thermal trimlines will be exposed as larger polythermal glaciers and ice caps retreat over the coming centuries.

Beyond the issue of correctly identifying ice marginal and thermal trimlines, further problems with trimline interpretation are associated with difficulties in establishing synchronicity between trimline features. Even in a small group of valleys there may be multiple separate trimlines and it is often not clear which trimlines formed at the same time (Figure 3.15). On a regional scale, attempts have been made to link together trimlines of assumed synchronous ages in order to reconstruct regional glaciation or equilibrium line altitude positions (e.g. Kelly *et al.* 2004). However, at present there is no standardised method for establishing trimline synchronicity and researchers have largely relied on morphological or altitudinal similarities (Kelly *et al.* 2004; Figure 3.5b). Studies using cosmogenic nuclide dating have linked trimlines of similar ages (e.g. Ballantyne *et al.* 2007; Fabel *et al.* 2012), but the error in the dating method is often too large to do this with any confidence. Synchronicity remains an area of on-going uncertainty in trimlines research.

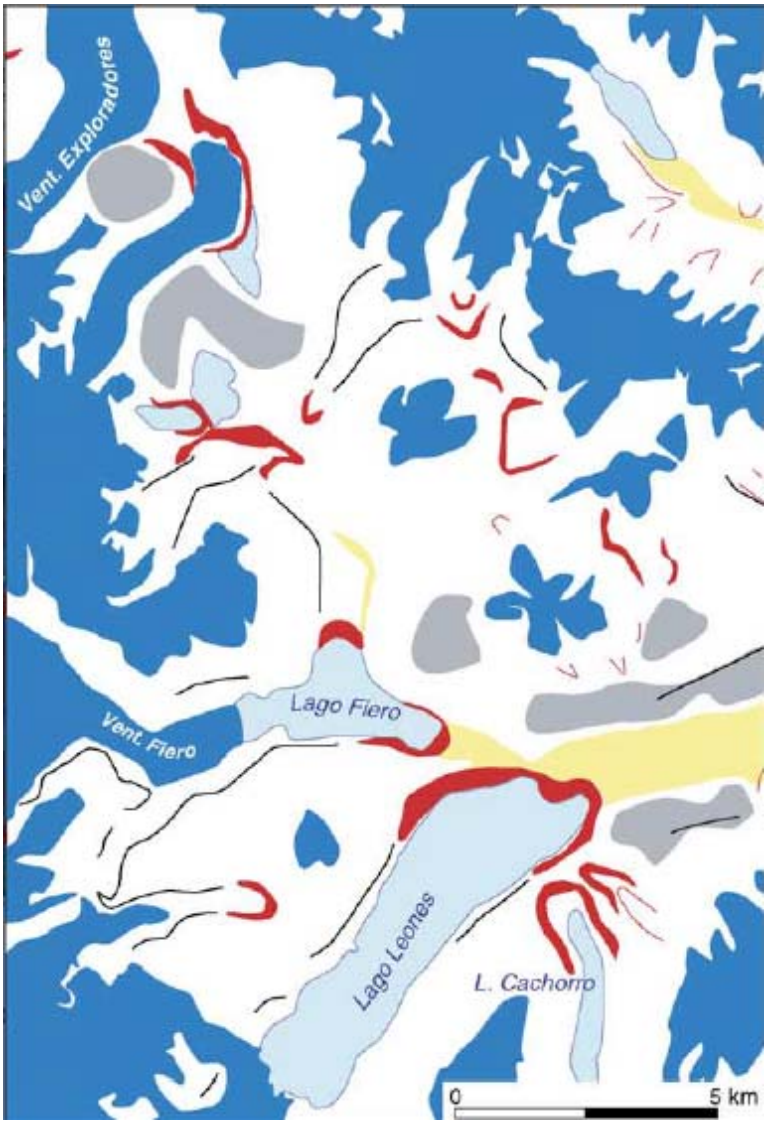

Figure 3.15 – In this extract of Glasser *et al.*'s (2005) geomorphological map of the North Patagonian ice sheet the following key is used: ice (shaded dark blue); lakes (shaded light blue); sandur (shaded yellow); scoured bedrock (shaded grey); moraines (shaded brown; purple lines); trimlines (black lines). This area has a lot of trimlines and it is possible to visually link up sets of trimlines surrounding single glaciers and also between glaciers. However, without either relative or absolute dating there is no way to establish synchronicity with any confidence. This is also a problem when linking trimlines to other glacial features, such as moraines. In Glasser *et al.*'s map there are clear instances of trimlines that link to specific moraines, for example around Lago Leones, but again it is not possible to establish synchronicity without further evidence. In many areas trimlines are not as easy to visually link to each other and to other glacial features as they are in this example, making the establishment of synchronicity very challenging. (Glasser *et al.* 2005, pp.269)

Whilst interpretation and problems of establishing trimline synchronicity are significant, arguably the most important problems lie with the identification and mapping of the trimlines themselves. If trimlines are not identified and mapped correctly, then any attempt to interpret or date these features will be flawed from the start. Early work with BIIS trimlines by Thorp (1981; 1986; 1987; Figure 3.5) provided some guidance on the identification and mapping of trimlines in the field and using aerial photographs (see Section 3.4). Subsequent expansion on Thorp's methods has largely focused on identifying specific trimline types, mapping trimlines in new study areas or expanding mapping methods using satellite imagery (Section 3.4; e.g. Csatho *et al.* 2005; Figure 3.7). However, trimlines are often very faintly expressed (e.g. Figure 3.9) and can be easily confused with non-glaciogenic linear features. In particular, geological strata and palaeo lake or sea shorelines can appear very similar to trimlines in remotely sensed imagery and even in the field. Furthermore, there has been only limited study of the preservation potential of trimlines and little is known about how trimline expression may change through time. Therefore, trimline features may be being overlooked where they are subdued or otherwise expressed in an atypical manner for their location. Better understanding of trimline formation and improved mapping methods including the use of secondary data, such as geological maps, alongside field validation and cosmogenic dating may resolve trimline identification problems and improve the accuracy of trimline mapping.

3.7 Unexplored territory

So far this literature review has described the development and state of the art in the field of glacial trimline research. Previous research has identified, mapped and interpreted glacial trimlines with a view to use these features in ice surface morphology and ice thickness reconstructions. This narrow focus has led to several under-researched areas, particularly: processes of trimline formation (beyond the ice marginal or thermal debate); the expression of glacial trimlines; the preservation of trimline features; the morphology or shape of individual trimlines; and the wider distribution of glacial trimlines.

In comparison to Quaternary trimlines, there has been far less research into the formation of historic trimlines. The examples of historic trimlines in Figure 3.1 and Figure 3.9 suggest why this is the case: these features tend to be self-evidently formed at the ice margin. However, the existence of thermal trimlines in historic settings cannot be ruled out and

examples may be found as trimlines research expands into new study areas. At present specific modes of trimline expression have not been demonstrated to be associated with either ice marginal or thermal trimline formation. However, consideration of the literature suggests that there may be links between trimline expression and the processes of trimline formation. For example, all vegetation trimlines studied so far have been identified as ice marginal (e.g. Figure 3.1; Wolken *et al.* 2005; McKinzey *et al.* 2004; Kelley *et al.* 2012;). Does this indicate that vegetation trimlines are only formed at the ice margin? What about weathering limits? Both ice marginal (e.g. Ballantyne *et al.* 1997; Ballantyne *et al.* 1998a; Stone *et al.* 1998) and thermal (e.g. McCormack *et al.* 2011; Fabel *et al.* 2012) examples of these features have been identified, which perhaps indicates that these are not diagnostic of a particular process of trimline formation. Further research into the factors affecting trimline formation may help to explain the links between mode of trimline expression and the process of trimline formation, which would assist in the interpretation of different trimline expressions.

The interpretation of different trimline expressions is hampered by the lack of a catalogue of all observable modes of trimline expression. Some existing terminology is descriptive of the expression of the trimline, such as 'vegetation trimline' or 'weathering limit' (see Section 3.2.2). However, many forms of trimline expression have no specific terms and have not been considered at all in the literature, for example discontinuities in erosional or depositional slope features that record a former ice margin position (e.g. Figure 3.9). Until all observable means of trimline expression have been described, it will be difficult to draw conclusions about the interpretation of different trimline expressions.

Similar to trimline formation, there has been not been sufficient consideration of trimline preservation. Some authors make passing comment, for example Thorp (1981) notes that Quaternary trimlines in Scotland are more clearly expressed on spurs and suggests that this is due to a relative lack of modification by postglacial streams, compared to the valley sides. It is also common for the relative sharpness of trimlines to be described; although this is most often used to suggest that sharper trimlines are ice marginal (e.g. Ballantyne *et al.* 1997; Ballantyne *et al.* 1998a) and not generally to considered to be linked to post-glacial trimline modification. Few papers go into detailed discussion of the factors affecting trimline preservation in their study area or into description of the relative preservation of the different modes of trimline expression. A rare exception is Kelly *et al.*'s (2004) Quaternary trimline mapping in the European Alps. Kelly *et al.* found that erosional trimlines were best

preserved where the bedrock resists weathering and that preservation is poor where bedrock is easily weathered and particularly where the bedrock is layered. This finding caused them to research the geology of their study area in greater detail and to use this information to aide in the interpretation of their trimlines. Further research along these lines may highlight other variables that affect trimline preservation and may aide in the interpretation of different modes of trimline expression.

It is possible that the distribution of different trimline expressions could be indicative of trimline preservation potential in different climates, glaciological settings or lithologies. For example, erosional trimlines are more common than vegetation trimlines in Quaternary settings and this is probably because these features preserve better over long timescales. If patterns of different trimline expressions could be linked to the period of time that the trimlines have been exposed to weathering, this may allow for relative dating of trimline features. Further study into trimline preservation in different climatic and geological settings is required to improve understandings of the way that trimline expression changes through time.

Research has yet to consider the possibility of trimline preservation beneath overriding ice cover (e.g. possible alternative explanation for the weathering zones in Figure 3.3). Where glacial features have survived being overridden, this can cause problems with relative dating and with establishing synchronicity. Conversely, the removal or modification of older features by overriding ice can leave gaps in the geomorphological record. It is unclear to what extent these problems affect glacial trimlines. However, the fact that trimlines are common components of palimpsest glacial landscapes, comprising landforms from multiple glaciations, suggests that study of the impact of overriding on trimlines may aide in the relative dating and interpretation of these features.

In many cases the presentation of a geomorphological map is the only clear description given of the morphologies, or shapes, of individual trimlines. The morphology of trimlines could contain information about the processes of trimline formation and could potentially be used to identify overridden trimlines. Figure 3.16 gives a theoretical example where a subtle kink in the morphology of a trimline could be diagnostic of a readvance during deglaciation. However, geomorphological maps do not generally show morphologically accurate individual trimlines but rather mark trimline locations using a generic symbol (e.g. Kelly *et al.* 2004 use single spots to mark individual trimline locations) or simply outline palaeo nunataks or patches of differing thermal regime and imply the presence of a trimline at the boundary

(e.g. Baroni *et al.* 2008). Some studies present field photographs of key trimlines (e.g. Kelly *et al.* 2004; Nesje *et al.* 2007; Forman *et al.* 2007; Glasser *et al.* 2011), but this is not standard practice. An example of good practice in describing individual trimline morphology is the Patagonian study of Glasser *et al.* (2005; 2008), who clearly describe the trimlines of their study area and also present morphologically accurate trimlines in their geomorphological maps (Figure 3.15).

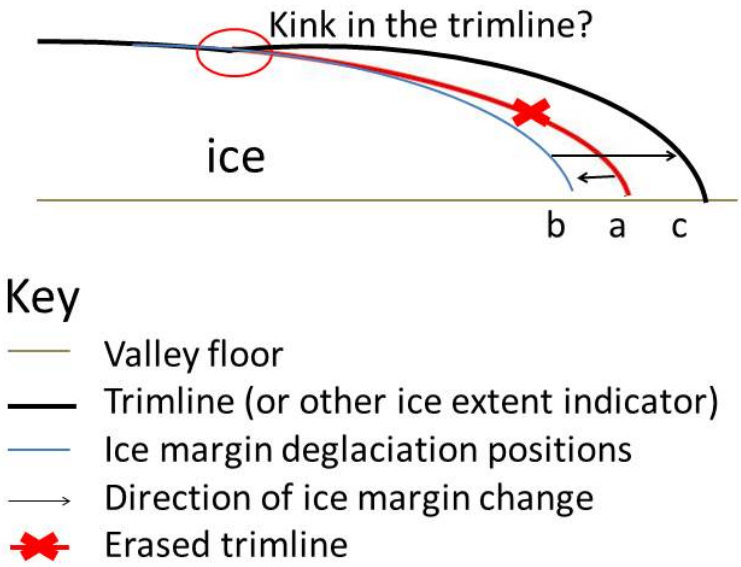

Figure 3.16 – Theoretical example of a small-scale morphological feature, in this case a kink in a glacial trimline, and a suggestion for how this feature may have formed via a readvance during deglaciation. At present, trimlines are not generally mapped in sufficient detail to recognise small-scale morphological features and there has been no discussion of these features in the literature. If these features do exist they may prove diagnostic of particular events, such as the readvance scenario theorised here. Small-scale trimline morphology may be particularly important in areas where surging glaciers are common because subtle differences in trimline morphology may be caused by surging, in the same way that morphological differences in other landforms have been linked to surging.

The one aspect of individual trimline morphology to have been widely discussed is the slope of ice marginal trimlines, which is considered when establishing trimline synchronicity to reconstruct the ice surface across several valleys or massifs (e.g. Figure 3.5b; Ballantyne *et al.* 1997; Ballantyne *et al.* 1998b). Additionally, the record of ice thickness gradients preserved in patterns of trimline slope has been used to deduce palaeo precipitation gradients and to estimate palaeo ELA (see Section 3.5; e.g. Glasser *et al.* 2008). Beyond these applications of trimline slope, have been no attempts to interrogate trimline morphology and determine what further information may be deduced from the morphological features of individual trimlines.

The distribution of trimlines at global and regional scales has also been under-studied. Records of glacial trimlines in a wide range of locations (see Figure 3.4) suggest that these features are not diagnostic of particular glaciological or climatic conditions, but there has not been an overall synthesis of global trimline distribution to confirm this observation. The distribution of specific modes of trimline expression, on the other hand, may well be correlated with glaciology or climatic factors. For example, erosional trimlines may be found to be more common in mid-latitudes compared to polar regions due to the higher percentage of warm-based glaciers, which have higher flow velocities and more erosive potential.

At a regional scale, topography and geology are likely to influence the distribution of trimlines due to the significant impact of these factors on patterns of glacial erosion and deposition. Some authors have mentioned the impact of geology on trimline expression (e.g. McCarroll *et al.* 1995; Kelly *et al.* 2004) but discussion of the impact on trimline distribution tends to be limited, if discussed at all. The impact of topography has been similarly overlooked. Barring brief mention of the concentration of trimlines on spurs by Thorp (1981), hardly any papers have discussed the relationship between topography and trimline distribution within a study area. If further research can better determine the impact of topography and geology on trimline distribution, this information may be significant for the identification and mapping for trimlines. For example, if Thorp's assertion that trimlines are more common on spurs is found to be correct, then this could cause mapping effort to be concentrated on spurs, potentially leading to the identification of subtle trimlines that may otherwise have been overlooked.

The link between the distribution of glacial trimlines and other glaciogenic features has also received little consideration. Glasser *et al.* (2008) briefly mention this subject when they describe that the trimlines of their study area in Patagonia tend to merge down-glacier with lateral and terminal moraines (Figure 3.15). They used this fact to help them interpret the trimlines as ice marginal and to establish synchronicity between the trimlines and the moraines. Aside from this example, the potential links between trimlines and other glacial landforms have received little attention. This omission is particularly significant in Quaternary trimline research because a better understanding of the links between trimlines and other glacial features could shed light on the interpretation of palimpsest glacial landscapes, particularly in establishing synchronicity between trimlines and other glacial features.

In summary, there exist several areas in which the trimlines literature is currently deficient. These 'unexplored territories' have the potential to resolve issues with identifying and mapping trimlines and could also help to establish synchronicity between groups of trimlines and between trimlines and other glacial features. Improvements in understandings of the relationships between trimline expression, morphology, formation and preservation are likely to be particularly significant because of key roles that trimline expression and morphology have in the interpretation of individual trimlines.

3.8 A new terminology

As discussed in Section 3.2, the terminology surrounding glacial trimlines is complex and non-standardised; a fact which is contributing to the issues raised in Section 3.6 and the literature gaps described in Section 3.7. This confusion in terminology leads to a lack of clarity in the discussion of trimline features and may be limiting research by causing papers using specific terminologies to be overlooked. Particular issues surround the blurred distinction between the description of glacial trimlines and their interpretation, as well as the lack of terms to accurately describe different modes of trimline expression.

To avoid confusion and to mitigate the above points, a new and more precise definition for the term 'glacial trimline' is here suggested:

"Glacial trimlines are glaciogenic features that are expressed as a break or transition in the vegetation, weathered material, erosion pattern, deposited material, or slope features on the slopes of a glacierised or glaciated valley."

Note that this definition is inclusive of all glaciogenic features that form any kind of break or transition on a glacierised or glaciated valley side – this means that features like lateral moraines and kame terraces are included as well as the features that have previously been called trimlines. It is clear that many of these features have different expressions and processes of formation, but their similar interpretations and uses in palaeoglacial reconstructions justifies discussing them collectively. Furthermore, the above definition of 'glacial trimline' allows room for both the concept of trimlines as linear features and as areas

of transition between two landsurface zones. The above definition also allows for both lateral and frontal trimline features – 'valley slopes' need not necessarily be lateral but can also refer to the valley floor in front of a glacier or former glacier. Using the above definition, a 'glacial trimline' can be of either ice marginal or thermal origin; both of these processes of trimline formation are glaciogenic so both can be described as 'glacial trimlines' (Figure 3.17).

However, the above definition implies a degree of interpretation to suggest that a given trimline feature is glaciogenic. In order to ensure adequate separation of pure description from any interpretation, the term 'apparent trimline' is suggested for a linear trace or transition on the side of a glacierised or glaciated valley of unknown origin (Figure 3.17).

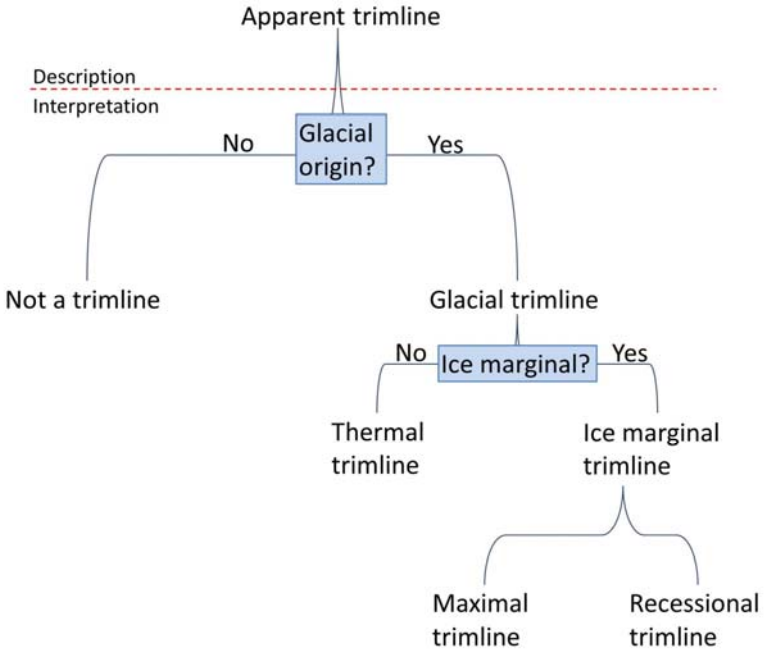

Figure 3.17 – Suggested decision tree for glacial trimline terminology. When a linear feature on the slopes of a glacierised or formerly glaciated valley is identified it is termed an 'apparent trimline', which is a purely descriptive term. The initial interpretation of the feature ascertains whether it is of glacial origin or not. If it is found to be glacial then it is termed a 'glacial trimline' and can be classified according to its expression (Figure 3.19a). Further analysis of the trimline's expression, morphology, preservation, location and age, if known, may allow the formation of the trimline to be determined as either ice marginal or thermal. If the trimline is thought to be ice marginal, further analysis may allow it to be identified as marking a maximal ice margin position, formed by a glacial advance, or as being a recessional feature created by a retreating ice margin.

By distinguishing between ‘apparent trimlines’ and ‘glacial trimlines’, as shown in Figure 3.17, it is hoped that a better separation between description and interpretation of trimline features can be achieved. Once an apparent trimline is determined to be of glacial origin, further interpretation steps can be used to identify it as an ‘ice marginal trimline’ or a ‘thermal trimline’. These terms are preferred to the various alternatives used in the literature (Table 3.1) because their meaning is clear and their usage will provide greater standardisation and clarity.

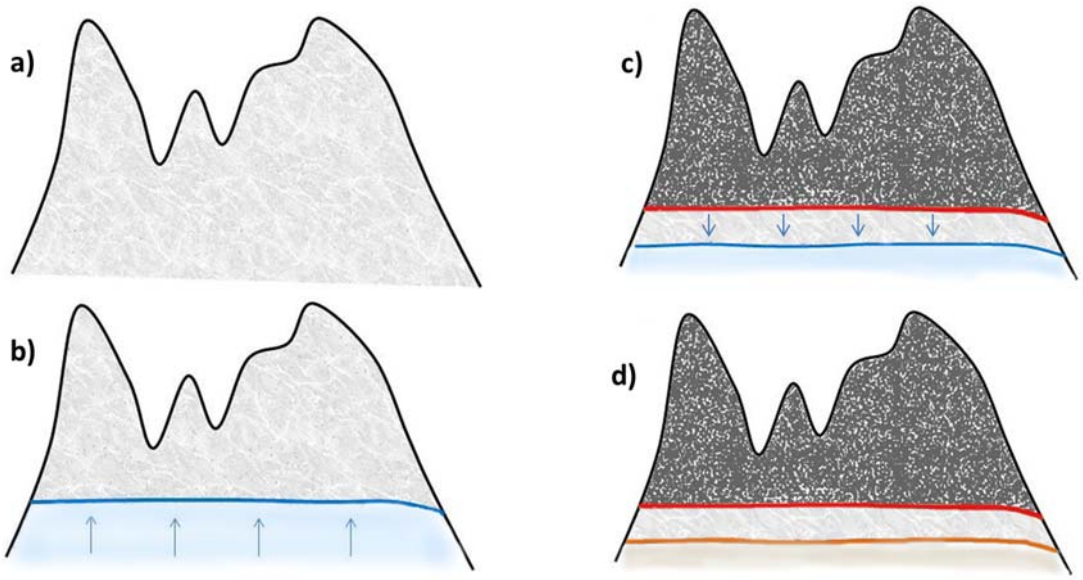

Figure 3.18 – Schematic representation of the difference between maximal and recessional ice marginal trimlines. a) Shows the initial conditions of a mountain side with a fairly uniform surface exposure age. At this stage it would generally be expected that any changes in the surface cover would be gradual and linked to altitude, for example frost-weathering debris cover increasing in thickness with increasing altitude. b) During a glaciation the ice margin advances up the mountain side and glacial erosion removes the surface of the mountain below the ice margin. c) As the ice retreats it exposes a maximal trimline, which records the ice margin position at the peak of the glaciation. The maximal trimline is expressed as a distinction between a zone of glacial scouring below the trimline and an older landsurface above the trimline, which may be distinguished by a sudden change in surface age markers such as vegetation density or depth of frost-weathered debris. d) A standstill or minor readvance during the overall retreat trend leaves a subtler recessional trimline. This trimline may also be expressed as a change in surface aging markers, but the change is likely to be subtler and possibly more diffuse than that of the maximal trimline.

A further terminology distinction, illustrated in Figure 3.17, is between the two possible types of ice marginal trimline: maximal and recessional (Figure 3.18). No research has been conducted into the relative prevalence of these two types of ice marginal trimline in historic settings; although they do appear to exist, for example Figure 3.9 shows a maximal trimline at the 1820 ice margin and a potential recessional trimline two-thirds of the way down to the 2014 ice margin position. In Quaternary settings, Ballantyne and others have given some consideration to distinguishing these two scenarios of trimline formation (Figure 3.13; Ballantyne 1998). Field observations of relative weathering across BIIS trimlines in Scotland have been used to suggest that these features are maximal trimlines, reflecting the LGM or Younger Dryas ice margin (e.g. McCarroll *et al.* 1995; Lamb and Ballantyne 1998; Rae *et al.* 2004; Nesje *et al.* 2007). The existence of observable recessional trimlines in Quaternary settings has not been conclusively demonstrated, possibly because these features may not be as well preserved as maximal trimlines. By introducing the terms 'maximal trimline' and 'recessional trimline', it is hoped that further research will be stimulated into identifying and distinguishing between these two types of ice marginal trimline.

Different types of glacial trimline expression have been called by a wide range of terms in the literature (Table 3.1). In Figure 3.19 an initial attempt at summarising the observable modes of glacial trimline expression is presented alongside specific terms for each of these types. By having individual terms for specific modes of glacial trimline expression it will be easier to clearly describe a given trimline feature and to distinguish and compare multiple glacial trimlines. However, the classification in Figure 3.19 requires testing and refinement to produce a final catalogue of glacial trimline expressions. By presenting this initial classification, is hoped further research will be stimulated that will ultimately lead to a more robust and transparent terminology for glacial trimline expression.

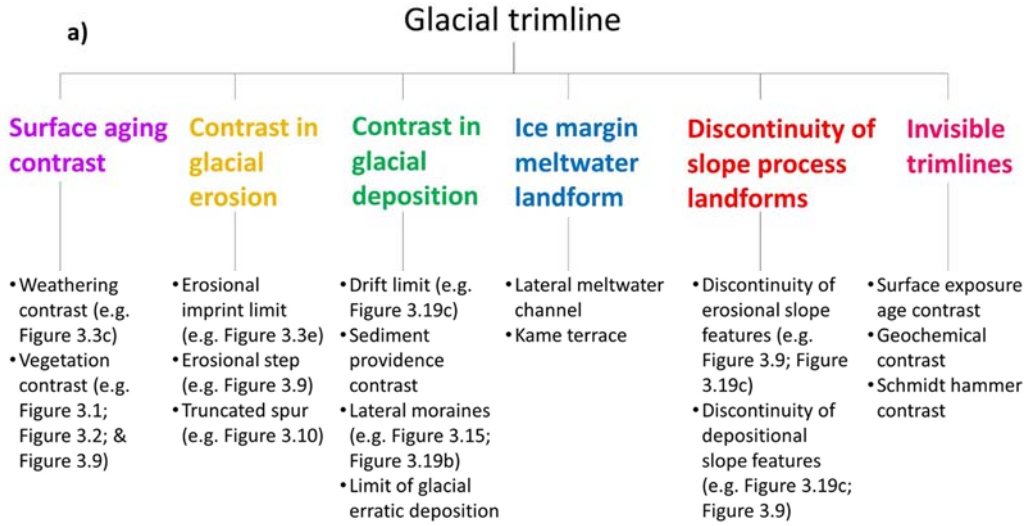

Figure 3.19 – a) Observable means of trimline expression as documented in the literature and from the author's personal experience. This is a suggested categorisation and terminology that requires testing and refinement. b) A series of a lateral moraine trimlines (white dashed lines) on the Pasu Glacier in the Karakorum (Google Earth; imagery from Landsat). Each lateral moraine records a former ice margin position and can be used in the same way as other types of trimline expression. c) This example shows how a trimline (white dashed line) can be expressed by a discontinuity in slope landforms, in this case depositional talus cones and erosional gullies above Conwaybreen in Svalbard (TopoSvalbard; imagery from Norwegian Polar Institute). In this example the trimline is also expressed as the limit of glacially deposited drift. It is very common for trimlines to be expressed in more than one way, which makes categorising them challenging.

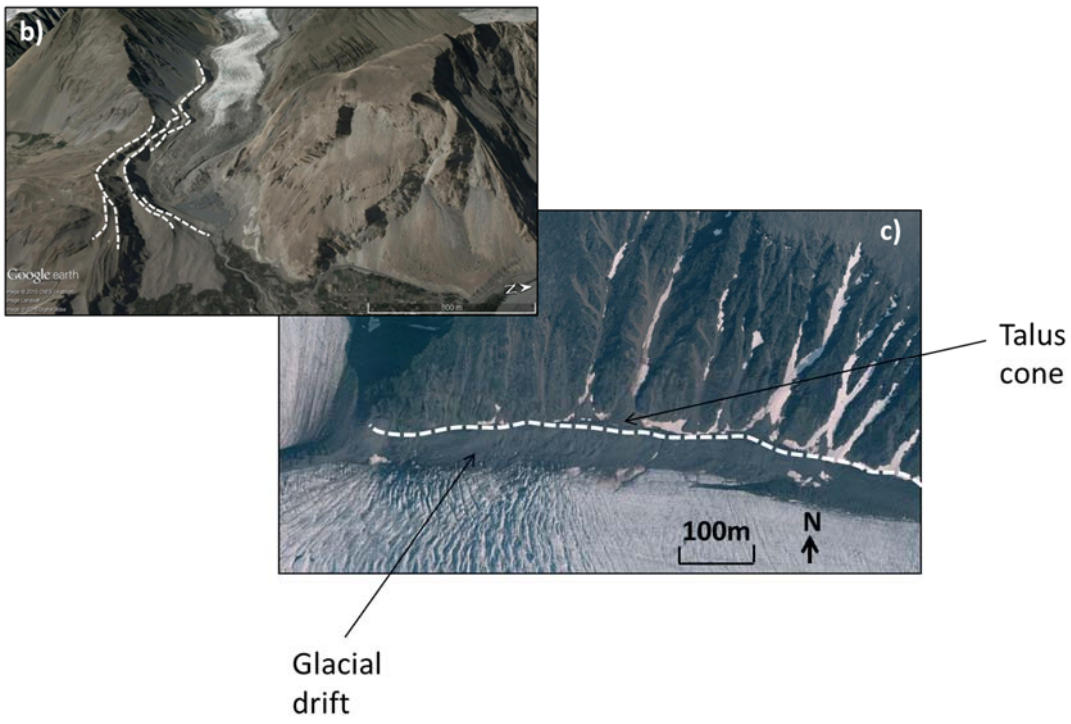

3.9 Conclusions

Overall there has been a significant lack of research into trimline features themselves, particularly their formation, expression, preservation, morphology and distribution. The limited picture that we have of glacial trimlines is potentially leading to inaccurate interpretations of Quaternary and historic trimline features. Additionally, the narrow focus of trimlines research in space and time, as well as the limited range of trimline expressions that have been studied, suggests that expanding the scope of trimlines research may be fruitful.

As well as further research into the trimlines themselves, greater clarity of language is required to progress trimlines research. This literature review has suggested a standardised definition of 'glacial trimline' and a new terminology for modes of trimline expression, which will improve communication within the field and promote research into a wider range of trimline expressions (Section 3.8). This terminology will now be used for the remainder of this thesis.

Improving and expanding the field of glacial trimline research is significant for producing better 3D reconstructions, with which to validate numerical ice sheet models. By allowing quantification of ice volume and elevation changes, as well as glacier response rates when rates of down-wasting are compared to climate records, trimlines are vital for improving predictions of glacier and ice sheet responses to on-going global climate warming. Additionally, better understanding of trimline formation and expression can enable more confident identification of ice marginal and subglacial trimlines, allowing these features to be used more confidently to constrain ice margin positions and reduce the need for subjective interpolation.

3.9.1 Recommendations for further research

From this review of the literature, the following areas have been identified for developing trimlines research:

1. Adoption of a clear and standardised terminology for glacial trimlines. A suggested terminology has been presented in Section 3.8 and Figure 3.17. In particular, clear distinction should be made between pure description and terms implying a degree of interpretation. The remainder of this thesis will demonstrate the use of this new terminology.

2. The production of a comprehensive catalogue of observable modes of trimline expression with specific terminology. This will be invaluable for researching the distribution of different trimline expressions and for determining how interpret these features. An initial attempt has been presented in Figure 3.19a, which will be refined and tested in Chapter 4.

3. Further research is required into the processes of trimline formation and the preservation potential of different types of trimline expression. The influence of climate, glaciological factors and geology/ topography on trimline formation and preservation is likely to be significant and these relationships will be explored further in Chapter 4.

4. The development of a standardised method for identifying and mapping glacial trimlines of different expressions using remotely sensed imagery, to promote more robust and comparable trimline mapping and reduce uncertainty in trimline identification. A new method is developed in Chapter 4 and used to map trimlines in central western Spitsbergen.

5. Closer study of trimline morphology, especially whether morphological features can be used to determine the process of trimline formation. It may be fruitful to consider the trimlines of surge-type glaciers because any particularities in the morphology or expression of surge trimlines could be added to the diagnostic surge landform assemblage. Exploration of the relationships between the modes of trimline expression (Figure 3.19a) and the surge-type glaciers of central western Spitsbergen will consider this possibility (Chapter 4).

6. Use of trimlines in a wider array of palaeoglacial reconstructions, particularly in historic settings where the trimlines can be used to compute ice volume changes compared to the modern glaciers. A reconstruction of the Little Ice Age glacial extent in central western Spitsbergen is presented in Chapters 5 and 6, utilising glacial trimlines alongside the GlaRe tool for producing 3D reconstructions (Pellitero *et al.* 2016).

7. Increased application of cosmogenic nuclide exposure dating to glacial trimlines, particularly outside the British Isles. From this a protocol for identifying synchronous trimlines could be produced. Environmental dating is beyond the remit of this study but this approach is commended to others for further investigation.

Chapter 4

Factors controlling the expression, morphology, distribution and preservation of trimlines: A case study from Svalbard

4.1 Introduction

The recent retreat of Svalbard glaciers since their Little Ice Age (LIA) maximum extent has exposed a wide range of glacial trimlines. These features tend to mark the peak LIA ice margin position, locally reached between 1850 and 1940 (Ziaja 2005; Mangerud and Landvik 2007; Flink *et al.* 2015), but can also record pauses during the overall retreat. The recent historical timing of Svalbard trimlines makes them relatively clear and well-defined features that are closely associated with modern ice margins, allowing the synchroneity of trimlines to be identified with reasonable certainty.

The wide range of observable trimline expressions present on the islands makes Svalbard an excellent location to study the factors influencing the formation of glacial trimlines. A study area in central western Spitsbergen, the largest of the Svalbard islands, was identified and the trimlines mapped and classified according to their mode of expression (Section 4.3). Analysis of the distribution, expression and elevation of the trimlines is presented in Section 4.4. Following this, the relative role of geology, topography and glaciology in controlling trimline formation in Svalbard will be discussed in Section 4.5. The implications for utilising trimlines in palaeoglacial reconstructions, both in Svalbard and in other glaciated and glacierised regions, will be also explored in the discussion (Sections 4.5 and 4.6).

4.1.1 Aims

1. To determine the factors influencing trimline formation by investigating the distribution, expression and elevation of trimlines in central western Spitsbergen.

2. To trial the trimline expression classification (Section 3.8 in Chapter 3) by applying it to the trimlines of central western Spitsbergen.

4.1.2 Research questions

Further to achieving the above aims, the following five research questions have been investigated:

1. What patterns are there in the distribution of trimlines in the study area? For example, are there patterns in the distribution of the different modes of trimline expression?

2. What contextual factors are associated with trimline distribution? Particularly, what is the impact of geological, topographical and glaciological factors on trimline distribution?

3. Are trimlines found above the equilibrium line altitude (ELA)? Are there differences in the expression of trimlines above and below the ELA? Previous research suggests that trimlines may be found above the ELA (e.g. Kelly *et al.* 2004). It is hypothesised that erosional trimlines are more common above the ELA and depositional contrast trimlines below the ELA.

4. Are there differences in the expression, elevation or distribution of trimlines associated with land-terminating glaciers compared to tidewater glaciers? It is expected that glaciers with active calving margins will have a higher ice flux, creating sharper trimlines that are predominantly erosional.

5. Are there differences in the expression, elevation or distribution of trimlines associated with surge-type glaciers compared to non-surging glaciers? Similar to calving glaciers, surge-type glaciers are hypothesised to preferentially create erosional trimlines.

4.2 Study area

The Svalbard archipelago is situated in the Barents Sea at a latitude range of 74^{o} to 81^{o} north. Spitsbergen, the largest island, has been well-studied and the glacial history is reasonably well constrained, particularly along the west coast (Ingólfsson 2011). The study area is located on the west coast of Spitsbergen in the central region between Kongsfjorden in the north and St. Jonsfjorden in the south (Figure 4.1). This area was chosen partially for logistical reasons but also because the glacial geomorphological evidence and stratigraphy has been previously documented. Previous studies have attempted to produce reconstructions of the LIA ice thickness (e.g. Lønne and Lysså 2005 Navarro *et al.* 2005; Ziaja 2005; Kohler *et al.* 2007; Mangerud and Landvik 2007; Nuth *et al.* 2007) but have made little to no use of glacial trimlines, despite the fact that these landforms are very widespread in the study area.

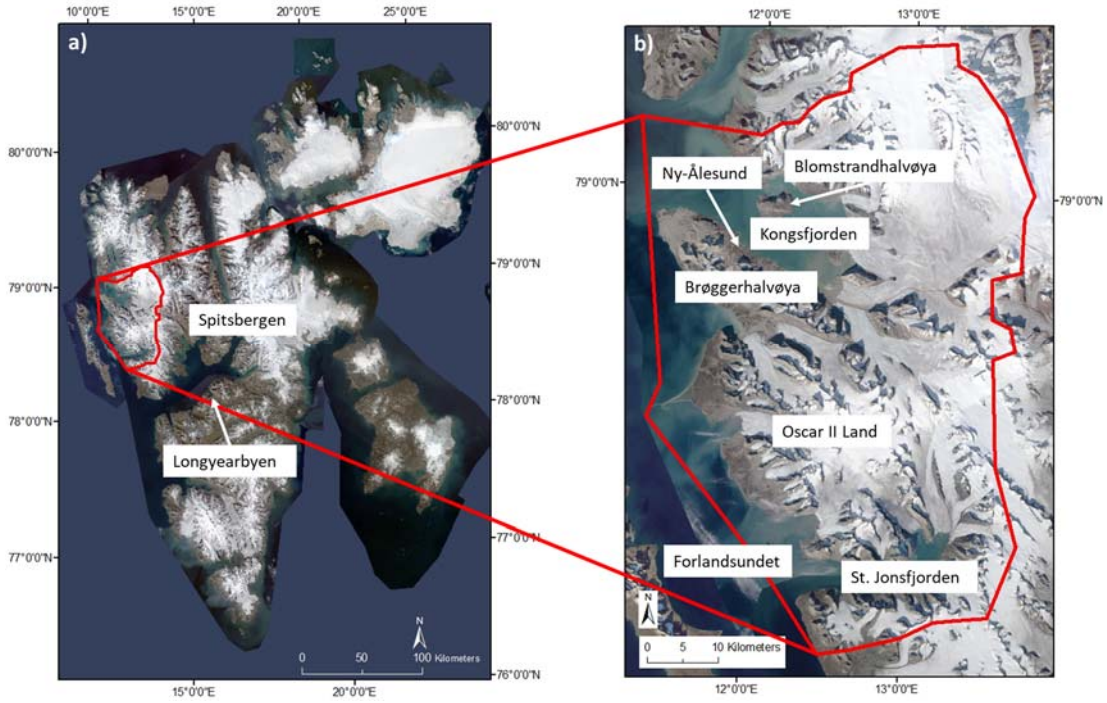

Figure 4.1 – a) The main Svalbard archipelago with the study area in central western Spitsbergen outlined in red. b) A closer view of the study area with place names referred to in the text. Map from the Norwegian Polar Institute (http://geodata.npolar.no/)

4.2.1 Geography, climate and modern glaciers

Central western Spitsbergen is a predominantly mountainous area bounded by two prominent fjords, Kongsfjorden in the north and St. Jonsfjorden in the south (Figure 4.1). The study area's location on the west coast of Spitsbergen means that the majority of valleys are orientated east-west, although the valleys flowing into the two fjords and those on the Brøggerhalvøya peninsula tend to be oriented north-south. The research town of Ny-Ålesund is located in the study area on the north shore of Brøggerhalvøya.

The area is heavily glacierised, with 78 glaciers covering 69% of the land area. The glaciers of central western Spitsbergen represent a wide range of different glacier types and morphologies. The majority are valley or cirque glaciers of 2-5 km length but there are several larger valley or icefield outlet glaciers, which can be up to 44 km long (Table 4.1). Of these larger glaciers, 15 are marine-terminating, flowing either into Kongsfjorden, St. Jonsfjorden or the Forlandsundet. These marine-terminating glaciers will be referred to as 'tidewater glaciers' in this study. The terrestrially-terminating glaciers in the study area tend

to be constrained to their valleys but Oscar II Land features a flat coastal plain on to which several valley glaciers flow out and form large piedmont lobes.

The study area has an Arctic maritime climate, which is typical for Svalbard. In the seas around Svalbard the West Spitsbergen Current brings heat and some precipitation to the archipelago but average temperatures remain low, with a mean annual air temperature of -6^{o}C at sea level (Ingólfsson 2011). These temperatures produce extensive permafrost cover and mean that the majority of Svalbard glaciers are polythermal, although the smallest valley and cirque glaciers may be completely cold-based (Nuth *et al.* 2007). Differences in the flow rates and erosive abilities of polythermal and cold-based glaciers in the study area may lead to observable differences in trimline expression. For example, it is hypothesised that erosional trimlines will be more prevalent around polythermal glaciers compared to cold-based ice masses, which may be primarily associated with trimlines expressed as a contrast in surface aging.

Svalbard is particularly known for surging glaciers. The study area features 30 surge-type glaciers, which have either been observed during a surge or are associated with glacial or geomorphological features that are diagnostic of surging (H. Sevestre pers. comm. 2015; Figure 4.2). These glaciers tend to be amongst the largest and are well distributed throughout the study area. There is a strong coincidence between tidewater and surge-type glaciers, with nine of the study area's 15 tidewater glaciers also classified as surge-type (Figure 4.2). Surging behaviour has been linked to several distinctive landforms, such as crevasse-squeeze ridges (Evans and Rea 2003), and here we hypothesise that surge-type glaciers may produce trimlines with different characteristics compared to the trimlines of non-surging glaciers. Where there is a coincidence of surge-type glaciers and tidewater glaciers this may also lead to distinctive trimlines.

Table 4.1 (next page) – This table lists all of the glaciers in the study area, alongside their lengths and areas. The glaciers are colour-coded to reflect their glacier type and are listed in size order by area, from smallest to largest. Normal glaciers are white, tidewater blue, terrestrial surge-type gold, and tidewater surge-type red. Inspection of this table shows that the glaciers of central western Spitsbergen vary greatly in size but several trends are apparent. Normal glaciers are generally smaller than either tidewater or surge-type glaciers. Tidewater glaciers amongst the largest, with nine of the ten largest glaciers by area being either tidewater or tidewater surge-type glaciers. Data from the Norwegian Polar Institute.

Glacier number	Name	Length (km)	Area (km^2)
94	Midtre Lovénbreen	0.4	114
28	Botnbreen	0.5	130
27	Unnamed	0.5	151
10	Unnamed	0.5	205
95	Unnamed	0.8	206
24	Unnamed	0.8	234
93	Midtre Lovénbreen	0.9	277
106	Holmeslettbreen E	0.5	281
47	Uversbreen	0.8	295
50	Arthurbreen	1.3	330
97	Unnamed	1.0	341
22	Unnamed	0.8	360
1	Holmeslettbreen E	0.5	386
26	Konowbreen	1.0	419
105	Holmeslettbreen W	0.8	425
96	Unnamed	1.0	430
92	Unnamed	1.1	430
2	Holmeslettbreen W	0.7	489
42	Unnamed	1.6	493
66	Kjærfjellbreen	0.9	529
31	Unnamed	1.5	673
37	Vestre Lovénbreen	1.6	829
67	Trongskarbreen	1.4	857
98	Unnamed	2.0	861
68	Mørebreen	0.9	958
40	Steenbreen	1.8	1000
13	Unnamed	1.6	1049
6	Unnamed	1.7	1123
57	Oliverbreen	1.9	1155
30	Tassbreen	1.8	1181
36	Vestre Lovénbreen	1.3	1217
52	Haakenbreen	1.8	1394
69	Olsønbreen	1.7	1550
18	Smalgangen	2.3	1607
51	Cissybreen	1.9	1630
16	Paulbreen	3.9	1953
14	Unnamed	2.0	1980
107	Vegardbreen	2.8	2351
59	Eivindbreen	3.0	2523

Glacier ID	Name	Length (km)	Area (km^2)
64	Skreifjellbreen	2.9	2662
34	Waldemarbreen	2.9	2792
0	Gunnarbreen	3.9	3159
3	Anna Sofiebreen	2.1	3235
32	Irenebreen	2.7	3455
29	Edithbreen	4.1	3616
21	Ankerbreen	2.6	4225
45	Vestre Brøggerbreen	3.6	4634
33	Erikkabreen	4.8	4646
49	Arthurbreen	3.8	4690
38	Austre Lovénbreen	3.4	5013
35	Midtre Lovénbreen	3.6	5202
58	Andreasbreen	4.2	5262
41	Botnfjellbreen	3.7	5869
39	Pedersenbreen	4.9	6245
62	Feiringbreen	5.7	7387
15	Vegardbreen	4.3	7782
46	Austre Brøggerbreen	4.9	9709
5	Løvliebreen	4.2	11039
63	Fatumbreen	6.8	11598
54	Elisebreen	6.6	12567
4	Bullbreen	4.2	14507
20	Gaffelbreen	6.0	21246
7	Charlesbreen	9.1	25641
17	Vintervegen	12.0	29315
19	Konowbreen	10.4	46556
60	Conwaybreen	14.7	53948
53	Comfortlessbreen	14.3	57819
56	Sidevegen	18.7	64499
48	Uversbreen	17.0	66091
43	Aavatsmarkbreen	13.2	73212
23	Osbornebreen	17.2	74371
99	Infantfonna	29.8	77899
25	Osbornebreen	18.0	82347
65	Blomstrandbreen	15.6	88620
55	Kongsvegen	25.5	108211
44	Dahlbreen	16.3	126490
91	Kronebreen	44.7	295209
61	Kongsbreen	37.4	378328

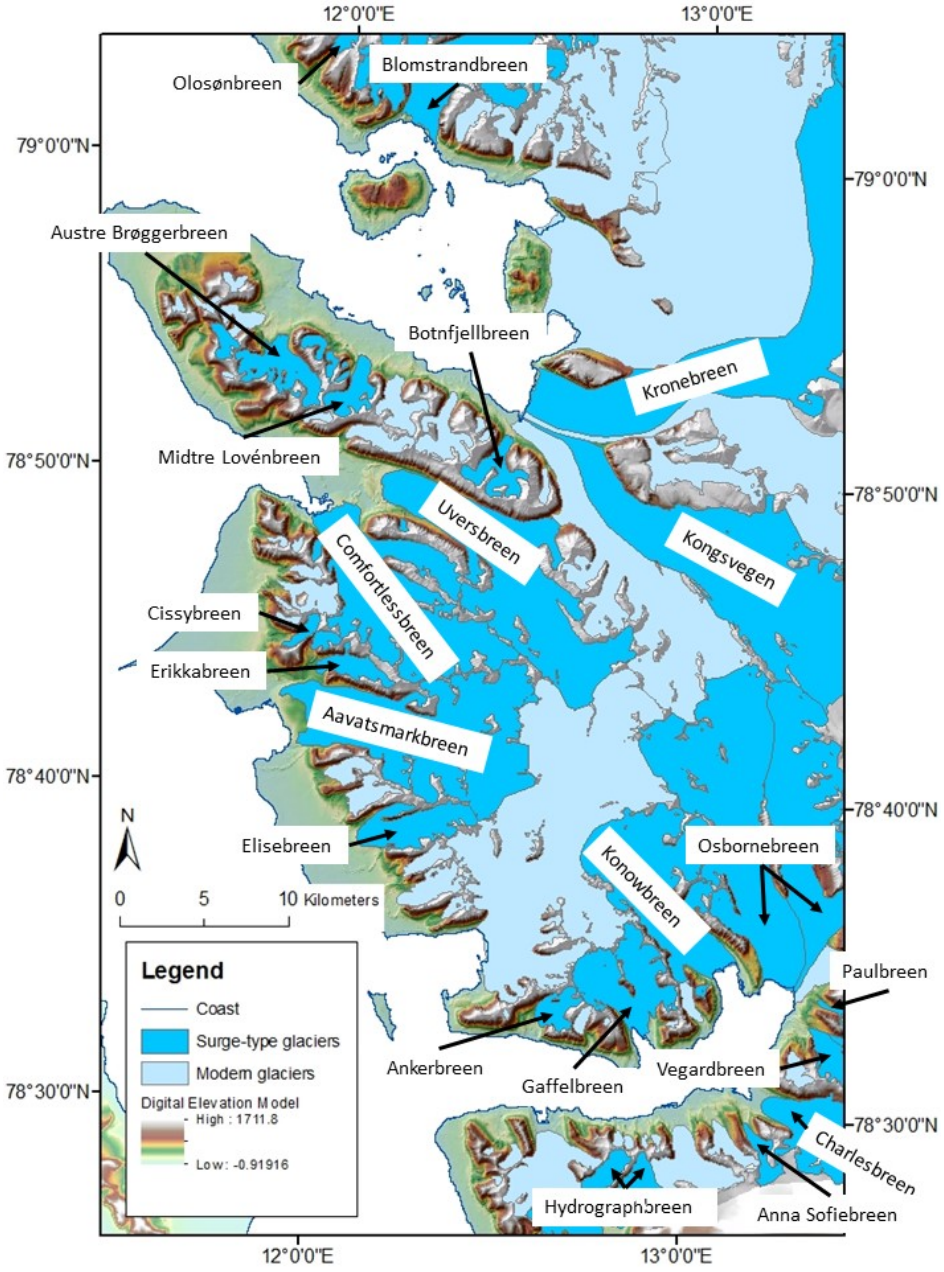

Figure 4.2 – this map shows the surge-type and non-surging glaciers of central western Spitsbergen. The surge-type glaciers are labelled, for easy comparison with Table 4.1. From this map it is clear that surge-type glaciers are distributed throughout the study area and that there is a strong coincidence between surge-type glaciers and tidewater glaciers, with nine of the 15 tidewater glaciers also thought to be surge-type. These tidewater surge-type glaciers tend to be amongst the largest glaciers in the study area, comprising six of the ten largest glaciers by area (Table 4.1). The size of these larger surge-type glaciers dominates the map but surge-type glaciers actually account for roughly half (55%) of the of the glaciated area in central western Spitsbergen. The glacier outlines and background DEM were sourced from the Norwegian Polar Institute (http://geodata.npolar.no/ [accessed 23/03/2016]). The surge-type glaciers were identified from H. Svestre's inventory of Svalbard surging glaciers (H. Sevestre pers. comm.).

4.2.2 Geology

The study area geology can be broadly divided into three categories: metamorphic Precambrian and Caledonian Hecla Hoek basement; sedimentary Permian and Triassic platform cover; and Tertiary and Quaternary deposits (Dallmann 2015; Figure 4.3a). The study area's complex geology is also reflected in the large number of faults in central western Spitsbergen, which has influenced the topography by favouring the development of valleys and fjords along fault lines (Figure 4.3b). This impact of geology on topography exerts a control over the location of glaciers, particularly larger glaciers, which indirectly influences the location of trimlines in the study area.

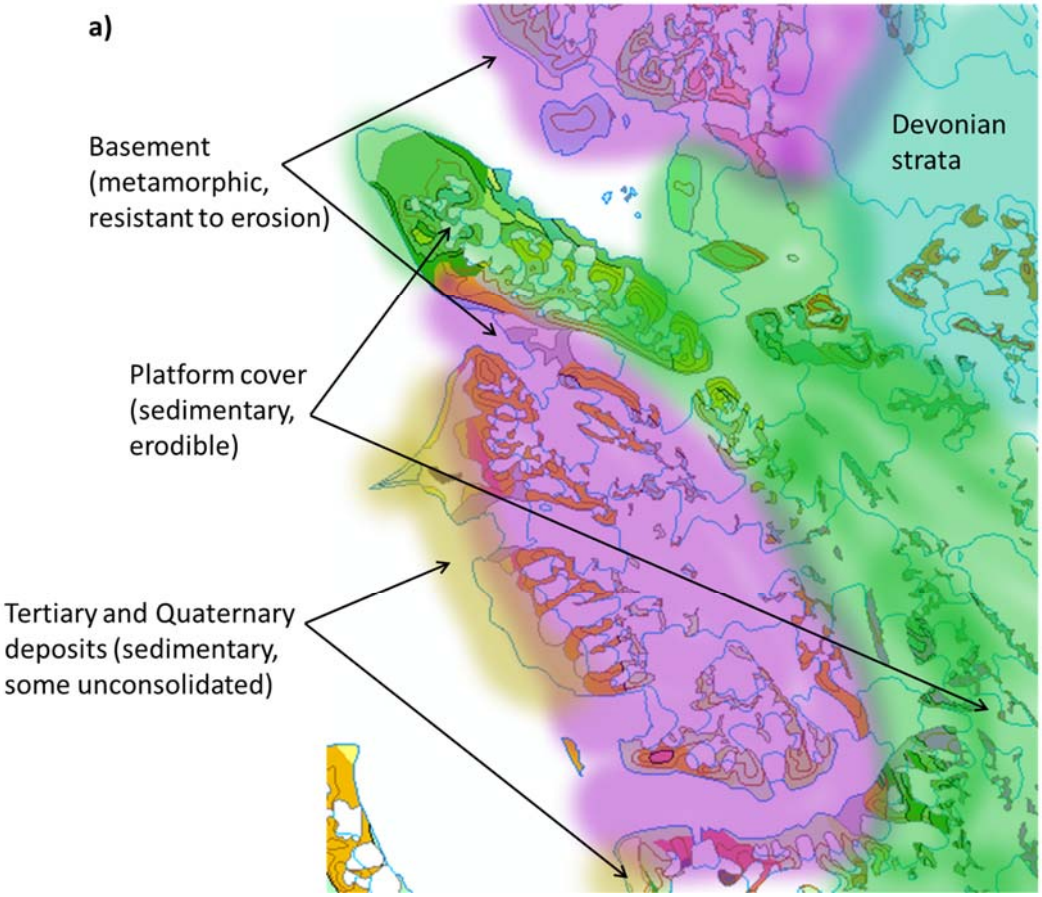

Figure 4.3 (4.3b on next page) **–** a) A generalised geological map of the study area, which has been simplified from the geological maps produced by the Norwegian Polar Institute (sheets A6G; A7G; A8G; and B8G). This map draws out the key distinction between the erosion resistant metamorphic basement and more erodible platform cover and sedimentary deposits. b) Shows the major geological faults in the study area, which are clearly associated with the topography and appear to exert a control over the locations of large glaciers. The fault map is taken from the Norwegian Polar Institute's online geological map (http://svalbardkartet.npolar.no/)

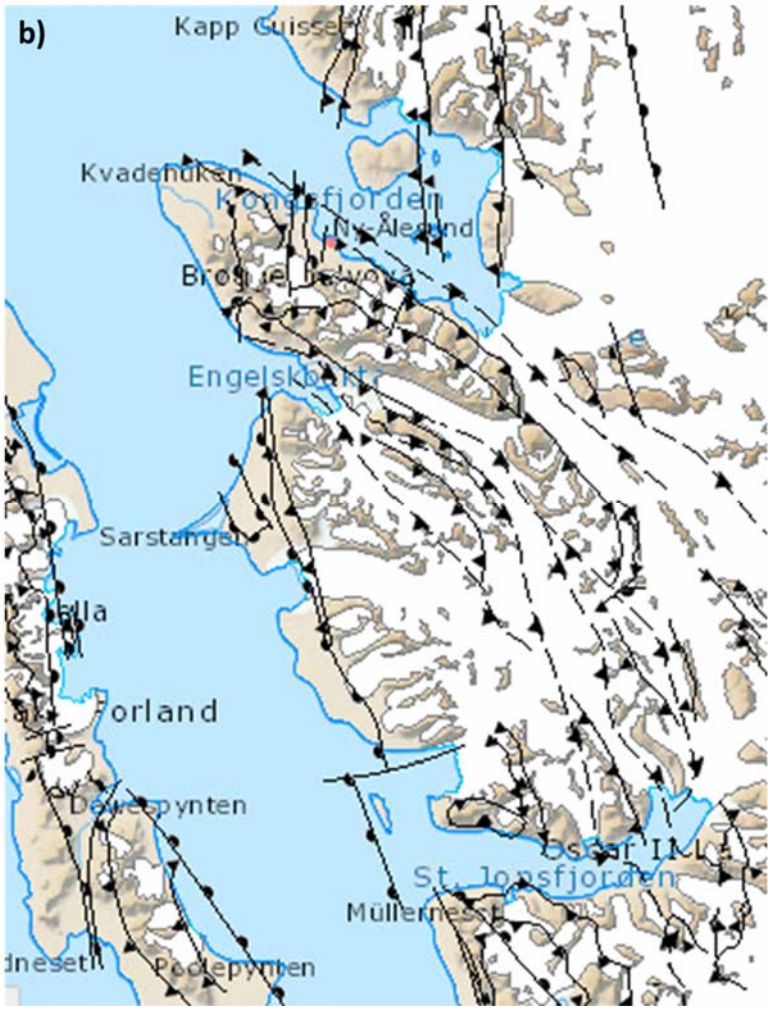

The contrast between the resistant basement and the more easily eroded platform cover and sedimentary deposits might also be expected to directly control patterns of trimline distribution, expression and elevation. Previous trimline research has observed differences in the concentration and expression of trimlines on more resistant bedrock. For example, Kelly *et al.* (2004) found that erosional trimlines were more prevalent in areas of more resistant bedrock within their study area in the European Alps. In order to better define the relationship between geology and trimlines, this study will consider the impact of geology on the distribution and expression of trimlines in central western Spitsbergen.

Geology can also cause problems in the identification and mapping of glacial trimlines. Geological faults and strata can be expressed in a similar way to glacial trimlines, leading to the potential misidentification of faults as trimlines. This issue will be considered in more detail in the discussion of the methods used to map trimlines in the study area (Section 4.3).

4.2.3 Glacial history

Svalbard has been wholly covered by ice several times during the Quaternary (Ingólfsson 2011). The most recent of these large-scale glaciations peaked at around 20,000 BP (Landvik *et al.* 1998; Ingólfsson and Landvik 2013) and is termed the Last Glacial Maximum (LGM), which covered the entire Barents Sea region with ice that was confluent with the continental Fennoscandian Ice Sheet (Landvik *et al.* 1998; Ingólfsson 2011). This glaciation has often been referred to as the Weichselian or Late Weichselian glaciation in the Svalbard palaeoglacial literature and these terms can generally be considered synonymous with the use of the term 'LGM' as applied by this study.

Since deglaciation from the LGM ice limits, Svalbard glaciers have readvanced on two occasions – during the Younger Dryas (YD c. 13,000 BP; Sejrup *et al.* 2005) and the Little Ice Age (LIA c. 1850-1940 AD). The majority of trimlines in central western Spitsbergen are likely to be associated with one of these post-LGM glacial events, due to the obliterative effect that these readvances may have had on any trimlines that may have formed as the ice sheet retreated from its LGM limits.

The extent of the ice cover in the Younger Dryas in Svalbard has been the subject of significant debate, particularly how the YD readvance compares to the LIA (Lønne and Lyså 2005; Hormes *et al.* 2013). Onshore evidence for the YD on Spitsbergen has been difficult to identify, with most well-studied landforms confidently linked to the LIA (Lønne and Lyså 2005). There are two potential explanations for the lack of YD landforms: 1) the YD ice cap extended offshore, so the evidence of this glacial event is concentrated offshore and the limited onshore evidence has been re-worked subsequently (Lønne and Lyså 2005); or 2) that the LIA on Svalbard was more extensive than the YD and removed any YD landforms (Mangerud and Landvik 2007). Recent bathymetric surveys of the Svalbard fjords and the surrounding continental shelf have shown no significant evidence of YD glaciation (Winsborrow *et al.* 2010). This finding supports the second theory, suggesting that the LIA glaciation was more extensive on Svalbard than the YD, particularly on the west coast of Spitsbergen (Mangerud and Landvik 2007).

The more extensive LIA glaciation on western Spitsbergen is at odds with North Atlantic glaciated regions, such as Scotland, where the YD was significantly more extensive than the LIA (Mangerud and Landvik 2007; YD in Scotland reviewed by Golledge 2010). The reasons for the larger LIA glaciation on Svalbard remains the subject of on-going debate (Hormes *et al.* 2013). However, the most popular theory at present suggests that a precipitation shadow

affected western Spitsbergen during the YD, limiting ice growth and leading to a reduced readvance compared to other North Atlantic glaciated regions (Mangerud and Landvik 2007). This situation mirrors the YD in Scotland, which was more extensive in the west but much reduced in the east, due to a precipitation shadow effect (Mangerud and Landvik 2007).

Regardless of the cause for the anomalously extensive LIA glaciation on Svalbard, this theory suggests that the trimlines of central western Spitsbergen are more likely to be LIA features and not associated with the YD. Therefore, a better understanding of these features will assist with the creation of 3-dimensional (3D) reconstructions of the LIA ice surface and ice thickness.

Previous studies have produced post-LIA retreat reconstructions for the glaciers of Svalbard, some of which include part or all of central western Spitsbergen (e.g. Bamber *et al.* 2005; Kohler *et al.* 2007; Nuth *et al.* 2007; Nuth *et al.* 2010). Of these reconstructions Nuth *et al.* (2007) is the most comprehensive and focuses on using historical maps to determine ice surface elevation change and estimate the geodetic mass balance during the retreat from the LIA ice limits. Nuth *et al.* (2007) produced their reconstruction by comparing topographic maps dating to just after the LIA maximum, produced from a 1936-38 aerial survey of Svalbard, with a Digital Elevation Model (DEM) produced from a repeat aerial survey conducted in 1990. This allowed them to compute changes in ice surface elevation relatively accurately. However, Nuth *et al.'s* method assumes that all the glaciers they studied reached their LIA maximum positions in the 1930s, which is far from certain. Other studies have suggested much earlier dates for the peak LIA in Svalbard, such as Mangerud and Landvik (2007) who dated the peak LIA at Scottbreen in southern Spitsbergen to 1900. Trimlines could be used to improve Nuth *et al.'s* reconstruction by providing a firm LIA ice margin position, from which the LIA ice surface could be reconstructed with greater confidence. Several other reconstructions of recent ice elevation or volume changes in Svalbard (e.g. Bamber *et al.* 2005; Kohler *et al.* 2007; Nuth *et al.* 2010) use similar methods to Nuth *et al.* (2007) and could also be constrained using the empirical evidence provided by glacial trimlines. Trimlines could also be used to expand the temporal range of these reconstructions, which at present are limited to the first aerial survey of Svalbard in 1936-38, and may potentially extend Svalbard LIA reconstructions into new areas that were not covered by the early aerial surveys.

Improving the spatial and temporal scale and better constraining 3D glacial reconstructions in Svalbard is important for understanding the relationship between these high Arctic

glaciers and the climate. A full comprehension of the impact of changing climate on ice extent and volume in Svalbard is necessary to predict how these glaciers will respond to on-going anthropogenic climate change, which is likely to have a particularly strong warming affect in the Arctic region (IPCC 2014). Nuth *et al.* (2007) compared their 1990 DEM with modern observations and found that glacier thinning rates have increased dramatically over the last 20-25 years compared with the period from 1936-90. This illustrates how rapidly the glaciers of Svalbard are changing and suggests that trimlines may even be identified from this most recent acceleration of thinning.

As well as aiding in attempts to understand the response of Svalbard glaciers to climate change, trimline research may shed light on the past and future behaviour of tidewater and surge-type glaciers in the archipelago. The work of Nuth *et al.* (2010) identified different thinning patterns for surge-type glaciers that were reflected in the geodetic mass balances of Svalbard surge-type glaciers since 1965. This different thinning response may be recorded in the trimlines of surge-type glaciers and similar trends may be identified in trimlines associated with tidewater glaciers, allowing the responses of these glaciers to post-LIA climate change to be better understood. Furthermore, trimlines may enable the position of LIA tidewater calving margins to be more accurately reconstructed and may also identify previously confluent glaciers. If distinctive trimline expressions, distributions or elevations can be linked to either surge-type or tidewater glaciers, then this information could be used to identify palaeo tidewater or surge-type glaciers in more ancient Quaternary settings.

4.3 Data and methods

4.3.1 Data sources

The trimlines in central western Spitsbergen were mapped from remotely sensed data. The primary imagery used for trimline mapping was a Landsat 7 scene (Figure 4.4a and Figure 4.4b), covering the whole study area, which was captured on 1st August 2015 using the Enhanced Thematic Mapper Plus (ETM+). The Landsat 7 ETM+ data is comprised of eight bands, with a resolution of 30 m for bands 1-7 and a higher resolution of 15 m for the panchromatic band 8. Alongside the Landsat satellite data, very high resolution (40-50 cm) aerial imagery from the Norwegian Polar Institute (NPI) was used to refine the trimline mapping and to assist in the classification of the modes of trimline expression (Figure 4.4c). The images were visually analysed in the NPI's TopoSvalbard online platform

(http://toposvalbard.npolar.no/) because it was not possible to acquire copies of the photographs for financial reasons. However, the combination of digitising trimlines directly onto the Landsat scene in ArcGIS 10.1 alongside visual comparison with the NPI aerial imagery was considered sufficiently accurate (see Section 4.3.2 for the resolution of the mapping method).

In addition to the satellite and aerial imagery, a 20 m resolution Digital Elevation Model (DEM) was acquired to provide elevation and slope information for the trimline features and to enable analysis of the surrounding topography (Figure 4.4d). The DEM was produced by the NPI in 2014 from stereo aerial imagery and was accessed from the NPI geodata website.

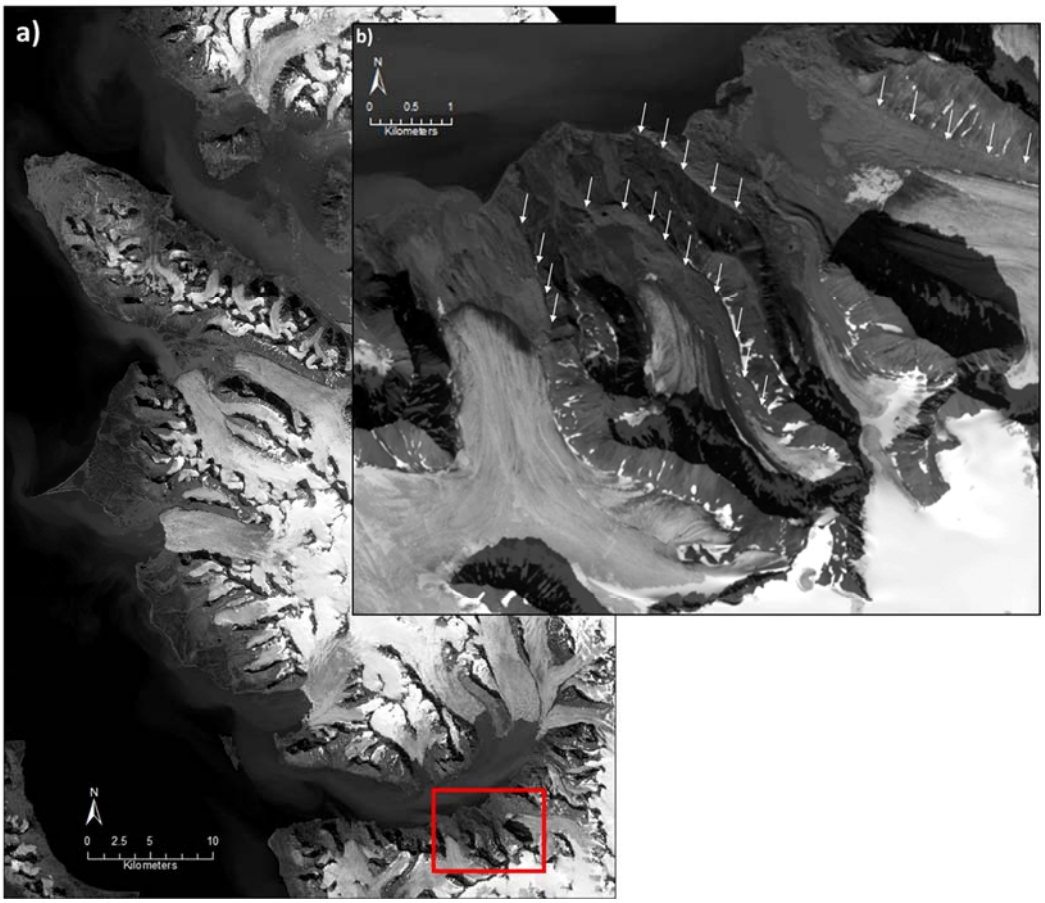

Figure 4.4 (4.4c and 4.4d on the next page) – Examples of the primary mapping data. a) The panchromatic band (number 8) of the 1st August 2015 Landsat 7 ETM+ image covering the entire study area. This band was used as the main imagery for trimline mapping because it has a resolution of 15 m compared to 30 m for the other ten bands. All 11 bands of the Landsat scene were downloaded from the United States Geological Survey (http://landsatlook.usgs.gov/viewer.html). b) A zoomed in section of the Landsat 7 image on the south side of St Jonsfjord, location indicated in Figure 4.4a by the red box. Example trimlines are marked by white arrows. c) An example of the NPI aerial imagery for the same region of the study area, again with trimlines marked by arrows. The NPI photographs were acquired during the summers of 2008-2012, in 2009 in this example, and have a resolution of 40-50cm. They were not used as the primary trimline mapping imagery because it was not

possible to purchase imagery covering the entire study area. However, it is possible to view the images online and this enabled them to be used as a visual reference during trimline mapping. d) Shows the 20m DEM covering the same area depicted in Figures 4.4b and 4.4c and the same trimlines are again marked with arrows. By manipulating the lighting of the DEM and comparing to the Landsat image and the aerial photographs, it was possible to identify and map trimlines with high confidence.

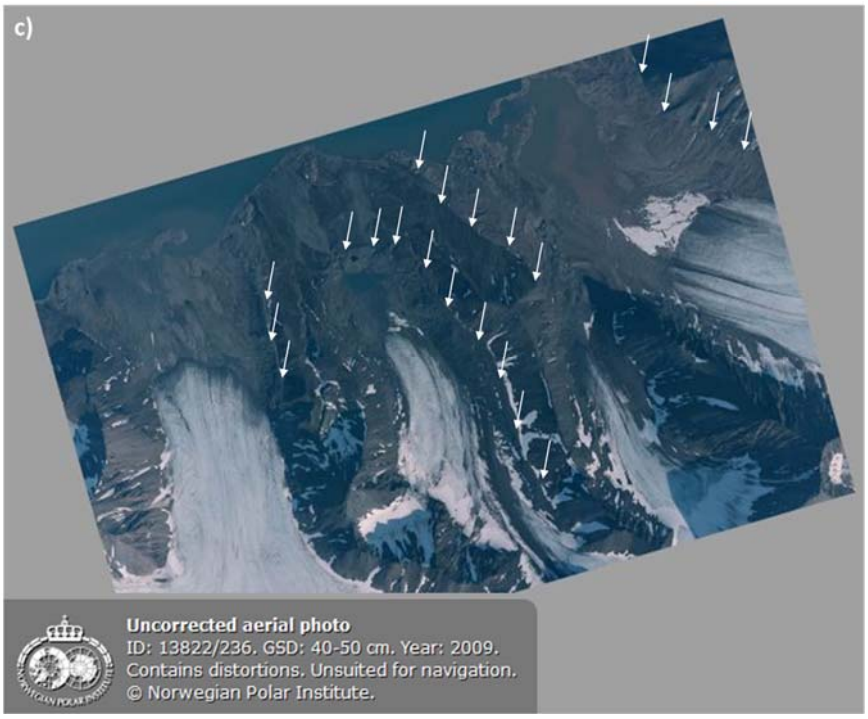

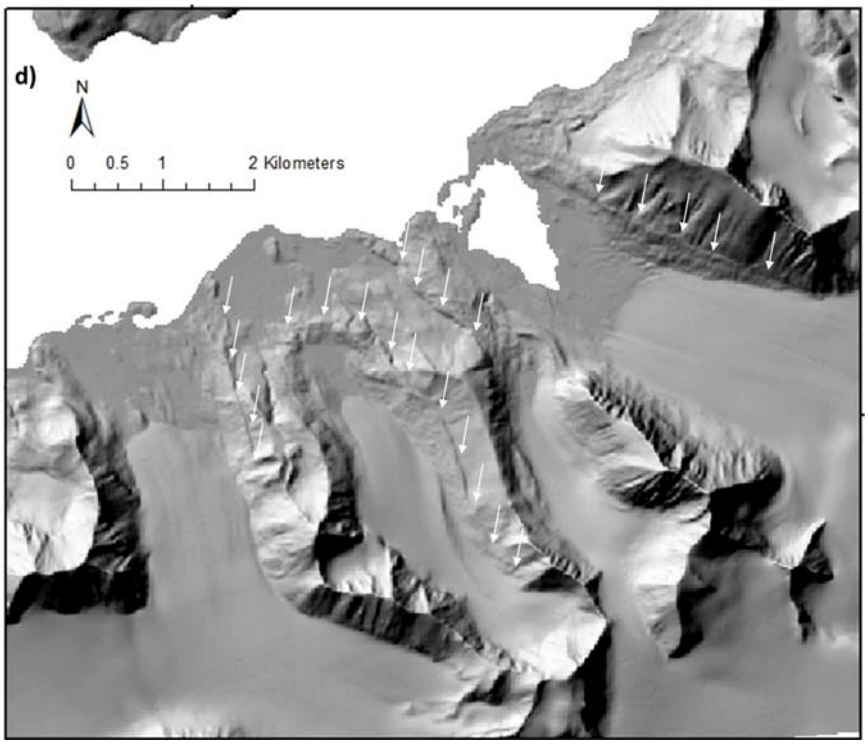

Various secondary data sources were used during the analysis. Paper geological maps of central western Spitsbergen, with a scale of 1:100,000, were purchased from the NPI and digital copies, with a scale of 1:250,000, were downloaded from the NPI geodata website for use in ArcGIS. The NPI geodata website was also the source of a GIS layer of glacier margins that provided polygon outlines of all the glaciers in the study area for the years 1936/1966-1971, 1990 and 2001-2010. A list of the surge-type glaciers in central western Spitsbergen was compiled using Sevestre's Svalbard surging glacier inventory (Sevestre 2015; Table 4.1).

Field photographs of several trimlines in central western Spitsbergen were acquired by the author and by M. Henriksen during July and August 2015. Although it was not possible to directly visit the trimlines in most cases, these photographs and associated field observations were used to provide additional validation of the mode of trimline expression.

4.3.2 Methods of trimline mapping

The primary trimline mapping was carried out in ArcGIS 10.1 using the panchromatic band (band 8) of the 1st August 2015 Landsat scene. This band has a resolution of 15 m. Further validation of the mapping was carried out by using other Landsat bands, which have a resolution of 30 m, to create composite images in ArcGIS. True and false colour composites were used to identify changes in surface colour that could represent trimlines. The DEM was also used to identify apparent trimlines by altering the direction and angle of illumination to pick out changes in surface texture and to identify moraine crests. Throughout the mapping process, the NPI aerial photographs were visually consulted to confirm each apparent trimline and to improve the accuracy of the mapping.

Tests of the geolocational accuracy of this mapping method were carried out using NPI aerial imagery of the town of Ny-Ålesund (acquired from the NPI geodata website: http://geodata.npolar.no/). Features of known positions, such as roads and buildings, were mapped directly from the aerial imagery and from the Landsat scenes, using the method outlined above. Comparison between the maps produced from these two types of imagery showed that the Landsat mapping had a locational accuracy of 17.5 m, only 2.5 m less accurate than mapping directly from the aerial imagery. This test justified the use of the Landsat scene as the primary data source for trimline mapping.

Once all apparent trimline elements had been mapped on to the Landsat image, steps were taken to identify any potentially non-glacial features. This involved consulting the NPI aerial imagery alongside the geological maps and glacier outlines to identify any apparent trimlines

that were likely to be of geological origin, i.e. marking a fault line or rock boundary, or were probably debris-covered ice margins. The primary mapping identified 408 apparent trimlines, of which 11 were found to be potentially not glacial trimlines. Therefore, these features were excluded from further analysis, leaving a data set of 397 confirmed glacial trimline elements in central western Spitsbergen.

4.3.3 Classification of trimline expression

Figure 4.5 shows the classification of the modes of trimline expression used in this study. Every glacial trimline in the study area was classified into one or more of six broad expression categories: 1) contrast in glacial deposition; 2) contrast in glacial erosion; 3) moraines; 4) ice margin meltwater landforms; 5) discontinuity of slope process landforms; 6) contrast in surface aging.

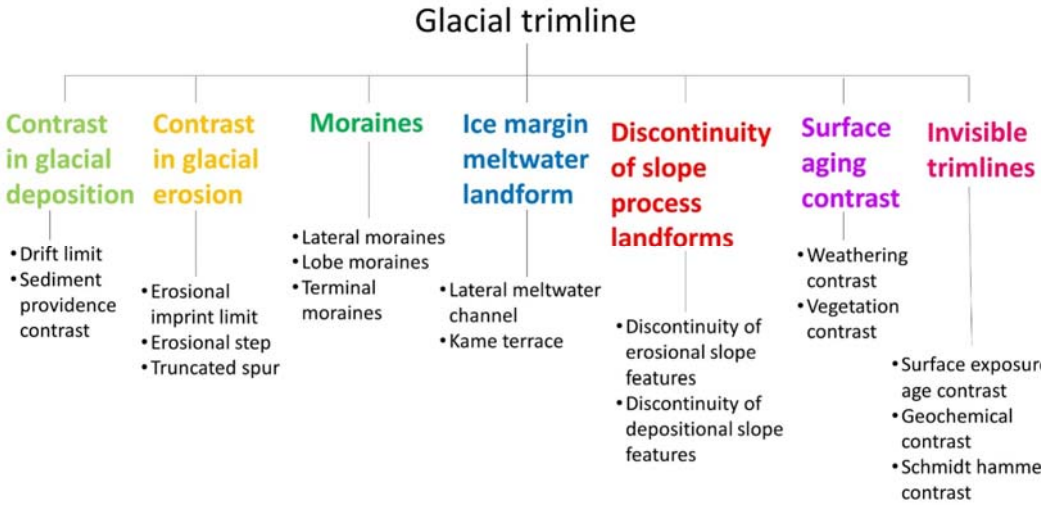

Figure 4.5 – The expression classification used to determine the mode of expression for the glacial trimlines in the study area. Due to the large number of complex moraine assemblages in central western Spitsbergen, it was decided to identify moraine trimlines separately from other depositional trimlines. No trimlines were classified in the seventh category – 'invisible trimlines'. These features would need to be identified by analysing soil or rock samples collected in the field, which was beyond the remit of the study. However, all of the remaining six trimline expression categories were found to be present in central western Spitsbergen. See Section 3.8 in Chapter 3 for more information about the development of the trimline expression classification.

The expression categories of the study area trimlines were identified by visual analysis of each trimline feature using the NPI aerial imagery. This technique generally allowed one or more of the expression categories to be easily identified for each trimline. In some cases, it was not possible to clearly identify the mode of trimline expression, in which case additional methods were applied to narrow down the trimline expression category. For example, a Normalised Difference Vegetation Index (NDVI) was computed from the Landsat data, which was used to identify the changes in vegetation that characterised some surface aging trimlines in the study area. Other additional methods involved consulting true and false colour composites, the DEM and any available field photos. This combination of methods allowed the mode of trimline expression to be identified with medium to high confidence for every glacial trimline in the study area.

4.4 Results

4.4.1 Overall trimline distribution

There are 397 trimlines in central western Spitsbergen and these features are evenly distributed throughout the ice-free land within the study area (Figure 4.6).

There are 78 glaciers in the study area, according to the Norwegian Polar Institute's Svalbard Glacier Inventory. However not all of these are distinct glaciers, which are defined as flowing bodies of ice that are not dependent on a larger ice mass. Several glaciers in the study area are tributaries of larger glaciers and others are relict areas of dead ice that have been abandoned by the retreat of a larger parent glacier. Neither of these can be considered to be distinct glaciers and may not be associated with their own trimlines, but both may have contributed to trimline formation as part of a larger glacial system. For example, the tributaries of Comfortlessbreen do not tend to have their own trimlines but are clearly associated with trimlines along the main trunk glacier (Figure 4.6c). Of the distinct glaciers in central western Spitsbergen, all bar two have at least one trimline feature (Table 4.2). Therefore, it can be stated that all areas of actively flowing glacial ice in central western Spitsbergen are associated with trimline features.

As well as being linked to almost every distinct glacier in the study area, there are 12 trimlines (3% of the total) without a clear association with a modern glacier (e.g. the isolated trimlines highlighted in Figure 4.6d). These trimlines indicate the existence of glaciers that have subsequently disappeared. This is evidence of a climate change since the date of trimline

formation, which is thought to be around the peak of the Little Ice Age cold event. Further evidence for glacial retreat in the study area is shown in the altitudinal sequences of trimlines associated with several of the larger glaciers, which suggest a period of glacial thinning. A particularly good example are the trimlines on Colletthøgda, a nunatak that is emerging as Kongsbreen and Kronebreen downwaste from either side of it (Figure 4.6b).

Further evidence of glacial retreat can be seen in some of the trimlines surrounding St. Jonsfjorden, which suggest that some glaciers were once marine-terminating but have since retreated on-shore (e.g. Bullbreen in Figure 4.6d). Trimlines can also suggest palaeo confluence points between glaciers that are now distinct. For example, following the line of the trimlines of Konowbreen and Osbornebreen in St. Jonsfjorden allows a potential palaeo confluence point to be identified (marked in Figure 4.6d). In some cases, the distribution of trimlines also suggests possible topographic pinning points, where the shape of the topography held the glacier stable for a significant period of time. An example is the pinning of Blomstrandbreen on the island of Blomstrandhalvøya in Kongsfjorden (Figure 4.6b). When this area was first mapped it was thought that Blomstrandhalvøya was a peninsula, but the retreat of Blomstrandbreen since the Little Ice Age has demonstrated that Blomstrandhalvøya is in fact an island (Figure 4.1). The trimlines on Blomstrandhalvøya and the surrounding area (Figure 4.6b) indicate the former position of Blomstrandbreen and show that the glacier was stably grounded on the island for some time, probably due to the effects of topographic pinning. The rapid retreat of Blomstrandbreen since it detached from the island supports the role of Blomstrandhalvøya as a topographic pinning point.

It is clear that the distribution of glacial trimlines in central western Spitsbergen records a wealth of information about the size, shape and configuration of the local glaciers at the time of trimline formation and during the subsequent retreat. A better understanding of these trimline features and the factors that influence their formation, preservation and expression will enable the trimlines of central western Spitsbergen to be interpreted with greater confidence, in order to produce more accurate palaeoglacial reconstructions. However, it is important to note that the duration of margin still-stands during retreat is likely to influence trimline distribution, with trimlines more likely to form during pauses in the overall retreat trend. Therefore, the trimlines are unlikely to be a complete record of the post-LIA retreat and information about rates and patterns of retreat is likely to be dominated by periods of slower retreat with more stable ice margin positions, which are more likely to produce trimlines.

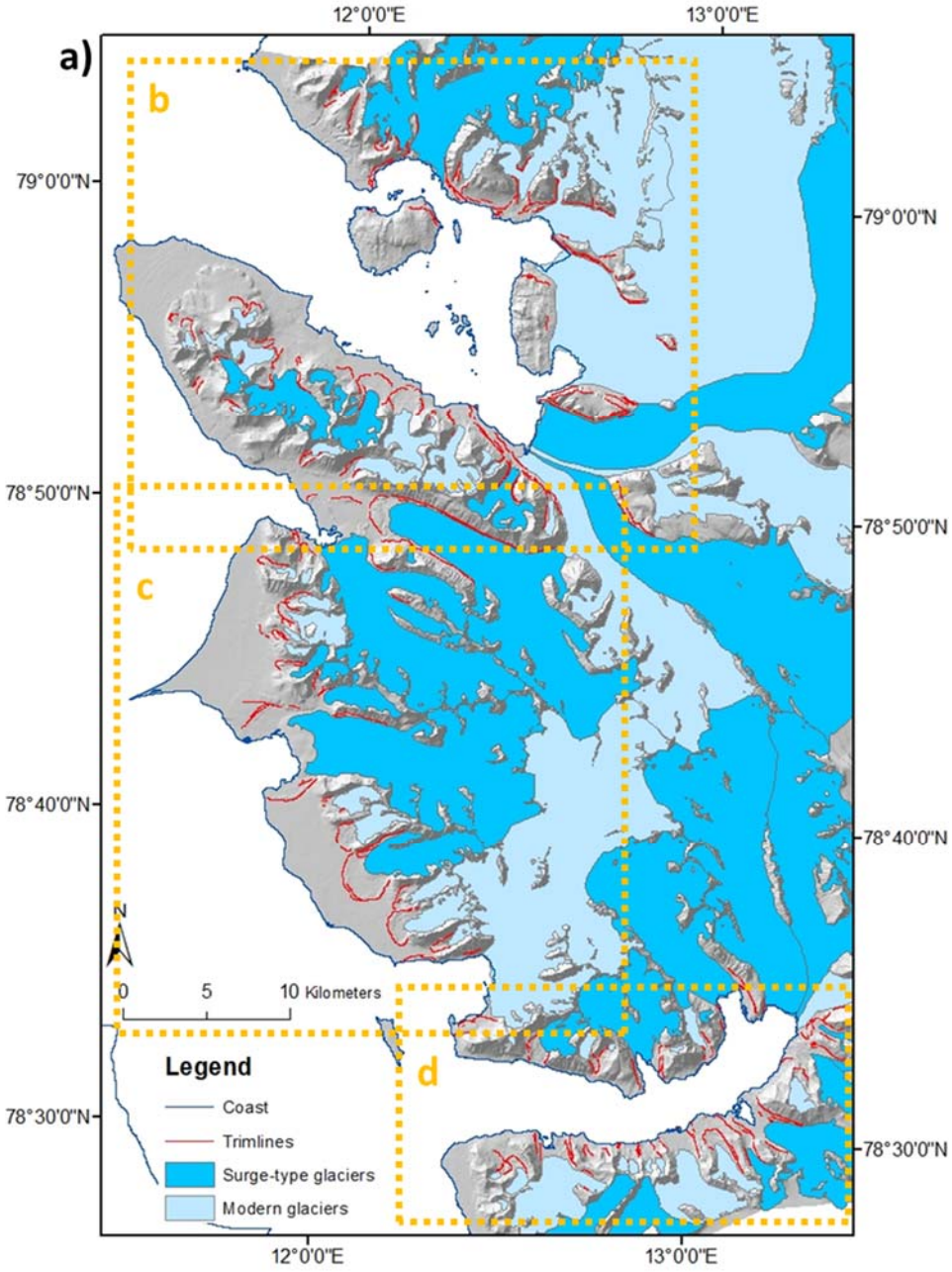

Figure 4.6 (4.6b, 4.6c & 4.6d on next page) – map of the trimlines and glaciers in central western Spitsbergen. a) shows the entire study area with the areas covered by Figures 4.6b, 4.6c and 4.6d indicated in orange; b) shows greater detail of Kongsfjorden and Brøggerhalvøya; c) shows coastal Oscar II Land; d) covers the area around St Jonsfjorden. These maps show that trimlines are found throughout the ice-free areas of central western Spitsbergen and are associated with almost all distinct glaciers in the study area, with most glaciers linked to multiple trimlines. It is also possible to pick out several interesting features of the study area trimlines, which are marked on the maps and discussed in the main text. The glacier outlines and background DEM were sourced from the NPI (http://geodata.npolar.no/ [accessed 23/03/2016]).

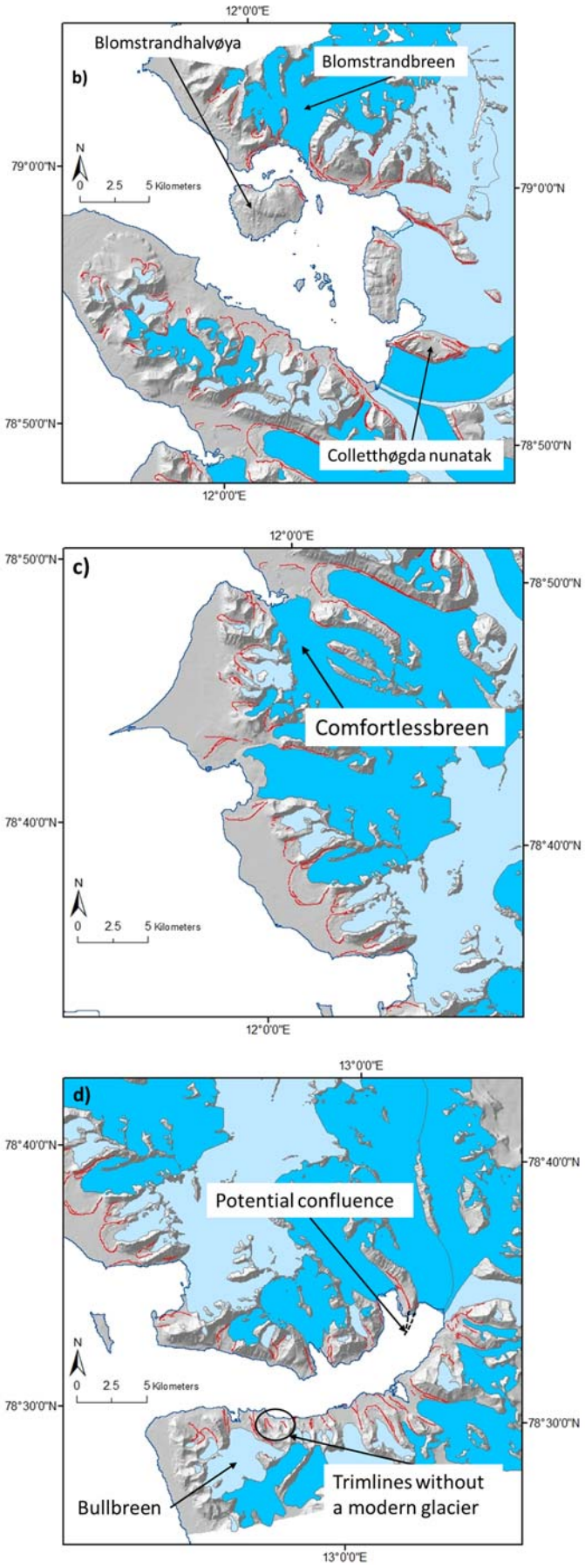
12°0'0"E
Blomstrandhalvøya
Blomstrandbreen
b)
N
0 2.5 5 Kilometers
79°0'0"N
78°50'0"N
Colletthøgda nunatak
c)
Comfortlessbreen
78°40'0"N
13°0'0"E
d)
Potential confluence
78°30'0"N
Bullbreen
Trimlines without
a modern glacier

4.4.1.1 Trimline distribution and geology

Central western Spitsbergen has a varied geology comprising a mixture of erosion-resistant metamorphic and more easily eroded sedimentary bedrocks (see Section 4.2.2 and Figure 4.3). It might be expected that the distribution of trimlines would be affected by the distribution of the different lithologies of differing erodibility in the study area. This has been found to be the case in previous trimline studies in other areas, for example in the work of Kelly *et al.* (2004) who found that erosional trimlines were better preserved on more erosion-resistant lithologies in the Alps.

However, comparison between the distribution of trimlines in central western Spitsbergen and the bedrock geology suggests that trimlines are evenly distributed throughout the study area and there is no clear link between trimline distribution and bedrock geology (Figure 4.7). The majority of trimlines (51%) are found on the most common bedrock lithology – Hecla Hoek metamorphic basement. The second most common bedrock lithology, sedimentary platform cover, is associated with 35% of trimlines, whilst Tertiary and Quaternary deposits are the least extensive in the study area and are linked to a lower percentage of trimlines (14%). This indicates that bedrock geology is not a direct control over trimline formation and does not strongly influence the preservation of glacial trimlines.

However, the geological setting is a control over the study area topography. Comparison of the faults in the study area (Figure 4.3b) with the distribution of glaciers (Figure 4.2) clearly shows that glacial erosion has been concentrated along fault lines, producing the valleys in which most glaciers and hence most trimlines are located. The easily eroded sedimentary bedrock of coastal Oscar II Land has also influenced the topography by allowing the creation of a wide coastal plain, which has enabled the formation of large complexes of trimline features around former glacier snout positions. Comparatively, the steeper topography associated with the resistant Hecla Hoek bedrock on the north side of Kongsfjorden and around St. Jonsfjorden has created less spatially extensive but more numerous trimlines. This evidence suggests that bedrock geology exerts an indirect control over the distribution of trimlines in the study area via its influence over the topography.

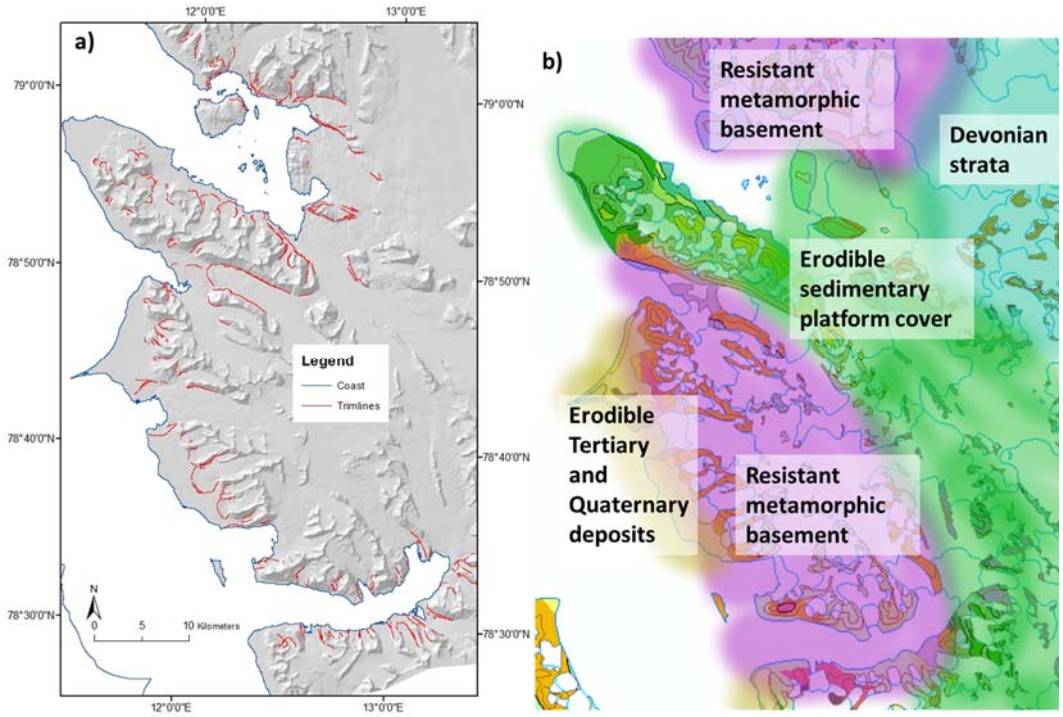

Figure 4.7 – comparison between the distribution of trimlines in the study area a) and the pattern of bedrock lithologies b). The geological map in b) has been simplified from the geological maps produced by the Norwegian Polar Institute (sheets A6G; A7G; A8G; and B8G). a) shows that trimlines are distributed fairly evenly throughout the ice-free areas of central western Spitsbergen. Comparison of the two maps shows there are no clear links between the bedrock lithologies shown in b) and the distribution of trimlines shown in a).

4.4.1.2 Trimline distribution and topography

Large-scale topography does appear to influence the distribution of trimlines in the study area (Section 4.4.1.1). Trimlines tend to be found on the sides of glacierised valleys or on areas of relatively flat topography in front of glaciers, which reflects the indirect influence of the underlying geology. Additionally, there appears to be some difference in the number of trimlines on north-facing and south-facing sides of the fjords in the study area, with a slightly higher trimline density on the north-facing side (Figure 4.6). These broad topographic controls over trimline distribution are difficult to quantify but are likely to be a factor of two key topographic variables: slope and aspect.

Topographic slope appears to have a direct influence over the distribution of trimlines in the study area (Figure 4.8). Figure 4.8 shows that trimlines in the study area can be found on all topographic slope angles in the study area, even approaching the maximum slope of 78.7°. However, most ice-free topographic slope angle in the study area are between 15-35° but most topographic slopes across which trimlines run are between 10-30°. This indicates that

trimlines are generally found on shallower than average topography in the study area and suggests there may be an optimum range of topographic slope angles for producing trimlines, of between 10-30° (Figure 4.8).

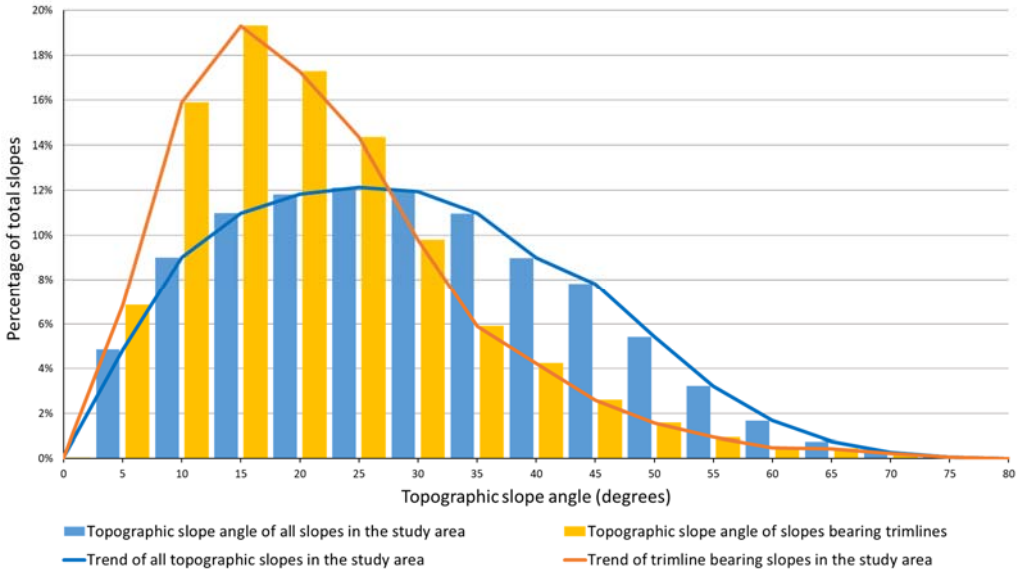

Figure 4.8 – Comparison of all ice-free topographic slope angles in the study area (blue) against the slope angles of those slopes across which trimlines run (orange). The slope angles of topographic slopes bearing trimlines shows a pronounced peak at slope angles of 10-30°. Conversely, the slope angles of all ice-free topographic slopes in the study area show a much more subdued peak located between 15-35°. This suggests that trimlines are more often found on relatively shallow topographic slopes in the study area and that topographic slope may exert a control over trimline formation or preservation.

The reasons for the strong preference for trimlines to be located on topographic slope angles between 10-30° is likely to be due to the influence of topographic slope angle over trimline formation and preservation. Certain modes of trimline expression that require high levels of glacial deposition, such as moraine trimlines, are likely to be preferentially formed on shallower topographic slopes, such as the areas around glacier snouts. Other modes of trimline expression may be more likely to form on steeper slopes but these higher slope angles may lead to these trimlines being more vulnerable to weathering and mass wasting processes. Therefore, the trimlines formed on steeper slopes may be relatively poorly preserved compared to trimlines formed on shallower slopes.

Topographic aspect was found to exert very little influence over the trimlines in the study area. Most trimlines were found to be located on the most common topographic aspects,

although there is a slight preference for trimlines to be located on north-facing topographic slopes compared to south-facing topography. This is likely to be due to differences in the rates of slope processes, in particular processes of weathering and mass wasting associated with freeze-thaw cycles. South-facing topography on Svalbard, which is in the northern hemisphere, receives more insolation than the north-facing topography, enhancing diurnal freeze-thaw cycles. Therefore, trimlines formed on south-facing topographic slopes are likely to have lower preservation potentials than those on north-facing topography. However, the difference between the numbers of trimlines found on north and south facing topography is only of the order of a couple of percentage points, making this distinction relatively minor. This suggests that topographic aspect does not exert a strong influence trimline distribution and that topographic slope is the more significant topographic variable.

4.4.1.3 Trimline distribution and glaciology

Trimlines are found associated with 97% of the distinct glaciers in the study area (Table 4.2; Section 4.4.1). However, the number of trimlines associated with a given glacier varies and it is hypothesised that both glacier size and glacier type will exert a control over this. Larger glaciers, both in terms of length and area, would seem likely to be associated with greater numbers of trimline elements. Faster flowing glaciers, such as surge-type or tidewater glaciers, might also be expected to create more trimline elements. The large and faster flowing glaciers have greater potential to work on the landscape via processes of glacial erosion and deposition, hence the expectation for such glaciers to create more trimlines and other glaciers.

Table 4.2 (next page) – The study area glaciers and the number of trimlines associated with them. The glaciers are colour-coded to reflect their glacier type and are ordered according to the number of trimlines, from lowest to highest. Normal glaciers are white, tidewater blue, terrestrial surge-type gold, and tidewater surge-type red. From this table it is clear that tidewater and surge-type glaciers are generally associated with higher numbers of trimlines than normal glaciers. Of the ten glaciers with no trimlines, three are tributaries of larger glaciers (which do have trimlines in all cases) and five are relict parts of larger glaciers (these are marked as 'split glaciers' in the table), with the larger parts of the glaciers again having trimlines in all cases. This leaves only two glaciers that have no trimlines are not part of a larger glacier systems. Both of these are relatively small glaciers, with lengths ≤ 1 km and areas of < 5 km^2, meaning that they are probably cold-based and no longer flowing. Twelve trimlines in the study area are not clearly associated with any modern glacier; these may indicate the positions of former glaciers.

Glacier ID	Name	Tributary of	Split glacier (Y/N)	No. of trimlines
63	Fatumbreen	Kronebreen		0
99	Infantfonna	Kronebreen		0
26	Konowbreen		Y	0
94	Midtre Lovénbreen		Y	0
93	Midtre Lovénbreen		Y	0
23	Osbornebreen	Osbornebreen		0
22	Unnamed			0
96	Unnamed			0
107	Vegardbreen		Y	0
37	Vestre Lovénbreen		Y	0
50	Arthurbreen		Y	1
1	Holmeslettbreen E		Y	1
25	Osbornebreen			1
30	Tassbreen			1
67	Trongskarbreen			1
27	Unnamed			1
24	Unnamed			1
97	Unnamed			1
42	Unnamed			1
47	Uversbreen		Y	1
36	Vestre Lovénbreen		Y	1
28	Botnbreen			2
51	Cissybreen			2
33	Erikkabreen			2
106	Holmeslettbreen E			2
10	Unnamed			2
92	Unnamed			2
6	Unnamed			2
14	Unnamed			2
3	Anna Sofiebreen			3
29	Edithbreen			3
59	Eivindbreen			3
52	Haakenbreen			3
2	Holmeslettbreen W		Y	3
55	Kongsvegen	Kronebreen		3
57	Oliverbreen			3
64	Skreifjellbreen			3
98	Unnamed			3
58	Andreasbreen			4

Glacier ID	Name	Tributary of	Split glacier (Y/N)	No of trimlines
38	Austre Lovénbreen			4
16	Paulbreen			4
95	Unnamed			4
31	Unnamed			4
34	Waldemarbreen			4
53	Comfortlessbreen			5
32	Irenebreen			5
66	Kjærfjellbreen			5
68	Mørebreen			5
13	Unnamed			5
49	Arthurbreen		Y	6
105	Holmeslettbreen W			6
19	Konowbreen		Y	6
35	Midtre Lovénbreen		Y	6
69	Olsønbreen			6
18	Smalgangen			6
40	Steenbreen			6
21	Ankerbreen			7
0	Gunnarbreen			7
15	Vegardbreen			7
17	Vintervegen	Osbornebreen		7
46	Austre Brøggerbreen			8
54	Elisebreen			8
62	Feiringbreen			8
20	Gaffelbreen			8
5	Løvliebreen			8
39	Pedersenbreen			8
43	Aavatsmarkbreen			9
4	Bullbreen			9
48	Uversbreen		Y	9
45	Vestre Brøggerbreen			9
44	Dahlbreen			10
91	Kronebreen			10
7	Charlesbreen			11
56	Sidevegen	Kronebreen		11
41	Botnfjellbreen			12
60	Conwaybreen			13
61	Kongsbreen			26
65	Blomstrandbreen			36

Study of Table 4.2 shows that all the glaciers associated with more than 10 trimline elements are either surge-type glaciers, tidewater glaciers or both. Blomstrandbreen, a tidewater surge-type glacier on the north side of Kongsfjorden, has the largest number of trimlines, with 36 individual elements. There are 11 glaciers with only one trimline and of these three are surge-type or tidewater glaciers, meaning that 73% of glaciers with only one trimline are terrestrial and non-surging (henceforward referred to as 'normal' glaciers). These findings suggest that tidewater and surge-type glaciers do produce more trimlines than normal glaciers and indeed the majority (62%) of trimlines in central western Spitsbergen are associated with either surge-type glaciers, tidewater glaciers or glaciers that are both tidewater and surge-type. Breaking this figure down shows that surge-type glaciers account for 25% of trimlines, tidewater 17% and glaciers that are both tidewater and surge-type account for 20% of trimlines. Normal glaciers account for 36% of trimlines, with the remaining 2% of trimline features not clearly associated with any modern glacier. Presumably, the glaciers that created these trimlines have since vanished in the period of climate warming experienced in Svalbard since the end of the Little Ice Age (c. 1850-1940 AD). Several currently normal-type glaciers in the study area show signs of having been tidewater glaciers at the time of trimline formation (e.g. Bullbreen in Figure 4.6d). If these are taken into account then the number of trimlines associated with either surge-type and/or tidewater glaciers rises to 70%, with normal glaciers accounting for just 27% of trimline features. These findings suggest that the glaciology of surge-type and tidewater glaciers promotes trimline formation, with surge-type glaciers seeming to produce the highest numbers of trimline elements (see Section 4.5.2).

However, when the relative abundance of each type of glacier in the study area is considered, it is tidewater glaciers that exert a more significant influence over trimline distribution than surge-type glaciers (Figure 4.9). Normal glaciers are associated with a lower than expected number of trimlines (36% of trimlines but 56% of glaciers) and surge-type glaciers with roughly the expected number of trimlines (25% of trimlines and 25% of glaciers). Tidewater glaciers, on the other hand, are associated with anomalously high numbers of trimlines. This is true for non-surging tidewater glaciers (17% of trimlines but only 7% of glaciers) and for tidewater surge-type glaciers (20% of trimlines but just 12% of glaciers). This would indicate that tidewater glacial behaviour is the most significant glaciological control on trimline formation and that surging behaviour does not produce many more trimlines than normal glaciers.

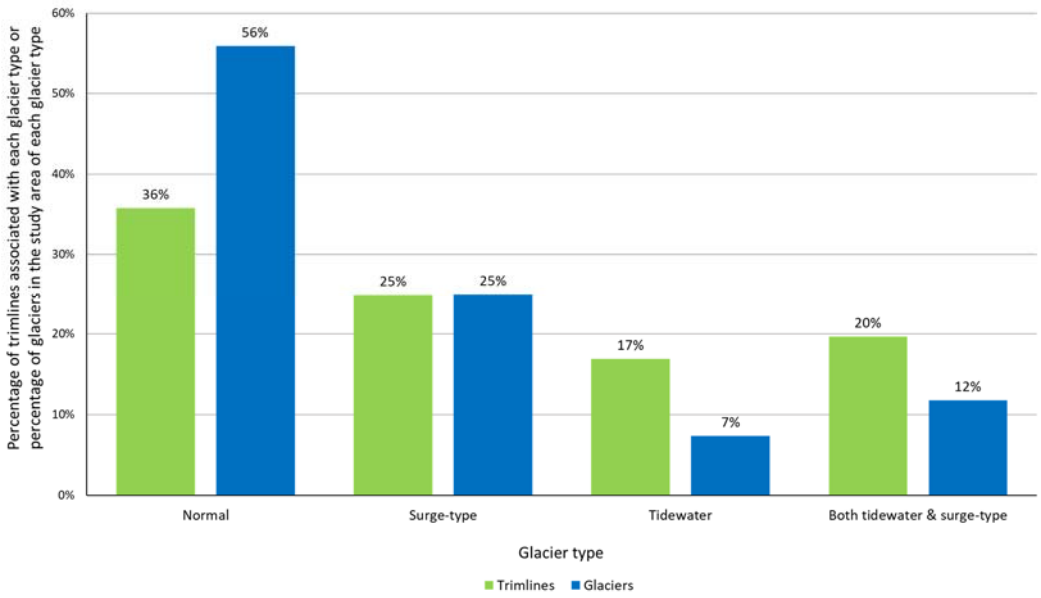

Figure 4.9 – The relative abundance of each glacier type in the study area is compared to the number of trimlines associated with that glacier type. This shows that normal glaciers are associated with fewer trimlines than would be expected, given that normal glaciers are by far the most common type of glacier in the study area. Surge-type glaciers produce roughly the expected number of trimlines, whilst tidewater and tidewater surge-type glaciers produce more trimlines than would be expected, given the prevalence of these glacier types in the study area. This suggests that the characteristics of tidewater glaciers promote increased trimline formation, compared to normal and surge-type glaciers.

The reason for this distinction between tidewater and surge-type glaciers may be due to the duration of high velocities, which increase the potential for a glacier to form trimlines by increasing rates of glacial erosion and deposition. Tidewater glaciers have consistently high velocities, due to their efficient mass-loss at the calving margin which causes a draw-down effect on upstream ice. Surge-type glaciers, on the other hand, experience relatively brief periods of high velocity, which may only last for a matter of a few years, between longer periods of more normal ice flow. It may be that the relatively short duration of glacial surges causes surge-type glaciers to create fewer trimlines, compared to continuously fast-flowing tidewater glaciers.

As well as glacier type, glacier size seems likely to affect the number of trimlines associated with a given glacier. In particular, it would seem reasonable to expect a larger glacier, with a greater perimeter, to produce more trimlines, with a positive linear relationship anticipated between glacier length or glacier area and number of trimlines. However, linear regression analysis demonstrates that neither glacier length nor glacier area produce a strong linear

correlation with the number of trimlines, with both variables producing r^2 values < 0.3. In both cases the weak correlations appear to be due to the high degree of variability in the number of trimlines associated with medium and large glaciers, which have lengths > 5 km and areas > 25,000 km^2. This variability suggests that another glaciological variable is more important than glacier size for controlling the number of trimlines associated with these medium and large glaciers.

For both glacier length and glacier area, the type of glacier appears to be an important influence over the amount of variability in the number of trimlines. Normal glaciers tend to be generally the shortest and smallest in area and show only a weak linear correlation between glacier size and number of trimlines, with r^2 values in the region of 0.2-0.3. Surge-type glaciers produce similarly weak correlations but tidewater surge-type glaciers show a much greater degree of variability and no correlation at all, with linear regression between glacier size and the number of trimlines producing r^2 values of < 0.1. Tidewater glaciers that do not surge, on the other hand, show a strong positive linear correlation between glacier area and the number of trimlines, producing an r^2 value of 0.67. However, tidewater glaciers do not show a relationship between glacier length and the number of trimlines, only glacier area produces a significant correlation. These findings suggest that surging behaviour is the reason for the majority of the variability obscuring any trends between glacier size and the number of trimlines, but that even non-surging glaciers do not generally produce significant relationships between glacier size and the number of trimlines. Therefore, it seems that glacier type is a more important control over trimline formation than glacier size in central western Spitsbergen. However, glacier size may be a significant control on trimline formation and distribution in areas without surge-type glaciers or in regions with large numbers of non-surging tidewater glaciers.

4.4.2 Trimline expression

All of the modes of trimline expressions described in Figure 4.5 were found in the study area with the exception of Invisible Trimlines, which can only be identified using methods such as cosmogenic nuclide dating that are not part of the remit of this study.

Trimlines formed by depositional processes were found to be the most common, with 19% of study area trimlines expressed as depositional contrasts and a further 34% as moraines (Table 4.3). Erosional trimlines were the next most common landform, comprising 17% of study area trimlines. Meltwater trimlines were the least common mode of trimline expression, representing just 5% of trimline features in the study area (Table 4.3). Several of

the trimlines in the study area were expressed as composite features and these often took the form of either erosional or depositional contrasts that were also expressed via changes in slope landforms or through surface aging contrasts. Despite the presence of composite features, the majority of trimlines in central western Spitsbergen are expressed in only one way.

Expression	% of trimlines
Depositional contrast	19%
Erosional	17%
Moraines	34%
Meltwater	5%
Slope landform discontinuity	13%
Surface aging contrast	11%
Composite features	22%

Table 4.3 – the percentage of trimlines in the study area classified into each mode of trimline expression. The colouring of the modes of expression are linked to the colour of the trimlines in the map of trimline expressions (Figure 4.10). Moraines are the most common mode of trimline expression and meltwater trimlines are the least common. Composite features are trimlines that are expressed in more than one way, often either erosional or depositional trimlines that are also expressed as slope landform discontinuities or surface aging contrasts.

Trimlines of every mode of expression are distributed throughout the study area but there is some clustering of particular expressions in certain places (Figure 4.10). Depositional contrasts and erosional trimlines are often found associated with the same glacier and are particularly clustered around the surge-type and tidewater glaciers of St. Jonsfjorden (Figure 4.10d) and Kongsfjorden (Figure 4.10b). Surface aging and slope landform trimlines follow broadly the same pattern as depositional contrasts and erosional trimlines. Conversely moraines are primarily found on the coastal plain of Oscar II Land (Figure 4.10c) and on Brøggerhalvøya (Figure 4.10b) and appear to have an equal association with all glacier types. Meltwater trimlines are rare in central western Spitsbergen but tend to form associated with surge-type glaciers. This clustering in the distribution of trimlines of different expressions indicates that geology, topography and glaciology may have an influence over the expression of glacial trimlines.

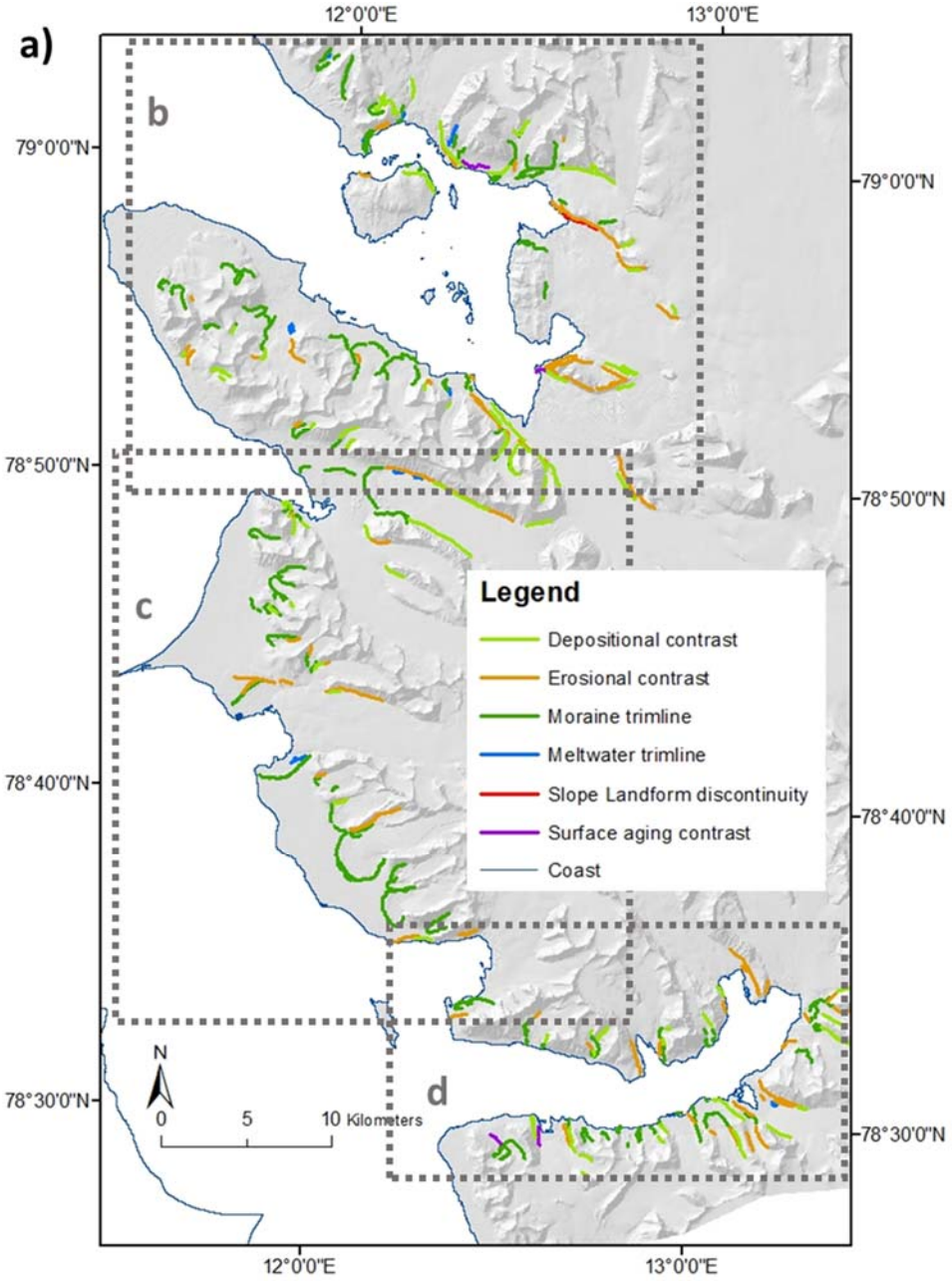

Figure 4.10 (4.10b, 4.10c & 4.10d on next page) – maps of the distribution of the different modes of trimline expression in the study area. The whole of central western Spitsbergen is shown in a), with the location of the Figures 4.10b, 4.10c, and 4.10d outlined; b) shows Kongsfjorden and Brøggerhalvøya; c) shows the coast of Oscar II Land; and d) covers the area around St Jonsfjorden. The majority of trimlines in all areas are either moraines (dark green), depositional contrasts (light green), or erosional (orange). Note that many slope landform and surface aging trimlines are not visible because they are often composite features, which are marked on this map by the dominate mode of trimline expression (usually erosional or depositional).

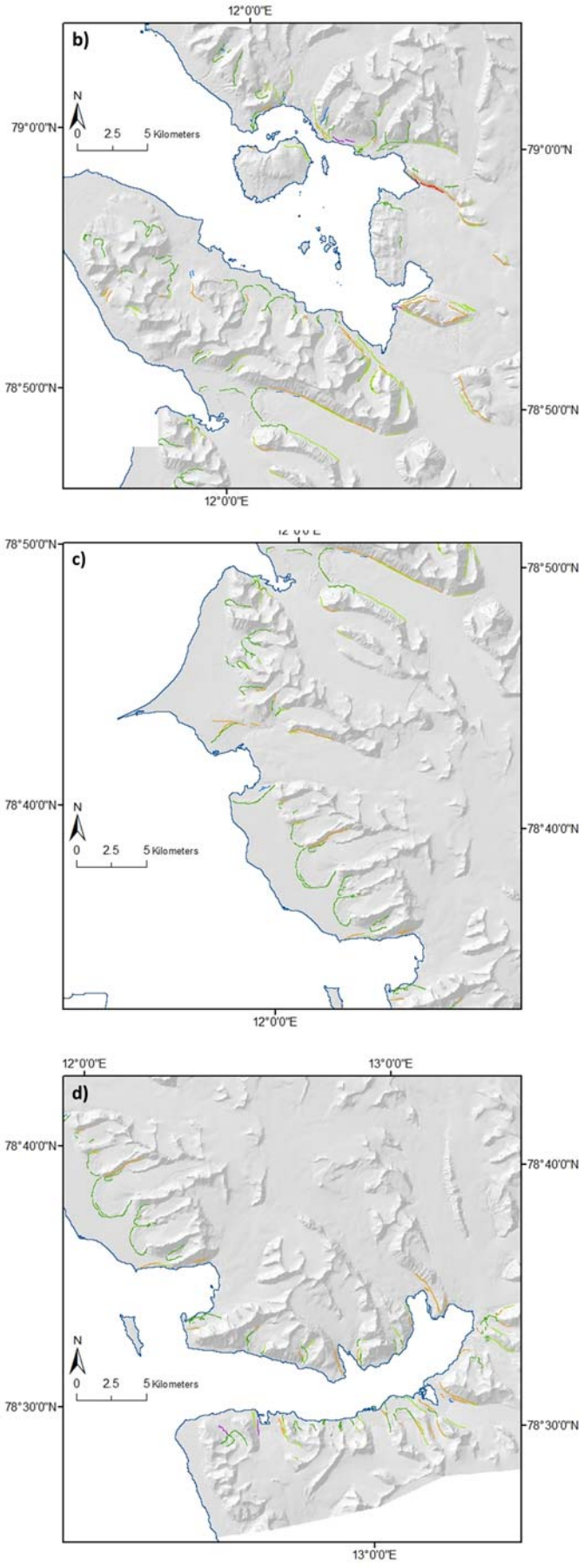
b)
12°0'0"E
79°0'0"N
78°50'0"N
N
0 2.5 5 Kilometers
c)
78°40'0"N
d)
13°0'0"E
78°30'0"N

4.4.2.1 Trimline expression and geology

Comparison of Figures 4.10 and 4.3 indicates that trimlines of all expressions are found on all types of bedrock in the study area. If bedrock lithology has a significant effect on trimline expression, it would be expected that higher proportions of trimlines of a particular expression would be associated with specific bedrock lithologies. In order to test this hypothesis, the percentage of all trimlines associated with each lithology was calculated (the 'expected value') and compared to the percentage of trimlines of each mode of expression associated with each lithology (Table 4.4). For all but two combinations of trimline expression and bedrock lithology, the values are within ± 10% of the expected value (i.e. the percentage of all trimlines associated with that bedrock lithology) and in the majority of cases the values are within ± 5%. This indicates that most trimline expressions are no more or less commonly associated with a given bedrock lithology than would be expected, given the percentage of all trimlines linked to that bedrock lithology.

The two exceptions are meltwater trimlines, which are more common than would be expected on sedimentary platform cover, and surface aging trimlines, which are anomalously common on Hecla Hoek bedrock. The greater erodibility of the sedimentary platform cover may explain the relatively high number of meltwater features found there. Alternatively, there may be a link between this softer bedrock and a higher prevalence of surge-type glaciers, with which meltwater trimlines are commonly linked (Section 4.4.2). The prevalence of surface aging trimlines on Hecla Hoek bedrock may be due to the greater resistance of this lithology to erosion, meaning that these often subtle trimlines might be better preserved here than elsewhere in the study area.

	Lithology	All trimlines	Depositional	Erosional	Moraines	Meltwater	Slope landform	Surface aging	Composites
Erodibility ▼	Hecla Hoek (metamorphic basement)	51%	51%	51%	47%	45%	51%	**63%**	43%
	Tertiary and Quaternary deposits	14%	6%	12%	22%	10%	7%	6%	13%
	Sedimentary platform cover	35%	43%	37%	30%	45%	42%	30%	43%

Table 4.4 – percentage of trimlines of each expression found on each bedrock lithology in the study area. This data has been estimated by comparing the ArcGIS map used to produce Figure 4.10 with Figure 4.3. The data entries are coloured to indicate the difference from the expected values, which are the percentage of all trimlines associated with a given bedrock geology. Black indicates values within ± 5% of the expected value; green is 5-10% greater than expected; red 5-10% lower than expected; and bold and underlined green are >10% greater than expected. For example, 63% of surface aging trimlines are found on Hecla Hoek bedrock compared to 51% of all trimlines, a difference of +12%, so the data entry is coloured bold green and underlined.

It is clear that geology is not a primary control on trimline expression in the majority of cases. However, certain types of trimline are more prevalent on more or less erodible bedrock. This may be due to a direct influence of geology over the processes of trimline formation and preservation, or to an indirect influence of geology via its effect on topography and glaciology.

4.4.2.2 Trimline expression and topography

Trimlines are found on a wide range of topographic slope angles in central western Spitsbergen (Figure 4.8) but several modes of trimline expression are confined to relatively flat topography (Figure 4.11). In particular, moraines always form on topographic slope angles < 60^{o} and meltwater trimlines are exclusively located on topographic slopes < 50^{o}. The trimlines found on topographic slopes steeper than 60^{o} in the study area tend to be either erosional trimlines, slope landform discontinuities or surface aging trimlines (Figure 4.11). Depositional contrasts can occasionally be found on these steeper slopes but this mode of trimline expression is predominantly found on shallower slopes of an angle < 30^{o} (Figure 4.11). These contrasts in the modes of trimline expression associated with different topographic slope angles suggests that topography exerts some control over trimline expression. Of particular interest is that the modes of trimline expression found on steeper slopes tend to be manifestations of glacial erosion, whereas trimlines expressed by glacial deposition or meltwater processes are more common on shallower slopes (Figure 4.11). Therefore, it may be that topographic slope is a secondary influence on trimline formation and expression, with glaciology as the primary control.

Figure 4.8 shows the distribution of trimlines of all expressions on different topographic slopes, demonstrating a strong preference for trimlines to form on slope angles between 10^{o}-30^{o}. However, this trend may be skewed by the large number of moraine trimlines in the study area, which account for 34% of all trimlines and are always found on slopes < 60^{o} (Figure 4.11). Comparison of Figure 4.12a and Figure 4.12b shows that the inclusion of moraines in Figure 4.8 has slightly increased the percentage of trimlines found on lower slope angles and has marginally decreased the percentage found on higher slope angles. However, the graphs shown in Figure 4.12 still supports the conclusion that trimlines of all expressions are most common on slope angles between 10^{o}-30^{o}, regardless of whether moraines are considered to be a type of trimline or not.

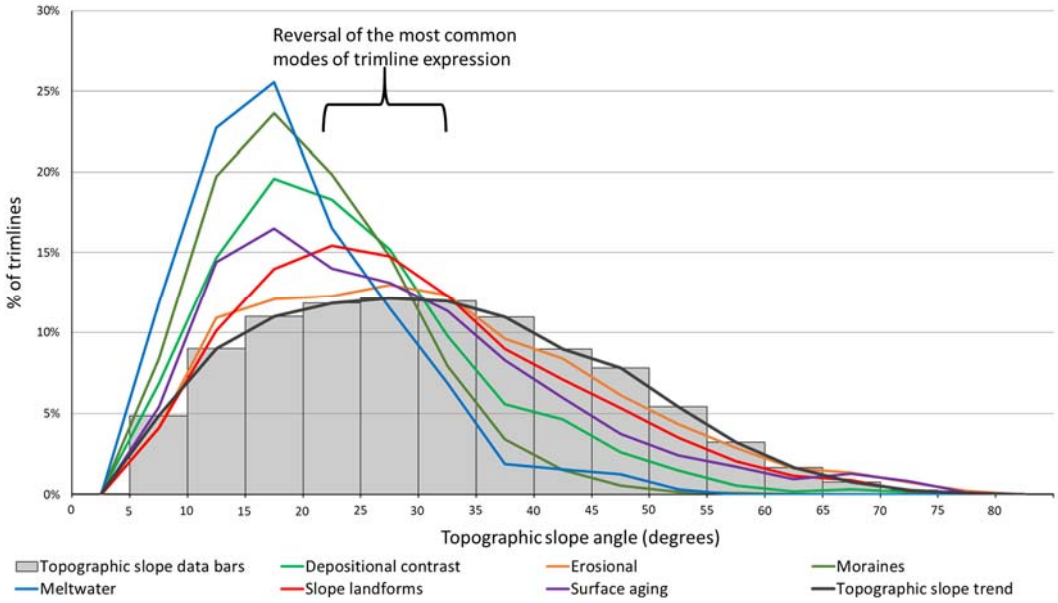

Figure 4.11 – the topographic slope angles of the slopes across which run trimlines of each mode of trimline expression (coloured lines) compared to all ice-free topographic slopes in the study area (bars & black line). From this graph it is clear that trimlines of all expressions tend to form on shallower than average topographic slopes in the study area (Figure 4.8). However, there are differences in the slope angles associated with specific types of trimline expression. For example, meltwater trimlines are much more common on shallower slopes and are highly uncommon on steeper slopes, compared the other modes of trimline expression. At topographic slope angles of around 30° there is a reversal in the most common modes of trimline expression. Below this slope angle most trimlines are depositional contrasts, moraines or meltwater features, whereas the trimlines on steeper topographic slopes are more likely to be expressed as contrasts in erosion, slope landforms or surface aging.

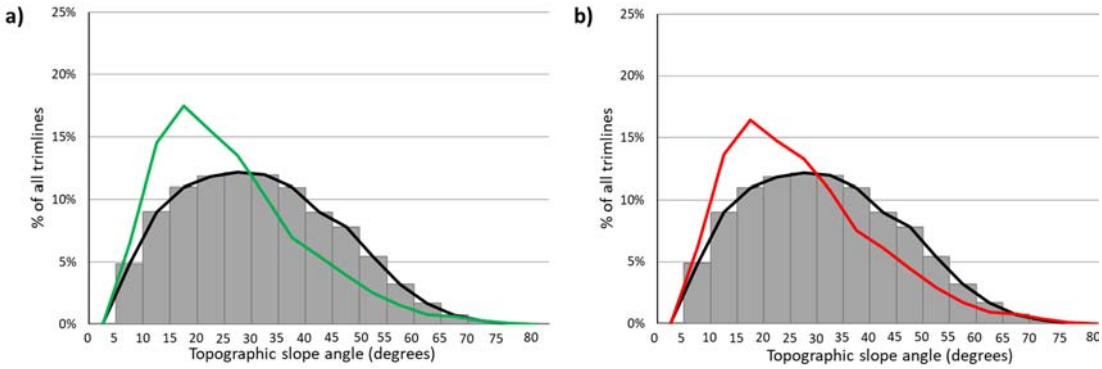

Figure 4.12 – comparison of the topographic slope angles associated with of all modes of trimline expression both including and excluding moraine trimlines. The large numbers of moraine trimlines (Table 4.3) and their strong association with shallower topographic slope angles (Figure 4.11) may have exerted a control over the overall trend shown in Figure 4.8, which could lead to misleading conclusions. However, comparison of the graphs in this figure show that the influence of moraine trimlines over the trend in Figure 4.8 is very small, with no change in the position of the peak between the graph including moraines a) and the one

excluding moraines b). The peak in a) is slightly higher than in b), suggesting that including moraines does marginally increased the percentage of trimlines found on the most common slope angles (between 10-30^{o}). However, this increase is not significant and the overall shape of the trend and position of the peak remains the same. Therefore, the conclusions drawn from Figure 4.8 stand for all modes of trimline expression, regardless of whether moraines are considered to be a type of trimline or not.

4.4.2.3 Trimline expression and glaciology

Table 4.5 shows that several modes of trimline expression are clearly associated with a particular type of glacier, or group of glacier types. Similar to Table 4.4, Table 4.5 compares the percentage of each mode of expression associated with each type of glacier to the percentage of all trimlines associated with that glacier type (the 'expected value'). For example, moraines are more commonly associated with normal glaciers than might be expected, with 51% of moraine trimlines linked to these glaciers compared just 37% of all trimlines (Table 4.5). Moraines are also more commonly linked to non-surging glaciers than to either terrestrial or tidewater surge-type glaciers. Conversely, meltwater trimlines are much more commonly associated with surge-type glaciers, which account for 73% of meltwater trimlines (Table 4.5). This suggests that processes associated with the formation of meltwater features are promoted by surging but that surging does not promote the high levels of glacial deposition required to form moraines. These findings suggest that surging behaviour favours the formation of particular modes of trimline expression and is likely to be a significant control over the way trimlines are expressed.

The data in Table 4.5 also demonstrates a link between tidewater glaciers and specific modes of trimline expression. In particular, trimlines related to processes of glacial erosion are more commonly found associated with tidewater glaciers. For example, 28% of erosional trimlines are linked to tidewater glaciers, compared to 17% of all trimlines (Table 4.5). Both slope landform and surface aging trimlines are also associated more closely with tidewater glaciers than terrestrial glaciers, with surface aging trimlines particularly strongly linked to tidewater surge-type glaciers (Table 4.5). This suggests that the faster velocities of tidewater glaciers may favour the formation of trimline expressions created by glacial erosional, with surface aging and erosional trimlines particularly likely to be formed by the combination of tidewater and surging characteristics.

Glacier type	All trimlines	Depositional	Erosional	Moraines	Meltwater	Slope landforms	Surface aging
Normal	37%	35%	**17%**	51%	**20%**	32%	**21%**
Surge-type	26%	26%	21%	24%	**47%**	30%	19%
Tidewater	17%	19%	**28%**	13%	7%	**28%**	24%
Both tidewater & surge-type	20%	20%	**34%**	13%	27%	**9%**	**37%**
All surge-type	46%	46%	54%	36%	**73%**	39%	56%
All non-surging	54%	54%	46%	64%	**27%**	61%	44%
All tidewater	37%	39%	**62%**	**26%**	34%	37%	**61%**
All terrestrial	63%	61%	**38%**	75%	67%	62%	**40%**

Table 4.5 – the percentage of trimlines of a given expression associated with each glacier type. The data entries are coloured to indicate difference from the expected value, which is the percentage of all trimlines associated with a given type of glacier. Black indicates values within ± 5% of the expected value; green is 5-10% greater than expected; red 5-10% lower than expected; bold and underlined green are >10% greater than expected; and bold and underlined red are >10% lower than expected. For example, 20% of meltwater trimlines are associated with normal glaciers compared to 37% of all trimlines, a difference of -17% so the data entry is coloured bold red and underlined.

It seems likely that glacier type is a significant control over the expression of glacial trimlines but glacier size may also play a role (Section 4.1.3). When all modes of expression are considered, there are weak positive linear relationships between glacier size and the number of trimlines associated with a given glacier, with r^2 values of around 0.32 for glacier area and 0.24 for glacier length. However, most individual modes of trimline expression have much weaker correlations, suggesting no significant relationship between glacier size and trimline expression in most cases.

The clear exception is erosional trimlines, which have a moderate-strength positive linear correlation with both glacier area (r^2 of 0.5) and glacier length (r^2 of 0.4). This indicates that larger glaciers, particularly those with larger areas, are more likely to create erosional trimlines. Surface aging trimlines also have a weak to moderate linear correlation with glacier size, suggesting that this type of trimline is also more likely to be created by larger glaciers. Conversely, all other modes of trimline expression have very weak relationships with glacier size. This suggests that large glaciers are no more likely than small glaciers to produce depositional contrasts, moraines, meltwater trimlines and slope landform trimlines.

However, erosional trimlines and surface aging trimlines are both associated with tidewater glaciers and are particularly strongly linked to tidewater surge-type glaciers (Table 4.5). Tidewater and tidewater surge-type glaciers are amongst the largest in the study area (Table 4.1), so the link between erosional and surface aging trimlines and larger glaciers may be

another expression of the relationship between these trimlines and tidewater glaciers. Examples such as this demonstrate the difficulties in separating glacier size from glacier type. However, the strong associations between specific modes of trimline expression and specific glacier types suggest that this is the more important influence compared to the relatively weaker correlations between specific modes of trimline expression and glacier size.

4.4.3 Trimline elevation

The majority of trimlines in the study area are located at relatively low elevations, with 55% below 150 m a.s.l. and 84% below 250 m a.s.l. (Figure 4.13). Trimlines at lower elevations are distributed evenly throughout the study area but trimlines at higher elevations are concentrated primarily on the north and east sides of Kongsfjorden. North-East Kongsfjorden has the highest and steepest topography in the study area, due to the resistant Hecla Hoek bedrock, so it is not surprising that this area has the highest concentration of trimlines at higher elevations. It would therefore appear that topography has a direct influence over trimline elevation, with geology indirectly controlling trimline elevations via its influence over topography. The role of glaciology is less clear, with no obvious visual relationship between surge-type or tidewater glaciers and particular trimline elevations.

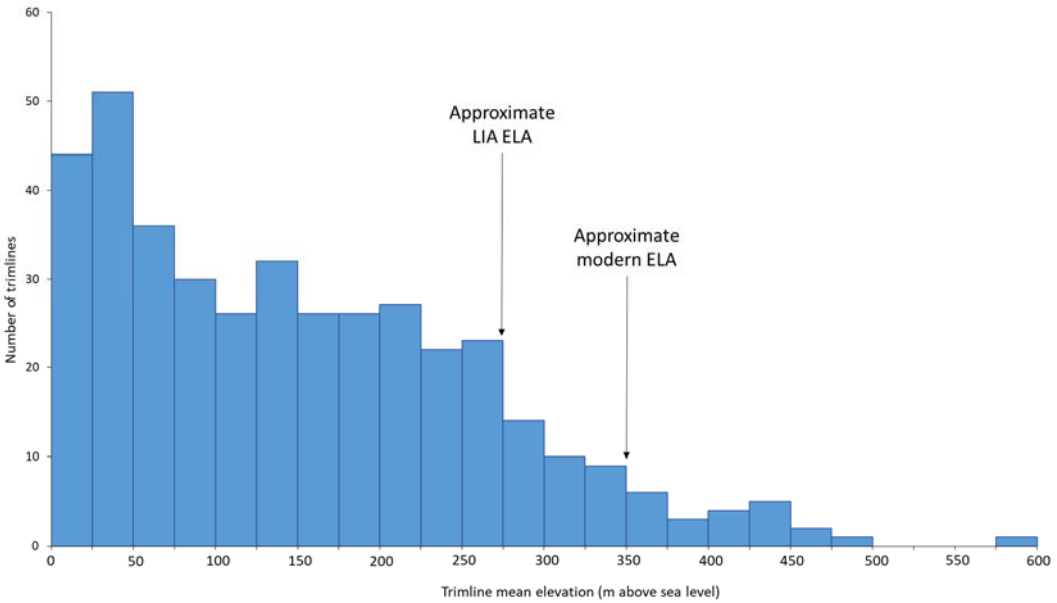

Figure 4.13 – this histogram shows that the majority of trimlines in central western Spitsbergen are located at low elevations, with almost a quarter (24%) situated below 50 m above sea level and 84% below 250 m. The highest trimlines are found between 400-600 m above sea level, accounting for 3% of all trimlines in the study area. Only 6% of trimlines are located above the modern ELA, which is at c. 350 m above sea level. However, the ELA at the time of trimline formation is likely to have been significantly lower, for example the local Little Ice Age ELA is around 273 m above sea level (Chapter 6).

The modern local ELA is approximately 350 m a.s.l. (Nuth *et al.* 2007), which is likely to be significantly higher than the ELA at the time of trimline formation for the majority of trimline features in the study area. Therefore, whilst only 6% of trimlines in central western Spitsbergen are located above the modern ELA (Figure 4.13), it is likely that a higher percentage were positioned above the ELA at the time of their formation. This would support the common notion that trimlines can be formed above the ELA, making them particularly useful for glacial reconstructions because they are often the sole record of the palaeo ice surface elevation in the accumulation area (Kelly *et al.* 2004).

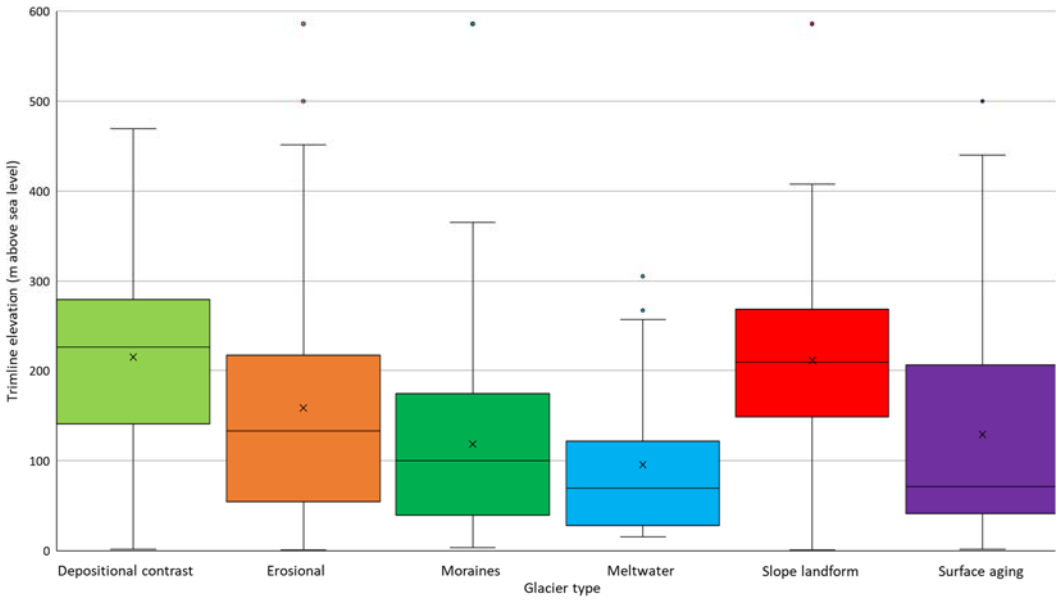

Figure 4.14 – these box plots show the elevations of trimlines of each mode of expression, with mean values shown as an x and outliers as dots (identified using the interquartile range method). The lack of overlap between some interquartile ranges indicates that there is a significant difference in the elevation of the different modes of trimline expression. There are also large differences between the mean elevations of the different expressions, for example meltwater trimlines have a mean elevation that is just 44% of the mean elevation of depositional trimlines. These significant differences indicate that trimline elevation is related to the mode of trimline expression, with particular expressions primarily forming at either lower or higher elevations.

The higher elevation trimlines in the study area tend to be either depositional contrasts or slope landform trimlines, which are the only modes of trimline expression with a mean elevation > 200 m above sea level (Figure 4.14). There are, however, some lateral moraines at elevations > 250 m a.s.l. and some erosional and surface aging trimlines are also found at these higher elevations. Meltwater trimlines and the vast majority of moraines, conversely, are found at lower elevations, with meltwater trimlines having a mean elevation of just 95 m, for example. These significant differences in the mean trimline elevation of different

expressions is supported by a lack of overlap in the interquartile ranges of several modes of trimline expression (Figure 4.14). This indicates that there is likely to be a relationship between the mode of trimline expression and the elevation of the trimline feature. This relationship is probably linked to the processes of trimline formation for the different modes of trimline expression. For example, meltwater trimlines may form only at lower elevations because the colder temperatures at higher elevations prohibit the formation of the large volumes of glacial meltwater required to form a meltwater trimline feature.

Qualitative visual analysis initially suggested no obvious relationship between trimline elevation and glacier type. However, quantitatively comparing normal glaciers to tidewater and to surge-type glaciers suggests that glacier type may influence trimline elevation. In particular, tidewater glaciers and surge-type glaciers both have a higher percentage (11%) of trimlines above the modern ELA then is the case for normal glaciers, of which only 8% are above the ELA. Histogram analysis of the trimline elevations for each glacier type shows that trimlines are most common at elevations of 0-50 m above sea level regardless of the type of glacier. However, all glacier types, except normal glaciers, show secondary peaks in their histograms, indicating greater numbers of trimlines than might be expected in specific ranges of elevations in the study area. Tidewater glaciers have an anomalously large percentage of trimlines at 100-150 m whilst surge-type glaciers produce more trimlines at 200-300 m than would be expected. Glaciers that are both tidewater and surge-type produce more trimlines than expected between these two peaks, at around 150-200 m. These secondary peaks suggest that the glaciology of tidewater glaciers produces a greater number of lower elevation trimlines, whereas surge-type glaciers produce more trimlines at slightly higher elevations. These differences between the trimline elevations of tidewater glaciers and surge-type glaciers may be causing glaciers that are both tidewater and surge-type to produce more trimlines of an intermediate elevation. These findings indicate that glacier type may be an influence over trimline elevation.

Whilst glacier type appears to exert some influence over trimline elevation, glacier size does not seem to be related. Neither glacier area nor glacier length show any form of relationship with trimline elevation, with most trimlines situated at lower elevations regardless of glacier size.

In summary, most trimlines in central western Spitsbergen are situated at relatively low elevations, particularly below 50 m above sea level. The vast majority of trimlines (94%) are situated below the modern ELA, although the ELA at the time of trimline formation is likely

to have been significantly lower. The mode of trimline expression, the underlying topography and the type of glacier all appear to directly influence trimline elevation. Glacier size, on the other hand, is not related to trimline elevation and geology appears to have only an indirect impact, via topography.

4.5 Discussion

4.5.1 Factors influencing trimline distribution, expression and elevation

This study has analysed the influence of topographic, geological and glaciological variables on the distribution, expression and elevation of trimlines in central western Spitsbergen. The topography, underlying geology and glaciology have all been found to have some influence over glacial trimlines, although some are much more significant as controls than others. Glacier type and glacier size appear to be the most important influences over the study area trimlines, with glacier type exerting the stronger control. Topographic variables also appear to be significant controls over some characteristics of the trimlines, whereas geological variables seem to be largely unimportant.

This study has only considered the trimlines of a single area, but it seems likely that glacier type, glacier size and topographic factors are important influences over trimlines regardless of location. However, it cannot be concluded that these variables are the only controls over glacial trimlines because other variables may be significant in other locations. There may also be some variables that have not been considered by this study but which do influence glacial trimlines. However, there is no clear evidence for the existence of any other variables influencing the trimlines of central western Spitsbergen and the clear relationships between glacier type, glacier size and topographic variables with the trimline characteristic considered suggests that this study has captured the primary influences over glacial trimlines.

The influence of topography, geology and glaciology varies for different trimline characteristics. These three variables will now be discussed separately in order to outline their relative importance as influences over the trimline characteristics considered in this study.

4.5.1.1 Topography

Two topographic variables have been considered in this study: slope angle; and aspect. Of these the topographic slope angle has been found to be by far the more important factor.

Topographic aspect has only been found to exert a very weak influence over trimline distribution, producing a slight preference for trimlines to form on north and west facing slopes. This partially reflects the more common aspects in the study area (which is on the west coast of Spitsbergen), but may also be influenced by differing rates of slope process on north-facing topography compared to south-facing topography, due to differences in insolation. This difference may cause trimlines to be better preserved on north facing slopes, compared to more active south facing topography.

Topographic slope angle is important for trimline distribution and also exerts some control over trimline expression. There is a strong preference for trimlines to be located on slope angles of 10-30^{o} (Figure 4.8). This suggests that this range of topographic slope angles either promotes trimline formation or increases the potential for trimlines to be preserved. Trimlines might preferentially form on these slopes due to the influence of topography on the glaciological processes of erosional and deposition, which may be more prevalent at specific topographic slope angles. For example, higher levels of glacial deposition on shallower slopes may be the reason behind the location of moraine trimlines only on topographic slopes of < 60^{o}. However, in this example it is difficult to say if the topographic slope angle is controlling the process of glacial deposition, or whether it is the location of these shallow slope angles within a glacial valley that is the primary influence. For example, moraine trimlines may only form where there is sufficient glacially transported material to build a moraine, which may only be the case at the snout end of the valley, coinciding with the location shallower topographic slopes. Therefore, topographic slope angle may have a direct influence on trimline formation and exert a direct control on the formation of specific modes of trimline expression, but it may be that larger-scale valley morphology is the primary control and topographic slope has only an indirect influence. In either case, however, topography appears to have a significant influence on the locations of trimlines of specific expressions.

The influence of slope angle on trimline preservation appears much more straight-forward, with steeper slopes likely to suffer from higher levels of mass wasting, which can damage or remove trimline features. The sharp drop-off in the number of trimlines associated with topographic slopes > 30-35^{o} suggests that the preservation potential of trimlines on steep slopes is indeed poor (Figure 4.8). However, it is difficult to separate the influence of slope angle on trimline preservation with its control over trimline formation. It would seem most likely that topographic slope angle exerts some influence over both trimline formation and

trimline preservation, which leads to the preference for trimlines to be located on topographic slopes of 10-30°. This finding has implications for the identification and mapping of glacial trimlines in new areas, suggesting that focusing efforts on topographic slopes of between 10-30° is more likely to identify trimline features.

There is a reversal in the most common modes of trimline expression at topographic slope angles of around 30-35°. At these slope angles there is a striking change from modes of trimline expression that are likely to have formed via depositional and meltwater processes, which are most common on shallower topographic slopes, and those formed by erosional processes, which are most common on steeper topography (Figure 4.11). This difference indicates that topographic slope directly influences trimline expression, probably by controlling the formation of specific modes of trimline expression. Again, there may be a preservation component, but the complete lack of certain modes of trimline expression, particularly meltwater trimlines and moraine trimlines, on steep topographic slopes suggests that these trimlines do not form in steep topography. Other modes of trimline expression, such as erosional trimlines, can clearly form on any of the studied topographic slope angles, which may mean that preservation factors are more significant for these modes of trimline expression. These findings may be relevant for the identification and mapping of glacial trimlines, informing the topographic slope angles to consider when looking for specific modes of trimline expression and assisting the application of the classification of trimline expressions.

As well as influencing trimline distribution and expression, a link has been found between topography and trimline elevation. However, topography appears to only influence trimline elevation in a very general fashion, whereby there are higher elevation trimlines in locations where the topography is generally higher elevation. This would suggest that topography is not so much a control over trimline elevation as a factor that facilitates higher elevation trimlines in certain locations, which is itself related to the bedrock geology.

In summary, topographic variables do influence glacial trimlines, in particular there are clear direct relationships between slope angle and trimline distribution and expression. Topographic aspect does not significantly influence glacial trimlines and it is difficult to separate the role of larger-scale topographic factors, such as valley morphology, from that of the underlying geology. The control of topography over trimline distribution and expression is likely to involve a combination of controls over both trimline formation and over mass wasting processes, which influences the preservation potential of trimlines.

4.5.1.2 Geology

The control of geology over the large-scale topography of the study area indirectly influences some characteristics of glacial trimlines, such as trimline elevation and trimline distribution. However, there is little evidence for a direct control of geology over individual trimlines, with only weak associations identified between specific modes of trimline expression and specific bedrock lithologies. The only exception is surface aging trimlines, which are 12% more common than expected on the erosion-resistant Hecla Hoek metamorphic basement (Table 4.4). In this case, it is likely that this particularly subtle mode of trimline expression is better preserved on the more resistant bedrock. The lack other of similar associations between bedrock lithologies and specific modes of trimline expression suggest that this case is unusual and that the bedrock geology does not generally exert a direct control over glacial trimlines.

4.5.1.3 Glacier type

Of all the variables considered in this study, glacier type appears to exert the strongest influence over glacial trimlines. Significant relationships have been identified between glacier type and all of the trimline characteristics considered in this study. It therefore seems that glaciology is the most significant control over the glacial trimlines in central western Spitsbergen, compared to the relatively weaker influences of topography and geology. This finding suggests that it is also likely that glacier type is an important influence for glacial trimlines in other areas with historic or Quaternary trimlines.

The type of glacier exerts a strong influence over the distribution of trimlines, with specific glacier types associated with either more or less trimline features than expected. Interestingly, normal glaciers are associated with far fewer glacial trimlines than would be expected, given that this is the most common glacier type in central western Spitsbergen (Figure 4.9). The lack of trimline features linked to normal glaciers suggests that most glaciers do not produce large numbers of trimlines and indeed the majority (62%) of all trimlines in the study area are associated with either tidewater or surge-type glaciers. This evidence indicates that these ‘abnormal’ glacier types tend to over-produce glacial trimlines compared to the majority of ‘normal’ glaciers.

Surge-type and non-surging tidewater glaciers are both associated with higher numbers of glacial trimlines than would be expected given the prevalence of these glaciers in the study area (Figure 4.9). Tidewater glaciers may produce more trimlines than terrestrial glaciers due to their greater ice flow rates, which promote higher levels of glacial erosion and create more

material that is then available for glacial deposition. It was initial hypothesised that terrestrial surge-type glaciers would also produce greater numbers of trimlines because these glaciers can also have high ice flow rates. However, this has not been found to be the case, with terrestrial surge-type glaciers found to produce roughly the expected number of trimlines given the prevalence of these glaciers in the study area (Figure 4.9). Surge-type glaciers only have high velocities for short periods of time during the surge-phase, which generally lasts 3-10 years for Svalbard surge-type glaciers, with much lower ice flow rates during the quiescent-phase, which is often much longer than the surge-phase and usually lasts for 50-500 years for Svalbard surge-type glaciers (Sevestre and Benn 2015; Dowdeswell *et al.* 1991). Therefore, it appears that high ice flow velocities do not promote the formation of greater numbers of glacial trimlines, unless they are sustained for extended periods of time, as is the case for tidewater glaciers but not for terrestrial surge-type glaciers.

Glacier type has also been shown to influence trimline expression, with most modes of trimline expression linked to a specific glacier type or group of glacier types. Depositional contrasts are the only mode of trimline expression that is no more or less commonly associated than expected with any given glacier type (Table 4.5). All other modes of trimline expression have been found to be associated with at least one glacier type. For example, meltwater trimlines are 21% more commonly found associated with surge-type glaciers than expected but 17% less likely to be linked to normal glaciers than expected (Table 4.5).

There are particularly strong associations between specific modes of trimline expression and either surge-type or tidewater glaciers. In particular, both erosional and surface aging trimlines are much more likely to be associated with tidewater glaciers, both surge-type and non-surging, whereas the reverse is true for moraine trimlines (Table 4.5). The lack of moraines is easily explained by the fact that there is less land area around the snout of tidewater glaciers, meaning that there is no space for large moraine complexes to form. The higher than expected numbers of erosional and surface aging trimline associated with tidewater glaciers is probably due to the high velocities of these glaciers, which promotes the processes of glacial erosion that produce these modes of trimline expression.

Surge-type glaciers are also linked to specific trimline expressions. In particular, 73% of meltwater trimlines are associated with surge-type glaciers but both erosional and surface aging trimlines are much less commonly linked to surge-type glaciers than would be expected. The reasons for the reduced numbers of erosional and surface aging trimlines may be due to the highly dynamic nature of surge-type glaciers, which creates a much less stable

ice margin. The formation of these types of trimline expression require a stable ice margin for an extended period of time, a condition that is not met by terrestrial surge-type glaciers but which is met by tidewater glaciers. This may explain the difference in the prevalence of these modes of trimline expressions for surge-type glaciers compared to tidewater glaciers. The high numbers of meltwater trimlines associated with surge-type glaciers (73% of these trimlines) also seem likely to be influenced by surging processes. Surge-type glaciers on Svalbard tend to surge via a polythermal mechanism, which can culminate with a release of meltwater from the snout area of the glacier during the surge phase (Murray *et al*. 2000; Fowler *et al.* 2001). This outflow of meltwater is likely to be the primary agent for producing meltwater trimlines in central western Spitsbergen, particularly given that the generally cold climate does not usually produce large quantities of meltwater.

As well as influencing trimline distribution and expression, the evidence suggests that glacier type exerts some control over trimline elevations. Whilst trimlines are generally found < 50 m above sea level, certain glacier types produce anomalously large numbers of trimlines at specific higher altitude ranges. For example, surge-type glaciers produce more trimlines at elevations of 200-300 m than any other glacier type, whereas tidewater glaciers produce the more trimlines at 100-150 m. Glaciers that are both tidewater and surge-type produce a higher number of trimlines at 150-200 m, falling between the peaks of tidewater and of surge-type glaciers. This suggests that glacier type influences the vertical distribution of trimlines, with tidewater glaciers more likely to produce trimlines at lower elevations and surge-type glaciers tending to produce more trimlines at higher elevations. This may be partially due to the fact that tidewater glaciers must always extend down to sea level, whereas terrestrial glaciers must terminate above sea level. However, visual analysis of the locations of glacial trimlines along their parent glacier suggests that tidewater glaciers do tend to produce more trimlines closer to the glacier snout than is the case for terrestrial glaciers, surge-type or otherwise (Figure 4.6). Visual analysis of surge-type glaciers also reveals a pattern in their trimline elevations, with slightly more trimlines at higher elevations, particularly above the ELA, than normal glaciers. This suggests that there is a glaciological influence on the elevation of trimline features, although the reasons for this are unclear.

In summary, glacier type is a significant control over trimline distribution, expression and elevation. Both tidewater and surge-type glaciers are associated with a range of specific trimline characteristics, which may make it possible to use trimline evidence for the identification of these glacier types in Quaternary settings. The reasons of the association

between specific trimline characteristics and certain glacier types is often unclear, which reflects the currently poor understanding of the processes of trimline formation.

4.5.1.4 Glacier size

As well as the type of glacier, glacier size has been considered in this study but has been found to be far a less significant control over glacial trimlines. Whilst glacier type influences trimline distribution, expression and elevation, glacier size is only related to trimline distribution and expression, with no impact over trimline elevation. There is a strong correlation between glacier size and tidewater or surge-type glaciers, which are generally larger than normal glaciers. Therefore, glacier type maybe behind some of the influence of glacier size or possibly vice versa. It is very difficult to distinguish between the impact of these variables but the fact that glacier type is linked to every trimline characteristic considered in this study suggests that this is the more significant glaciological variable.

Glacier size, both in terms of glacier length and area, has been shown to be weakly related to the number of trimline features associated with a given glacier, with larger glaciers producing slightly more trimlines on average. This relationship was expected because a larger glacier has a greater ability to work on the landscape, via glacial erosion and deposition, and is therefore more likely to produce glacial landforms, such as trimlines. However, there is a lot of variability in the relationship between glacier size and the number of trimlines. This variability is caused by the type of glacier, with surging behaviour creating unpredictable numbers of trimline features compared to normal glaciers or non-surging tidewater glaciers. This suggests that the relationship between glacier size and the number of trimlines is moderated by the type of glacier, indicating that glacier type is the more important variable. Considering the different glacier types individually gives a wide variety of trend strengths between glacier size and number of trimlines, supporting the conclusion that glacier type is the more significant influence over trimline distribution.

Glacier size has also been found to be associated with the mode of trimline expression, with correlations found between glacier length or area and certain modes of trimline expression. In particular, erosional trimlines and surface aging trimlines have been found to be positively related to glacier size, with both larger and longer glaciers more likely to produce this mode of trimline expression. This would seem likely to be due to the greater erosional potential of larger glaciers. However, the majority of modes of trimline expression are no more commonly associated with larger or smaller glaciers, indicating that the greater depositional potential of larger glaciers does not lead to more moraine trimlines, for example.

Additionally, both erosional and surface aging trimlines are more commonly associated with tidewater and tidewater surge-type glaciers, which are generally amongst the largest glaciers. Therefore, glacier type may again be the dominate variable and could be indirectly influencing trimline expression via glacier size.

4.5.1.5 Summary

In summary, glacier type has been found to be the most significant control over the characteristics of glacial trimlines in central western Spitsbergen. Geology and topographic aspect have little impact over glacial trimlines and topographic slope influences only trimline distribution and elevation. The role of glacier size is difficult to distinguish from that of glacier type but is likely to be less significant and exerts an influence only over trimline distribution and certain modes of trimlines expression.

The influence of topographic slope over glacial trimlines is likely to be due to a control over the processes of trimline formation and of trimline preservation. The precise nature of this control is not clear, largely due to limited understanding of the formation and preservation potential of glacial trimlines. Further research into glacial trimlines in a wider range of settings may shed more light on the role of topography as a control over the characteristics of glacial trimlines. In the meantime, the findings of this study have suggested a range of topographic slope angles (10^{o}-30^{o}) within which glacial trimlines are most likely to be found. This information may prove useful for the identification and mapping of trimlines in other areas.

The dominant influence of glacier type may be due to differences in the ice flow velocities between the different types of glaciers. The higher flow rates of surge-type and particularly tidewater glaciers promote greater rates of glacial erosion and deposition, leading to higher numbers of trimlines and favouring the development of specific modes of trimline expression. The strong influence of glaciological factors over glacial trimlines in this historic setting may be reflected in Quaternary settings, potentially allowing the type of glacier to be identified from an assemblage of trimlines. The use of trimline evidence in conjunction with other landforms may be particularly useful for identifying surge-type glaciers in both historic and Quaternary settings.

4.5.2 Trimlines of tidewater and surge-type glaciers

This study has shown that tidewater and surge-type glaciers produce trimlines with differing characteristics, which may allow the glacier type to be identified from a trimline assemblage.

This would be especially useful in Quaternary settings, where the glaciers responsible for creating the trimlines no longer exist and the sea level may have been different. Trimlines may also prove useful for positively identifying surge-type glaciers, which can be difficult if the glacier has not been observed during a surge event (Sevestre and Benn 2015). Due to the relatively short time that glaciers spend surging, compared to the time spent in the quiescent phase, landform assemblages are often used to try and identify potential surge-type glaciers (Sevestre and Benn 2015; Ottesen *et al.* 2008; Evans and Rea 2003). Specific trimline characteristics associated with surge-type glaciers could be added to the existing assemblage of surge landforms, adding further evidence to the positive identification of surge-type glaciers in both historic and Quaternary settings.

Former tidewater glaciers are often easy to distinguish in historic settings. For example, the trimlines associated with several glaciers on the southern side of St. Jonsfjord show that the glaciers previously reached the coast, suggesting that they were once tidewater glaciers (Figure 4.6d). However, it is not always so easy to identify former tidewater glaciers in historic settings and it is usually much more difficult in Quaternary settings, particularly due to the complicating factor of fluctuations in sea level. This study has shown that tidewater glaciers produce more trimlines than any other glacier type and that the trimlines of tidewater glacier may be distinguishable by their mode of expression and by the clustering of trimlines in specific elevation ranges. These findings suggest that it may be possible to identify former tidewater glaciers in more difficult historic and Quaternary settings.

In particular, the tidewater glaciers in central western Spitsbergen are strongly associated with erosional and surface aging trimlines and have far fewer moraine trimlines than other types of glacier. All glacier types were found to have a majority of trimlines at elevations below 50 m above sea level but tidewater glaciers can be distinguished by their secondary peak of trimlines clustered between 100-150 m above sea level. A clustering of trimlines at this elevation, alongside evidence from the pattern trimline expressions, may allow the positive identification of former tidewater glaciers.

Where a glacier is tidewater and non-surging, the above characteristics hold true and there is also an association with greater numbers of trimlines expressed as slope landform discontinuities. Surge-type tidewater glaciers, on the other hand, do not show this particular association, which may potentially help to distinguish surge-type and non-surging tidewater glaciers. There is also a difference in the location of the secondary trimline elevation cluster for surge-type tidewater glaciers (150-200 m above sea level) compared to non-surging

tidewater glaciers (100-150 m above sea level). Therefore, analysis of trimline elevations and expressions may enable surging behaviour to be distinguished in tidewater glaciers, both in historic and Quaternary settings.

Terrestrial surge-type glaciers produce a differing set of trimline characteristics. Surge-type glaciers are also associated with particular modes of trimline expression, most significantly 73% of meltwater trimlines in the study area were linked to surge-type glaciers. Moraine trimlines and slope landform discontinuities are less commonly associated with surge-type glaciers than with other glacier types, whilst erosional and surface aging trimlines are more often found associated with surge-type glaciers. Terrestrial surge-type glaciers also produce a different secondary cluster in the elevation of their trimlines, at 200-300 m above sea level. A combination of these trimline characteristics may enable the identification of surging behaviour in historic and Quaternary settings, particularly when found in conjunction with other evidence of glacial surging.

There are two surge-type glacier landsystems already in use in Svalbard – Evans and Rea's (2003) terrestrial surging glacier landsystem and Ottesen *et al.*'s (2008) tidewater surging glacier landsystem. Both of these landsystems were developed by studying Svalbard surge-type glaciers and both include a wide range of landforms but neither landsystem includes glacial trimlines. Given the findings of this study, it may be time to update these two landsystems to include the trimline characteristics that have been shown to be associated with terrestrial and tidewater surging behaviour in central western Spitsbergen.

In summary, this study has shown that tidewater and surge-type glaciers produce differing sets of trimline characteristics, which may assist with identifying these glacier types. However, it is unclear how applicable these identifying characteristics will be outside of Svalbard. The glaciers of Svalbard surge via a thermal switch mechanism (Sevestre and Benn 2015), whilst surge-type glaciers in other areas can surge via a range of different processes. This may mean that surge-type glaciers outside of Svalbard could produce very different trimlines. Further research in other areas is required to confirm whether the trimline characteristics found by this study to be associated with surging behaviour are common to all mechanisms of glacier surging. The characteristics of trimlines associated with tidewater glaciers in central western Spitsbergen, on the other hand, are much more likely to be robust outside of Svalbard, although further research in other areas will be required to confirm this.

4.5.3 Trimlines above the ELA

Previous research has suggested that trimlines are unusual compared to other glacial landforms because they can form above the ELA (Thorp 1981; Kelly *et al.* 2004). If true, this makes trimlines a rare source of information about the ice margin position and ice thickness in the accumulation area. This study has found that trimlines can indeed form above the ELA, with 6% of trimlines in central western Spitsbergen located above the modern ELA (c. 350 m above sea level). However, the majority of trimlines in the study area are thought to have formed at the peak of the Little Ice Age glacial readvance. At this time, the ELA is likely to have been at a significantly lower elevation, meaning that a higher percentage of trimlines would have been above the ELA at the time of trimline formation.

It is clear that trimlines can form above the ELA, supporting the conclusions of previous research (e.g. Kelly *et al.* 2004). Therefore, trimlines can be used to determine the palaeo ice thickness in the accumulation area as well as in the ablation area. This makes glacial trimlines a very significant landform for producing 3D palaeoglacial reconstructions in both historic and Quaternary settings, which can then be used to produce reconstructions of palaeo temperature and precipitation.

4.5.4 Trimline expressions in central western Spitsbergen

The mode of trimline expression has been found to be most strongly related to the type of glacier, although glacier size, topographic slope, and bedrock geology may all influence trimline expression. Most modes of trimline expression have been found to be preferentially associated with a specific type of glacier, with depositional contrasts being the only exception (Section 4.5.1.3). Particularly, significant differences have been noted between the trimline expressions associated with surge-type compared to non-surging glaciers and between tidewater and terrestrial glaciers (Section 4.5.1.3). These findings suggest that consideration of the expression of trimline features is fruitful and can provide useful evidence to help in the identification of glacier type.

4.5.4.1 Review of the trimline expression classification

This study utilised a new classification system for the mode of trimline expression (Figure 4.5). Overall this classification system was easy to use and it was generally possible to separate the different modes of trimline expression. However, a significant minority of trimlines (22%) were found to be expressed in more than one way – these features are referred to as ‘composite trimlines’. These composite trimlines were classified according to

their most dominate expression, which was generally easy to identify but this was necessarily a subjective decision. The most common composite trimlines were dominantly erosional or depositional contrasts, combined with either slope landform discontinuities or surface aging contrasts.

Aside from issues classifying composite trimlines, the classification system performed well when applied by eye to the high resolution aerial imagery of the study area but was more difficult to use with the lower resolution Landsat imagery. However, the system was still useable with the Landsat imagery, which has a maximum resolution of 15 m in the panchromatic band (Band 8) and 30 m for all other bands. Identification of the mode of trimline expression was greatly aided by the use of composite images, particularly true and false colour images and Normalised Difference Vegetation Index analysis (Section 3.3). The use of the Digital Elevation Model (DEM) also assisted in identifying the mode of trimline expression, particularly by altering the angle of illumination. It is therefore recommended that the trimline expression classification system is used with aerial imagery where possible but it can be applied to lower resolution satellite imagery, where DEMs and compound images can be utilised to aid the classification process.

4.5.5 Implications for the use of trimlines in palaeoglacial reconstructions

This study has found that glaciological factors, particularly the type of glacier, are the primary controls over the characteristics and locations of glacial trimlines. This finding means that studying glacial trimlines in greater detail can potentially yield more information about former glaciations than simply constraining the areal extent and ice thickness. This is especially significant in Quaternary settings, where the glacier that created the trimlines no longer exists and where there are often few other sources of information about the glacier type and behaviour. It is particularly important that tidewater and surge-type glaciers create differing assemblages of trimlines, meaning that trimlines may be added to the existing landsystems used to identify these glacier types.

Glacial trimlines are very useful landforms both for their traditional use (creating 3D palaeoglacial reconstructions), and for providing additional information about the glacier type and behaviour. Studies of glacial landforms can now justify spending more time analysing the glacial trimlines, particularly by considering their distribution, expression and elevation. Analysis of these variables can then be used, alongside other evidence, to suggest the type of glacier. Further study of glacial trimlines may allow improved understanding of trimline formation and preservation to be developed further, potentially allowing for more

information to be extracted from trimlines and for increased confidence when using trimlines to suggest the glacier type. In particular, testing of a new surging glacier landsystem, including trimlines, in a range of different locations is needed to verify that the surge-type glacier trimline characteristics identified by this study hold true in other locations and for other mechanisms of glacial surging.

As well as expanding the potential uses of glacial trimlines in palaeoglacial reconstructions, this study has also identified trimline characteristics that may make the identification, mapping and expression classification of trimlines much easier. Glacial trimlines have been shown to be much more common on topographic slope angles of 10-30^{o} (Figure 4.8). Therefore, researchers looking for glacial trimlines would be best advised to concentrate their efforts on areas meeting this criterion. However, this study has found trimlines at almost all slope angles in the study area, so future efforts to map and identify trimlines should not limit themselves to a narrow range of possible trimline locations. Additionally, this study has confirmed previous research and identified trimline features above the ELA, suggesting that the accumulation area is an important place to look for trimlines.

The new expression classification presented and tested in this study provides a new way to look at glacial trimlines and a functional system to determine the expression of a given trimline feature. The mode of trimline expression has been shown to be related to glacier type, meaning that the use of the trimline expression classification can provide a relatively straight-forward way to deduce information about glacier type and behaviour.

4.5.6 Sources of uncertainty and limitations of this study

The accuracy of the mapping of trimlines in the study area was tested and it was determined that features could be identified to a geolocational accuracy of 17.5 m using a combination of very high resolution aerial images alongside the Landsat 7 images. The mapping process did not identify any trimlines that were shorter than 30 m in length (i.e. covering roughly two pixels in the Landsat 7 imagery), indicating that features shorter than this may have been missed. However, extensive use of the aerial images (with a resolution of 40-50 cm) in areas where relatively short trimlines were identified minimised the chance that any trimline features < 30 m in length were overlooked, although this cannot be completely ruled out. The use of multiple different data sets and the high resolution of the mapping, compared to the size of the trimline features, suggests that high confidence can be placed in the results of the trimline identification and mapping process. The methods used to map trimlines in

this study are also likely to work well in other areas, although the availability of high resolution aerial imagery may limit the resolution of trimline mapping outside of Svalbard.

Some of the trimline elements identified by this study are continuous trimlines of considerable length but others are much shorter features. Visual analysis of these shorter trimlines suggests that, in some cases, several trimline features may be fragments of a larger trimline, which presumably was once continuous and has since been broken up by weathering and mass wasting processes. It is not always possible to positively distinguish fragments of previously larger features without the use of environmental dating, which is beyond the remit of this study. For this reason, this study has made the assumption that all trimlines are discrete features. As it was not possible to verify the accuracy of this assumption, the problem of trimline fragmentation and its potential impacts on the conclusions of this study were investigated.

In order to avoid any confusion, all features discussed thus far are termed 'trimline elements'. This term means that these are visually identifiable trimline features, which may include both whole trimlines but also fragments of trimlines. 'Interpolated trimline margins' are produced by using a degree of subjective interpretation to 'join up' trimline elements into a continuous ice margin. For example, in Chapter 5 a reconstruction will be produced that will involve the synthesis of the trimline elements presented in this chapter into interpolated trimline margins. The use of these two terms is encouraged to clearly distinguish between empirically mapped trimline elements and subjective interpolated trimline margins. The issue of trimline fragmentation impacts only on the trimline elements, so the impacts of this problem are considered in the context of this chapter because fragmentation will not affect the interpolated trimline margins in Chapter 5.

An estimate of the prevalence of fragmentation in the study area was made by considering the relationship between the number of trimline elements per glacier and the total length of trimline elements per glacier. This analysis indicated that levels of fragmentation are likely to be low in the study area, so probably not significantly impacting on the conclusions of this study. However, the lack of environmental dating means that this conclusion cannot be empirically verified. Therefore, further testing was carried out to determine whether fragmentation had affected the conclusions of this study. This testing was carried out on the two analyses that were deemed to be most likely to be sensitive to the problem of fragmentation: the number of trimline elements per glacier; and the number of trimline elements associated with each type of glacier. It was found that controlling for fragmentation

did not significantly impact the conclusions of either of these analyses. In all cases the same overall conclusions were drawn and there was very little difference in any individual data values. This testing process validates the results of this study and supports the evidence that fragmentation is not likely to widespread in the study area. Furthermore, it can be confidently stated that, where it is present, fragmentation does not significantly affect the analyses used in this study and has not impacted the conclusions of this research.

4.6 Conclusions

In summary, this study has demonstrated that analysis of glacial trimlines can tell us much more than simply where the ice margin was. In particular, analysis of the expression and elevation of glacial trimlines can shed light on the type of glacier that formed them, potentially allowing the identification of surge-type and tidewater glaciers in Quaternary settings. This study has also confirmed that trimlines can be formed above the ELA, supporting the conclusions of previous research and validating the use of these features as indicators of palaeo ice thickness in the accumulation area. A new classification system for trimline expressions has been tested and found to work well in practice. Several trimline characteristics have been identified that will enable more targeted mapping of glacial trimlines by future studies and will enable more confident use of the trimline expression classification.

Analysis of the trimlines of central western Spitsbergen suggests that the type of glacier is the primary control over trimline characteristics, with differing trimline assemblages found to be associated with tidewater glaciers and with surge-type glaciers in particular. Geological factors have been shown to have little direct influence over glacial trimlines and topography is also generally not a significant factor. Therefore, trimline analysis can be used to deduce information about the type of glacier responsible for forming the trimlines, without the risk of misinterpreting the influence of non-glaciological variables.

The findings of this study may lead to a significant expansion in the potential uses for glacial trimlines in palaeoglacial reconstructions. Where previously trimlines have been used only as a constraint on the ice margin position and as a measure of ice thickness, they can now potentially be used to diagnose the type of glacier. Further research is required to confirm that these trimline assemblages are robust in multiple locations, but these initial findings justify further study into glacial trimlines and suggest that these features are being under-

utilised at present. Additionally, the better understanding of the glacial trimlines of central western Spitsbergen enables more confident use of these features to constrain 3D reconstructions of glacial fluctuations in the local area, a demonstration of which will now follow in Chapters 5 and 6.

Chapter 5

Reconstruction of the Little Ice Age glacial extent in central western Spitsbergen from glacial trimlines using GlaRe

5.1 Introduction

In Chapter 4 the trimlines of central western Spitsbergen were mapped and in this chapter they will be used to produce a 3-dimensional (3D) reconstruction of 15 Little Ice Age (LIA) glaciers. The LIA reconstruction will comprise the following components:

- a LIA ice surface elevation model;
- the ice margin (based on trimlines) and glacier area;
- ice thickness and ice volume measurements;
- estimated local Equilibrium Line Altitude (ELA).

The use of glacial trimlines for 3D reconstructions of LIA glaciers in central western Spitsbergen is a new concept, with previous studies attempting to reconstruct the LIA ice thickness without this empirical constraint (e.g. Lønne and Lyså 2005 Navarro *et al.* 2005; Ziaja 2005; Kohler *et al.* 2007; Mangerud and Landvik 2007; Nuth *et al.* 2007). In this study, the glacial trimlines will be pivotal to constraining the ice margins and ice thickness of the LIA glaciers, allowing greater confidence to be placed in the 3D reconstructions and enabling more accurate estimation of the LIA ice volume and ELA. The GlaRe method of Pellitero *et al.* (2016) will be used to produce the 3D reconstructions – a Geographic Information Systems (GIS) toolbox for spatial interpolation of an ice surface based on ice flow physics along a central flowline. This is a relatively new method and this study will provide a demonstration of its use and an example of the combination of glacial trimlines and GlaRe for producing robust 3D glacial reconstructions.

5.1.1 Choice of reconstruction glaciers

The trimline mapping and analysis in Chapter 4 utilised a large sample of 78 glaciers, in order to draw robust and reliable conclusions about the relationships between trimlines and various glaciological, topographic, and geological variables. For the LIA reconstruction, a smaller sample of 15 glaciers will be used to enable a more detailed analysis. The glaciers for the reconstruction were chosen as a representative sample, including all types of glacier in

the study area and a range of glacier sizes (Table 5.1). The area around Ny-Ålesund is included in the reconstruction sample because of the availability of glacier bed topography Digital Elevation Models (DEMs) produced using ground penetrating radar (GPR) in this area. Access to a GPR DEM for one or more glacier was needed to validate the estimated bed topography used in the production of the 3D LIA reconstructions (see Section 5.4).

Glacier ID	Name	Type	Glacier area (km^2)	Ice volume (km^3)
32	Irenebreen	Normal	3.5	0.2
33	Erikkabreen	Surge-type	4.6	0.4
34	Waldemarbreen	Normal	2.8	0.2
35	Midtre Lovénbreen	Surge-type	5.2	0.4
38	Austre Lovénbreen	Normal	5.0	0.4
39	Pedersenbreen	Normal	6.2	0.5
41	Botnfjellbreen	Surge-type	5.9	0.5
43	Aavatsmarkbreen	Tidewater surge-type	73.2	15.8
44	Dahlbreen	Tidewater	126.5	26.3
48	Uversbreen	Surge-type	66.1	16.7
53	Comfortlessbreen	Tidewater surge-type	57.8	11.7
54	Elisebreen	Surge-type	12.6	1.5
57	Oliverbreen	Normal	1.2	0.1
58	Andreasbreen	Normal	5.3	0.4
59	Eivindbreen	Normal	2.5	0.2

Table 5.1 – The chosen reconstruction glaciers represent the full range of glacier types and sizes within the larger sample of glaciers described in Chapter 4. This table summarises the key statistics for each of the reconstruction glaciers. A map of the numbered glaciers is shown in Figure 5.6.

To avoid confusion between the two study areas in this thesis, the larger area used for the trimline analysis presented in Chapter 4 is termed the 'study area' whilst the smaller area used for the LIA reconstruction is the 'reconstruction study area' (Figure 5.1). The group of glaciers for which LIA reconstructions were produced are called the 'reconstruction glaciers' to distinguish them from the 'study area glaciers' discussed in Chapter 4.

In this chapter, the methods used to produce the 3D LIA reconstructions will be described and explained using an example glacier that has been chosen to provide a demonstration of the various processes. Glacier 32 has been chosen because it is a medium-sized normal valley glacier that has not be identified as exhibiting any surging behaviour, which might complicate its reconstruction (Figure 5.2).

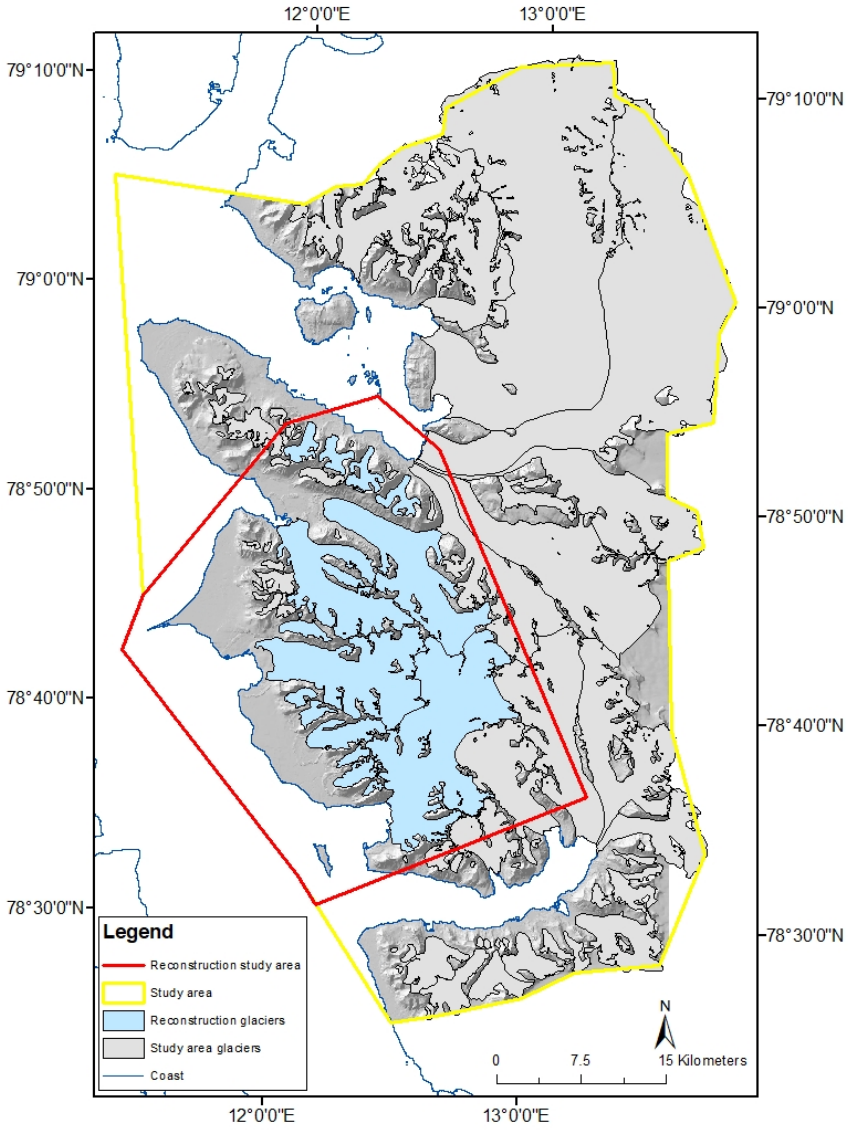

Figure 5.1 – The study area for the trimline mapping presented in Chapter 4 is shown in yellow, with the smaller reconstruction study area in red. The glaciers used in the reconstruction are picked out in blue, whilst the rest of the larger sample of glaciers used in the study of trimlines in Chapter 4 are coloured grey.

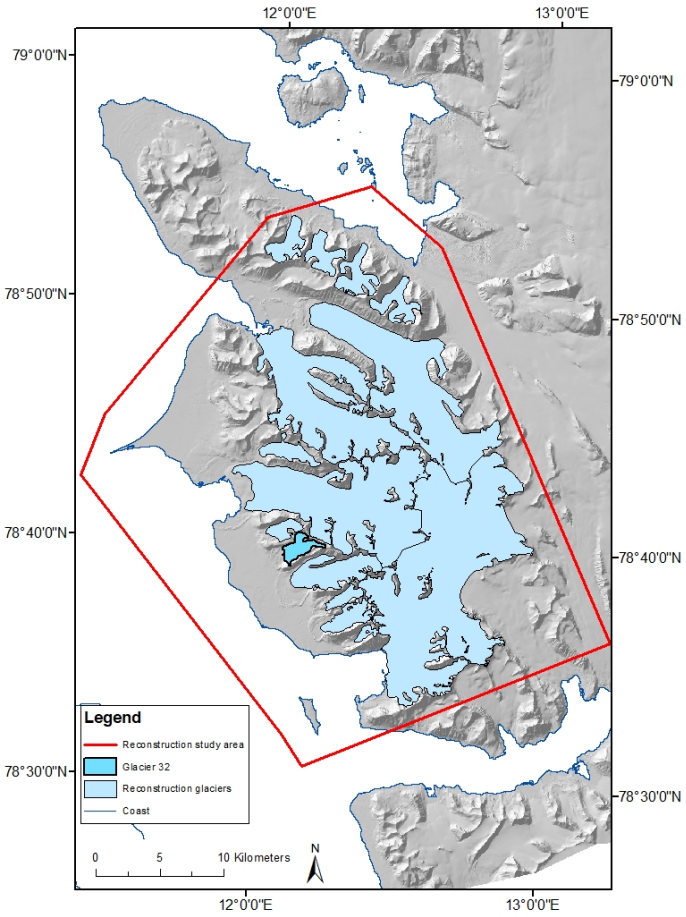

Figure 5.2 – This map shows the position of Glacier 32 within the reconstruction study area and in relation to the other reconstruction glaciers. Glacier 32 is a medium-sized valley glacier that has not been classified as surge-type, meaning that it has not been observed during a surge and is not associated with any diagnostic surge-type landforms.

5.2 Overview of the production of LIA glacier surface elevations

This study will demonstrate the use of the relatively new GlaRe method for producing 3D glacier reconstructions, in this case utilising trimlines. GlaRe was produced by Pellitero *et al.* (2016) and consists of a toolbox for use in ArcGIS that outputs a DEM of the reconstructed ice surface elevations. The DEM is interpolated from ice thickness values computed along flowlines using standard ice flow laws (details in Section 5.5 and Pellitero *et al.* 2016).

The GlaRe method was chosen because it works well for valley glaciers as well as ice cap and ice field outlets (Pellitero *et al.* 2016). Additionally, the method requires testing in a wider range of glacial environments and this study will provide a good example of GlaRe's usage in an Arctic maritime glacial environment.

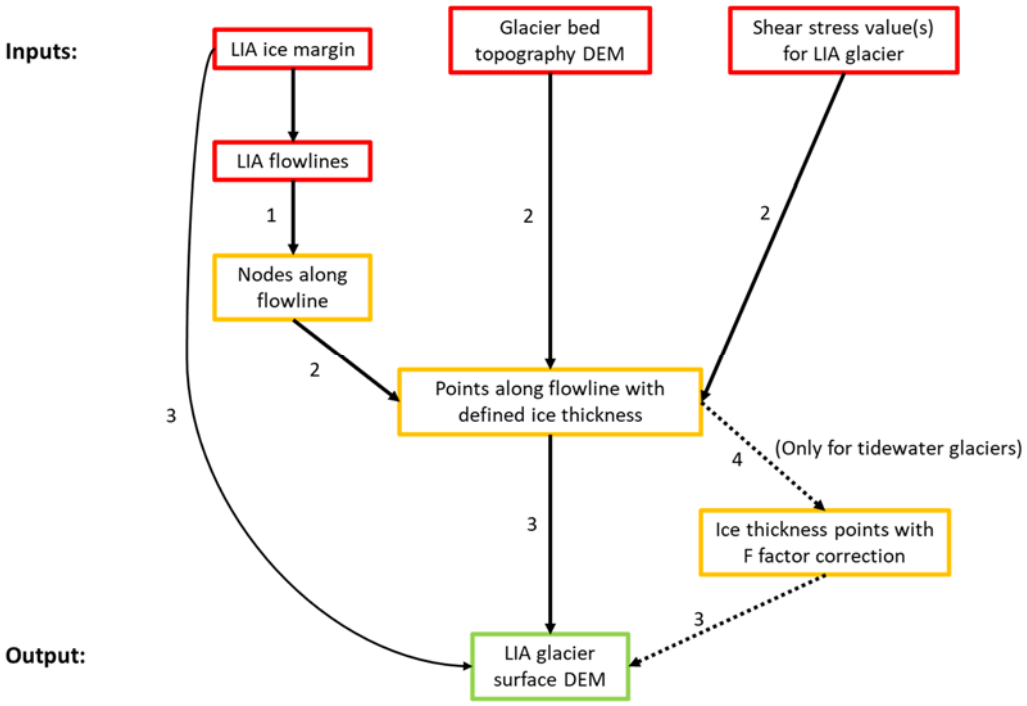

Figure 5.3 – Simplified flowchart showing the main steps of the GlaRe reconstruction process. User-defined inputs are shown in red, although it is possible to produce the glacier bed topography DEM within GlaRe (see Section 5.4). Intermediate layers produced during the use of the GlaRe toolset are coloured yellow and the final output is coloured green. The dotted arrows indicate an optional additional step that was used to improve the accuracy of the tidewater glacier reconstructions by using an F factor correction to include a measure of lateral drag into the ice thickness calculations (see Section 5.5.2). The numbers alongside the arrows identify specific named tools within the GlaRe toolset. These are: 1) 'Construct interval nodes'; 2) 'Flowline ice thickness tool'; 3) 'Glacier surface interpolation'; 4) 'Automatic ice thickness recalculation with F factor'.

Figure 5.3 shows the essential core steps in the GlaRe method that are required to produce a reconstructed ice surface DEM. The inputs required for this core method are:

- a DEM of the glacier valley without ice (i.e. the bed topography);
- LIA ice margin;
- centreline flowline for the LIA glacier, with attached centreline flowlines of major tributaries;
- estimated basal shear stress value(s) for the LIA glacier;
- measurement of the largest width of the LIA glacier snout, narrowest width of the LIA trunk glacier, and approximate mean width of the LIA glacier snout.
- a defined interval distance for points along the GlaRe flowline.

Additional processing steps were required to produce some of the input data required for the core GlaRe method. Section 5.3 details the production of the LIA ice margins by interpolation between the mapped trimline elements, which were first grouped by estimated age. Optional steps in the GlaRe toolbox, explained in Section 5.4, were used to produce the bed topography from the modern ice margin and modern ice surface DEM. Finally, the basal shear stress values were calculated using the *Profiler* tool of Benn and Hulton (2010), which is recommended for use with GlaRe and detailed in Section 5.5.1. An optional step in GlaRe utilised F factors to add a measure of lateral drag to the reconstruction, which is described in Section 5.5.2.

Once the LIA ice margin had been produced from the trimlines, this could be easily used to produce the centreline flowline for the LIA glacier and the LIA glacier measurements in ArcGIS (see the appendix to Pellitero *et al.* 2016 for instruction on creating suitable flowlines for GlaRe and details of the glacier measurements needed). The interval distance for the GlaRe flowline points was set as 20 m to correspond to the resolution of the DEM used to map the trimlines.

The glacial trimlines mapped in Chapter 4 are clearly a key component of the LIA ice margin and were also used to constrain the ice surface elevation in the calculation of the basal shear stress values. Without the trimlines it would not be possible to estimate the basal shear stress during the LIA and instead a default value of 100 kPa would have to be used, which does not produce realistic ice surfaces in the majority of cases in the reconstruction study area (see Section 5.5.1 for examples).

5.3 Trimline-based ice margins

The process of interpolation by eye was used to link together individual trimline elements to form continuous LIA ice margins for each of the reconstruction glaciers. Interpolation is a subjective process but at present there is no other reliable and reproducible method for producing continuous ice margins from fragmentary geomorphological evidence (see Chapter 2). Figure 5.4 shows the LIA trimlines of Glacier 32 and how these were linked using interpolation to produce a likely ice margin position.

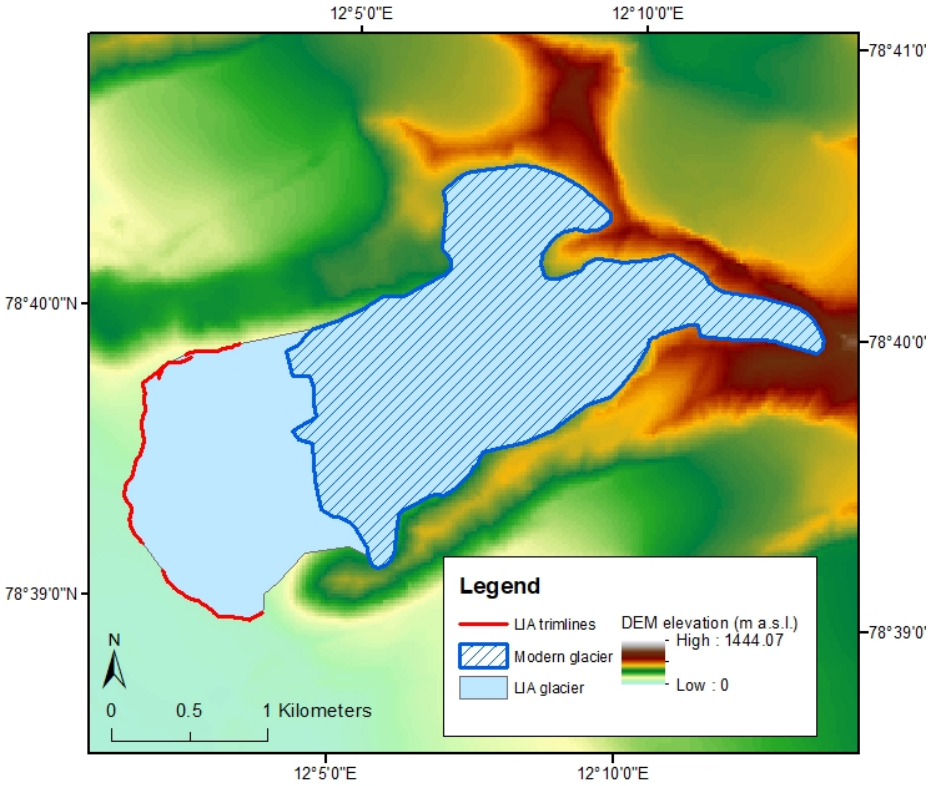

Figure 5.4 – Both the modern and LIA ice margins of Glacier 32 are shown alongside the LIA trimlines associated with this glacier. The modern ice margin was used to guide the form of the LIA ice margin in the confined area of the upper glacier, whilst the LIA trimlines were used to guide the shape of the LIA glacier's snout and ablation area. Where no trimlines were present, the process of interpolation by eye was used to link up the trimline features, which was guided by the form of the glaciers' valley to produce a glaciologically plausible LIA ice margin.

5.3.1 Grouping trimlines by relative age

The first step in producing the LIA ice margins was to identify the trimline elements that were most likely to be associated with the LIA maximum glacial extent for each glacier. Initially, a survey of all of the trimlines in the study area was carried out to identify how many glacial events were represented. From this survey it was found that five glacial events are represented in the glacial trimlines of central western Spitsbergen. Based on the relative position of the trimlines, these five events were suspected to represent the following time periods:

1. Recent ice margin fluctuations;
2. Retreat from the LIA to the modern ice margin position;

3. LIA ice margin;
4. Retreat from an older glacier to the LIA ice margin position;
5. Older glaciation ice margin/ possible retreat onshore from the offshore Last Glacial Maximum ice margin position.

Having identified these five broad time periods, each individual trimline element needed to be assigned to the correct group. Absolute trimline dating was not possible within the remit of this study, although this would be the optimum method for confidently dating the trimlines and verifying the dates of each time period. Even had absolute dating (with typical error ranges) been possible, these methods do not always provide separate and distinguishable age categories and may not have been able to distinguish the five time periods represented in the reconstruction study area. Therefore, relative dating methods were used to age the trimlines and to group them into the above time periods.

There are several glaciers within the study area that had a set of trimlines including several of the age groups. These glaciers were used as benchmarks to guide the relative dating of other glaciers' trimlines. Various methods of comparison were trialled and it was found that the most reliable way to relatively date the trimline elements in the study area was to consider the approximate area change of the glaciers between the different time periods. The benchmark glaciers with mostly complete trimline sets were used to estimate a percentage area change between each time period, for example approximately -25 % area change was identified between the glaciers at the LIA maximum compared with the modern glacier area. By applying these percentage area changes to other glaciers in the study area, it was possible to identify the trimline elements that were most likely to belong to each time period (Figure 5.5). Although this method is subjective, it was possible to support the identification of the LIA trimlines by comparing the glacial area change, as well as the expression and the morphology of the trimlines, to confidently dated LIA landforms of other glaciers in Svalbard (Lønne and Lysså 2005; Mangerud and Landvik 2007). With the LIA maximum trimlines reasonably well constrained, the relative dating of the remaining four time periods was able to be carried out with greater confidence.

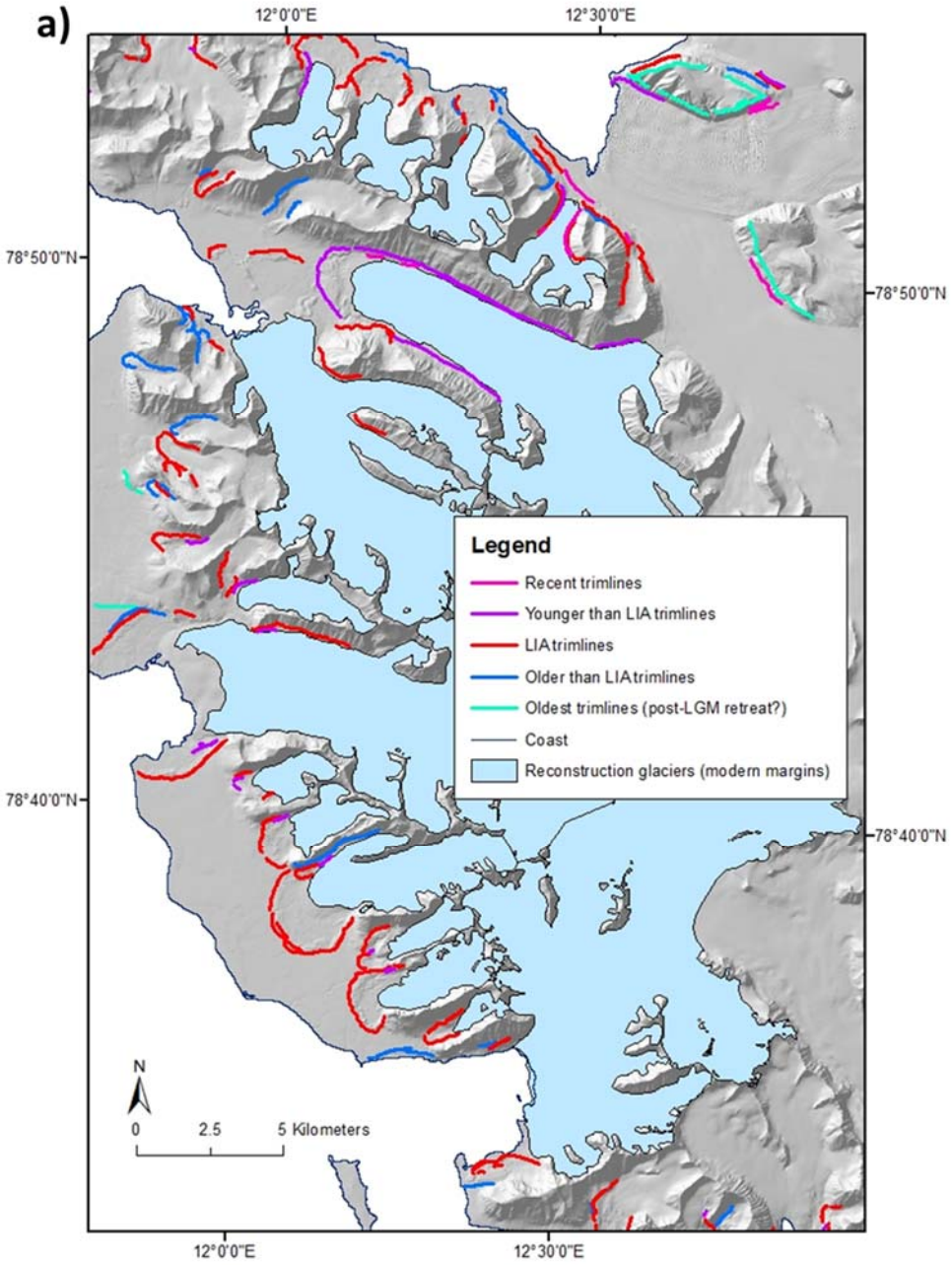

Figure 5.5 (5.5b on next page) – The age classification of the five named time periods applied to the reconstruction study area trimlines. a) shows the entire reconstruction study area, whilst b) shows the trimlines around Glacier 43 in more detail because this area has examples of four of the five named time periods.

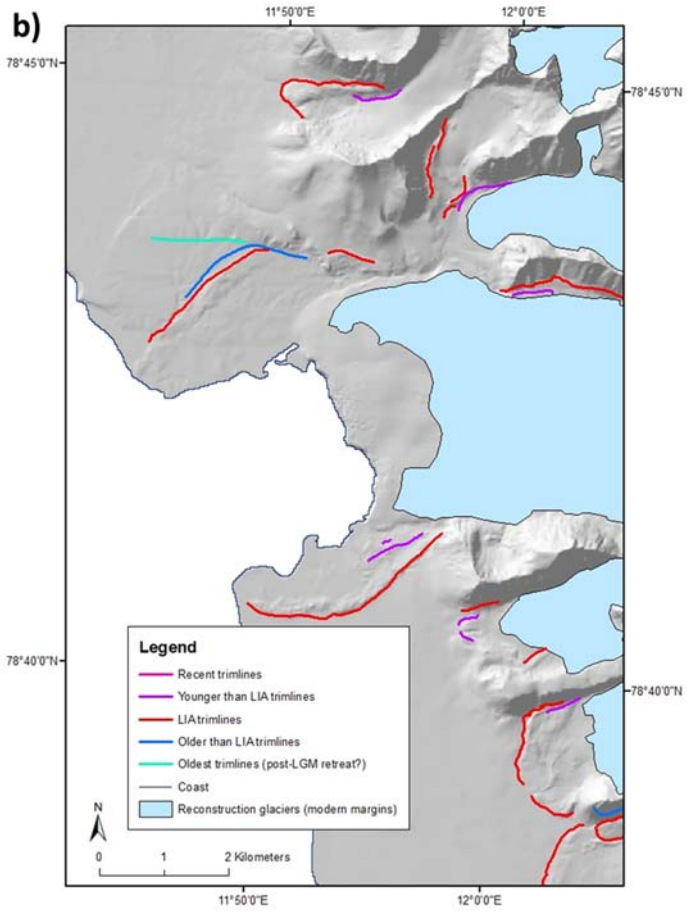

5.3.2 Interpolating the trimlines into ice margins

Once the trimline elements had been grouped by relative age and the LIA maximum features identified, these could then be linked together using the process of interpolation. There is a long history of interpolation between fragmentary geomorphological evidence in the production of continuous ice margins for use in palaeoglacial reconstructions (Chapter 2; Sissons 1974; Benn and Hulton 2010; Clark *et al.* 2012). Generally, interpolation is performed by simply 'joining the dots' by eye, although this is a highly subjective process. Extensive efforts, detailed in Chapter 2, were made to develop a more robust and reproducible framework for interpolation. However, this was ultimately unsuccessful and it was not possible to produce a method that was sufficiently refined as to be usefully applied to reconstructing LIA ice margins in central western Spitsbergen. Therefore, this study utilised the by eye method of interpolation to produce a likely LIA ice margin for each glacier from its relatively aged trimline elements (Figure 5.6). Despite the subjective nature of this process, previous research suggests that an experienced human eye can do a reasonably

good job of approximating ice margins from fragmentary evidence and it is not anticipated that this step has introduced significant uncertainty.

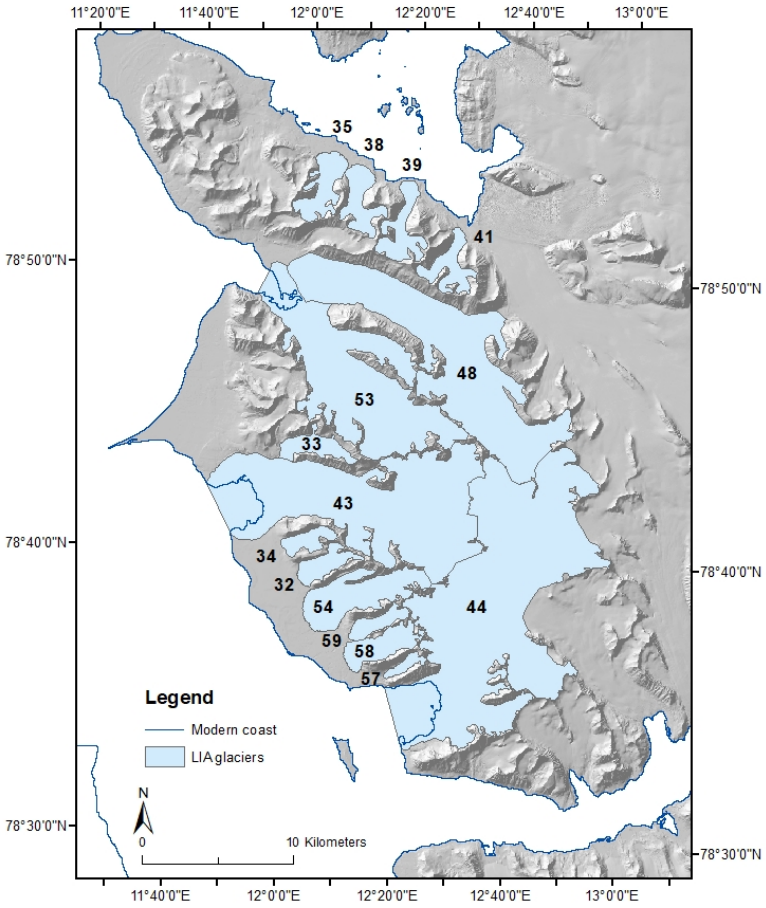

Figure 5.6 – The LIA ice margins produced from the LIA trimlines for the 15 reconstruction glaciers are shown. The glaciers are labelled with their ID numbers.

To guide the interpolation, the morphologies of the trimlines were considered, particularly by extending the ends of each trimline or moraine crest in a straight line to identify their intersection with the next feature (e.g. the small gap between the trimlines in front of Glacier 32 in Figure 5.4). This method often allowed straight forward interpolation between proximate trimline features but the topography of the glacier's valley also frequently needed to be considered to ensure glaciological plausibility, particularly for larger gaps (e.g. between the trimline and modern ice margin on the south side of Glacier 32 in Figure 5.4). The snouts and ablation areas of most of the reconstruction glaciers are well demarcated by the geomorphological record but the empirical evidence is generally more dispersed in the accumulation area. Therefore, the modern ice margin was used to guide the form of the LIA ice margin in the accumulation area, when required (e.g. Figure 5.4). Where a glacier was

tidewater during the LIA, the final landforms on each side of the fjord were connected using a straight line across the water as an approximation of the palaeo calving margin.

5.4 Deriving bed topography from the modern ice surface

The GlaRe method requires a DEM of the topography of the glacier valley without any ice cover (i.e. the glacier's bed topography). This is simple to produce in areas without extant ice cover but is much harder where the valleys are still occupied by glaciers, such as within the reconstruction study area. In central western Spitsbergen there are only two or three glaciers that have had their bed topography empirically measured using ground-penetrating radar (GPR), all of which are close to the research settlement of Ny-Ålesund. The other glaciers in the reconstruction study area have no existing measurements of their bed topography.

Therefore, it was necessary to employ a process to estimate the bed topography of the glaciers in the study area. The GlaRe tool provides an option to produce an estimate of the bed topography from an ice surface DEM of the modern glacier. This tool uses the method of Huss and Farinotti (2012), which computes ice thickness based on glacier mass turnover and ice flow mechanics (developed from Farinotti *et al*. 2009). The GlaRe bed topography tool produces these ice thickness values and uses them to output a bed topography DEM, created by subtracting the ice thickness from the modern ice surface elevation. The use of the modern ice surface to produce a DEM of the bed topography introduces a circularity to the LIA reconstruction method because the bed topography produced this way will then be used to reconstruct the LIA ice surface. However, there was no other way to derive bed topography DEMs for the reconstruction glaciers because of the lack of GPR data for the vast majority of glaciers in the central western Spitsbergen.

In order to test the accuracy of the GlaRe bed topography tool for the reconstruction glaciers, a comparison was performed with a bed topography DEM derived from GPR. Saintenoy *et al.* (2013) used extensive GPR surveys in April 2010 to produce a bed topography DEM for Austre Lovénbreen, a glacier near Ny-Ålesund in the north of the reconstruction study area (numbered 38 in Figure 5.6; Figure 5.7a & 5.7b). This GPR-derived DEM was compared to the bed topography DEM for the same glacier produced using the GlaRe bed topography tool. The two DEMs were compared using long profiles as well as a subtraction of the GlaRe DEM from the GPR DEM. This enabled a visual and statistical comparison of the two DEMs.

From the comparison with the GPR-derived DEM, it was shown that the Huss & Farinotti (2012) method, as used in the GlaRe tool, tends to slightly overestimate bed topography elevation along the centre line of the glacier valley (Figure 5.7c). Cross sections of the glacier valley were taken near the modern glacier snout, around the ELA, and in the upper glacier, which indicted that there was greater deviation between the two DEMs in the upper glacier area. To produce a final estimate of the deviation between the DEMs, a subtraction of the GlaRe DEM from the GPR DEM was carried out. This gave a value of + 4.35 m on average, supporting the finding that the Huss and Farinotti (2012) method slightly overestimates bed topography elevation. This will likely mean that the resulting reconstruction will underestimate the LIA ice thickness by approximately the same amount. The slight underestimation of ice thickness across the whole glacier could lead to a more significant underestimate of ice volume. However, the GPR bed topography DEM has a minimum error of 0-5 m below the GPR tracks and a maximum error of 15-19 m for the areas of most interpolation. Therefore, the DEM produced by the GlaRe bed topography tool is within the error range of the GPR DEM and can be considered a reasonably accurate match. Due to the GlaRe bed topography DEM falling within the error range of the GPR DEM, it was decided not to adjust the GlaRe bed topography DEM to remove the + 4.35 m bias identified. Instead, an error value for the GlaRe bed topography of ± 4.35 m was used to indicate the level of uncertainty in the DEMs produced by this method.

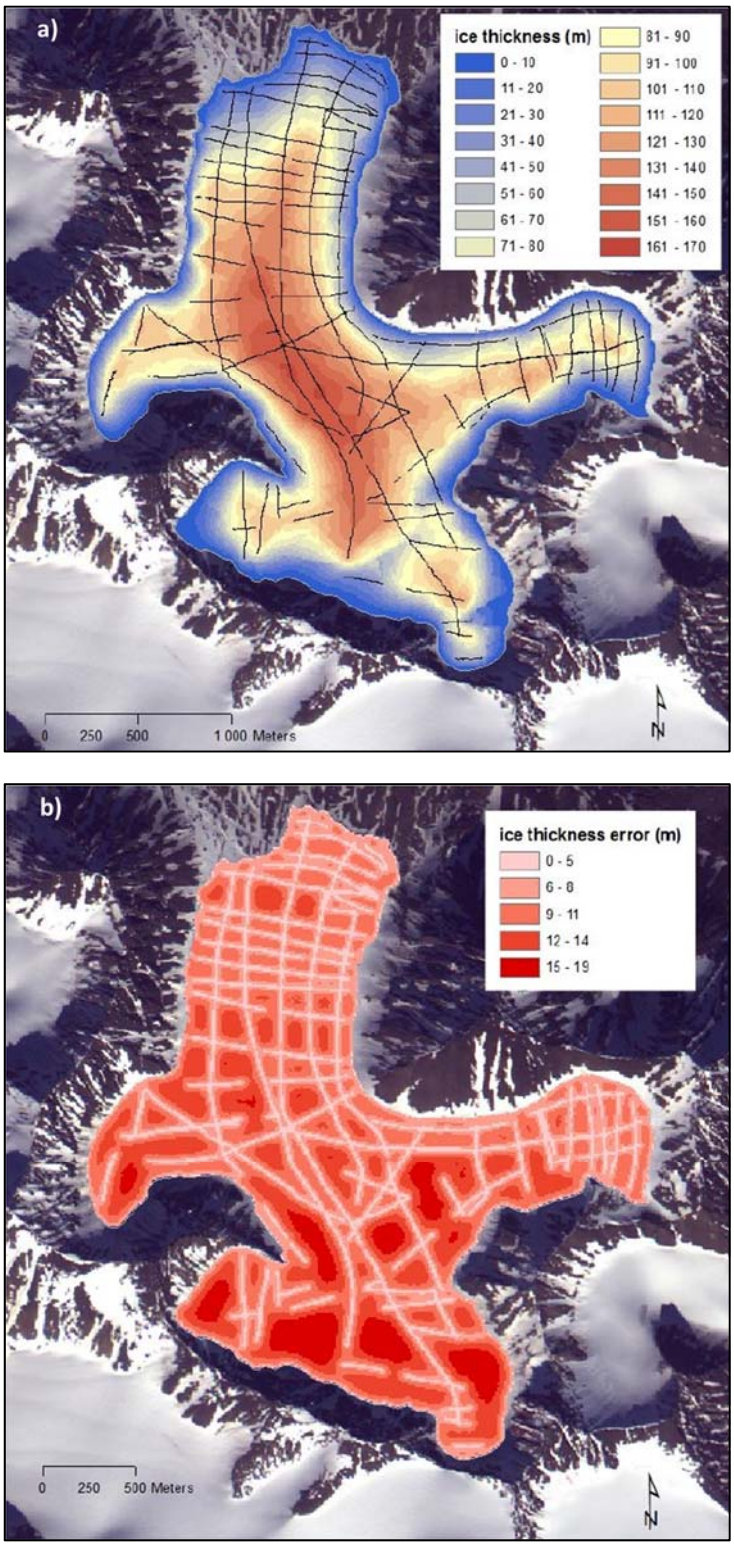

Figure 5.7 (5.7c on next page) – a) black lines indicate GPR tracks on the surface of Austre Lovénbreen, collected by Saintenoy *et al.* (2013) and used by them to produce a bed topography DEM for the glacier from the ice thickness data shown here. b) the estimated error of Saintenoy *et al.'s* ice thickness data. The error of the ice thickness, and also the bed topography DEM, is linked to the distance from the GPR tracks, which were interpolated between to produce a continuous bed topography DEM. c) shows a long profile along the centre line of the glacier valley for both the GPR bed topography DEM and a bed topography

DEM inverted from the modern ice surface using the method of Huss & Farinotti (2012) via the GlaRe bed topography tool. Comparing these two long profiles shows that there is very little deviation of the GlaRe bed topography compared to the GPR bed topography. The magnified section shows that there is some deviation, but the mean difference between the profiles is just +0.42 m.

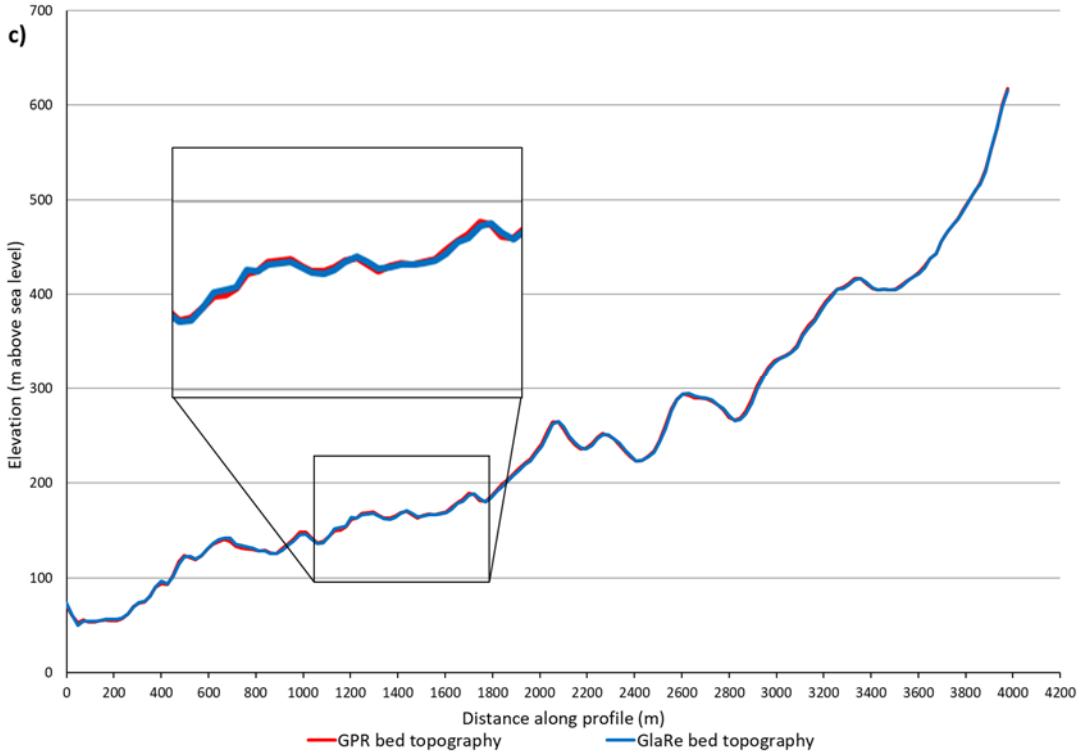

5.5 Deriving the 3D ice surface elevations (the GlaRe method and key parameters)

The GlaRe tool was developed by Pellitero *et al.* (2016) and uses a numerical approach to produce ice surface elevations for a palaeoglacier when given the bed topography. The method is based on an assumption of perfect plasticity for the ice rheology (Pellitero *et al.* 2016; Benn and Hulton 2010), which is used to produce a 2-dimesional (2D) equilibrium profile of the glacier along a user-defined central flowline. At this point, there is an optional step available to recalculate the ice thickness values along the 2D profile by applying an F factor to incorporate the impact of the lateral drag from the valley sides on ice flow rates along the central flowline.

In order to create the 3D ice surface reconstruction, the final 2D equilibrium profile (with or without F factor correction) is extrapolated using a choice of standard GIS interpolation tools. For the reconstructions in this study, the 'Topo to raster' interpolation tool was chosen because it provided the most realistic glacier surface that also passed through all of the input

ice thickness points. To improve the accuracy of the interpolation step, the GlaRe tool uses optimised parameters for the various interpolation methods and also generates additional ice thickness points orthogonal to the original 2D profile.

Whilst the GlaRe tool is relatively simple and user-friendly, it still requires a series of choices to be made at different steps in the process. To refine the best method options and parameters for the GlaRe method it was necessary to test different combinations of parameters for the different glacier types in the study area. These tests were performed by attempting to reproduce the modern ice surface from the bed topography produced using GlaRe, which allowed for comparison between the GlaRe method's outputted ice surface DEM and a measured ice surface DEM produced by the Norwegian Polar Institute from aerial surveys in 2009-2010 (referred to as the NPI DEM). In this way, multiple different input parameters and settings within the GlaRe method were trialled to identify those that produced the most accurate output. These optimum settings were then applied to the LIA ice surface reconstructions.

5.5.1 Shear stress calculation and parameterisation

One of the most important primary inputs to the GlaRe method is the choice of basal shear stress value, which is a first order control on the calculation of the ice surface elevation (Pellitero *et al.* 2016). GlaRe can be used either with a single shear stress value for the entire glacier, or with two shear stress values applied to different sections of the glacier. For many valley or cirque glaciers, a single value of basal shear stress may be sufficient but multiple shear stress values could be required where there are significant changes in bed lithology/ roughness, subglacial sediment cover, bed topography, or in the area surrounding an ice divide of an icefield or ice cap.

The Microsoft Excel™ *Profiler v. 1* tool developed by Benn and Hulton (2010) was used to calculate a basal shear stress value along the central flowline of each reconstruction glacier. The *Profiler* tool is recommended for use with GlaRe and is also based on an assumption of perfect plasticity for the ice rheology. *Profiler v. 1* outputs a single basal shear stress value for the entire glacier, whilst *Profiler v. 2* allows multiple basal shear stress values to be applied for different steps along the central flowline. Both versions of the tool require 'target elevations' to be identified, which are used to test different shear stress values with the optimum value being the one that produces ice surface elevations that most closely match the target elevations (Figure 5.8).

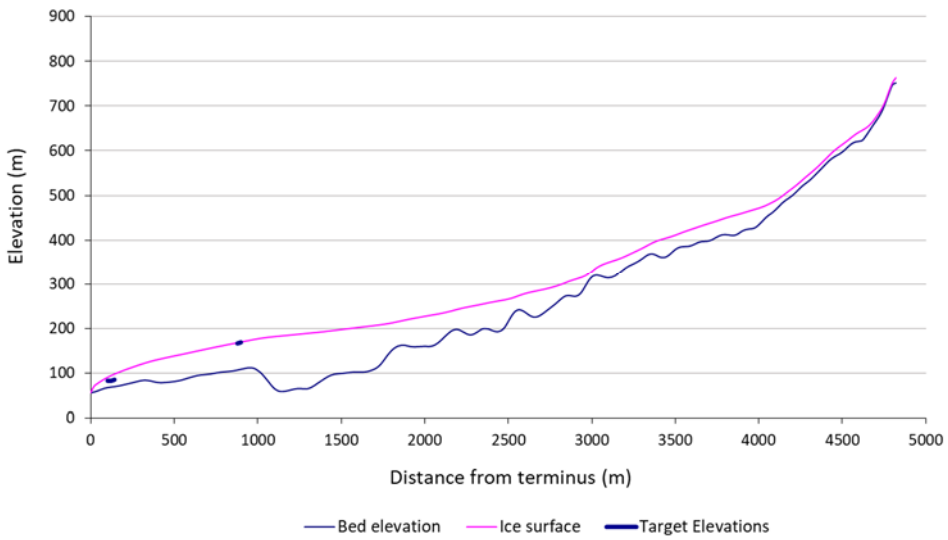

Figure 5.8 – Output chart from the *Profiler v.1* tool for Glacier 32. In this case the LIA trimlines (termed 'target elevations') have been used to constrain the basal shear stress value for the entire glacier by adjusting the shear stress to achieve the ice surface that intersects most closely with all of the LIA trimlines. This adjustment was done through experimentation and judgment of fit, producing a LIA basal shear stress value of 40 kPa for Glacier 32. However, it is clear from the graph above that this shear stress produces a realistic looking snout but forces the glacier to be too thin in the accumulation area (See Figure 5.9 for the impact of using this basal shear stress value in GlaRe).

For the modern glacier tests of GlaRe, the NPI DEM was used to extract the modern ice surface elevations along the central flowline. These values were then used as the target elevations for the *Profiler* tool, which defined a single mean shear stress value for each modern glacier. Utilising a single shear stress value worked well when GlaRe was used to reproduce the modern ice surface. Therefore, a single shear stress value was initially used for the LIA reconstructions. The shear stress value for each LIA glacier was determined using the trimline elevations as the target elevations to which the shear stress was tuned in the *Profiler* tool (e.g. Figure 5.8). However, inspection of long profiles for the glaciers indicated that the trimline-based shear stress value, whilst producing a realistic snout, was causing the accumulation areas of most of the glaciers to be unrealistically thin (e.g. Figure 5.9a). Testing the use of the modern shear stress value in the LIA reconstructions produced glaciers that looked correct in the accumulation area but were far too thick in the snout area, tending to be well above the elevation of the LIA trimlines. This finding suggests that neither the trimline-based shear stress value nor the modern shear stress value is a suitable estimate of the mean basal shear stress for the entire LIA glacier.

The likely explanation for this conclusion is that there was a difference in the basal shear stress in the snout area of the glaciers compared to the accumulation areas, during the LIA. The cause of the difference in basal shear stress is probably a difference in the substrate, which affects ice flow velocities due to its roughness and ability to deform. The accumulation areas of the glaciers are most likely to be underlain by bedrock, with only very limited sediment deposits; but the LIA snouts had advanced across the unconsolidated outwash sediments deposited by the previously smaller glaciers. This significant difference in the substrate probably explains why using the trimline-based shear stress value for the whole glacier produces an excessively thin accumulation area - this basal shear stress value is far too low for the higher basal shear stress expected as the glacier flows over bedrock in the accumulation area.

To reflect the likely difference in substrate and produce LIA reconstructions with a more realistic accumulation area, the decision was taken to use two different shear stress values in the GlaRe tool. For the area of the glacier downstream of the highest trimline elevation, the shear stress value based on the LIA trimlines was used (Figure 5.9b). The use of LIA trimlines to constrain this area of the reconstructed glacier means that the snout region is likely to be much more accurate than if the modern shear stress value was used for the entire glacier. Where there was no access to trimlines with which to constrain the palaeo ice surface in the accumulation area of a glacier, the decision was taken to use the mean shear stress value of the modern glacier in this area. As both the modern and LIA glaciers were likely to be flowing over bedrock in the accumulation area, it is probable that the basal shear stress value has not changed significantly in this area. Therefore, using the modern shear stress value upstream of the elevation of the highest trimline should produce a realistic LIA glacier when the trimline-based shear stress value is used downstream of this elevation (e.g. Figure 5.9b).

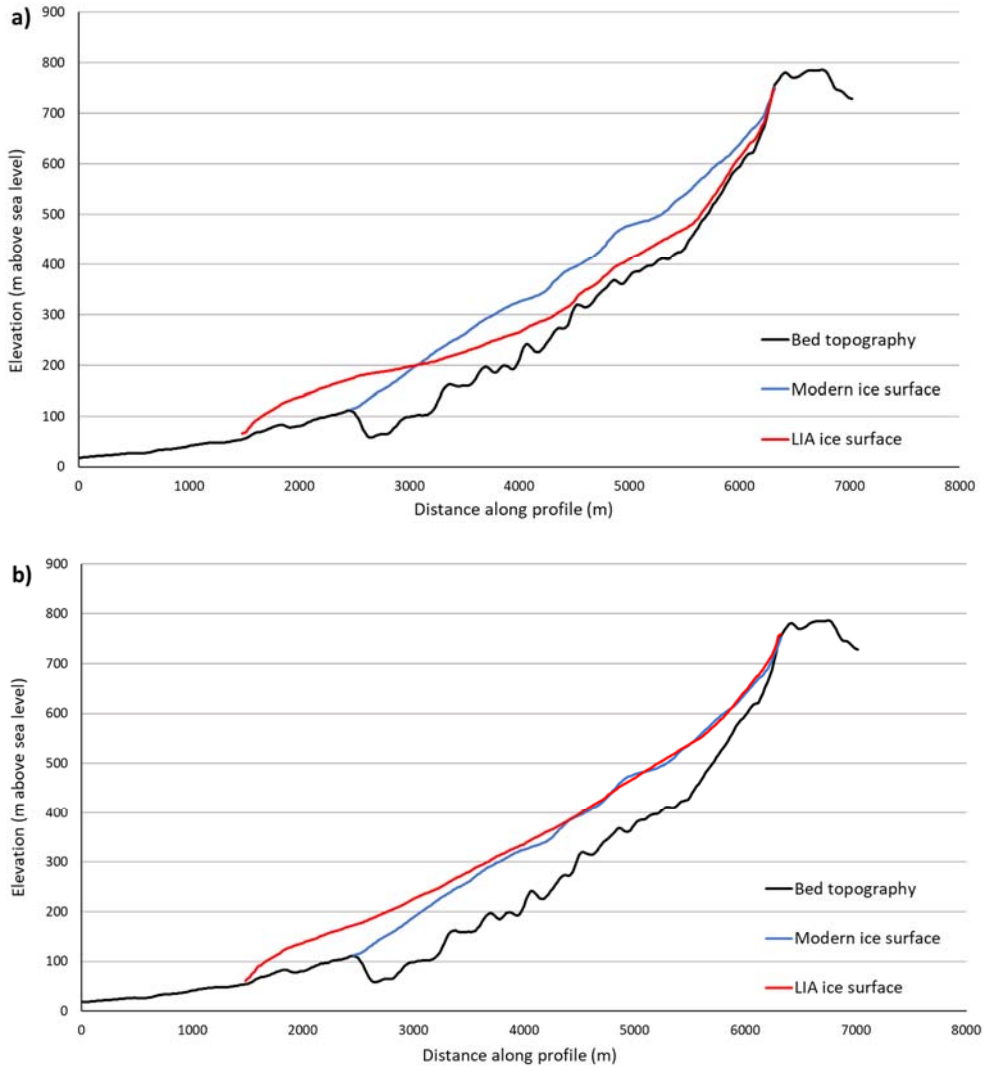

Figure 5.9 – These two long profiles demonstrate the difference between using a single value for the basal shear stress, compared to using two values. a) shows the long profile of Glacier 32 in the modern day compared to the LIA reconstruction produced in GlaRe using only a single basal shear stress value (based on the LIA trimlines). The reconstruction looks reasonable in the snout area of the glacier, but it is clear that this shear stress value is too low for the accumulation area because the glacier is too thin. Comparatively, b) shows the difference to the reconstruction produced when multiple shear stress values are used; with the basal shear stress derived from the LIA trimlines used downstream of the elevation of the highest trimline and the modern glacier's basal shear stress is applied upstream of this point. This reconstruction has a much more realistic accumulation area ice thickness and still maintains a snout that matches well with the LIA ice margin and trimline elevations.

It is anticipated that the use of two shear stress values defined individually for each of the reconstruction glaciers in this study will produce a much more realistic and accurate reconstruction than using a default shear stress value. To test this, a set of LIA reconstructions was produced using a single default basal shear stress value. The GlaRe tool comes with a recommended basal shear stress value of 100 kPa and this value has previously been used as a default basal shear stress for valley glaciers and ice cap outlets (Pellitero *et al.* 2016; Cuffey and Paterson 2010). Therefore, this value was chosen for use to produce a set of test reconstructions ('default shear stress reconstructions') for comparison with the reconstructions produced using the two shear stress values described above ('multiple shear stress reconstructions'), with all other inputs and variables remaining the same between the reconstructions. This allowed for comparison of ice volumes and Equilibrium Line Altitudes (ELAs) between the multiple shear stress reconstructions and the default shear stress reconstructions.

When the two sets of reconstructions were compared, they visually look similar because the area of the glaciers were constrained in both cases by the LIA ice margin, based on the LIA trimlines. However, the ice volumes are considerably different, with all of the default shear stress reconstruction glaciers having larger ice volumes than the multiple shear stress reconstructions. There is a lot of variability in the ice volumes of individual glaciers, but the mean difference in ice volume between the two sets of reconstructions is 4.25 km^3 and the median is 0.23km^3, which is probably more representative. As a percentage of the total ice volume of each glacier, the mean and median differences between the reconstructions are very similar, at 31% and 33% respectively. This indicates that the default shear stress value of 100 KPa produces glaciers with an ice volume roughly a third greater than that of multiple shear stress reconstructions. The larger ice volumes are particularly pronounced for the tidewater glaciers, which have ice volumes 54%, 38% and 40% greater when the default shear stress value of 100 KPa is used compared to the multiple shear stress values. These findings suggest that using a single default shear stress value for all glaciers in the reconstruction study area produces reconstructions with significantly overestimated ice volumes, particularly for the tidewater glaciers. As the areas of the glaciers were constrained by the same ice margin, it must be the influence of the choice of basal shear stress value over the reconstructed ice thickness that is altering the ice volumes.

When the ELAs of the two sets of reconstructions are considered, a similar picture emerges. The Accumulation Area Balance Ratio (AABR) ELAs of the default shear stress reconstructions

(excluding the tidewater glaciers – see Section 5.6.2) are all higher than the ELAs of the multiple shear stress reconstructions. On average the default shear stress reconstruction ELA is 45 m higher than that of the multiple shear stress reconstruction, but there is a lot of variability between individual glaciers (with a range of 2 m – 148 m). However, all but one glacier has a difference >21 m between the two reconstructions' ELAs, indicating that the choice of basal shear stress value generally has a strong influence on the position of the reconstructed ELA. This finding demonstrates that using a default shear stress value of 100 KPa may cause an underestimation of the size of the LIA accumulation area, compared to a reconstruction using multiple shear stress values constrained by trimlines and the modern ice surface. This could mean that any climate metrics based on reconstructions using a default shear stress value may also be inaccurate. Considering the results of comparing the default reconstructions with the multiple shear stress reconstructions, it is clear that the use of trimlines and the modern ice surface to constrain shear stress values marks a significant improvement in the methods of this study compared to a typical 3D reconstruction utilising a default value for the shear stress. It was therefore decided to go ahead with using multiple shear stress values in the final LIA reconstructions. Table 5.2 gives the shear stress values that were used in the final reconstructions.

Glacier ID	LIA trimline-based shear stress (kPa)	Modern shear stress (kPa)
32	40	120
33	19	75
34	70	72
35	55	90
38	50	90
39	165	100
41	130	98
43	30	75
44	50	80
48	15	100
53	70	105
54	40	102
57	130	65
58	135	85
59	145	55

Table 5.2 – The final multiple basal shear stress values utilised in the reconstructions of the LIA glaciers using GlaRe. These were all produced using the *Profiler v.1* tool with either the LIA trimlines or the modern ice surface used as the target elevations.

5.5.2 Adding lateral drag in GlaRe

The GlaRe tool box allows for the addition of an F factor that influences the ice thickness values along the central flowline of the glacier by including a measure of the effect of lateral drag with the valley sides on the ice flow. The different glacier types in central western Spitsbergen are likely to flow at different velocities, with the tidewater glaciers expected to flow much faster than either surge-type or normal glaciers on average. Therefore, it was suspected that the tidewater glaciers may require a lateral drag component to be included in their GlaRe reconstructions, whereas the surge-type and normal glaciers may not need this.

In order to test this, a set of three test glaciers were chosen and the modern ice surface was reproduced using GlaRe for each of these glaciers both with and without lateral drag. The glaciers were chosen because they are representative of the size and morphology of the glaciers of their type in the reconstruction study area. The test glaciers are:

- Glacier 32 – a normal valley glacier.
- Glacier 35 – a surge-type valley glacier.
- Glacier 44 – a non-surging tidewater glacier.

For each of these glaciers, GlaRe was run twice using the same input values, including a single shear stress produced using the *Profiler v. 1* tool with the modern ice surface as the target elevation. In one run of GlaRe the lateral drag tool was used, whilst the second run did not use the lateral drag tool but otherwise used identical inputs and parameters. The outputs of these two runs were compared to the modern ice surface using a long profile drawn down the GlaRe central flowline of each glacier (Figure 5.10). Visual and statistical comparison along these profiles showed that the use of the lateral drag tool made the reproduction of the modern ice surface less accurate for Glaciers 32 (Figure 5.10a) and Glacier 35 (Figure 5.10b). Glacier 44, on the other hand, showed a marked improvement in the reproduction of the modern ice surface when lateral drag was included, particularly in the snout and mid-glacier areas (Figure 5.10c).

From the results of the lateral drag tests, it was decided to include the lateral drag tool only in reconstructions of tidewater glaciers. The normal and surge-type glaciers in the reconstruction study area are likely to be cold-based or polythermal and probably have low flow rates, which may explain why the addition of a lateral drag component actually reduced the accuracy of the simulated modern ice surfaces. Climate conditions in the study area were

most likely a similar temperature or even slightly colder during the LIA, therefore it is probable that these glaciers would also have been slow-flowing at this time. The tidewater glaciers, conversely, are much faster flowing at present and are highly likely also to have been fast-flowing during the LIA. Therefore, the results of the lateral drag tests reproducing the modern ice surface are likely to hold for the LIA, justifying the use of the lateral drag tool only for the tidewater glaciers in the production of LIA ice surface reconstructions.

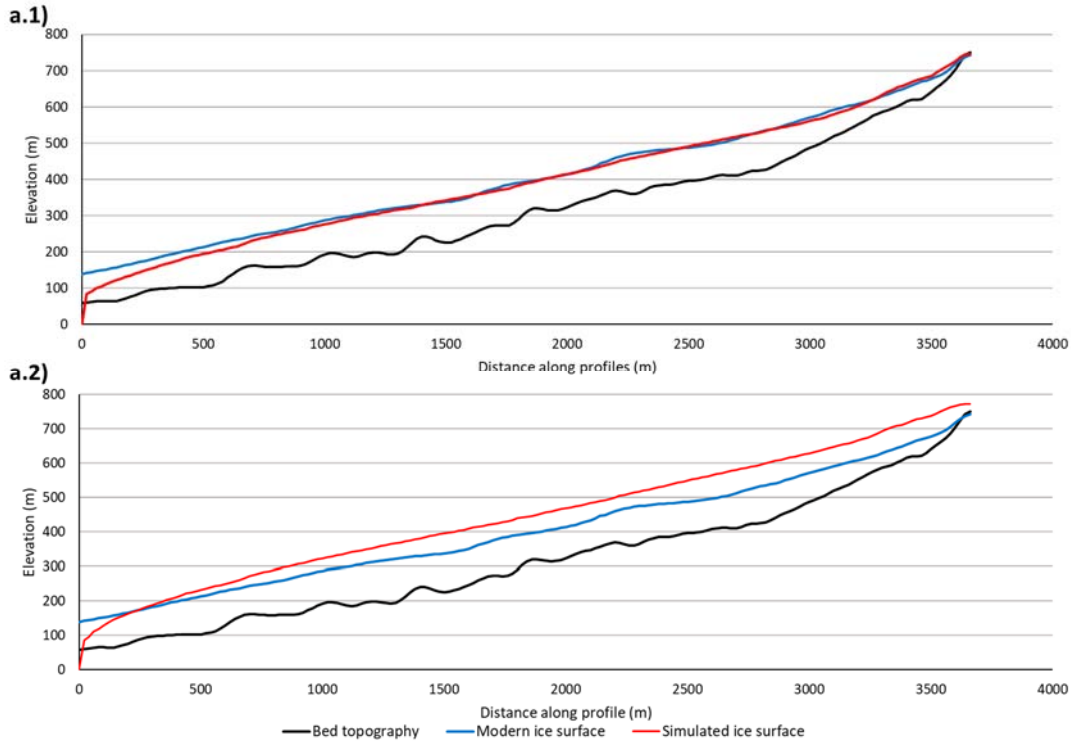

Figure 5.10 (5.10b and 5.10c on next page) **–** The effect of using F factors to add a measure of the lateral drag with the valley sides for the three test glaciers when trying to reproduce the modern ice surface using GlaRe. a.1) Shows the output for Glacier 32 without F factors; a.2) is the same glacier with F factors, showing that adding a lateral drag element actual reduces the accuracy with which the modern ice surface is reproduced. The same can be seen in the graphs for Glacier 35 - b.1) without F factors and b.2) with F factors. Whereas, the graphs for the tidewater Glacier 44 show the reverse, with F factors improving the reproduction of the modern ice surface up until the accumulation area. The deviation between the simulated GlaRe ice surface and modern ice surface in the accumulation area may be due to the impact of the riegel, which is likely to cause a difference in the shear stress upstream of it. c.1) is without F factors and c.2) is with F factors.

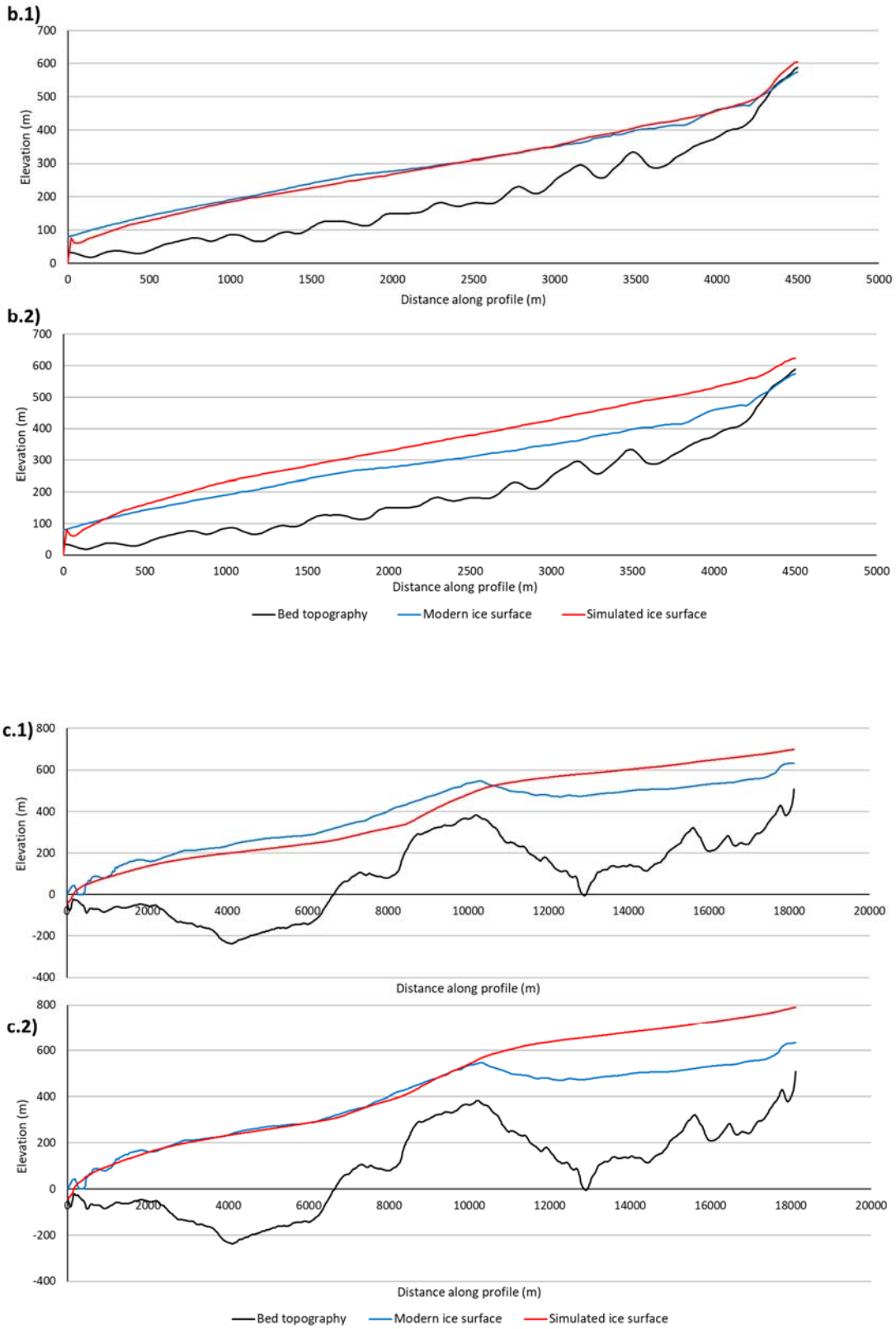
b.1)
Elevation (m)
Distance along profile (m)
b.2)
Elevation (m)
Distance along profile (m)
Bed topography
Modern ice surface
Simulated ice surface
c.1)
Elevation (m)
Distance along profile (m)
c.2)
Elevation (m)
Distance along profile (m)
Bed topography
Modern ice surface
Simulated ice surface

5.6 Analysing the LIA reconstructions

Using the inputs outlined in Section 5.2 and the parameters discussed in Section 5.5, the GlaRe tool was run for each individual glacier in the reconstruction study area. This produced a final LIA ice surface DEM for each glacier and these were then used to produce a series of glaciological and climatological outputs (Section 5.6.2). However, before any further analysis could be carried out using the LIA reconstruction DEMs, it was necessary to produce an estimate for the uncertainty in the ice surfaces produced using GlaRe.

5.6.1 Deriving uncertainty estimates for the LIA reconstructions

In order to produce a vertical uncertainty estimate for the LIA ice surface elevations produced using GlaRe, it was first necessary to define the vertical uncertainty of the LIA trimlines, the modern ice surface DEM, and the bed topography DEM for each glacier. These data are significant because they were used to constrain the basal shear stress values produced using the *Profiler v. 1* tool for each glacier. Tests of the GlaRe method indicated that it is sensitive to changes in the basal shear stress (see Section 5.5.1), so it is likely that the vertical uncertainty in the GlaRe LIA ice surfaces is linked to the vertical uncertainty of the data used to determine the basal shear stress input values.

The trimlines in the study area were mapped on to the Norwegian Polar Institute's (NPI) 20 m resolution DEM of the whole of Svalbard and this surface was used to provide elevations for the vertices of each trimline feature. The use of the NPI 20 m DEM as the source of the trimline elevations allows the vertical uncertainty of this DEM to be used as the vertical uncertainty for the trimline features. This DEM was also the source of the modern ice surface DEMs, so their vertical uncertainty will be the same as that of the trimlines. The NPI 20 m DEM is comprised of a variety of smaller DEMs produced at different times using different methods and so there is no single uncertainty for the entire product. However, the entire reconstruction study area falls within a region of the DEM that was wholly produced from stereo models based on aerial photography surveys conducted in 2009-2010 (for more information see http://geodata.npolar.no/). This allows a uniform vertical uncertainty of ± 2 m to be used for the entire reconstruction study area (Faste Aas pers. comm. 2017).

The vertical uncertainty of the bed topography DEMs produced using the Huss and Farinotti (2012) method, via the relevant GlaRe tool, was calculated using the comparison with a GPR-derived bed topography DEM of Austre Lovénbreen (see Section 5.4). This comparison yielded a vertical uncertainty of ± 4.35 m for the bed topography DEMs. This uncertainty was

applied to all of the reconstruction glaciers' bed topography DEMs because it was not possible to determine uncertainties for individual glaciers due to the absence of GPR data for the other reconstruction glaciers.

Having determined estimates of the vertical uncertainties for the trimlines, modern ice surface DEM, and bed topography DEM, it was decided to see how these influenced the final LIA ice surface reconstructions. This was done by using the uncertainty estimate for each input variable to produce an upper and a lower elevation profile for that variable. For example, the uncertainty of the modern ice surface is ± 2 m, so the upper profile was produced by adding 2 m to the original measured profile points (produced from the NPI 20 m DEM) and the lower profile was made by subtracting 2 m from the measured profile (Figure 5.11). The bed topography elevation profile and the trimlines were likewise adjust to produce upper and lower profiles, in addition to the original profiles. These upper, original, and lower profiles could then be input into the *Profiler* tool to derive three estimates of the basal shear stress for each glacier (Figure 5.11). These shear stress estimates were:

1. **Maximum estimate**: with shear stress values based on the upper profiles of the trimline and modern ice surface elevations and the lower bed topography elevation profile.
2. **Measured estimate**: with shear stress values based on the measured trimline, modern ice surface, and bed topography elevations.
3. **Minimum estimate**: with shear stress values based on the lower profiles of the trimline and modern ice surface elevations and the upper bed topography elevation profile.

The *Profiler v. 1* tool was used as before to compute the basal shear stress values (see Section 5.5.1), with the only difference between shear stress estimates being the choice of the input elevation profiles. Once the full set of basal shear stress values had been produced for each glacier, each value was run through GlaRe using the multiple shear stress method outlined in Section 5.5.1. In every case the only difference was the basal shear stress values used; all other parameters, inputs, and settings in the GlaRe toolset remained the same between the three scenarios. From GlaRe, three different LIA ice surfaces were output: one using the maximum estimate of basal shear stress; one using the measured estimate of basal shear stress; and one using the minimum estimate of basal shear stress (Figure 5.12).

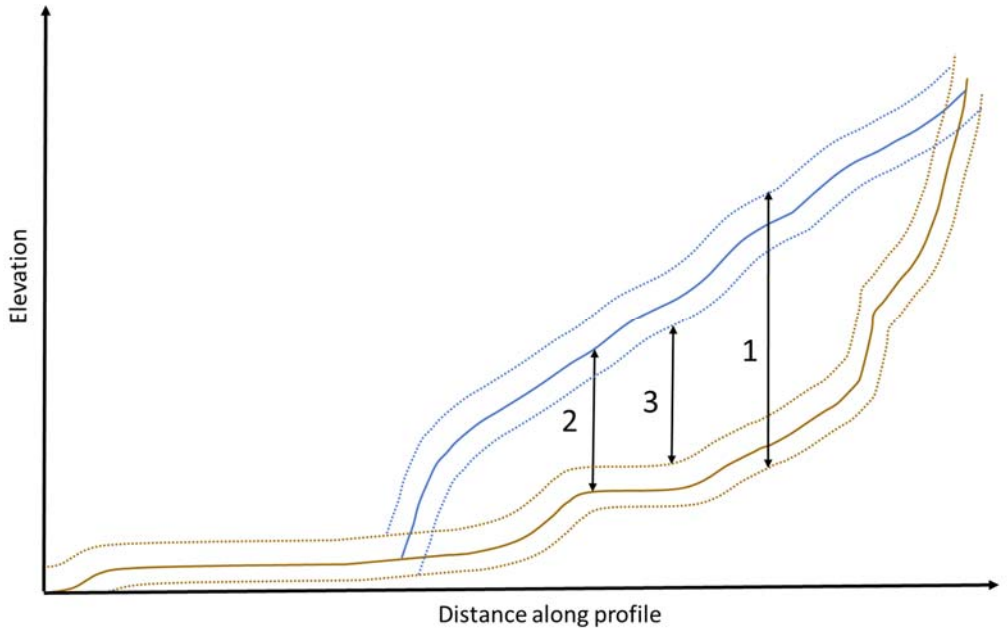

Figure 5.11 – In this example, the modern ice surface is shown in solid blue with the upper and lower error range of this surface shown as dashed blue. The bed topography is shown in brown with its upper and lower error range shown in dashed brown. The three shear stress estimates are indicated by the arrows between the bed topography and modern ice surface that were used to produce them, with the numbers referring to the numbering in the main text.

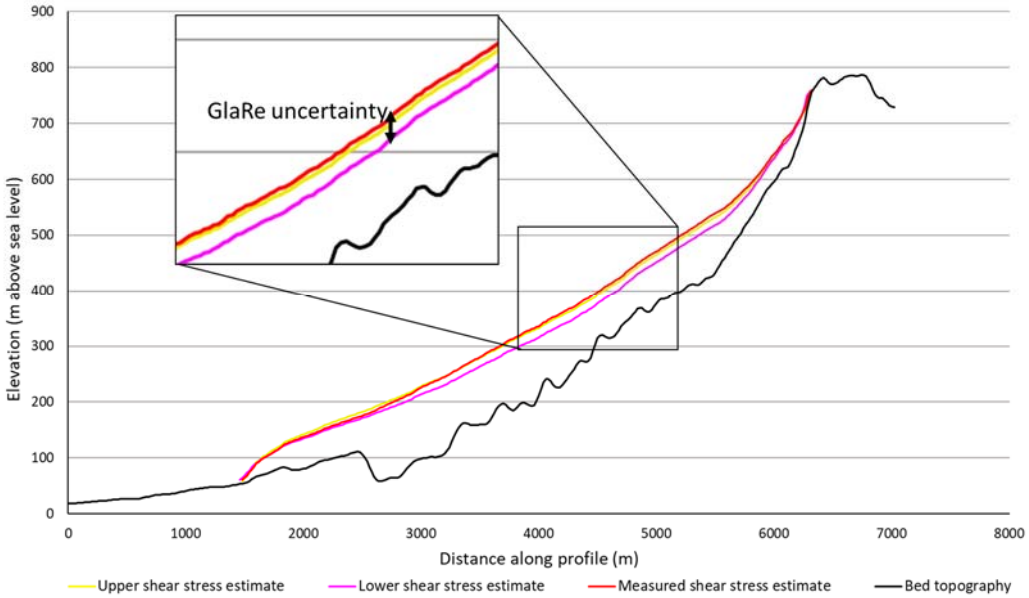

Figure 5.12 – The three shear stress estimates for Glacier 32 are shown as a long profile of the outputted GlaRe reconstructions. The magnified area shows the difference between the three reconstructions more clearly and indicates how these long profiles were used to determine a measure of the vertical uncertainty for the LIA reconstruction produced using GlaRe for this glacier.

To compute a single vertical uncertainty value of the GlaRe LIA ice surface for each glacier, the elevations of the three long profiles produced from the three shear stress scenarios were subtracted from each other. The two profiles with the largest total difference were then identified and the mean difference between these two profiles was taken as the estimated vertical uncertainty of the GlaRe method for each individual glacier (Figure 5.12; Table 5.3).

Glacier FID	GlaRe uncertainty (m)	GlaRe uncertainty %
32	11.81	14.7
33	9.77	13.4
34	12.46	13.4
35	11.28	13.7
38	7.77	11.9
39	28.36	35.2
41	7.96	10.0
54	9.12	7.5
57	3.84	6.3
58	6.24	6.2
59	5.84	10.3

Table 5.3 – The ± vertical uncertainties for the ice surface elevations, hence ice thickness, of the LIA GlaRe reconstructions are given for each glacier. These values show that the GlaRe method is sensitive to the choice of basal shear stress value, but ice surface elevation values vary by only around 9-10% on average for the range of basal shear stress scenarios tested. Glacier 39 has a significantly larger GlaRe uncertainty than the other glaciers, it is unclear why this is the case but it may be to do with the glacier's hypsometry within a steep and narrow valley (see Chapter 6 for a full discussion of this anomaly). The tidewater glaciers are missing from this table because the use of the different shear stress scenarios caused GlaRe to crash without outputting ice surface reconstructions, so it was not possible to compute an ice thickness error for these glaciers.

With the ice thickness uncertainties calculated, it was necessary to also compute the uncertainty in the glacier areas before an estimate of the uncertainty in the LIA and modern ice volumes could be determined. In order to compute an uncertainty estimate for the area of the glaciers, four factors needed to be considered:

1. The uncertainty of the background image from which the mapping was carried out. This is 15 m for the Landsat band 8 scenes used to map the glacial trimlines (see Chapter 4 Section 4.3.1). The modern ice margins were mapped from a combination

of a 40 m resolution DEM and 5 m resolution orthophotos (König *et al.* 2014). For the purposes of uncertainty estimation, the lower accuracy DEM resolution was applied to the modern ice margins.

2. The measurement uncertainty of the mapping of the glacial trimlines and modern ice margins. For the trimline mapping, this error was found to be ± 17.5 m (see Chapter 4 Section 4.3.2). For the modern glacier ice margins, a stated uncertainty of ± 10.0 m was given for the mapping of Svalbard glaciers by the NPI (König *et al.* 2014). The LIA ice margins were based primarily on the glacial trimlines in the ablation area, with the modern ice margin used to guide form of the accumulation area. Therefore, the larger trimline mapping uncertainty of ± 17.5 m was used for the entire LIA ice margin.

3. The uncertainty in the position of the ice margin. In the modern day, rockfalls, snow, and debris cover can make it difficult to distinguish the ice margin when mapping glaciers. This leads to an additional uncertainty in the modern ice margins and these factors may also cause some uncertainty in the mapping of the glacial trimlines. The effect of these factors on the mapping of the glacial trimlines and modern ice margin means that this source of uncertainty will also affect the LIA ice margins.

4. The natural variability of the ice margin from year to year and intra-annually means that mapped ice margins may not represent the mean position of the ice margin because they tend to be mapped from a single remotely sensed image, taken on a single day. This creates a further source of uncertainty in the mapping of the modern ice margins. The position of the LIA trimlines is more likely to be representative of a position sustained by the ice margin for an extended period of time, however the use of the modern ice margins in the production of the LIA ice margins means that this source of uncertainty also applies to these features.

These factors have been grouped into 'total measurable uncertainty' (comprising 1 and 2) and 'potential variability error' (made up of 3 and 4) by previous authors (Beason 2017). The total measurable uncertainty can be easily calculated using an established formula that combines the uncertainty in the background image and the measurement uncertainty of the mapping (Carisio 2012; Beason 2017). The potential variability error is harder to quantify but previous researchers have suggested that a percentage error of 2-5% of the glacier area is appropriate, with larger errors associated with smaller glaciers (Post *et al.* 1971; Sitts *et al.*

2010; Riedel *et al.* 2015; Riedel and Larrabee 2016; Beason 2017). Due to the variability in the size of the reconstruction glaciers (Section 5.1.1), it was decided to apply the maximum uncertainty of 5% to the glacier areas (Table 5.4). With numerical values for both the total measurable uncertainty and the potential variability error, the final uncertainty estimates for the modern and LIA glacier areas were computed by summing these two uncertainties for each individual glacier (Table 5.4).

Glacier FID	LIA area (km²)	5% LIA area (km²)	Background image resolution (km)	Trimline mapping uncertainty (km)	Total measurement error (km²)	Final area uncertainty (km²)	Area uncertainty %
32	5.08	0.25	0.015	0.0175	0.1035	0.36	7.0
33	5.10	0.25	0.015	0.0175	0.1038	0.36	7.0
34	3.51	0.18	0.015	0.0175	0.0861	0.26	7.5
35	7.54	0.38	0.015	0.0175	0.1262	0.50	6.7
38	6.96	0.35	0.015	0.0175	0.1212	0.47	6.7
39	7.11	0.36	0.015	0.0175	0.1226	0.48	6.7
41	6.20	0.31	0.015	0.0175	0.1145	0.42	6.8
43	92.87	4.64	0.015	0.0175	0.4429	5.09	5.5
44	137.34	6.87	0.015	0.0175	0.5386	7.41	5.4
48	76.54	3.83	0.015	0.0175	0.4021	4.23	5.5
53	70.97	3.55	0.015	0.0175	0.3872	3.94	5.5
54	17.71	0.89	0.015	0.0175	0.1934	1.08	6.1
57	1.75	0.09	0.015	0.0175	0.0607	0.15	8.5
58	7.77	0.39	0.015	0.0175	0.1281	0.52	6.6
59	3.51	0.18	0.015	0.0175	0.0861	0.26	7.5

Table 5.4 – The uncertainties in the mapped areas of the LIA glaciers are given, both as absolute figures and percentages, as well as the intervening steps in the calculation of these values. These uncertainties are relatively small, in the order of 7% of the total glacier area on average. This suggests that the larger uncertainty associated with the ice thickness values produced using the GlaRe tool (Table 5.3) are the major source of uncertainty in the ice volume calculations, but the glacier area uncertainty is large enough to play a role.

With final uncertainty estimates for both the ice thickness (Table 5.3) and glacier areas (Table 5.4), it was possible to compute the uncertainty in the modern and LIA ice volumes. To do this the area and ice thickness uncertainties were given as percentage errors of the glacier area and mean ice thickness respectively. These percentage errors could then be summed to give the final ice volume percentage error, which was then converted into a numerical uncertainty (Table 5.5).

Glacier FID	Area uncertainty %	Ice thickness uncertainty %	LIA volume uncertainty %	Ice volume uncertianty (km³)
32	7.0	14.7	21.7	0.089
33	7.0	13.4	20.4	0.076
34	7.5	13.4	20.8	0.060
35	6.7	13.7	20.4	0.134
38	6.7	11.9	18.6	0.085
39	6.7	35.2	42.0	0.240
41	6.8	10.0	16.8	0.083
54	6.1	7.5	13.6	0.293
57	8.5	6.3	14.8	0.016
58	6.6	6.2	12.8	0.101
59	7.5	10.3	17.8	0.035

Table 5.5 – Combining the percentage ice thickness (Table 5.3) and glacier area (Table 5.4) uncertainties produced ice volume percentage uncertainties of around 20% on average. This is a large uncertainty but one that reflects the difficulties in producing 3D palaeoglacial reconstructions from fragmentary evidence. The tidewater glaciers are missing from this table because their lack of clear ice thickness uncertainties made it impossible to compute ice volume uncertainties for these glaciers.

5.6.2 Deriving glaciological and climatological metrics

There were four glaciological and climatological metrics that were desired outputs of the LIA reconstruction: glacier area (km^2); ice thickness (m); ice volume (km^3); and an estimate of the local equilibrium line altitude (ELA) during the LIA (Section 5.1). Additionally, computing the change from the LIA to modern in each of these metrics was also a desired output of this study.

The glacier area was easily computed from the LIA ice margins that were produced using the glacial trimlines (Section 5.3). Maps of the LIA ice thickness was produced by subtracting the bed topography DEM from the GlaRe LIA ice surface DEM for each glacier. The mean LIA ice thickness was produced from these thickness maps, with an estimated uncertainty value for each glacier based on the process described in Section 5.6.1. From the LIA ice thickness maps, along with the LIA glacier area, it was possible to produce an estimate of the LIA ice volume. The same methods were used to produce the modern glacier areas, mean thicknesses, and volumes, with suitable uncertainties.

The local LIA ELA was computed using an ArcGIS toolbox created by Pellitero *et al.* (2015). This tool requires the ice surface DEM as the primary input and can produce estimates of the ELA using the following methods: Accumulation Area Ratio (AAR); Accumulation Area Balance Ratio (AABR); Altitude Area (AA); and Kurowski (see Pellitero *et al.* 2015 for a full

explanation of these methods). The AAR and AABR are the most widely used techniques for ELA reconstruction, with the AAR method the more common of the two, despite the AABR method being recognised as the more robust option, because it is simpler and does not require a 3D glacier reconstruction (Pellitero *et al.* 2015; Furbish and Andrews 1984). The AA ELA estimate is produced during the process of calculating the AABR, whilst the Median Glacier Elevation (MGE) or Kurowski method is an alternative to the AAR. The Kurowski/ MGE method is based on the idea that a glacier in an equilibrium state will have an ELA at or near the median glacier elevation (Pellitero *et al.* 2015; Kurowski 1891; Braithwaite and Raper 2007). This method had fallen out of favour but was shown by Braithwaite and Raper (2007; 2009) to have a very high correlation with the measured ELA in a sample of 144 glaciers, leading to a recent increase in usage (e.g. Hughes 2009; Hannah *et al.* 2017).

For the AAR method it is necessary to define the approximate ratio between the accumulation and ablation areas and the AABR method requires a balance ratio based on the glacier hypsometry to be defined. Pellitero *et al.* (2015) reviewed the ratios used in the literature and produced a series of suggested values for different glacial environments and different glaciers sizes. The choice of ratios used in this study were taken from this literature summary. An AAR ratio of 0.64 ± 0.04 was selected for glaciers > 4 km^2 in area, with a ratio of 0.54 ± 0.07 for the smaller glaciers between 1-4 km^2 (both from Kern and László 2010). The ratio chosen for the AABR calculation was taken from Rea (2009), who computed a mean balance ratio for Svalbard glaciers of 2.13 ± 0.52.

To confirm the suitability of these ratios, the ELA tool of Pellitero *et al.* (2015) was first used to reproduce the modern ELA in the reconstruction study area. This has been estimated to be around 350 m above sea level in the larger regional area of central western Spitsbergen (Nuth *et al.* 2007). The ELA tool, with the above input ratios, was applied to the modern ice surface DEMs for all of the reconstruction glaciers, excluding the tidewater glaciers. These glaciers were excluded because the ELA methods are designed for terrestrial glaciers and may not produce reliable results when applied to tidewater glaciers due to the complex impact of calving on the mass balance and ice throughput. From the ELA tool, the mean ELA was calculated for each of the four ELA methods by averaging the ELAs of the individual glaciers. Each of the ELA methods produced a reasonable value for the modern ELA: 398.5 m (MGE/ Kurowski); 378.6 (AA); 358.5 (AAR); and 338.5 m (AABR). The close proximity of the AAR and AABR ELA values to the previously estimated ELA of 350 m for the regional area suggests that the choice of ratios for the AAR and AABR calculations are reasonable and that

the ELA tool of Pellitero *et al.* (2015) is working well in the reconstruction study area. Therefore, this tool and these ratios were applied to the estimation of the ELAs for the LIA reconstructions.

For the LIA ELA calculations, it was decided to focus on the AABR method because this method is generally thought to be the most robust (Pellitero *et al.* 2015) and is only possible for 3D reconstructions, such as those produced using trimlines in this study, due to the inclusion of the glacier hypsometry in the calculation. As with the modern ELA calculations, the tidewater glaciers were not included in the analysis. Using the Pellitero *et al.* (2015) tool, it was possible to run the AABR calculation for each glacier using three values for the balance ratio: the given value stated above (i.e. 2.13 for Svalbard glaciers); the upper limit of the stated error range (i.e. 2.13 + 0.52 = 2.65); and the lower limit of the stated error range (i.e. 2.13 – 0.52 = 1.61). Using these three input balance ratios produced three possible values for the LIA AABR ELAs, from which a measure of the uncertainty was produced by subtracting the highest and lowest ELAs. The mean study area ELA was computed as for the modern glaciers, using the median ELA value produced from the three AABR balance ratio values for each glacier. To compute the uncertainty for the mean ELA, the lowest AABR ELAs for the glaciers were averaged and the highest AABR ELA values were similarly averaged. These two lowest and highest mean AABR ELAs were then subtracted to produce an uncertainty for the mean study area ELA.

5.7 Summary of the adopted method for the LIA reconstructions

In summary, the GlaRe method of Pellitero *et al.* (2016) was used to produce 3D LIA reconstructions of 15 glaciers in central western Spitsbergen using the trimlines mapped in Chapter 4 to constrain the LIA ice margin and basal shear stress (Section 5.3; Section 5.5.1). It was found that a second basal shear stress value based on the modern ice surface was required to improve the reconstruction of ice thickness in the accumulation area. This second basal shear stress value was used upstream of the elevation of the highest trimline (Section 5.5.1), with the shear stress value based on the trimlines applied below this point. A lateral drag component was applied to the reconstructions of tidewater glaciers because this was found to improve the accuracy of GlaRe for this type of glacier (Section 5.5.2). Before running the reconstruction tools, it was necessary to produce bed topography DEMs for the glaciers. This was also carried out using GlaRe, which has a tool that can invert the bed topography

from the modern ice surface using the method of Huss and Farinotti (2012), which was tested against GPR bed topography for one of the glaciers and found to be a very good match (Section 5.4). These methods enabled a 3D reconstruction of each glacier to be produced using the GlaRe tool, from which further analysis was required to determine the LIA ice thickness (Section 5.6.1), ice volume (Section 5.6.1), glacier area (Section 5.6.1), and ELA (Section 5.6.2). Figure 5.13 shows the final method for producing the 3D LIA reconstructions using GlaRe and including the additional pre- and post-processing steps.

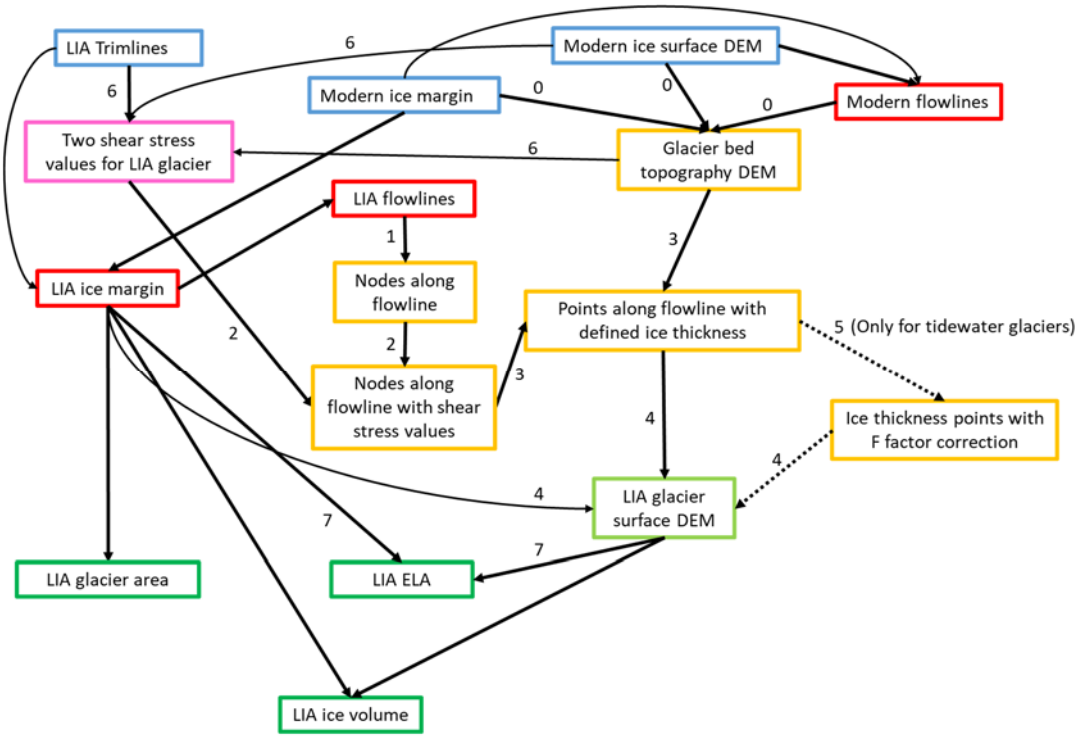

Figure 5.13 – This flowchart summaries the final process used to produce the 3D LIA glacier reconstructions for the 15 reconstruction study glaciers. Initial input data are coloured blue; red indicates a manually produced layer; pink shows the basal shear stress values produced using the *Profiler v.1* tool (Benn and Hulton 2010); layers produced by intermediate steps in the GlaRe toolbox are coloured yellow; the final LIA glacier reconstruction is light green; and additional outputs created by further processing of the reconstruction DEM are coloured dark green. All non-optional steps are shown as solid arrows, whilst the optional steps to add a lateral drag component are shown with dashed arrows. The numbering on the arrows refers to the tool used to create that connection, with unnumbered arrows indicating manual steps utilising standard tools in ArcGIS or Microsoft Excel™. 0 is the GlaRe tool 'Bed elevation from ice surface'; 1 is the GlaRe tool 'Construct interval nodes'; 2 is the GlaRe tool 'Define shear stress'; 3 is the GlaRe tool 'Flowline ice thickness tool'; 4 is the GlaRe tool 'Glacier surface interpolation'; 5 is the GlaRe tool 'Automatic ice thickness recalculation with F factor'; 6 is the *Profiler v.1* shear stress tool; 7 is the ELA tool of Pellitero *et al.* (2015) 'AAR and AABR (AA) for several ratios'.

Chapter 6

The Little Ice Age glacial extent in central western Spitsbergen – interpretation of the reconstruction

6.1 Introduction

The 3-dimensional (3D) reconstruction of the Little Ice Age (LIA) glacial extent in central western Spitsbergen aimed to demonstrate a method for using trimlines in a palaeoglacial reconstruction (Chapter 5). However, the reconstructions produced also provided new information about the LIA in the reconstruction study area and about the retreat of the local glaciers from the LIA maximum extent to the modern day. Figure 6.1 shows the full set of reconstructions, produced using the GlaRe method constrained with the glacial trimlines, alongside their modern ice margins. All of the glaciers have retreated and there has been a rise in the local equilibrium line altitude (ELA) of 64 m ±39 m on average. This rise in the ELA and consequent increase in the size of individual glaciers' ablation areas has not translated to a uniform loss of ice volume, with a large variation in the percentage ice volume change and even a possible gain in ice volume for one glacier. This chapter will attempt to resolve the causes of this variability in the responses of the glaciers to the post-LIA climate change in central western Spitsbergen.

The reconstructions of each individual glacier will be presented in Section 6.2, alongside an initial interpretation. Variables potentially influencing the responses of the glaciers were analysed to determine which were the most significant in the reconstruction study area (Section 6.3). From spatial patterns in the response of the glaciers, further light was shed on the variables that have influenced the responses of individual glaciers or groups of glaciers (Section 6.4). In Section 6.5 the results of these analyses are drawn together to identify the most significant factors that have led to the variation in ice volume changes since the LIA in central western Spitsbergen. Following this analysis of glacial responses in the reconstruction study area, the use of trimlines in the production of the reconstruction and the potential to expand the use of these features for producing 3D palaeoglacial reconstructions will be discussed in greater detail in Chapter 7.

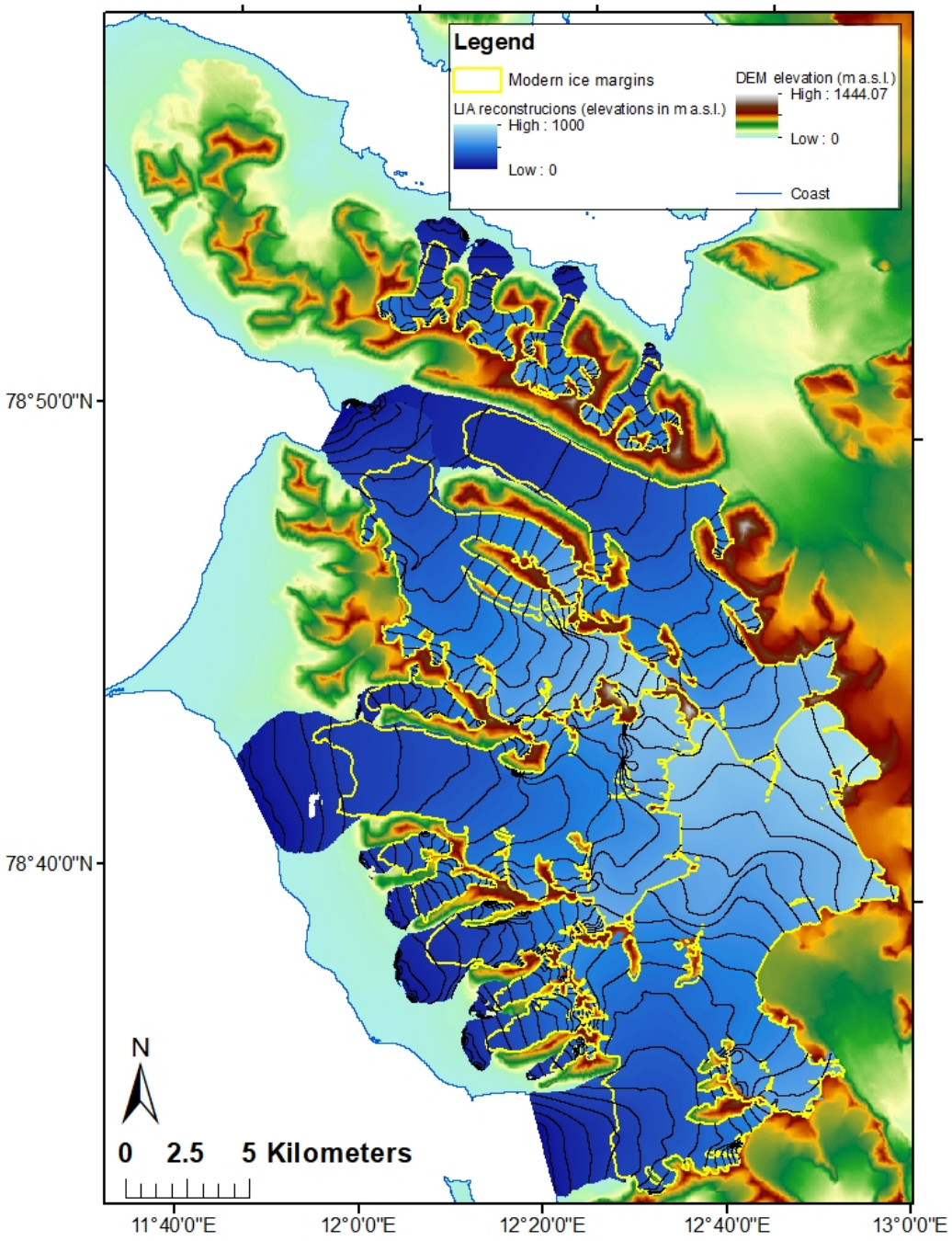

Figure 6.1 – The full set of LIA glacier reconstructions produced using GlaRe and the glacial trimlines. The modern ice margins are also included, allowing the scale of the post-LIA retreat to be visually shown. Ice surface contours are at intervals of 50 m.

6.2 Individual glacier reconstructions and metrics

Although four tidewater glaciers were included in the reconstruction study area (Figure 6.1), these glaciers will not be discussed in detail in this chapter. The reason for this is that the GlaRe tool is not designed for use with tidewater glaciers and the attempts at producing LIA reconstructions of these glaciers have proved difficult and subjective, with the accuracy of the resulting ice surface reconstructions consequently highly uncertain. Figure 6.2, for example, shows that the tidewater glaciers appear to have extreme responses to the post-LIA climate change, compared with the other glaciers in the reconstruction study area. Given the high degree of uncertainty in the tidewater glacier reconstructions, it is likely that these extreme responses are an artefact produced by the lack of inclusion of ice loss through calving in the GlaRe tool and in the calculation of the ELAs. Therefore, any conclusions drawn from analysis of the tidewater glacier reconstructions are not likely to be robust, so the decision was taken to exclude these glaciers from further analysis.

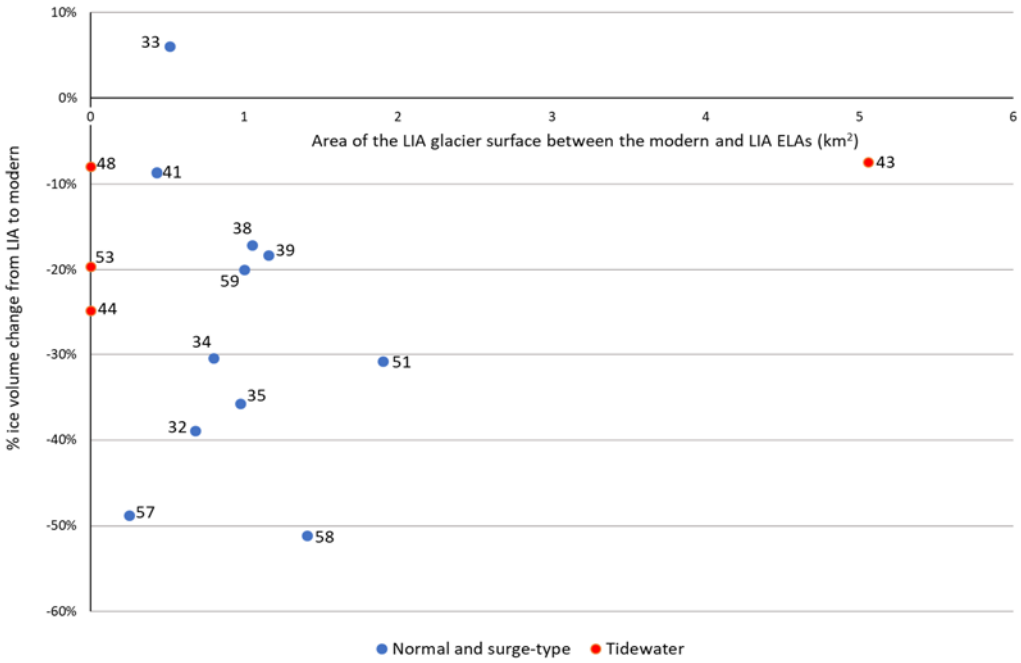

Figure 6.2 – This example shows that the percentage ice volume change from LIA to modern is similar for both the tidewater glaciers and the other glacier types, but the tidewater glaciers appear to have unusual changes in the ELA position in the modern day compared with the LIA. This is probably because the method used to compute the ELAs (see Chapter methods) is not optimised for tidewater glaciers, which lose mass predominantly via calving rather than through melting, so the ELA values produced for these glaciers are likely to be inaccurate. The GlaRe tool is also not optimised for use with tidewater glaciers and produced reconstructions that seemed too thin, which is possibly why the tidewater glaciers appear to have lost relatively little ice volume compared to the other glaciers in the study area. Due to the high levels of uncertainty and likely inaccuracies involved in using GlaRe and the ELA toolset with tidewater glaciers, these glaciers were excluded from further analysis. The numbers next to each point reflect the identification number of the glacier.

For each of the remaining glaciers in the reconstruction study area the following outputs were produced by the methods outlined in Chapter 5:

- a LIA ice surface elevation model;
- the ice margin (based on the glacial trimlines) and glacier area;
- ice thickness and ice volume measurements;
- estimated local equilibrium line altitude (ELA).

As well as the above outputs, long profiles and hypsometric curves for the LIA and modern ice surfaces were also produced. In this section these outputs will be presented, described, and initial interpretations suggested for each glacier, before more detailed analysis and interpretations are presented in Sections 6.3 and 6.4. Figure 6.3 shows a map of the locations of all of the glaciers along with their identification numbers.

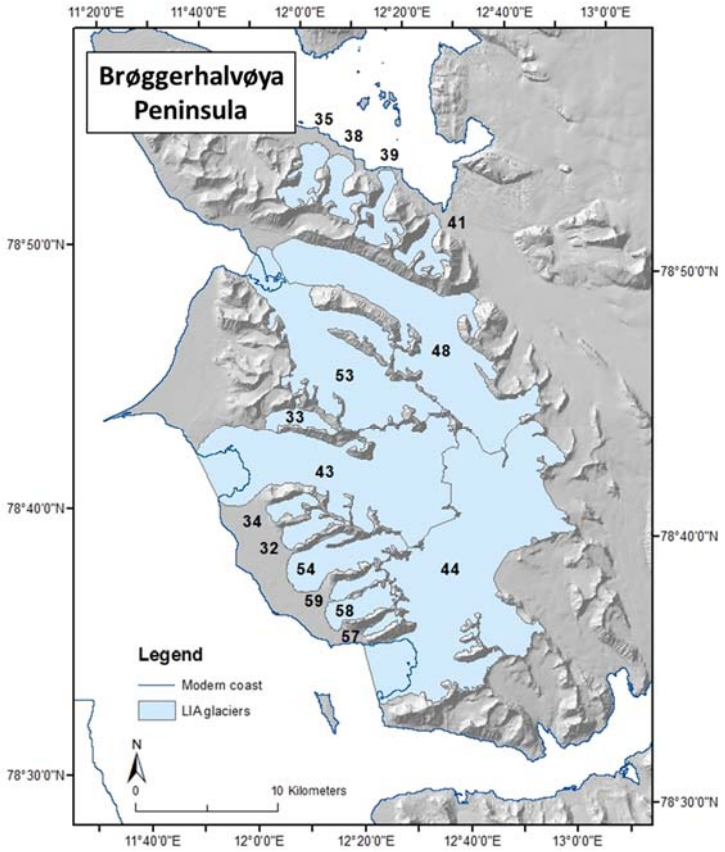

Figure 6.3 – The identification numbers for the reconstruction study area glaciers are shown in this map, so that their relative locations can be appreciated. The tidewater glaciers are also included because these are mentioned in the later analysis due to the possible confluences between these glaciers and various others during the LIA.

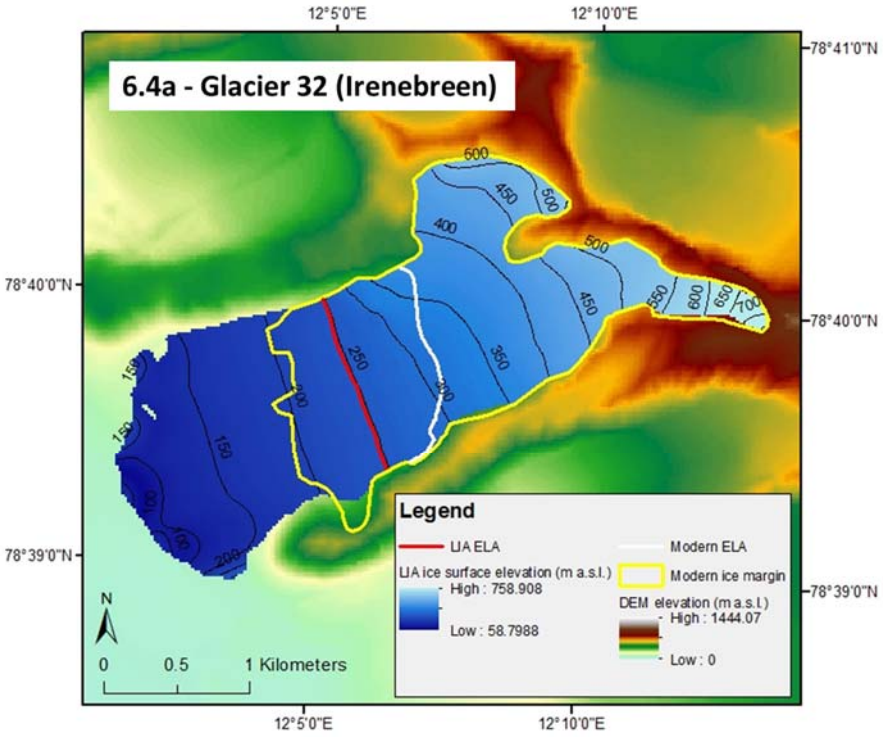

Measurement	LIA		Modern		Change since LIA	
Area (km^2)	5.08	± 0.36	3.45	± 0.32	-1.62	± 0.48
Mean thickness (m)	80.32	± 11.81	72.01	± 2.00	-8.31	± 11.98
Volume (km^3)	0.41	± 0.09	0.25	± 0.03	-0.16	± 0.09
AABR ELA (m a.s.l.)	248	± 40	303	± 20	55	± 45

Figures 6.4 - 6.14 (over pages 190-201)**–** Each of these figures shows the reconstruction outputs for an individual glacier, the identification number of which is stated in the figure (see Figure 6.3 for a map of the glacier locations). For every glacier the table shows the key metrics for that glacier during the LIA and in the modern day, alongside the change in each metric (coloured red for a negative change and black for a positive change) and the uncertainty ranges of the metrics and of the changes (see Chapter 5 for explanation of the calculation of these uncertainties). a) is a map of the LIA ice surface reconstruction with the modern ice margin also shown, as well as both the modern and LIA ELAs. b) the long profile of the modern and LIA glaciers are compared and the upper and lower estimates of these ice surfaces are also shown, giving a visual indication of the vertical ice surface uncertainty. c) the hypsometry curve of the LIA glacier is shown as a series of yellow bars whilst the modern glacier's hypsometry is given by the blue line. The LIA and modern ELAs are marked and labelled.

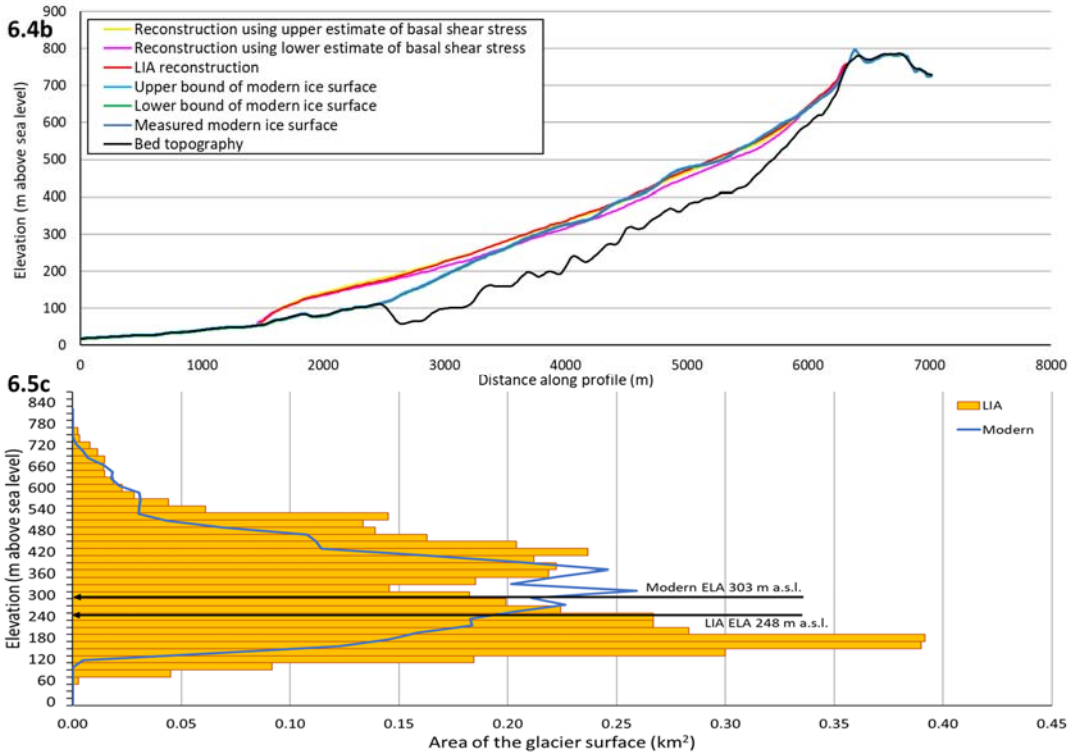
6.4b
Reconstruction using upper estimate of basal shear stress
Reconstruction using lower estimate of basal shear stress
LIA reconstruction
Upper bound of modern ice surface
Lower bound of modern ice surface
Measured modern ice surface
Bed topography
Elevation (m above sea level)
Distance along profile (m)
6.5c
LIA
Modern
Modern ELA 303 m a.s.l.
LIA ELA 248 m a.s.l.
Elevation (m above sea level)
Area of the glacier surface (km²)

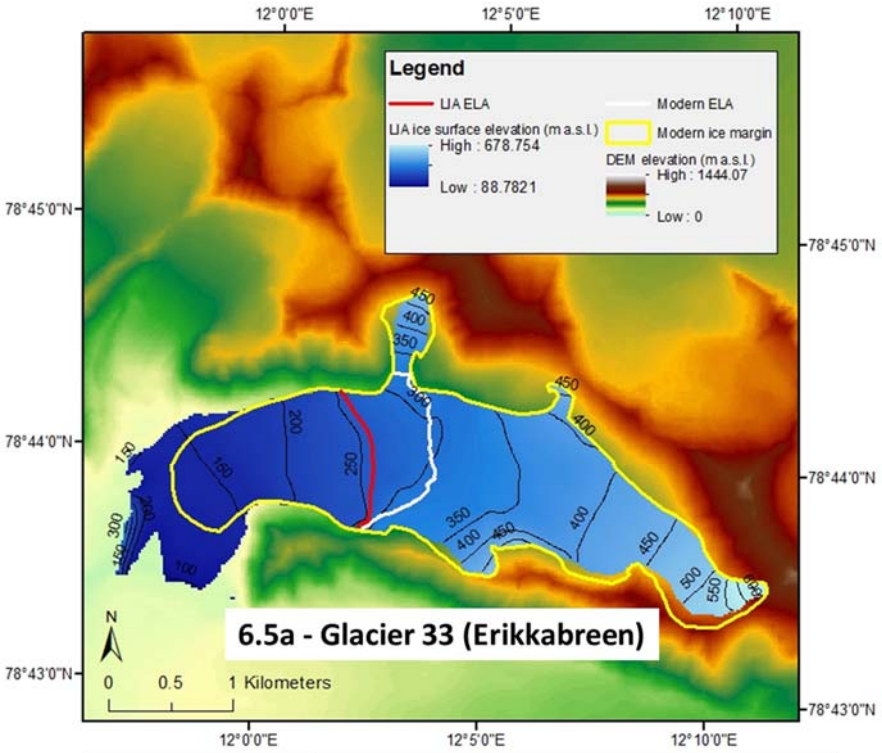

Measurement	LIA		Modern		Change since LIA	
Area (km^2)	5.10	± 0.36	4.65	± 0.41	-0.45	± 0.54
Mean thickness (m)	73.18	± 9.77	85.20	± 2.00	12.03	± 9.97
Volume (km^3)	0.37	± 0.08	0.40	± 0.04	0.02	± 0.09
AABR ELA (m a.s.l.)	258	± 20	304	± 20	46	± 28

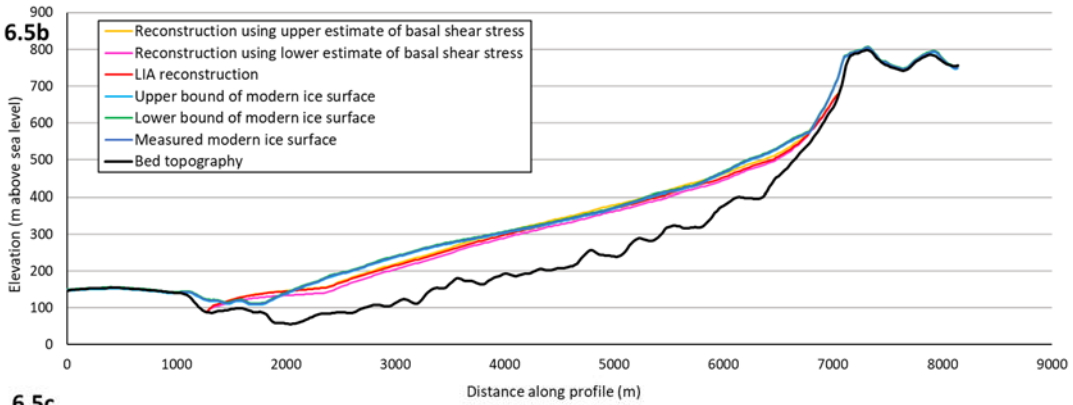

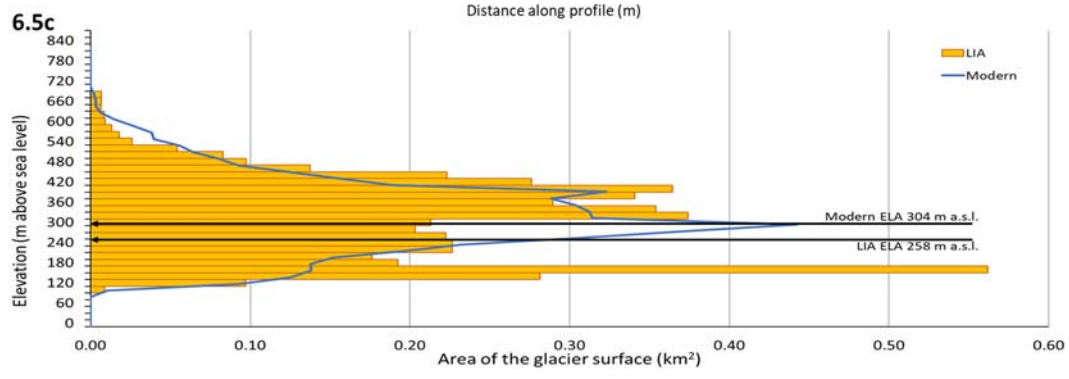

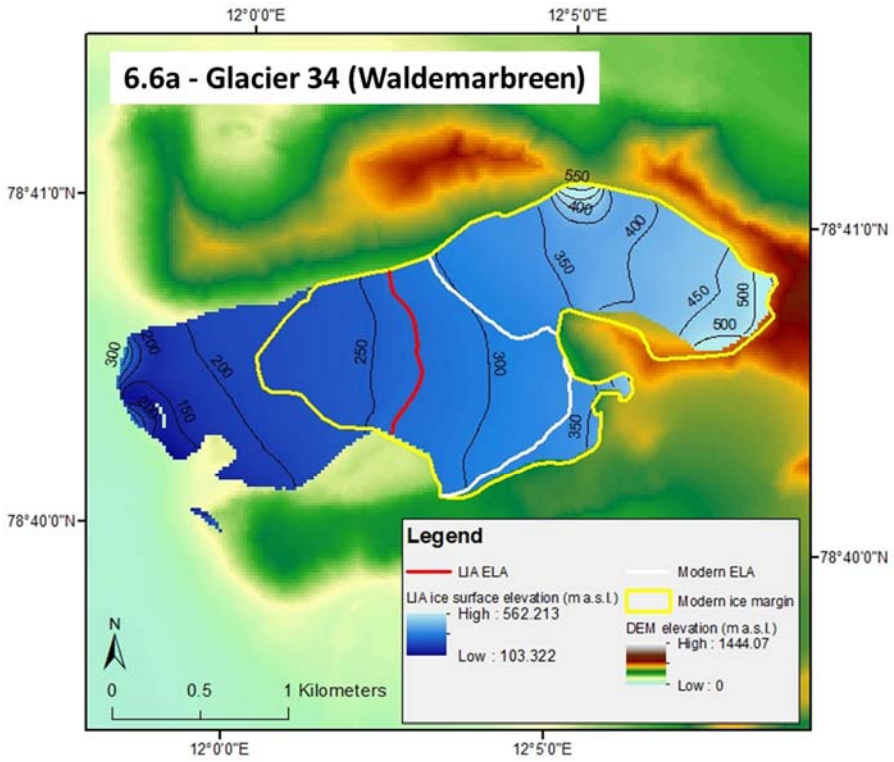

Measurement	LIA		Modern		Change since LIA	
Area (km^2)	3.51	± 0.26	2.79	± 0.28	-0.72	± 0.38
Mean thickness (m)	93.06	± 12.46	72.13	± 2.00	-20.93	± 12.62
Volume (km^3)	0.29	± 0.06	0.20	± 0.03	-0.09	± 0.07
AABR ELA (m a.s.l.)	273	± 0	291	± 20	18	± 20

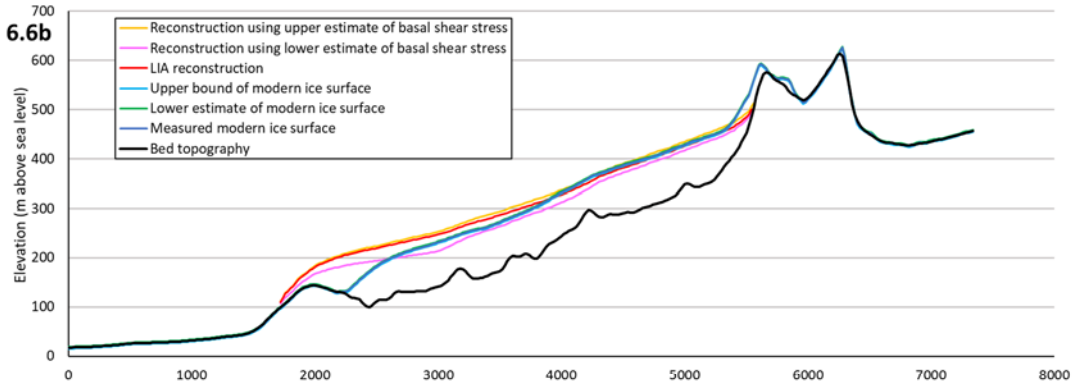

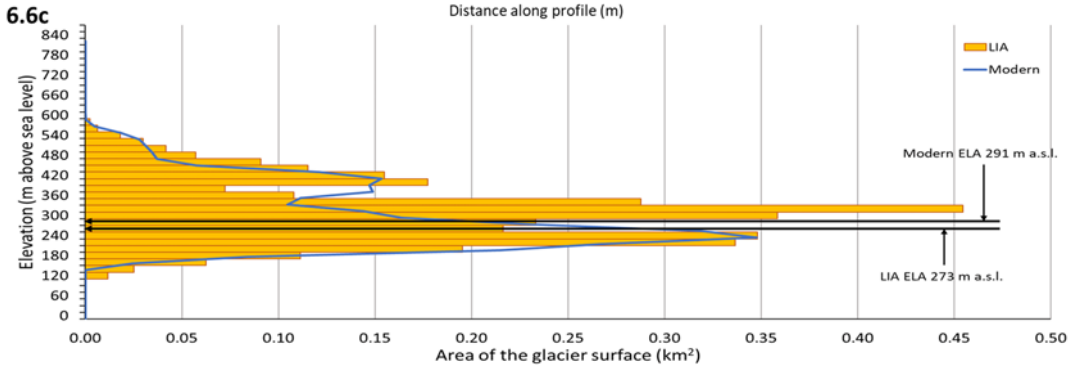

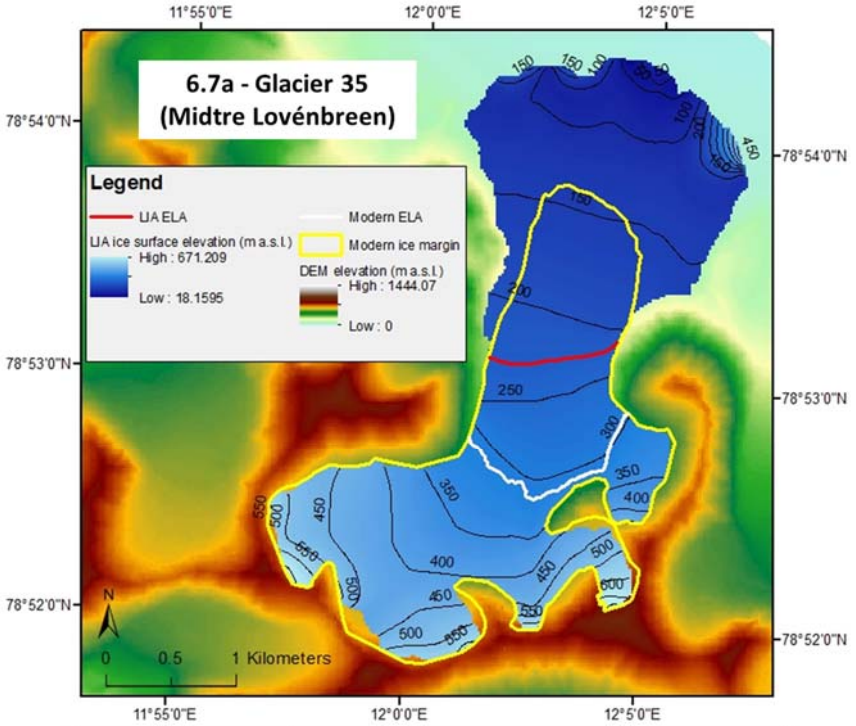

Measurement	LIA		Modern		Change since LIA	
Area (km^2)	7.54	± 0.50	5.20	± 0.45	-2.34	± 0.67
Mean thickness (m)	82.37	± 11.28	81.49	± 2.00	-0.88	± 11.46
Volume (km^3)	0.66	± 0.13	0.42	± 0.05	-0.24	± 0.14
AABR ELA (m a.s.l.)	228	± 40	303	± 20	75	± 45

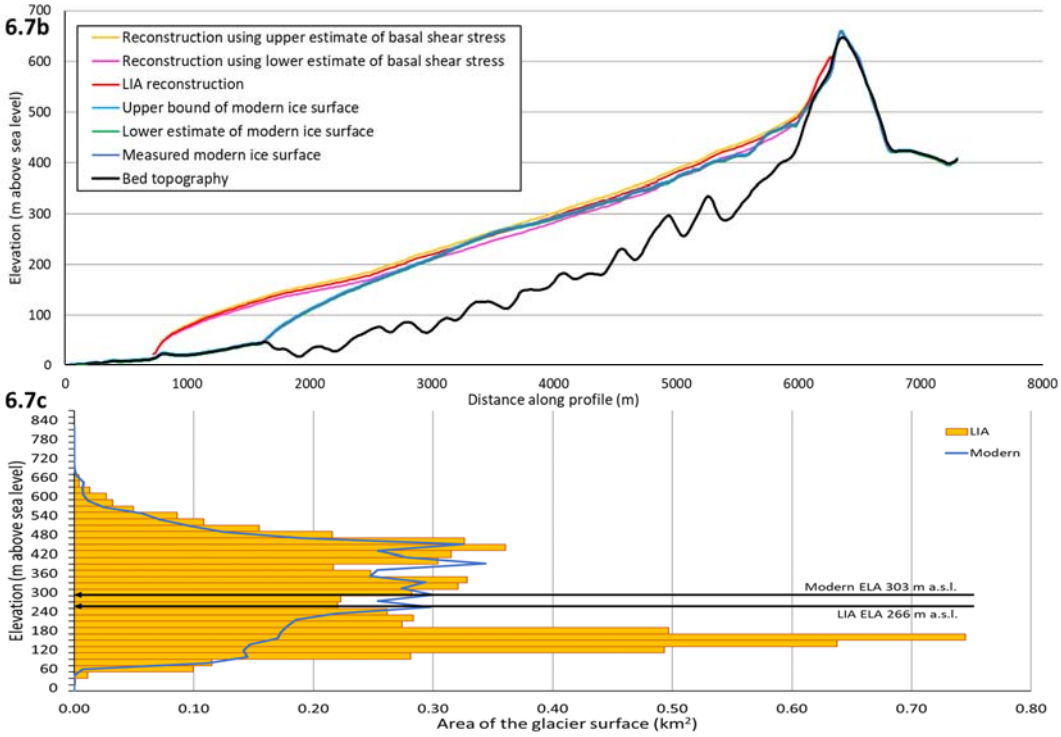

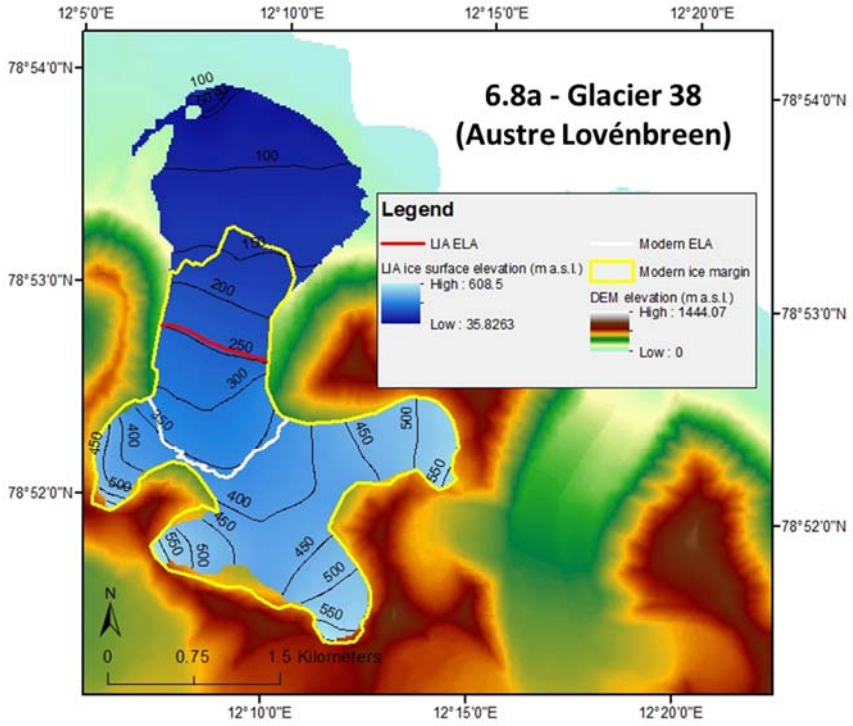

Measurement	LIA		Modern		Change since LIA	
Area (km^2)	6.96	± 0.47	5.01	± 0.43	-1.95	± 0.64
Mean thickness (m)	65.51	± 7.77	75.03	± 2.00	9.52	± 8.02
Volume (km^3)	0.46	± 0.08	0.38	± 0.04	-0.08	± 0.09
AABR ELA (m a.s.l.)	245	± 40	348	± 20	103	± 45

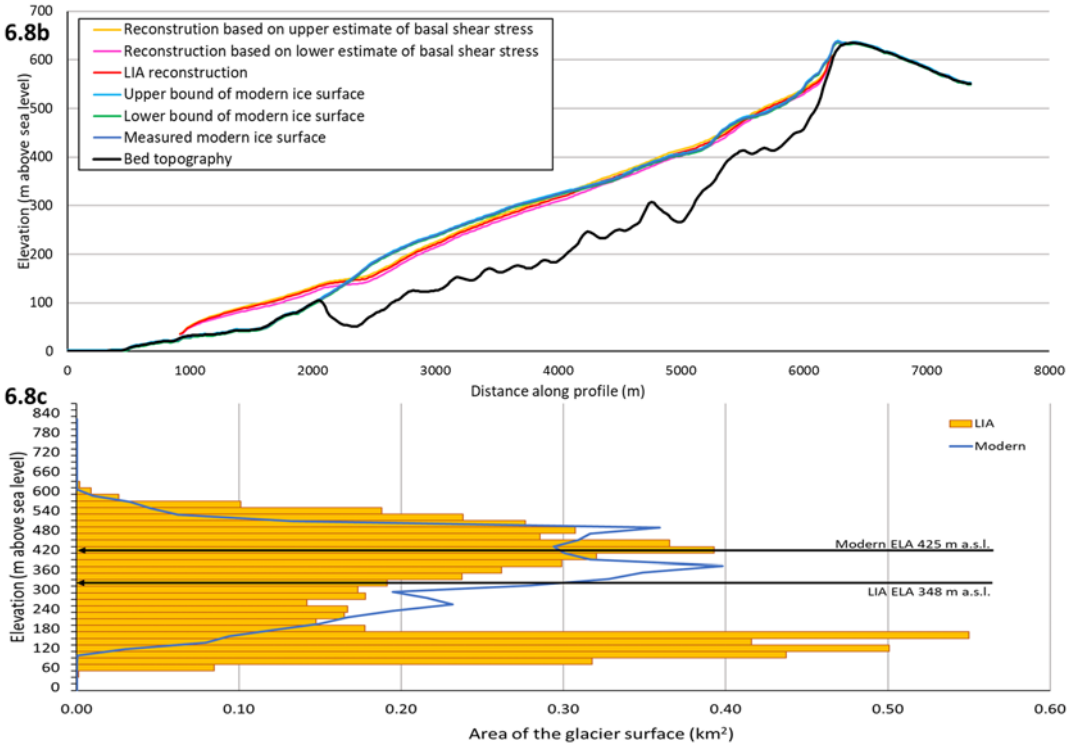

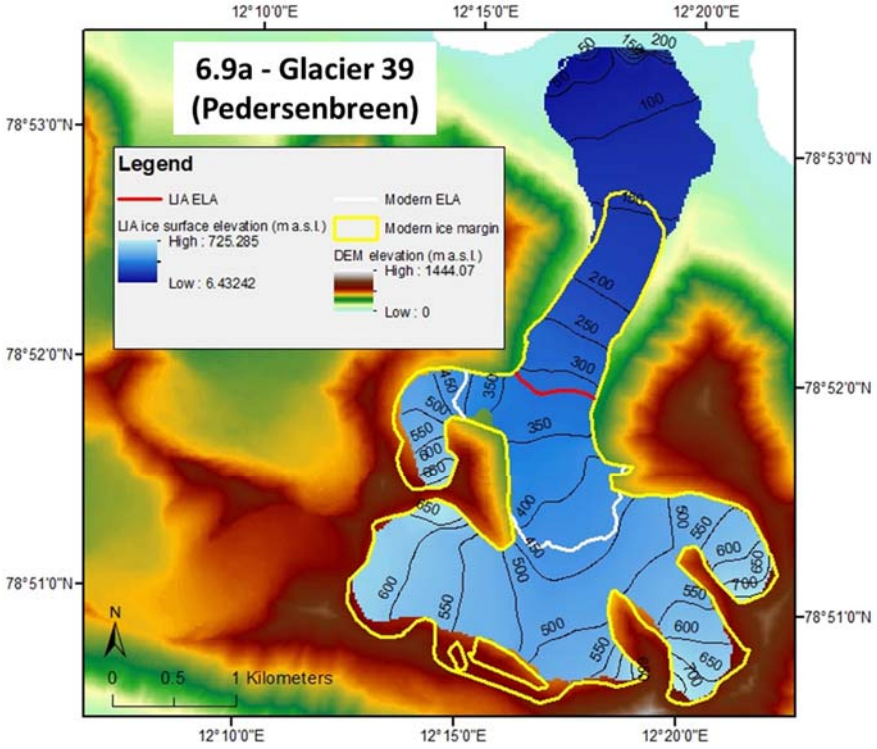

Measurement	LIA		Modern		Change since LIA	
Area (km^2)	7.11	± 0.58	6.24	± 0.52	-0.87	± 0.70
Mean thickness (m)	80.46	± 28.36	74.53	± 2.00	-5.93	± 28.43
Volume (km^3)	0.57	± 0.24	0.47	± 0.05	-0.10	± 0.25
AABR ELA (m a.s.l.)	316	± 40	426	± 40	110	± 57

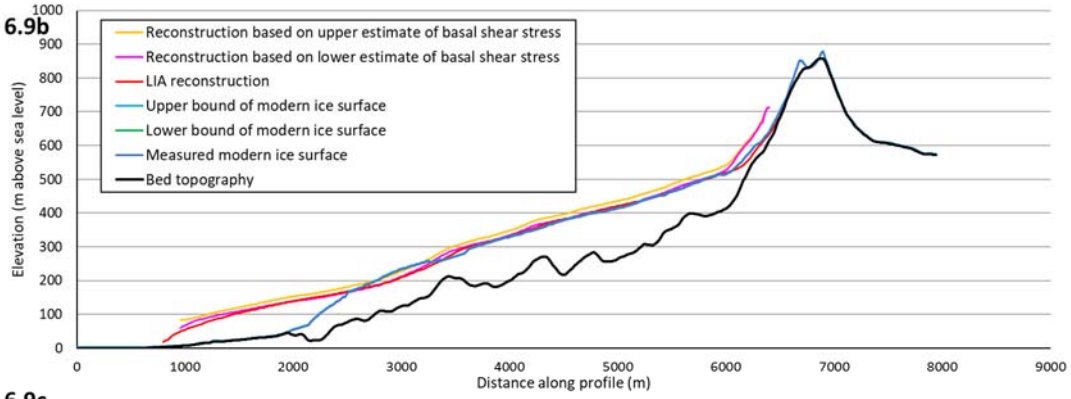

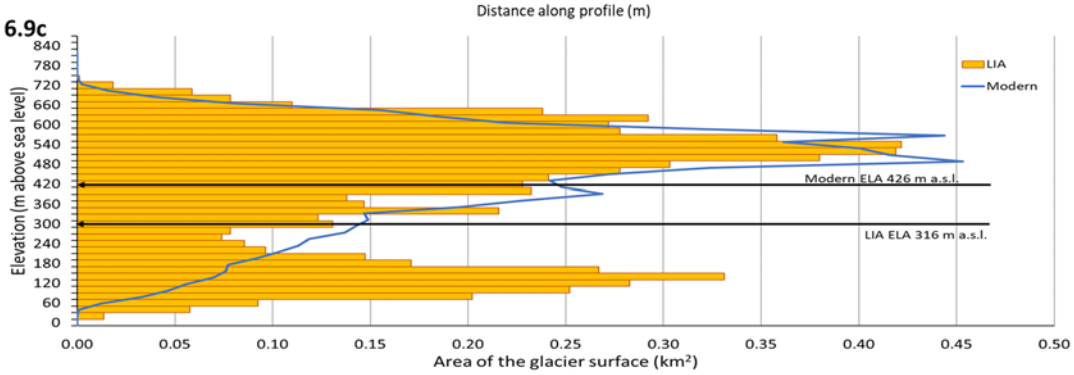

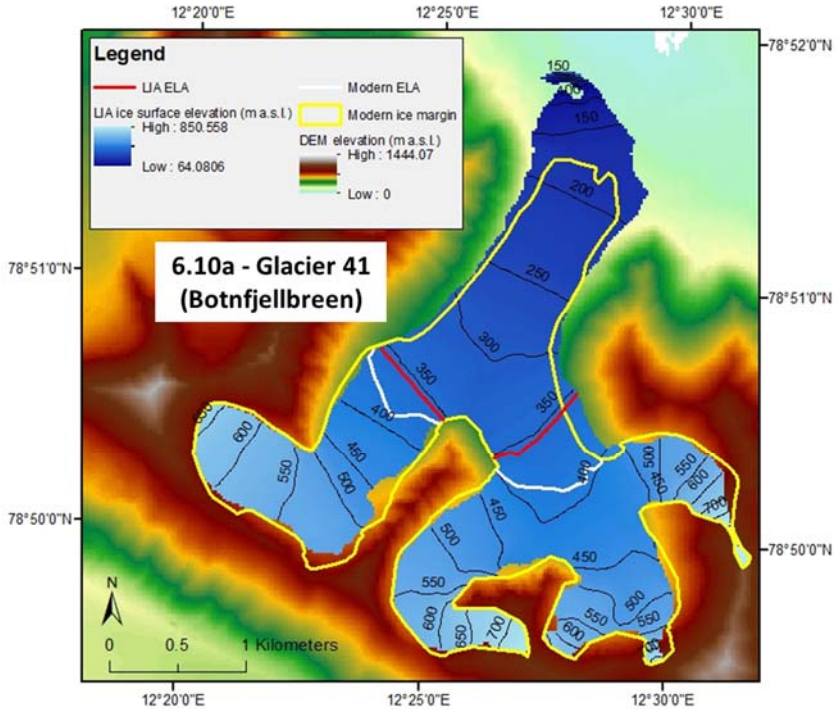

Measurement	LIA		Modern		Change since LIA	
Area (km^2)	6.20	± 0.42	5.87	± 0.49	-0.33	± 0.65
Mean thickness (m)	79.77	± 7.96	76.97	± 2.00	-2.79	± 8.21
Volume (km^3)	0.49	± 0.08	0.45	± 0.05	-0.04	± 0.10
AABR ELA (m a.s.l.)	354	± 40	381	± 20	27	± 45

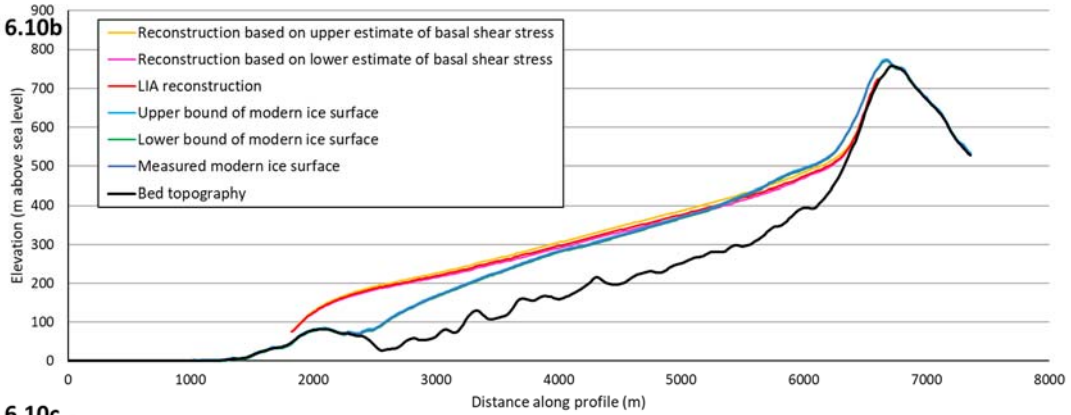

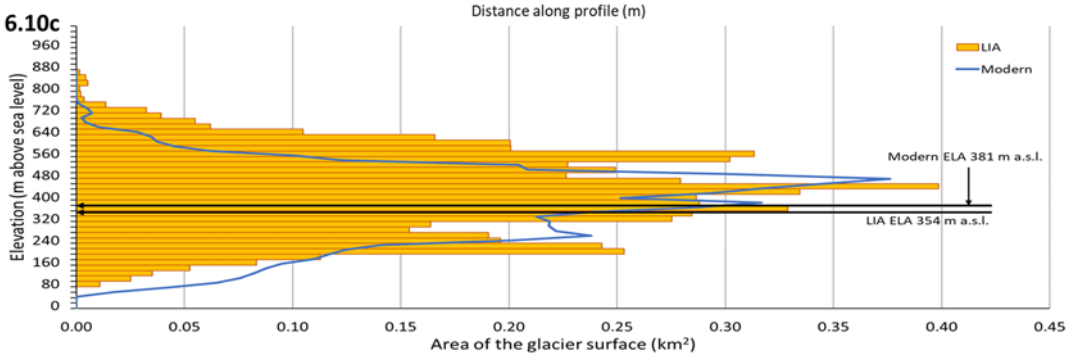

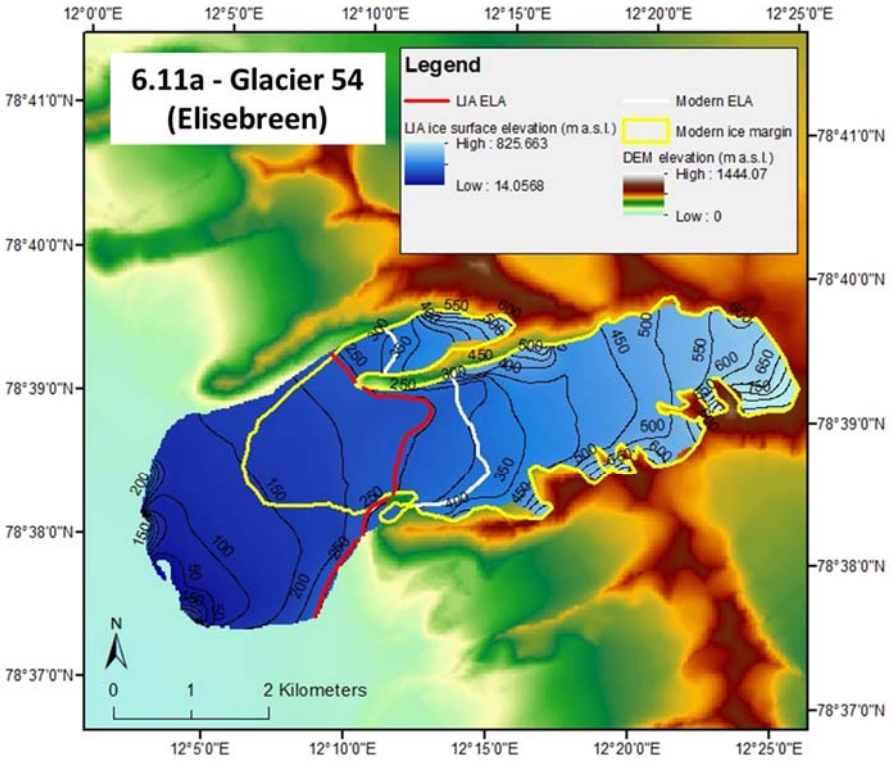

Measurement	LIA	Modern	Change since LIA
Area (km^2)	17.71 ± 1.08	12.57 ± 0.92	-5.14 ± 1.42
Mean thickness (m)	122.11 ± 9.12	118.69 ± 2.00	-3.42 ± 9.34
Volume (km^3)	2.16 ± 0.29	1.49 ± 0.13	-0.67 ± 0.32
AABR ELA (m a.s.l.)	244 ± 20	322 ± 40	78 ± 45

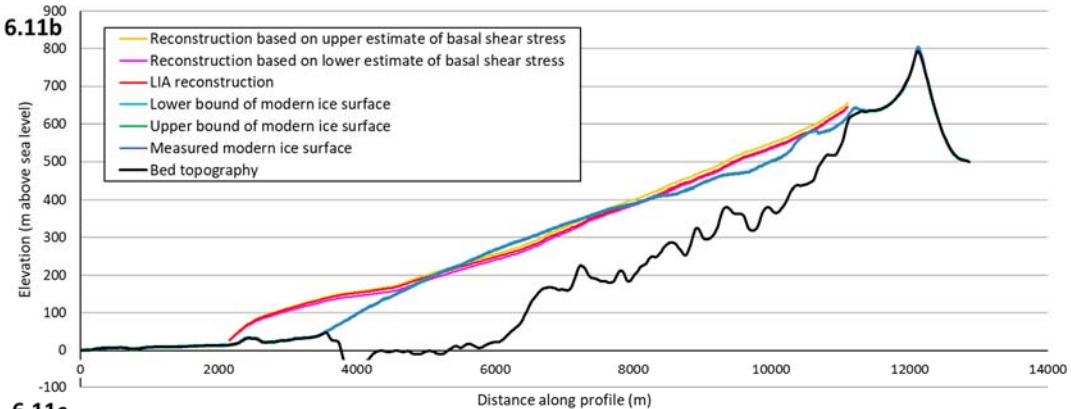

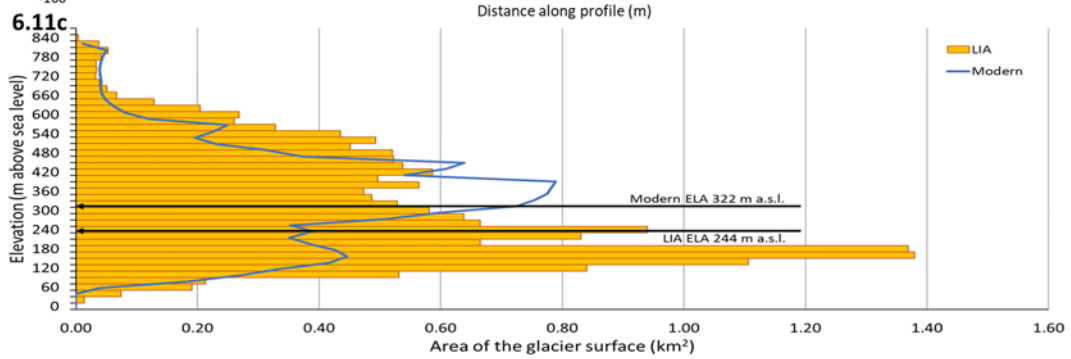

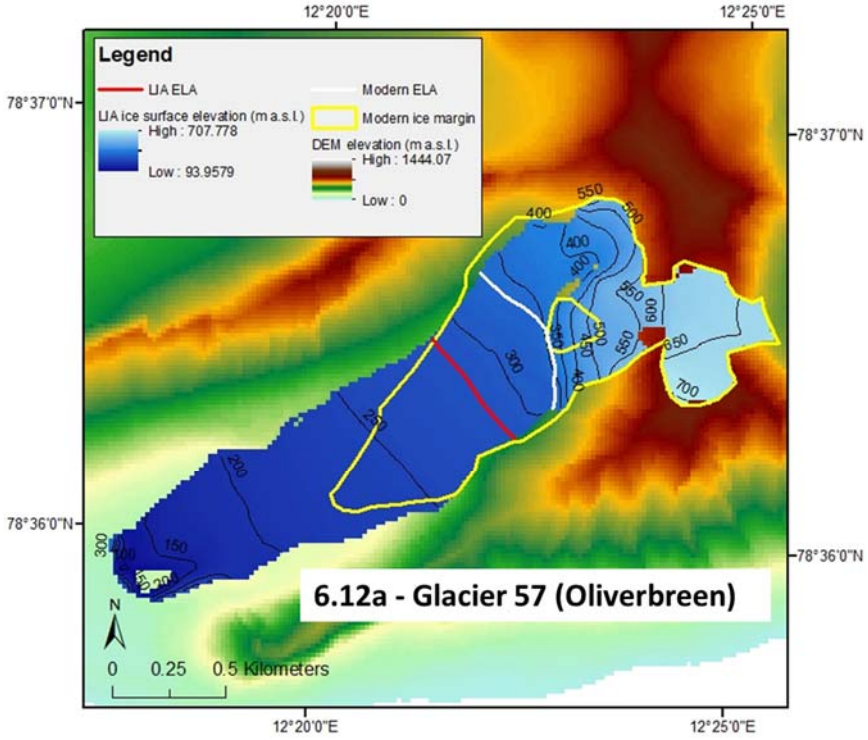

Measurement	LIA		Modern		Change since LIA	
Area (km^2)	1.75	± 0.15	1.15	± 0.14	-0.59	± 0.21
Mean thickness (m)	60.82	± 3.84	47.16	± 2.00	-13.65	± 4.33
Volume (km^3)	0.11	± 0.02	0.05	± 0.01	-0.05	± 0.02
AABR ELA (m a.s.l.)	283	± 20	352	± 40	69	± 45

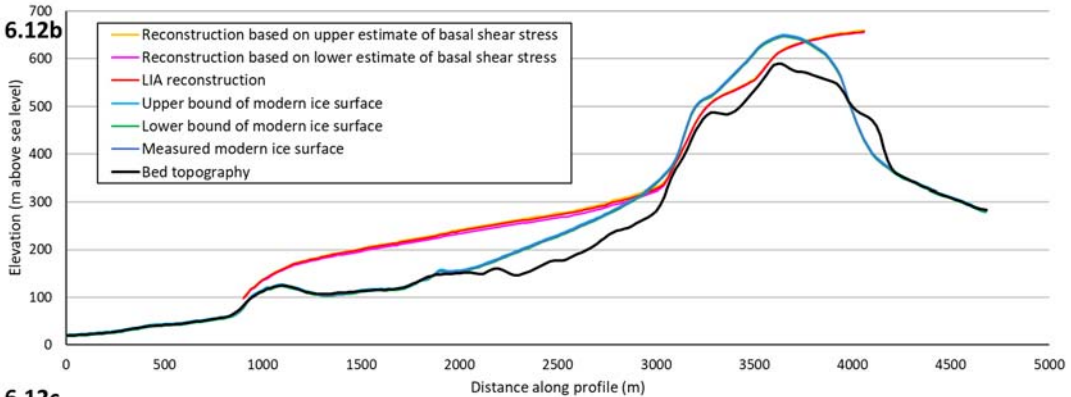

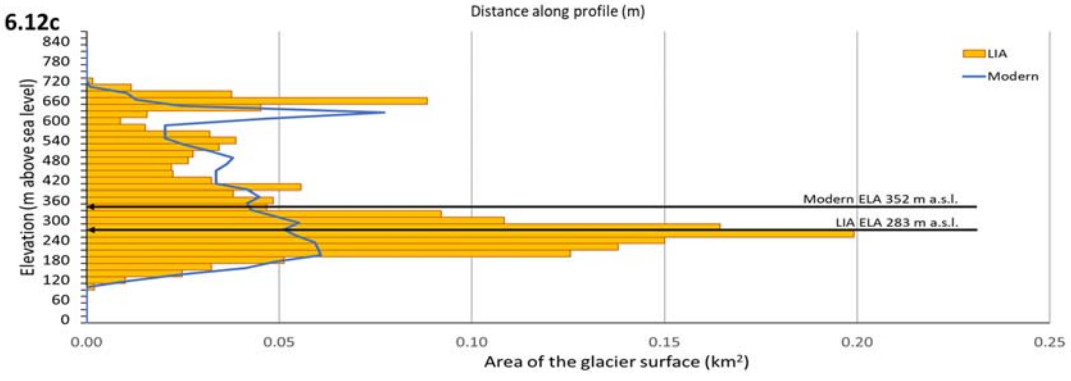

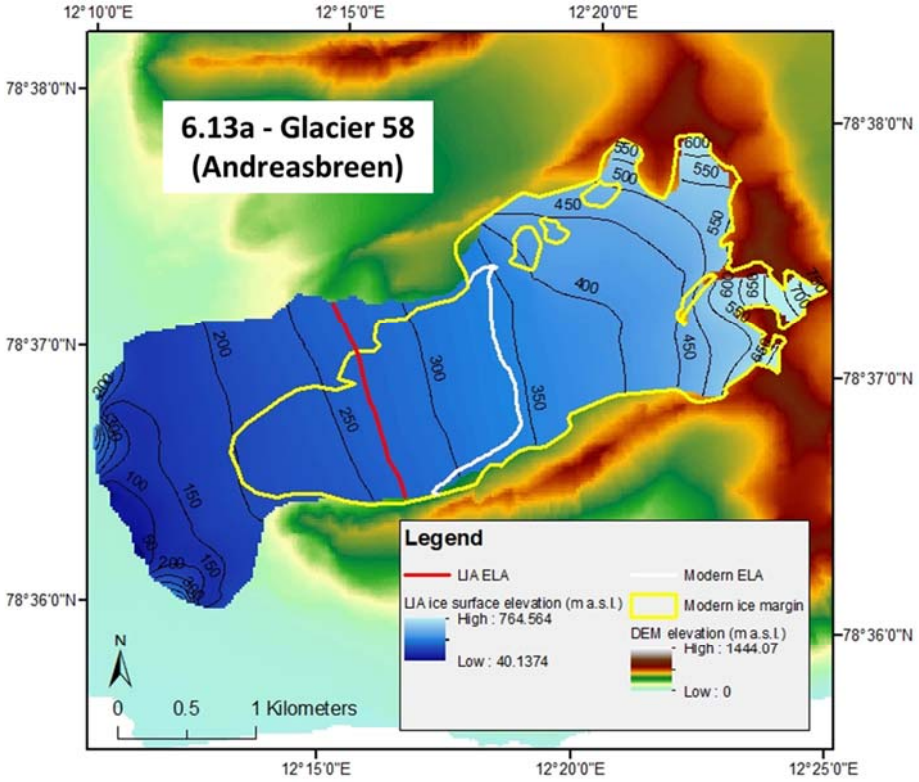

Measurement	LIA		Modern		Change since LIA	
Area (km^2)	7.77	± 0.52	5.27	± 0.45	-2.50	± 0.69
Mean thickness (m)	101.36	± 6.24	73.06	± 2.00	-28.30	± 6.55
Volume (km^3)	0.79	± 0.10	0.38	± 0.04	-0.40	± 0.11
AABR ELA (m a.s.l.)	270	± 20	309	± 20	39	± 28

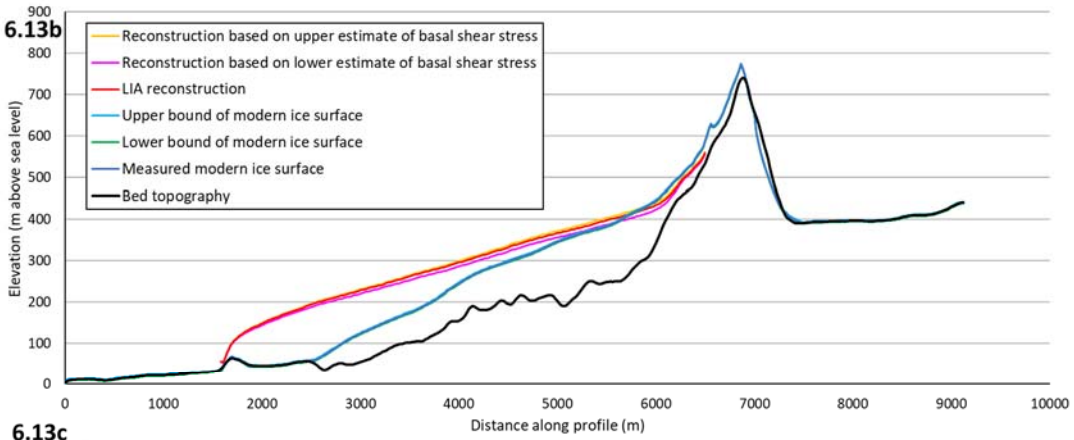

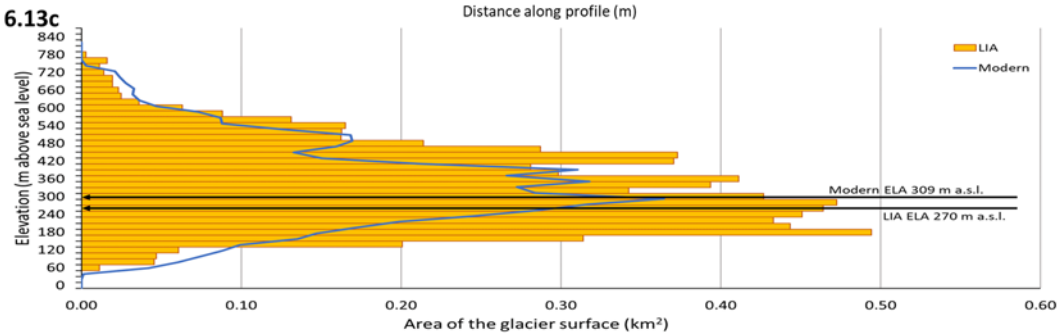

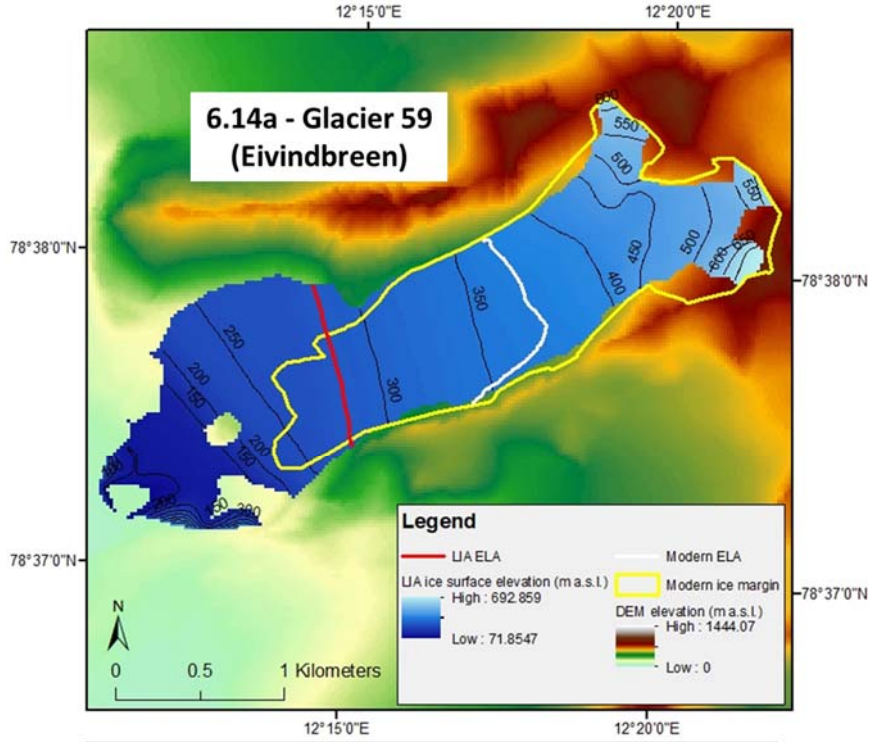

Measurement	LIA		Modern		Change since LIA	
Area (km^2)	3.51	± 0.26	2.53	± 0.26	-0.98	± 0.37
Mean thickness (m)	56.59	± 5.84	62.47	± 2.00	5.87	± 6.17
Volume (km^3)	0.20	± 0.04	0.16	± 0.02	-0.04	± 0.04
AABR ELA (m a.s.l.)	281	± 20	367	± 20	86	± 28

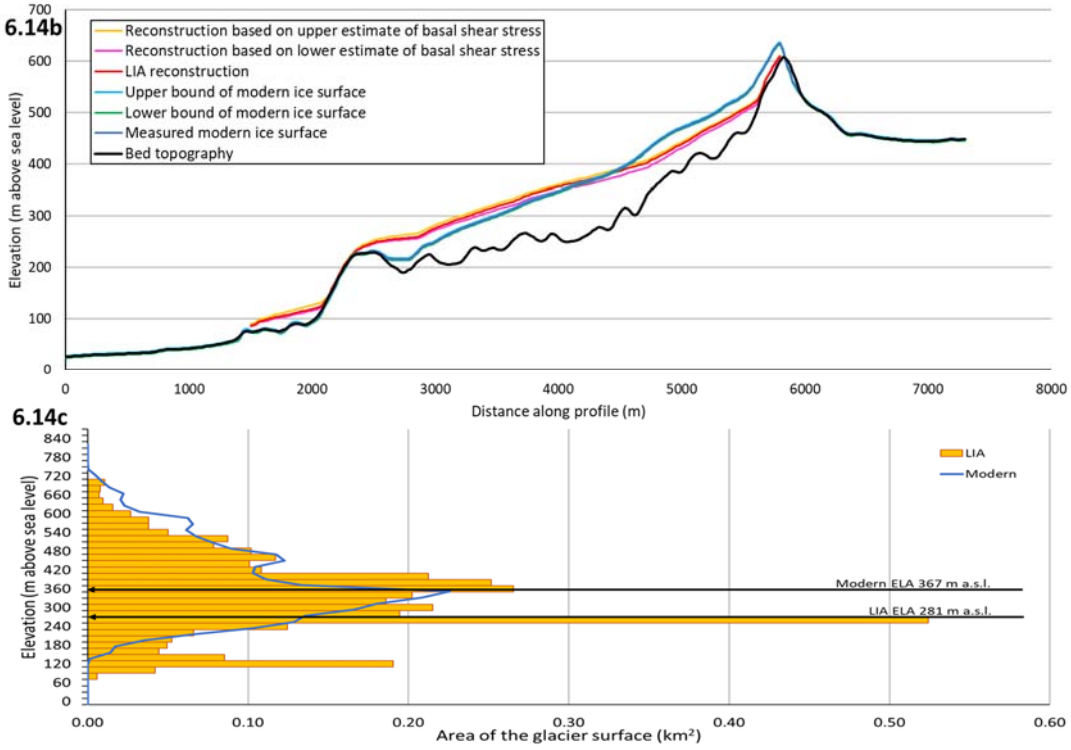

Glacier 32 is located on the west coast of Spitsbergen (Figure 6.3) and is a normal valley glacier. Figure 6.4 shows the reconstruction outputs for this glacier, which has retreated over a kilometre since the LIA. This retreat has been associated with a glacier area change of -1.62 km^2 (-32%) and a similar ice volume change of -0.16 km^3 (-39%). The glacier's ELA has risen by around 55 m since the LIA, increasing the size of the ablation area by 13% and probably accounting for the change in ice volume and glacier area due to the exposure of a larger proportion of the ice surface to mass loss via melting. The hypsometric curves for the glacier support this (Figure 6.4c), with a large part of the glacier's LIA ice surface area located near the snout, much of which has been lost in the modern hypsometric curve. This indicates that there has been significant loss of ice in the ablation area of the glacier but the similar hypsometries above the modern ELA suggests that the accumulation area of the glacier has remained relatively stable. Overall, Glacier 32 appears to have had a reasonably consistent response to post-LIA climate change, with the ELA change reflected in glacier area and ice volume changes of similar magnitudes.

Glacier 33 has undergone a very different response from that of Glacier 32, having actually gained ice volume since the LIA (Figure 6.5). This glacier is the only one in the reconstruction study area to have increased its ice volume (by 6%), despite the ELA rising by a similar amount to other glaciers (46 m), leading to a comparable increase in the glacier's ablation area (10%). However, the uncertainty for the ice volume change of this glacier gives a possible range of percentage ice volume changes from +30% to -17%. This means that there is a chance this glacier may have actually lost volume since the LIA, although it is most likely to have slightly gained ice volume. The glacier is located on the west coast of Spitsbergen and is likely to have been confluent with the tidewater Glacier 43 during the LIA (Figure 6.3), which may perhaps be the reason for its unusual response. Glacier 33 is also thought to be surge-type (H. Sevestre pers. comm. 2015), although it is not known if it has undergone any surges during the LIA or in the subsequent retreat period.

Both Glaciers 34 and 35 have responded in a similar way to Glacier 32, with ice volume losses of 30% and 36% respectively (Figure 6.6; Figure 6.7). This is despite the significant difference in the locations of these glaciers (Figure 6.3) and the fact that Glacier 35 is nearly twice the area of Glacier 34. This indicates that perhaps a similar change in the size of the glaciers' ablation areas might be behind the similar responses of these glaciers and that of Glacier 32. However, the ELA change for Glacier 34 is 18 m (± 20 m), producing an ablation area increase of 23%, whilst Glacier 35 has seen its ELA rise by 75 m (± 45 m) and its ablation area increased

in size by just 13%. This suggests that there may be other variables influencing the responses of these glaciers. A potentially important factor is that Glacier 35 is known to be a surge-type glacier, with the most recent surge thought to have taken place around 1880 (Hansen 2003), placing it around the most likely time of the LIA maximum extent.

Unlike Glacier 35, the other glaciers on the Brøggerhalvøya Peninsula have not responded in a way that is similar to any of the glaciers along the west coast of Spitsbergen. Glaciers 38 and 39 have both lost a slightly smaller ice volume (17% and 18% respectively) despite both glaciers undergoing an even larger ELA change than Glacier 35's 75 m, with Glacier 38's ELA rising by 103 m and Glacier 39's by 110 m (Figure 6.8; Figure 6.9). However, these larger changes in ELA have not translated in to particularly large increases in the size of the glaciers' ablation areas. Glacier 38 has seen an ablation area increase of 15% whilst Glacier 39 has had an increase of 16%. As both of these values are in line with the ice volume changes for these glaciers, it may be that they have actually responded in a more straightforward manner and it is the response of the nearby Glacier 35 that has been more strongly influenced by other factors. Alternatively, it is possible that both Glaciers 38 and 39 have slightly gained ice volume since the LIA, with change of +4% and +25% respectively possible within the uncertainty range of ice volume changes for these glaciers. However, it seems much more likely that both have lost ice volume, particularly Glacier 38 with a potential range of percentage ice volume changes from -38% to +4%. Glacier 39, on the other hand, has a much wider range on uncertainty, by far the largest for any normal glacier (surge-type glaciers seem to produce greater uncertainty). The possible percentage ice volume changes for this glacier could be from -61% to +25%. Despite the uncertainty surrounding Glaciers 38 and 39, it still seems most likely that they have responded in a reasonably straightforward fashion, given the correspondence between the sizes of their ablation area increases and most likely ice volume losses.

Glacier 41 has lost even less ice volume than the other three glaciers on the Brøggerhalvøya peninsula (Figure 6.3). It has lost just 9% of its LIA volume but has also had a relatively smaller change in ELA (27 m) (Figure 6.10). It is worth noting that there is a chance that Glacier 41 may have even gained ice volume since the LIA, with potential ice volume changes from -28% to +11% possible within the range of uncertainty for this glacier. The ELA change of the glacier is comparable to the sort of changes seen amongst glaciers along the west coast of Spitsbergen, such as Glaciers 34 and 32, which have lost significantly more ice volume than Glacier 41. Therefore, some other factor appears to have mitigated the impact of the rise in

ELA on rates of ablation for Glacier 41. A possible explanation may be that Glacier 41 is thought to be a surge-type glacier but it is not known when the glacier last surged (H. Sevestre pers. comm. 2015). It may be more important that the glacier was most likely confluent with the tidewater surge-type glacier Kongsvegen during the LIA.

Glacier 54 is unusual amongst the west coast glaciers because it extended out on to the coastal plain and formed a large piedmont lobe during the LIA (Figure 6.3). However, the response of the glacier to post-LIA climate change is broadly in line with the responses of Glaciers 32, 34 and 35. Glacier 54 has lost around 0.67 km^3 of ice volume (31%) with an ELA rise of 78 m and a consequent 11% increase in the size of the glacier's ablation area (Figure 6.11). Considering the glacier's hypsometric curves (Figure 6.11c), it seems that the modern glacier has gained ice surface area in the accumulation area slightly above the modern ELA. This may have offset the loss of ice from around the LIA snout when the glacier retreated in to its valley and lost its lobe. The reasons for this glacier to have gained mass in the accumulation area are unclear but it has been suggested that Glacier 54 may have experienced a surge during the LIA, which may be related to the large lobe size and subsequent ice thickening above the modern ELA (Christoffersen *et al.* 2005; Larsen *et al.* 2006).

Glaciers 57 and 58 have both lost larger proportions of their LIA ice volume than any other glaciers in the reconstruction study area, with losses of 49% and 51% respectively (Figure 6.12; Figure 6.13). The ELA rises for the glaciers, however, are in line with their neighbours along the west coast of Spitsbergen (69 m and 39 m respectively). They have also retreated by a similar amount as their neighbours and have similar percentage area changes (-34% and -32% respectively). Given these similarities, it is not clear why these glaciers have undergone such a large ice volume loss, suggesting that another variable must be influencing their responses to the post-LIA climate change.

Glacier 59 is located very close to Glaciers 57 and 58 (Figure 6.3) but it has undergone a relatively small ice volume loss of just 20% despite having a larger ELA rise than either of these two glaciers (86 m) and a similar percentage change in the size of its ablation area (-28%). Considering the glacier's hypsometric curve (Figure 6.14c) and long profile (Figure 6.14b) suggests that there has been a thickening of the ice in the accumulation area since the LIA, which may have offset the retreat from the LIA maximum extent. It is not clear why the glacier has thickened above the modern ELA – unlike Glacier 54, Glacier 59 is not thought to be a surge-type glacier.

6.3 Understanding glacier responses to post-LIA climate change

From the reconstruction results presented above, it is clear that there has not been a uniform response to the post-LIA climate change in the reconstruction study area. This is surprising given that this is a small group of glaciers under very similar geological, climatic and glaciological conditions.

There has been a relatively standardised rise in the ELA across the reconstruction study area, with the mean ELA rising by 64 m from 273 m during the LIA to 337 m in the modern day. The majority of glaciers (64%) have seen ELA rises within one standard deviation of the mean and all are within two standard deviations, suggesting that the ELA change has been fairly uniform between the glaciers. Comparatively, the percentage change in ice volume has varied considerably, with a maximum ice volume loss of 51% for Glacier 58 compared with a gain of 6% ice volume Glacier 33; two glaciers that are just 13 km apart (Figure 6.3). These findings lead to the question: why is the change in ice volume so variable, given the relatively uniform rise in ELA?

The relatively uniform change in ELA suggests that the post-LIA climate change has not varied significantly across the reconstruction study area, meaning that there must be one or more other variables influencing the volume changes of individual glaciers in response to this climate forcing. Several potential variables were identified and compared to the percentage change in ice volume, to determine if any one variable/ group of variables was exerting an influence over the response of all of the glaciers in the reconstruction study area. The variables tested were:

- Glacier area
- Glacier aspect
- Outlet glacier or independent valley glacier
- Glacier snout elevation
- Ice surface gradient
- Glacier snout distance from the coast
- Glacier type (i.e. surge-type or normal)

In all cases the percentage ice volume change was graphically compared to the LIA, modern, and change from LIA to modern for each of the above variables, unless these three values were all the same (e.g. it is not thought likely that the glacier types will have changed since the LIA).

When the above variables were compared to the percentage ice volume change it was found that most did not produce any kind of clear pattern or relationship (Figure 6.15). The variables that were found not to be important controls over the percentage change in ice volume from LIA to modern were: glacier area (Figure 6.15a); the glacier snout distance from the coast; glacier aspect; outlet glacier or independent valley glacier; glacier snout elevation (Figure 6.15c); and glacier type (Figure 6.15b).

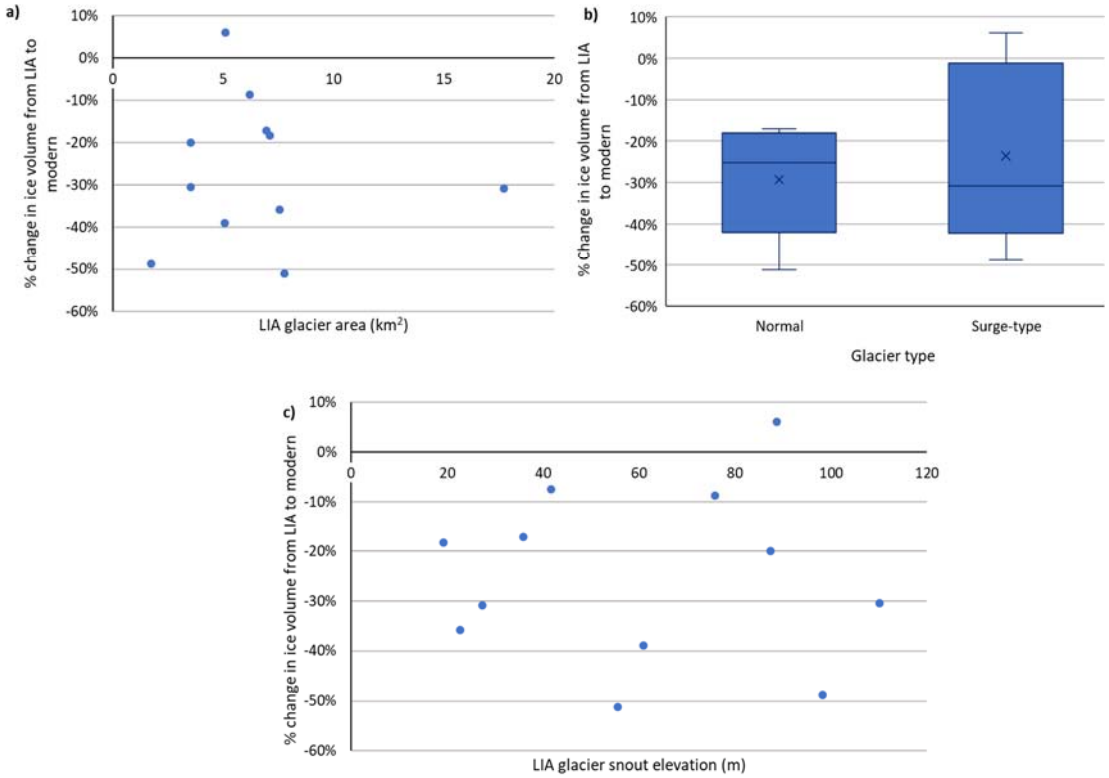

Figure 6.15 – These three examples demonstrate the sort of analysis carried out when comparing the percentage change in ice volume from LIA to modern to the potential controlling variables. These examples also show the lack of a clear link, relationship, or strong correlation between the percentage change in ice volume and most of the variables tested. In this case the variables tested were: a) glacier area (r^2 = 0.0004); b) glacier type; c) glacier snout elevation (r^2 = 0.000006).

The change in ice surface gradient since the LIA was found to have slightly stronger relationships with the percentage change in ice volume from LIA to modern (Figure 6.16). The average gradient of the ice surface was measured along the central flowline of the main trunk glacier, giving an idea of the overall steepness of the glacier during both the LIA and the modern day. The change in the gradient of the ice surface from LIA to modern was found to have a negative linear association with the change in ice volume (Figure 6.16), suggesting that glaciers which have steepened during their retreat have lost larger proportions of their ice volume than those that have maintained a similar ice surface gradient. A glacier retreating in to a steeper valley would have a greater proportion of its ice surface area falling below the ELA, as the ELA rose from the LIA position to that of the modern day. This may explain the possible mechanism by which the change in ice surface gradient influences the change in ice volume. However, the relationship between the change in glacier gradient and the change in ice volume is not especially strong and does not seem to be able to explain all of the variability in ice volume change (Figure 6.16).

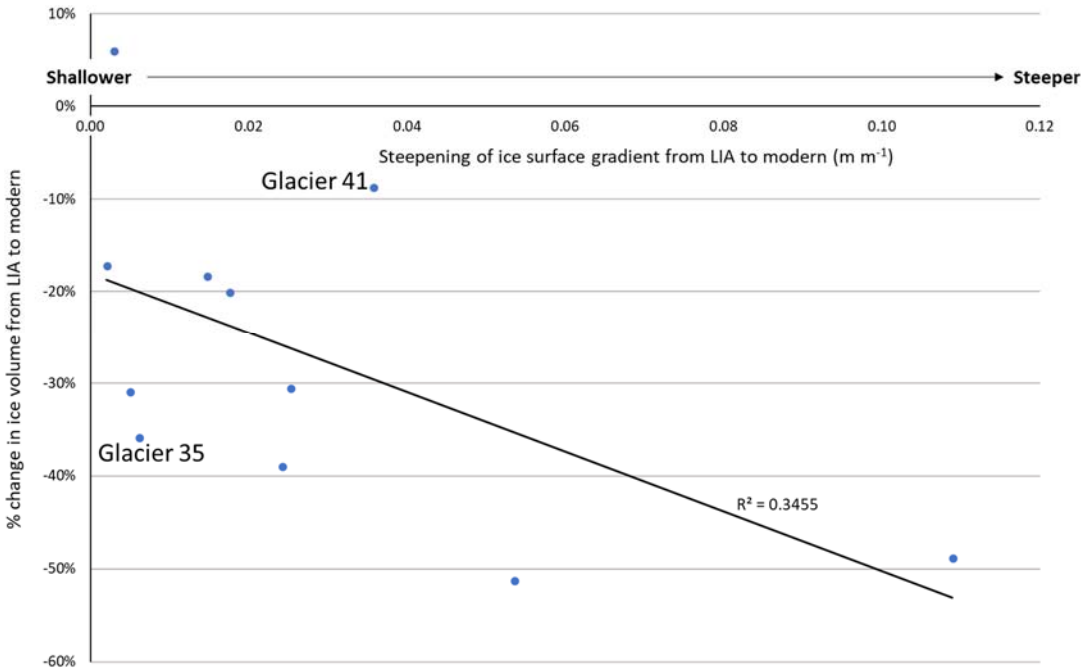

Figure 6.16 – A moderate negative linear correlation was identified between the change in glacier gradient and the percentage change in ice volume from LIA to modern. This correlation suggests that the changing steepness of a glacier as it retreats up its valley influences the proportion of ice volume lost, indicating that the topography of the valley into which the glacier retreats may be a factor that exerts influence over the glacier's response to a given climate forcing. This is particularly true given that the percentage change in ice volume does not correlate as strongly with either the LIA ice surface gradient or modern ice surface gradient, only with the change in ice surface gradient. The modest strength of the trend and the presence of several glaciers that do not conform well to the pattern, for example Glaciers 41 and 35, suggests that the change in ice surface gradient is not able explain all of the variability in ice volume changes.

From the above analyses, no single controlling variable has been identified as exerting a strong influence over the responses of all of the glaciers in the reconstruction study area to the post-LIA climate change. The change in the ice surface gradient of the glaciers appears to have some influence but it is not able to fully explain all of the variation in the ice volume changes (Figure 6.16). It was, therefore, decided to consider the spatial relationships between the glaciers, to determine if there were any spatial patterns or groupings in the way that the glaciers had responded to the post-LIA climate change.

6.4 Spatial variations in glacier responses

Visual analysis of the pattern of ice volume changes and the pattern of ablation area changes was used to identify glaciers with unusual responses to the post-LIA climate change, as well as groups of glaciers with similar responses. Figures 6.17 and 6.18 show the maps produced to enable this analysis, with the glaciers colour-coded to reflect their relative ablation area or ice volume changes. From comparison of these maps, a series of groupings were produced that identify the glaciers with similar or differing responses (Table 6.1).

It is clear from Figure 6.17 that the percentage changes in the size of the glaciers' ablation areas have been reasonably uniform across the study area, reflecting the fairly standardised change in the glaciers' ELAs. There are only three glaciers with unusual ablation area percentage changes: Glacier 41; Glacier 34; and Glacier 59 (Table 6.1). Of these, Glaciers 41 and 34 are slightly outside the range of ablation area changes that most of the glaciers have seen (of around 10-18%), with Glacier 41 seeing only a 7% increase and Glacier 34 a 23% increase. Glacier 59, comparatively, has seen a much larger change in the size of its ablation area (28%) than the majority of other glaciers studied. Despite these anomalous glaciers, the overall picture from the analysis of the ablation area changes is one of a reasonably uniform response to the post-LIA climate change across the glaciers in the reconstruction study area.

Figure 6.18 shows that the ice volume change responses have been far more variable, with glaciers generally grouped in twos or threes in terms of their percentage volume changes. Four groups of ice volume responses have been identified (Figure 6.18; Table 6.1), with the scale of the ice volume change ranging from +6% to -51% across the reconstruction study area. There is no clear pattern of similarly-responding glaciers being grouped together spatially, with adjacent glaciers sometimes behaving in the same way and sometimes differing significantly in their responses. Therefore, it is unlikely that any localised variation

in the post-LIA climate change or in the bedrock geology is responsible for the variety in the ice volume changes. It seems more likely that some other external factors are impacting on the responses of the glaciers, particularly as some glaciers at almost opposite ends of the reconstruction study area have undergone very similar responses. To explain the variety of responses, it has been necessary to consider these factors potentially affecting the responses of individual glaciers or groups of glaciers. The remainder of this section will detail the findings of this investigation.

Glacier ID	Ablation area group	Ice volume group	Area between modern and LIA ELAs (km^2)	Area between ELAs as % of LIA ice surface	Ice volume change from LIA to modern (km^3)	Ice volume change as % of LIA ice volume
32	2	3	0.68	13%	-0.16	-39% ± 22%
33	2	1	0.52	10%	0.02	6% ± 20%
34	3	3	0.80	23%	-0.09	-30% ± 21%
35	2	3	0.98	13%	-0.24	-36% ± 20%
38	2	2	1.05	15%	-0.08	-17% ± 19%
39	2	2	1.16	16%	-0.10	-18% ± 42%
41	1	1	0.43	7%	-0.04	-9% ± 17%
54	2	3	1.90	11%	-0.67	-31% ± 14%
57	2	4	0.25	14%	-0.05	-49% ± 15%
58	2	4	1.41	18%	-0.40	-51% ± 13%
59	4	2	1.00	28%	-0.04	-20% ± 18%

Table 6.1 – The groupings of glacier responses shown in Figures 6.17 and 6.18 are reproduced in this table alongside the actual ablation area and ice volume changes and percentage change values for each glacier. The colouring of the numbers in the two group columns reflects the colour of these groups in Figures 6.17 and 6.18. Consideration of the percentage uncertainty for the ice volume changes shows that glaciers in ice volume groups 3 and 4 have all seen ice loss in excess of the possible uncertainty, whereas the glaciers in ice volume groups 1 and 2 have predominantly seen ice volume changes within the possible uncertainty range. This indicates that the proposed ice volume groupings reflect the amount of uncertainty in the responses of the glaciers, highlighting glaciers that may have responded in more complex or more straight-forward ways to the post-LIA climate change in the study area.

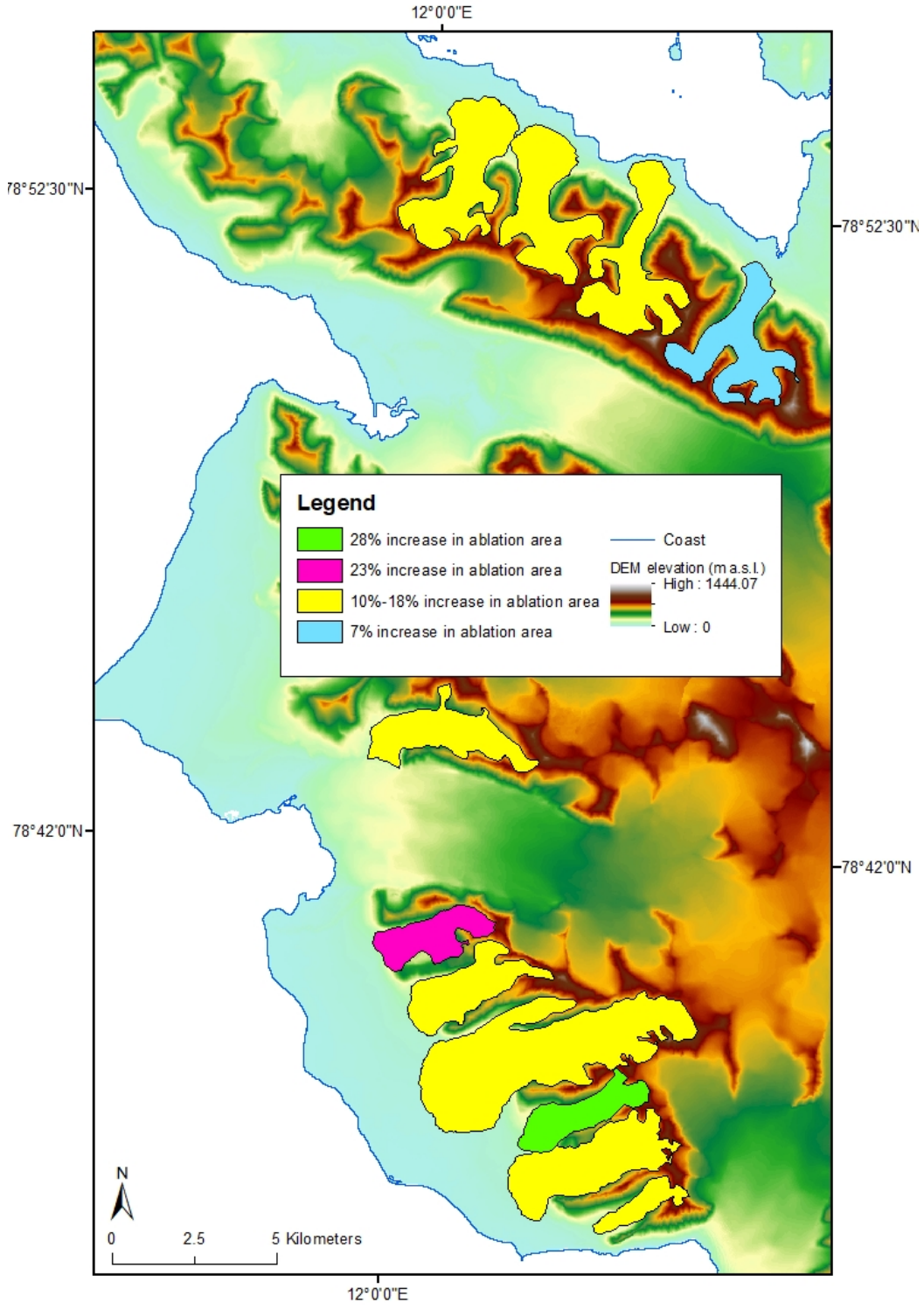

Figure 6.17 – The glaciers in this map are coloured according to their percentage change in ablation area, caused by the increase in the elevation of their ELAs since the LIA. From this map it is clear that most glaciers have had a fairly uniform change in their ablation area, with Glacier 41 (in blue) having a slightly smaller change than the other glaciers and Glacier 34 (in pink) having a slightly larger change. Glacier 59 (in green) is the only marked anomaly, with a significantly larger change in the size of its ablation area relative to the other glaciers in the reconstruction study area.

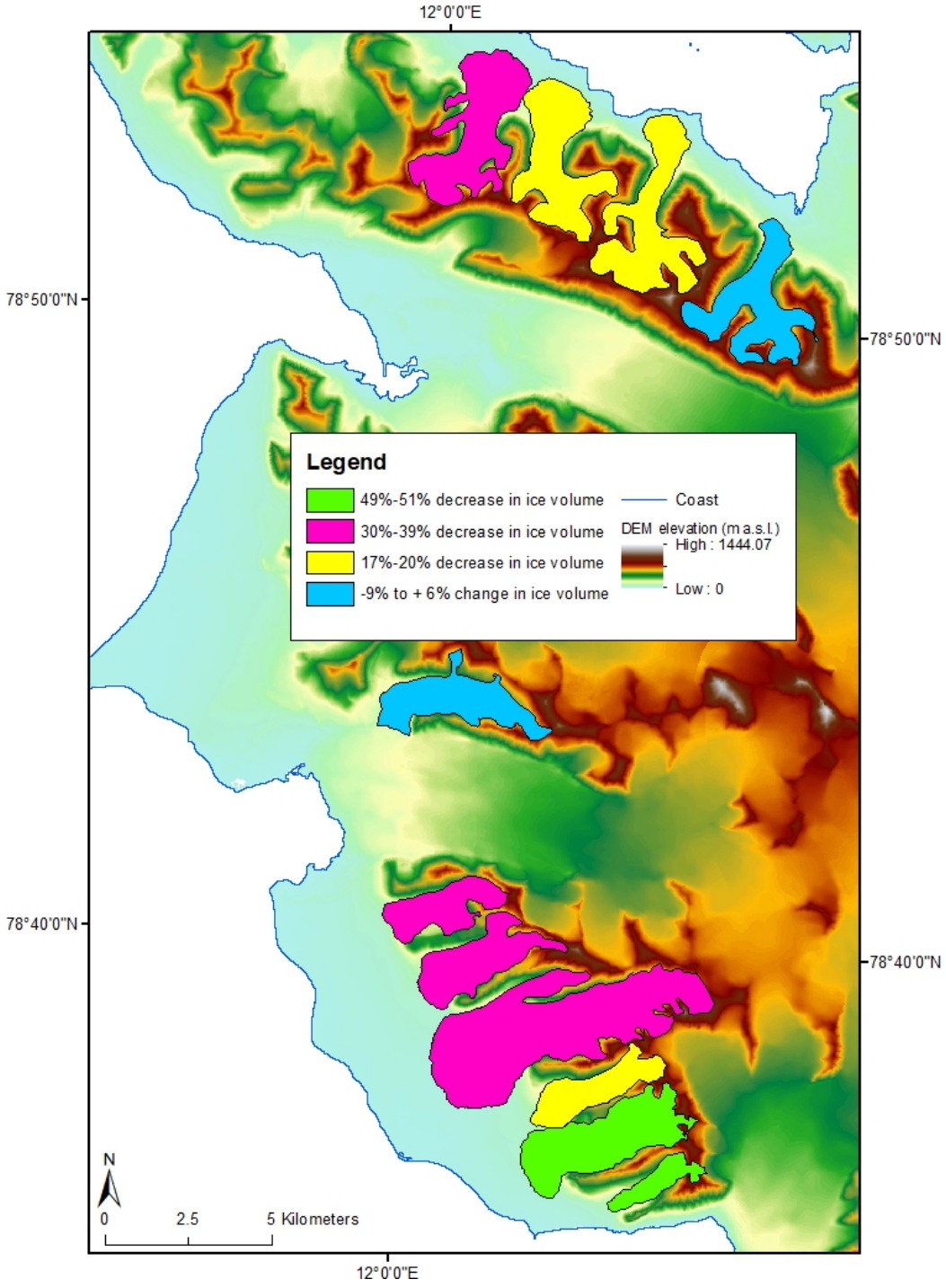

Figure 6.18 – The colouring of the glaciers in this map reflects the percentage change in their ice volumes from LIA to modern day. Comparing to Figure 6.17 clearly shows that the volume change response of the glaciers is much more varied than the change in the size of their ablation areas. Four groupings of two or more glaciers can be identified in this map (see legend) and there are no markedly anomalous responses of any one individual glacier, with the exception of a single glacier that is more likely to have gained ice volume since the LIA (Glacier 33, blue in the centre of the map).

From the patterns identified in Figures 6.17 and 6.18 and in Table 6.1, there are four glaciers that appear to have responded particularly unusually: Glacier 33; Glacier 34; Glacier 41; and Glacier 59. Glacier 33 is highly unusual because of it is the only glacier to have gained ice volume since the LIA, although there is a possibility that it may have lost as much as 17% of its LIA ice volume (Section 6.2). Closer analysis of this glacier shows that it has slightly increased its ice thickness near the snout of the glacier (Figure 6.5b), which could be the reason for the increase in ice volume because the rest of the glacier is a very similar thickness during both the LIA and the modern day. The glacier is thought to be surge-type and this can affect the ice thickness, particularly during polythermal surging of the type common on Svalbard (H. Sevestre pers. comm. 2015; Murray *et al*. 2000; Fowler *et al.* 2001). However, increased ice thickness near the snout of the glacier is most likely towards the end of the active phase of a surge cycle but there have been no observations of Glacier 33 exhibiting surging behaviour in recent times (H. Sevestre pers. comm. 2015). A more likely cause of the ice thickening near the snout of Glacier 33 is the separation from Glacier 43 during the post-LIA retreat. Figure 6.19 shows the likely confluence of these glaciers based on their LIA ice margins, reconstructed from the trimline record, and clearly showing Glacier 33 flowing into the lateral margin of Glacier 43. Due to the faster flow of the tidewater Glacier 43, it is likely that this glacier would have increased the mass loss from Glacier 33 via a drawdown effect. During the retreat from their LIA maximum positions these two glaciers must have separated, as they are no longer confluent in the modern day (Figure 6.1), and the loss of ice from Glacier 33 to Glacier 43 must have come to a halt. This may explain the ice thickening seen near the snout of Glacier 33 and hence why this particular glacier has gained ice volume since the LIA, rather than losing it.

Glacier 34 has a percentage volume change that fits with several other glaciers, both near neighbours and elsewhere in the study area, but it has the second largest increase in the size of its ablation area (Table 6.1). The other glaciers with a similar ice volume change all have much smaller ablation area increase (10-13% compared to 23% for Glacier 34), so it seems strange that Glacier 34 has not lost more ice volume. The long profile of the glacier in Figure 6.6b shows a marked lump in the bed topography around the position of the LIA snout, which may be a bedrock riegel. The modern ice margin sits on the up-valley side of this lump and this may be acting as a topographic pinning point, particularly as it coincides with a slight narrowing of the glacier's valley (Figure 6.6a). The presence of topographic pinning points can reduce the response of a glacier to a given climate forcing by restricting the size of the ablation area near the snout, leading to a reduction in ice loss and a pause or stabilisation of

the retreat (Barr and Lovell 2014). In the case of Glacier 34, the pinning point may have reduced the rate of ice loss sufficiently to slow the glacier's retreat and lead to a lower loss of ice volume than would otherwise have been the case given the change in the size of the glacier's ablation area.

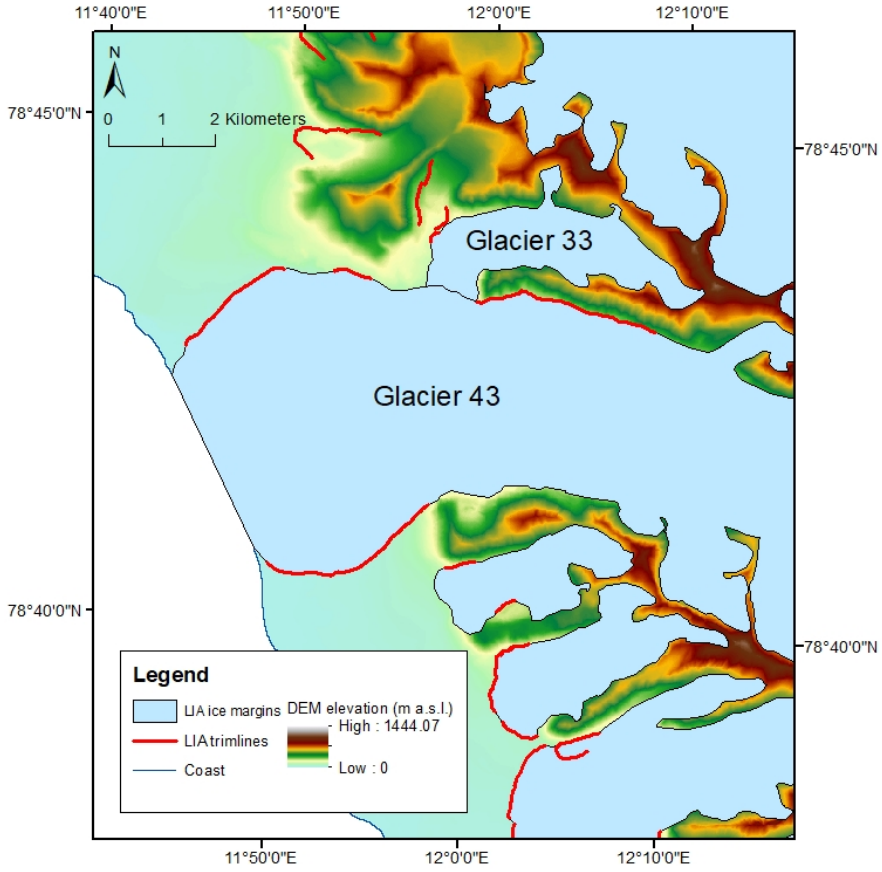

Figure 6.19 – The LIA ice margins of Glaciers 33 and 43 clearly show that these two glaciers were confluent during the LIA. These margins were produced from the trimline evidence shown and confidence in the identification of this palaeo-confluence is high. As Glacier 43 is a tidewater glacier it is likely to have flowed much faster than Glacier 33, potentially causing a drawdown of ice from the smaller tributary glacier.

Glacier 41 has also lost ice volume but only 9% (Table 6.1), compared to an average ice loss of 27% for all of the glaciers in the reconstruction study area. The relatively small ice loss is matched by a small change in the size of the ablation area, which has only increased in size by 7% for Glacier 41 since the LIA. This may explain the limited change in the ice volume of the glacier but the reason for the unusually small change in the size of the ablation area requires further investigation. The morphology of the glacier's valley has forced the glacier to develop two distinct branches, which split just below the position of the LIA ELA (Figure 6.10a). This branching reduces the portion of the glacier affected by the change in the position of the ELA, reducing the resulting change in the size of the glacier's ablation area. The relatively small change in the size of the ablation area may be entirely responsible for the small ice volume loss but Glacier 41 is thought to have been confluent with the tidewater Kongsvegen glacier during the LIA (Figure 6.20). A drawdown effect, very similar to that affecting Glacier 33, may have been increasing the ice loss from Glacier 41 during the LIA. Therefore, the subsequent separation of the glaciers may have further reduced the scale of ice volume loss from Glacier 41 and reinforced the effect of the relatively small increase in the size of the ablation area.

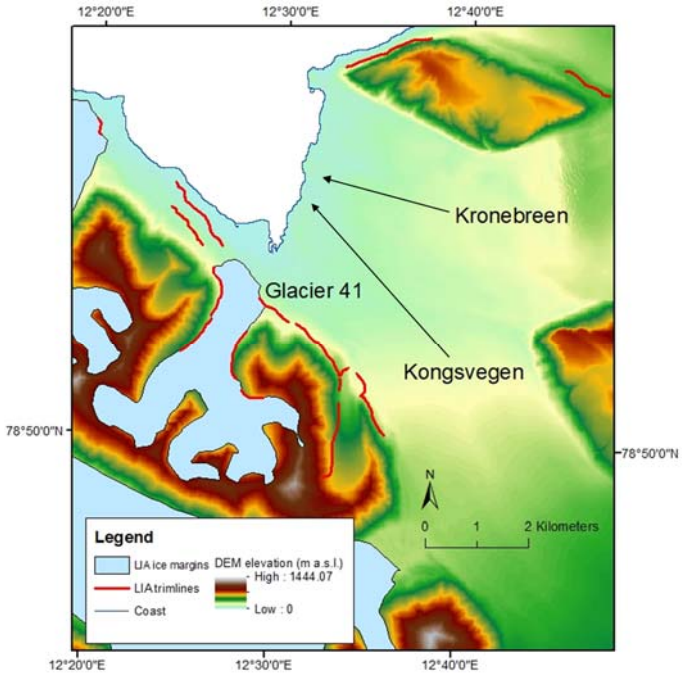

Figure 6.20 – There is evidence of palaeo confluence between Glacier 41 and Kongsvegen due to the pattern of LIA trimlines associated with these glaciers and the reconstructed morphology of Glacier 41's snout. It appears that the fast-flowing tidewater Kongsvegen connected to Glacier 41 and dragged its snout down-fjord towards the sea. This confluence was probably a significant source of ice loss for Glacier 41 during the LIA and the separation of the glaciers may help to explain the unusual response of this glacier.

The final unusual glacier response is that of Glacier 59, which has seen by far the largest increase in the size of its ablation area (28%) but has not undergone a similarly large loss of ice volume, losing just 20% of its LIA volume. The long profile of the glacier (Figure 6.14b) reveals a similar story to Glacier 34, with a marked bedrock riegel near the modern snout position. Also similar to Glacier 34 is that the glacier has retreated in to a constricting valley (Figure 6.14a) and, combined with the presence of the riegel, this may well constitute a topographic pinning point that has restricted the ice loss from the glacier. The position of the supposed pinning point roughly coincides with the LIA ELA and it is clear from the glacier's hypsometric curve (Figure 6.14c) that there has been little change to the ice surface area above this point, supporting the theory that topographic pinning has mitigated the large increase in the size of Glacier 59's ablation area.

Aside from these unusual responses, the remaining glaciers can all be more easily grouped together in terms of their ablation area and ice volume changes. These groupings area: Glaciers 38 & 39; Glaciers 32, 35, & 54; and Glaciers 57 & 58.

Glaciers 38 and 39 have both seen a very similar change in the size of their ablation areas, increasing by 15% and 16% respectively. This has translated into a similar ice volume loss of 17% and 18% respectively. The similarity between these values, despite the reasonably large uncertainty in the ice volume change of Glacier 39, suggests that both of these glaciers have undergone a more straight-forward response to the post-LIA climate forcing than the glaciers discussed so far. It seems unlikely that there are any significant external factors influencing the responses of these glaciers and their similarity to each other is probably due to the fact that they are immediately adjacent and are of a similar size and valley morphology. Unlike their neighbours on the Brøggerhalvøya peninsula, both Glaciers 38 and 39 are normal valley glaciers and are not suspected to be surge-type. This may have contributed to their 'textbook' response to the post-LIA climate forcing compared to the other glaciers in the reconstruction study area.

The grouping of Glaciers 32, 35, and 54 has seen a more complex change since the LIA. These glaciers have all undergone a similar increase in the size of their ablation areas of 11-13%, which is slightly smaller than that of Glacier 38 & 39 (Table 6.1). However, these three glaciers have lost a much greater percentage of their ice volumes than Glaciers 38 & 39, with Glacier 32 losing 39% of its volume whilst Glacier 35 lost 36% and Glacier 54 lost 31%. These three glaciers are dispersed throughout the reconstruction study area (Figure 6.3), so this relatively large ice volume change is not likely to be due to unusual local climatic conditions.

One thing that all of these glaciers have in common is that they have retreated into their valleys from their LIA maximum extents, when they had flowed out over the relatively flat coastal plains and formed piedmont lobes of varying sizes. From the hypsometric graphs of the three glaciers (Figures 6.4c, 6.7c and 6.11c) it can be seen that they all have a large peak in the proportion of their ice surface areas located around the LIA snout position. These peaks are all much reduced in the modern day hypsometries, indicating that all of these glaciers have lost a significant portion of their total ice loss from around the LIA snout. The relative similarities of their modern and LIA hypsometric curves in the accumulation areas suggests that mass loss here has been relatively small, supporting the theory that the loss of the piedmont lobes around their LIA snouts is the factor that has contributed most to these glaciers' relatively large decreases in ice volume. The slight differences in the scale of the ice volume loss for the three glaciers may be explained by considering their accumulation areas, with Glacier 32 losing the highest percentage of its ice volume (39%) and also losing some mass in the accumulation area whereas Glacier 54 has lost the smallest percentage of its ice volume (31%) and has actually gained mass in the accumulation area, offsetting the loss of its larger piedmont lobe.

Glaciers 57 and 58 have not had particularly similar ablation area changes (gaining 14% and 18% respectively) but they are grouped together due to their extremely large ice volume losses of -49% and -51% respectively. Similar to Glaciers 32, 35 & 54, Glaciers 57 and 58 had started to extend out of their valleys at the LIA maximum and Glacier 58 had even begun to form a piedmont lobe (Figures 6.12a and 6.13a). The subsequent retreat back in to their valleys has caused a significant loss of ice in the ablation areas of both glaciers, which can be clearly seen in their hypsometries (Figures 6.12c and 6.13c). However, the retreat back from the coastal plain cannot totally explain why these particular glaciers have undergone such a large ice volume loss compared to others that have lost similar piedmont lobes during their retreat, such as Glaciers 32, 35, and 54. When the long profiles of Glaciers 57 and 58 are considered (Figures 6.12b and 6.13b), what is unusual about these glaciers is that they have particularly steep valleys. Consideration of the ice surface gradients of the glaciers also reveals that they have seen the largest changes in their surface gradients since the LIA of any glaciers in the reconstruction study area. This means that the glaciers have become much steeper as they retreated, compared the other glaciers in the reconstruction study area, leading to a relatively larger loss of accumulation area and a stronger impact of the LIA climate forcing. It is likely to be this factor that has caused their larger than usual ice volume losses.

From this analysis of the responses of individual glaciers and small groups of glaciers in central western Spitsbergen it is clear that no single factor has been wholly responsible for the variety of ice volume changes seen. However, the valley-scale topography of individual glacier valleys does seem to be important in many cases and confluence with another glacier during the LIA has an influence where this is present. The findings from this group analysis can be summarised as:

- Glacier 33: the unusual gain in ice volume since the LIA appears to have been caused by the separation of this glacier from the neighbouring Glacier 43 during the retreat, which would have removed an important source of ice loss for Glacier 33.

- Glacier 34: a relatively large increase in the size of this glacier's ablation area has not resulted in a similarly large loss of ice volume due to the influence of a topographic pinning point, which appears to have reduced the rate if ice loss and slowed the glacier's retreat.

- Glacier 41: a small loss of ice volume has been caused by a relatively small change in the size of this glacier's ablation area. The most likely cause appears to be the branching morphology of the glacier's valley, which has led to the rise in ELA covering a smaller area of the ice surface. However, palaeo-confluence with Kongsvegen may also be a factor.

- Glacier 59: a relatively large increase in this glacier's ablation area has not been reflected in the ice volume lost. A topographic pinning point appears to be the explanation for the limited ice loss experienced by this glacier.

- Glaciers 38 & 39: these glaciers appear to have responded in a 'textbook' fashion, with strong correspondence between the change in the size of their ablation areas and the amount of ice volume lost.

- Glaciers 32, 35, & 54: a relatively small change in the size of these glaciers' ablation areas has led to a relatively large loss of ice volume. The cause appears to be the loss of piedmont lobes as these glaciers retreated from the coastal plains into more confined valleys.

- Glaciers 57 & 58: very large ice volume losses for these glaciers are not linked to similarly large changes in ablation area, but rather seem due to an increase in their ice surface gradients as the glaciers retreated into steeper sections of their valleys.

6.5 Summary and conclusions

Climate change since end of the LIA has impacted the glaciers within the reconstruction study area in central western Spitsbergen. Little is confidently known about LIA climate on Svalbard because this period largely pre-dates accurate record-keeping. Mean annual temperatures during the 1890s are thought to have been 3-4°C lower than in the 1980s-1990s (Ziaja *et al.* 2005; Førland *et al.* 1997) but other temperature records for the early 1900s show a more marked mean annual temperature rise of 4-5°C from 1912-1920, with summer temperatures rising by 2-3°C on average over the same period (Lønne and Lysså 2005; Førland *et al.* 1997). Most studies note little change in precipitation during the 20th Century (e.g. Førland *et al.* 1997; Ziaja *et al.* 2005), indicating that the modern mean annual precipitation of around 200 mm (measured from 1988-2000 at Svalbard airport) is likely to be roughly accurate for the LIA (Ziaja *et al.* 2005). Therefore, the complex responses of the glaciers of central western Spitsbergen are likely to be primarily driven by the increase in mean annual and summer air temperatures, with little influence of precipitation.

The glaciers reconstructed by this study have responded in an complicated way to the temperature change that has occurred since the end of the LIA. In particular, the change in the glaciers' ice volumes have been highly variable compared to the fairly uniform change in the position of the ELA and the associated increase in the size of the glaciers' ablation areas. This variability in ice volume change is not strongly linked to any single variable tested, although there is an association with the change in glacier gradient since the LIA. The identification of this particular variable suggested that that topography may well be an important influence over the responses of the glaciers in the reconstruction study area. Further analysis of individual glaciers and small groups of glaciers has supported this and identified valley-scale topography as being the primary influence over the variation in ice volume changes since the LIA in central western Spitsbergen.

Topographic features within and around the valleys of the glaciers have been found to be an important control over the responses of all but three of the reconstructed glaciers. Most glaciers have been affected by topography in one of three key ways:

1. The presence of topographic pinning points/ bedrock riegels that have led to slowdowns or standstills in their retreat from the LIA maximum (Glaciers 34 and 59);

2. Retreat from a LIA maximum position on the coastal plain into a confined valley, often including the loss of a piedmont lobe (Glaciers 32, 35, and 54);

3. Retreat into a steep valley since the LIA, leading to an increased impact of the change in ELA and a greater loss of ice volume (Glaciers 57 and 58).

Aside from the glaciers mentioned in the above list, Glacier 41 has also been affected by the branching topography of its valley, which has reduced the impact of the rise in its ELA since the LIA. However, it is difficult to determine if this is the dominate factor controlling this glacier's response because it was also confluent with a neighbouring tidewater glacier (Kongsvegen) during the LIA. The presence of confluence with other glaciers during the LIA and especially the subsequent parting of the glaciers during retreat appears to also be an important influence over the change in ice volume. Whilst the impact of confluence on Glacier 41 is difficult to separate from the role of topography, the lack of a clear topographic control over Glacier 33's unusual gain in ice volume since the LIA suggests that this is wholly down to the change in its confluence with the tidewater Glacier 43.

For Glaciers 38 and 39, neither topography nor confluence appear to have had a strong influence. These glaciers have seen increases the size of their ablation areas that are reflected by losses of ice volume that are within one percentage point of the change in their ablation areas. This suggests that these glaciers have undergone a relatively simple response to the post-LIA climate change, with a rise in their ELA leading to a level of ice volume change that might have been predicted from the change in the size of the ablation area and hence increase in the proportion of the ice surface losing mass via melting.

The significant influence of the valley-scale topographic factors outlined above over the responses of most of the glaciers in central western Spitsbergen suggests that these factors deserve more consideration in palaeoglacial reconstructions. The role of palaeo-confluence is also something that appears to have a potentially significant impact, particularly with the loss of confluence appearing to have a strong impact on the ice volume of the tributary glacier involved. These two factors seem to have affected the way in which individual glaciers have responded to the same climate forcing, leading to the very different changes in ice volume observed in this study. Future palaeoglacial reconstructions may need to give more

consideration to these factors and to the potential for highly variable responses between glaciers within a relatively small study area with a fairly uniform change in climate and ELA.

The use of glacial trimlines in this study was vital to the identification of palaeo-confluence (Figures 6.19 and 6.20) and also helped to identify the influence of topography by allowing more accurate reconstruction of the LIA ice margins and ice thickness. This study suggests care must be taken when utilising the outputs of reconstructions based on limited geomorphological evidence because these reconstructions may well be missing important information about the responses of poorly-recorded glaciers, which may potentially not be accurately extrapolated from the behaviour their near neighbours. This finding means that large-area palaeoglacial reconstructions may miss much of the variability between glaciers, if they are not adequately constrained by geomorphological evidence, and should be produced and used with caution to avoid missing the impacts of valley-scale topography and palaeo-confluence. It is therefore important that all forms of glacial geomorphological evidence, including glacial trimlines, are well studied to ensure that the maximum possible amount information can be extracted from them for use in palaeoglacial reconstructions.

Chapter 7

Summary, conclusions and implications for palaeoglaciology

7.1 Summary and conclusions

This thesis aimed to improve understanding of the geomorphological signature of ice margins in rugged terrain, in order to increase the accuracy and confidence of empirical palaeoglacial reconstructions. To achieve this aim, research has been carried out into glacial trimlines, developing a deeper understanding of these landforms and their best usage in 3-dimensional (3D) reconstructions, and into the process of interpolation, in order to reduce subjectivity within palaeoglacial reconstructions. This work has included the production of a new 3D reconstruction of Little Ice Age (LIA) glaciers in central western Spitsbergen, Svalbard, utilising glacial trimlines (Figure 7.1; Section 7.1.2).

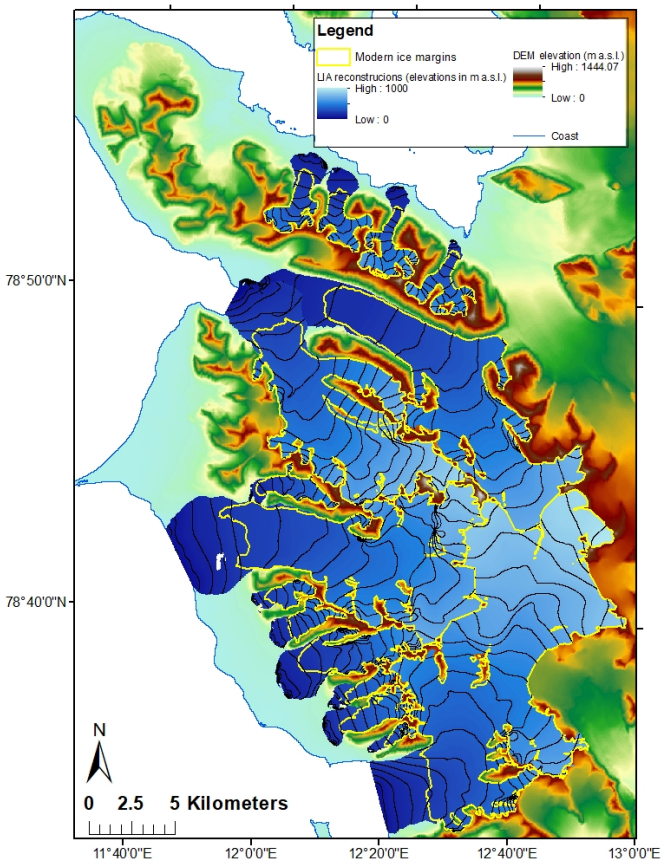

Figure 7.1 – The Little Ice Age (LIA) glaciers of central western Spitsbergen were reconstructed in 3-dimensions from their glacial trimlines and compared to the modern glaciers, in order to determine their responses to the local post-LIA climate change (Section 7.1.2).

7.1.1 The phenomena of glacial trimlines

Glacial trimlines are glaciogenic features that are expressed as a break or transition in the vegetation, weathered material, erosion pattern, deposited material, or slope features on the slopes of a glacierised or glaciated valley. These features have been shown to be relatively under-studied compared to other types of glacial geomorphological features, despite holding much promise for the production of 3D palaeoglacial reconstructions (Chapter 3). Trimlines are particularly significant landforms because they record both the ice margin position and a measure of the ice thickness at their time of formation, making them valuable empirical constraints for ice volume changes. Three-dimensional reconstructions are an increasingly important output of palaeoglaciology because they can be used for testing and refining numerical glacial models and they can also be used to estimate the palaeo Equilibrium Line Altitude (ELA), permitting inference of climate changes. Better use of glacial trimlines, therefore, has the potential to improve understanding of the geomorphological signature left by glaciers in rugged terrain and to increase the accuracy and confidence of 3D palaeoglacial reconstructions based on this empirical evidence (Chapter 1).

This thesis has produced several improvements to the understanding of glacial trimlines and their use in 3D palaeoglacial reconstructions. These include: developing and testing a new classification scheme for glacial trimlines to aid in their identification, correlation and interpretation (Chapter 3; Chapter 4); improving understanding of the formation and preservation of glacial trimlines (Chapter 3; Chapter 4); providing an example of best practice for the identification and mapping of glacial trimlines (Chapter 4); and demonstrating all of these outputs by producing a case study example of a 3D palaeoglacial reconstruction underpinned by the mapping and interpretation of glacial trimlines (Figure 7.1; Chapter 5; Chapter 6; Section 7.1.2).

Trimlines have generally been under-utilised and this has often been due to poor identification and mapping of these features, as well as because of a lack of clear terminology for discussing glacial trimlines. A clearer and more concise terminology for trimline features and a classification scheme for trimline expressions was developed from a review of the literature surrounding glacial trimlines (Chapter 3). This new terminology and classification scheme for trimline expressions was applied to the central western Spitsbergen case study, which helped the identification and discussion of the trimlines features (Chapter 4). The analysis of the trimlines of central western Spitsbergen also provided an example of trimline

mapping and has produced a recommended process for reliably identifying trimline features from remotely sensed imagery (Chapter 4). From the trimlines mapped in this case study, a 3D palaeoglacial reconstruction was produced, the implications of which will be discussed in more detail in Section 7.1.2.

The production of a new terminology and classification scheme for trimline expressions will hopefully facilitate more widespread identification of these features, as well as enabling further research into the processes of trimline formation and preservation. The use of the new trimline expression classification scheme and the detailed analysis of the trimlines in central western Spitsbergen has already provided some hints about the formation of glacial trimlines, particularly in finding that glaciological factors appear to have a much stronger influence than geological or topographic variables. This goes against some previous research, which has suggested that geology is an important constraint over the formation, preservation and expression of glacial trimlines in other areas (e.g. Kelly *et al.* 2004 in the European Alps).

The links identified between glaciological variables, such as glacier type, and the expression of glacial trimlines may open up new potential for extracting information about glacier behaviour from trimlines, making them more useful than simply as markers of palaeo ice margin positions or estimates of palaeo ice thickness. Of particular note is the potential for glacial trimlines to be added to the diagnostic landform assemblage used to identify possible surge-type glaciers. This could enable trimlines to assist in the identification of surge-type glaciers in Quaternary settings, where glacier surging is often harder to diagnose. Targeted research into the trimlines of surge-type glaciers in a range of glacial environments, particularly regions containing temperate surging glaciers, is now required to further tease apart the links between surging behaviour and trimline expression. Further research in to trimline formation and preservation in a wider range of glaciological, geological, and climatic settings is also recommended to build on the results of this thesis and develop a deeper understanding of the factors influencing trimline formation, preservation and expression and whether these differ in different areas.

The successful classification of trimline expressions in central western Spitsbergen suggests that this scheme should now be used as a regular component of trimline identification and analysis. In particular, the classification scheme should be applied to Quaternary glacial environments, where there are no extant glaciers. This setting is likely to produce a different array of trimline expressions to those of central western Spitsbergen and this will test the

universality of the classification scheme. Use of environmental dating in conjunction with the classification scheme is also recommended in order to identify examples of invisible trimlines and confirm the existence of this type of trimline expression (Chapter 3). These features were not discernible in the case study presented in this thesis because they are not associated with visible landforms or surface contrasts but are marked by invisible boundaries in surface exposure age, which could potentially be identified by strategic sampling of slope profiles using environmental dating. Additionally, the use of environmental dating in conjunction with the trimline expression classification scheme may resolve the issue of trimline fragmentation identified in Chapter 4, for which a better understanding of trimline formation and preservation is required.

7.1.2 Trimlines in palaeoglacial reconstructions

A 3D reconstruction of the Little Ice Age (LIA) glacial extent in central western Spitsbergen was produced utilising the advances to trimline identification, mapping, and interpretation presented in this thesis (Chapter 5; Chapter 6). Following the mapping and analysis of glacial trimlines in the study area (Chapter 4), the trimlines were relatively dated to identify those most likely to be LIA in origin and a smaller sample of 15 glaciers were selected for the reconstruction (Chapter 5). The trimlines were then used to produce continuous LIA ice margins using 'by eye' interpolation to connect the trimline features (Chapter 5). The GlaRe toolbox produced by Pellitero *et al.* (2016) was used to produce the 3D reconstructions, constrained by the LIA ice margins and by basal shear stress values produced using the glacial trimlines as a constraint over the ice thickness (Chapter 5). The GlaRe method is a relatively new tool for inverting ice margins produced from glacial geomorphological evidence into 3D palaeoglacial reconstructions using ArcGIS software. The 3D reconstruction in this thesis is a demonstration of the use of the toolbox, as well as being the first time it has been used alongside glacial trimlines (Chapter 5). Developing a clear method for the use of trimlines and GlaRe together could enable more widespread use of trimline features in 3D palaeoglacial reconstructions. In particular, by utilising the trimlines both as ice margin constraints and in the production of basal shear stress values this thesis has demonstrated a method for extracting the maximum empirical evidence from these landforms, enabling better constraint of the 3D palaeoglacial reconstructions produced.

The reconstruction of LIA glaciers in central western Spitsbergen also produced new information about the local LIA maximum extent and the subsequent retreat to the modern glacier positions. The glaciers in this area of central western Spitsbergen have been found to

have lost a total of 17.50 km^2 in area (24% of the total LIA glacierised area) and 1.85 km^3 of ice volume (28% of the LIA total ice volume) since the LIA maximum extent. A surprising finding was that, despite this overall pattern of ice loss and retreat, the behaviour of individual glaciers has been highly variable in terms of the percentage of the LIA ice volume that has been lost (Figure 7.2; Chapter 6). Analysis of the responses of individual glaciers to the post-LIA climate change suggests that valley-scale topographic factors have an important influence over the responses of glaciers in rugged terrain. Changes in confluence between glaciers were also found to be particularly important for the glaciers that have separated from their neighbours during the retreat from their LIA maximum positions. These findings highlight the importance of reconstructing individual glaciers, where sufficient geomorphological evidence is available, and stress the potential for inaccurate reconstructions to be produced when interpolating between spatially disparate sets of geomorphological features in rugged terrain. The variability between the glaciers of central western Spitsbergen suggests that interpolation across large gaps in the geomorphological record and extrapolation of glacier responses across neighbouring valleys may introduce substantial uncertainty to a reconstruction of local glacial responses to a given climate change (Chapter 6).

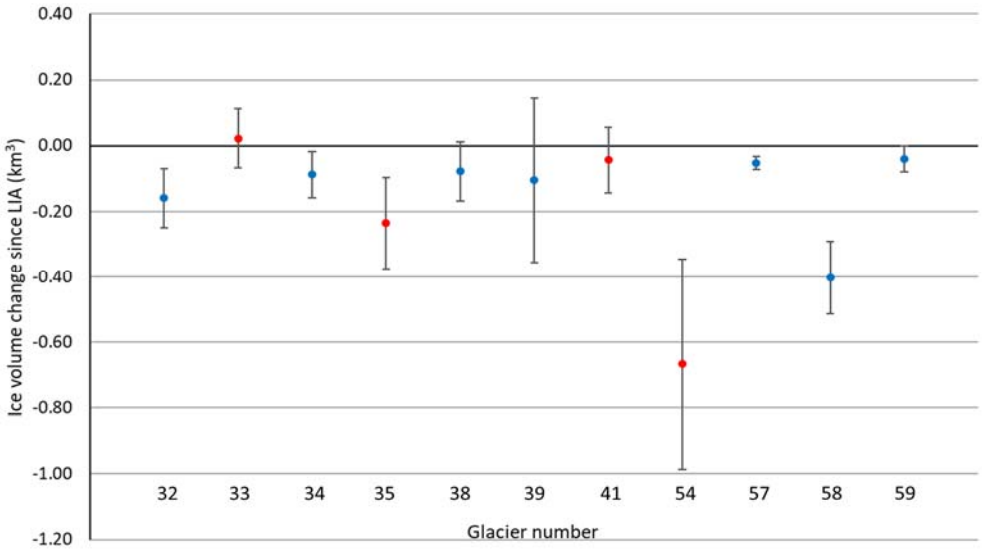

Figure 7.2 – The responses of glaciers in central western Spitsbergen to the post-LIA climate change have been highly variable. The volume changes produced by comparing the 3D LIA reconstructions with the modern glaciers are shown alongside the associated error bars. The four surging glaciers in the reconstruction study area are marked in red. These are amongst the most extreme responses but excluding the surging glaciers still shows a wide variety of responses. This is particularly true when considering the change as a percentage of the LIA ice volume, with a range of changes from -51% to +6% including the surging glaciers and -51% to -17% excluding the surging glaciers. Note that the four tidewater glaciers are not shown in this graph because it was not possible to compute reliable error bars for these glaciers (Chapter 5; Chapter 6).

Glaciology and palaeoglaciology make frequent use of relatively well studied 'type glaciers', the behaviour and responses of which are extrapolated over potentially large areas deemed to contain similar glaciers. The high levels of variability in the responses and behaviour of the glaciers of central western Spitsbergen suggests that the use of type glaciers to study the response of the glaciers in this area would not be appropriate. Consideration of the responses of the individual glaciers in central western Spitsbergen suggests that the variability identified is not primarily caused by the presence of surge-type glaciers but is rather due to valley-scale topographic factors (Figure 7.2; Chapter 6). This indicates that this level of variability in individual glacier responses may well be relatively common in other areas of rugged terrain (e.g. Koffman *et al.* 2017) and may not be confined to areas with surge-type glaciers, such as Svalbard. If this is the case then the use of type glaciers may be introducing uncertainty into research in a wide range of rugged terrain settings, both historic and Quaternary. It is, therefore, important that more 3D palaeoglacial reconstructions at the scale of individual glaciers are produced, for which continued improvements in the use of glacial trimlines are required, so that the variability in responses between glaciers can be further studied and better taken into account.

7.1.3 Improving interpolation between fragmentary geomorphological evidence

In addition to better use of glacial trimlines, improving methods for interpolation between disparate glacial geomorphological features, such as trimlines but also including other types of glacial features, is an area of palaeoglaciology that could improve the accuracy and reliability of 3D palaeoglacial reconstructions. Attempts at standardising the common but also very subjective 'by eye' method of interpolation have been presented in this thesis, focusing around utilising the angles made where the ice margin abuts the valley side topographic contours (Chapter 2). It was hypothesised that researchers were unconsciously using an understanding of the way in which the morphology of the valley affects the form of the ice margin when interpolating 'by eye', which might be quantifiable by considering these 'contour angles'. However, it has not proved possible to produce a robust rule for the pattern of contour angles from the snout to the headwall of a glacier, which was needed to guide interpolation and reduce the subjectivity of the 'by eye' method. A key factor has been the significant levels of variability within the contour angles measured, which has prevented the identification of a clear pattern or trend between glaciers (Chapter 2). Nonetheless, it was possible to identify links between the pattern of contour angles and the presence of larger-scale features of the valley topography, such as truncated spurs and bedrock steps. This

suggests that further exploration of contour angles may enable more confident interpolation of ice margins in rugged terrain, where these topographic features are common.

Use of a much larger sample of glaciers across different glaciological and climatic settings may improve on the findings presented in this thesis, allowing for a robust contour angle trend to emerge, despite the variability of individual glaciers, and facilitating the use of contour angles to guide interpolation around valley-scale topographic features. However, this study was not able to produce accurate measurements of contour angles without manual steps that were deemed too subjective to yield meaningful and reliable outputs, preventing the collection of a large enough data set of contour angles. The contour angles approach to improving interpolation is still thought to be potentially useful and developing on the work presented in Chapter 2 is commended to others for further investigation. On-going improvements in computer technology and GIS software may resolve the issues that led to this work being discontinued for the purpose of this thesis. In particular, developments in machine learning may well facilitate quicker and more reliable automated computation of contour angles, enabling a large enough sample of glaciers to be measured for a robust rule to become apparent.

7.1.4 Overall summary and conclusions

In summary, this thesis has achieved its overall aim of improving the reconstruction of palaeo ice margins in rugged terrain, primarily by advancing understandings of glacial trimlines and demonstrating best practice for using these features in 3D palaeoglacial reconstructions. It has not proved possible to adequately improve on the subjective 'by eye' method of ice margin interpolation, but the approaches trialled in this study may enable others to work on this problem. Glacial trimlines have previously been under-used in palaeoglaciology and this thesis has provided new methods for identifying, mapping, interpreting, and utilising glacial trimlines in 3D palaeoglacial reconstructions. A new terminology and classification system for the expression of glacial trimlines has facilitated study into the formation and preservation of trimlines, leading to the identification of potential relationships between glacier type and trimline expression. A demonstration of the use of glacial trimlines in the 3D reconstruction of the LIA maximum extent in central western Spitsbergen also yielded new information about the retreat of the local glaciers to their modern positions. The large variability in the ice volume lost by individual glaciers responding to the same climate forcing highlights the need for numerous and detailed 3D palaeoglacial reconstructions and calls in

to question the use of type glaciers and the extrapolation of glacier responses from one glacier to another.

7.2 Implications for palaeoglaciology

The implications for palaeoglaciology of the improvements made by this thesis will now be discussed in greater detail and suggestions for further research identified.

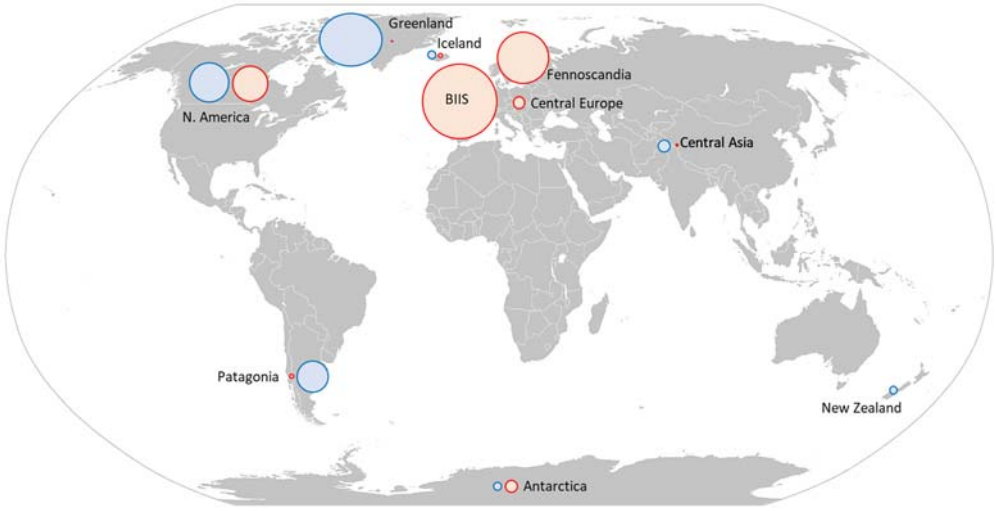

Figure 7.3 – Trimlines have been identified in a wide range of glacial environments within the existing literature but have rarely been studied in detail or used to constrain 3D palaeoglacial reconstructions. The size of the circles on this map indicates the number of papers mentioning trimlines in each location, with red circles indicating Quaternary trimlines and blue historic trimlines. The confirmed presence of trimlines in most historic and Quaternary glacial settings suggests that these landforms can be considered both widespread and common, indicating that much greater use of these features may be possible than is currently the case. Additionally, it is highly likely that trimlines will be identified in more areas now that a better system of trimline terminology and recommended procedures for mapping and identifying these features exist. Background map from Wikipedia Commons (file name: BlankMap-World6.svg).

Figure 7.3 shows the widespread global distribution of reported glacial trimlines (Chapter 3). This map includes only trimlines specifically mentioned in the existing literature, so this should be considered a minimum potential distribution of these features. Informal investigation by the author suggests that perhaps only 40-50% of all trimlines globally are currently known, i.e. have been identified, but only around 10-20% have been studied in any detail or used to constrain 3D palaeoglacial reconstructions. Therefore, there is a large potential for further research into glacial trimlines, particularly given the marked clustering

of previous trimline research in North-West Europe and North America (Figure 7.3). Examples of previously unidentified and unstudied trimlines in new areas are easy to find using readily available tools, such as Google Earth, and some examples are given in Figure 7.4. Suggestions for potentially fruitful study areas for future trimlines research include but are not limited to: the YD in Scotland; LGM in the European Alps; LGM in the Torngat mountains of Canada; and recent ice margin fluctuations in the Karakorum (e.g. Figure 7.4).

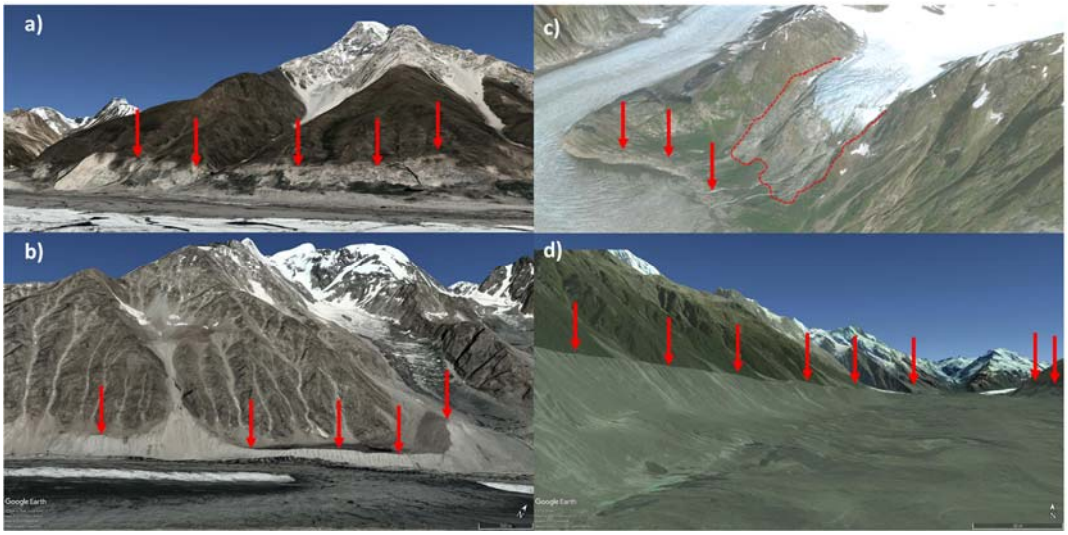

Figure 7.4 – These images contain examples of previously unrecognised trimlines (marked by red arrows) that have not been studied scientifically. a) and b) are trimlines associated with the debris-covered Pasu glacier in the Karakorum, Pakistan. The trimline in a) appears to be a surface aging contrast, marked by a distinction in the vegetation cover, whilst b) could be a contrast in glacier deposition, with some sections that appear to be lateral moraines, but could also be an erosional step. In c) an unnamed glacier in Alaska (Lat. 57.6224° Long. -132.9562°) has a surface aging/ erosional contrast trimline along the main trunk glacier, with a smaller nearby glacier's former ice margin marked by an almost continuous surface aging trimline (red dotted line). d) shows a clear lateral moraine trimline along the side of the Tasman Glacier, New Zealand. There is also a smaller surface aging/ erosional contrast on the opposite side of the glacier. Like the Pasu glacier (a and b), the Tasman glacier (d) is debris-covered and the glacial trimlines of this type of glacier have received little or no detailed study in the literature to date. All images from Google Earth and sourced from: a) Landsat/ Copernicus ©CNES/ Airbus; b) Landsat/ Copernicus ©CNES/ Airbus and ©DigitalGlobe; c) ©DigitalGlobe; d) Landsat/ Copernicus ©CNES/ Airbus and ©DigitalGlobe.

The improvements from this thesis may encourage more widespread use to be made of these very common landforms, enabling trimlines to be better utilised where they have already been identified and assisting in the identification and mapping of trimline features in new areas (e.g. Figure 7.4). Applying the trimline expression classification scheme outside of Svalbard will enable further study into the factors affecting trimline formation and preservation in a wider range of glacial environments. Better understanding of the formation and preservation of glacial trimlines will aid in their interpretation and may confirm the relationship identified in this thesis between glacier type and trimline expression. More spatially extensive use of trimlines in 3D palaeoglacial reconstructions can also now progress using the methodology for combining trimlines with the GlaRe toolbox, opening up new areas for detailed 3D reconstructions that may shed more light on the role of topography in controlling the response of individual glaciers in rugged terrain.

As well as being widespread spatially, trimlines have also been found to be associated with a range of temporal periods (Chapter 3). The majority of trimline research has so far focused on Quaternary trimlines, particularly those associated with the Last Glacial Maximum (LGM) and the Younger Dryas (YD) (Chapter 3), but historic trimlines associated with Holocene glacier fluctuations have also been identified, such as the Little Ice Age (LIA) trimlines of central western Spitsbergen. The relative lack of robustly dated trimline features in the literature makes it hard to define the best glacial periods for trimline research to focus on and means that it is not known if the trimlines in many areas are associated with older or younger glacial events than the LGM or LIA respectively. This study has focused on the historic LIA trimlines of central western Spitsbergen, partially because of the relatively under-studied nature of historic trimlines, but it is hypothesised that many of the methods and conclusions produced from this case study will be applicable in other areas and for trimlines associated with other glacial events. Further research is required to test this hypothesis and particularly to test the classification of trimline expressions in Quaternary settings.

Research building on the initial study of trimline formation and preservation presented in this thesis may also facilitate better relative dating of trimlines. More widespread use of environmental dating techniques applied to glacial trimlines is also highly recommended and may reveal more information about trimline formation, as has already been the case in Britain and Ireland (Ballantyne 2010; Fabel *et al.* 2012; McCarroll 2016; Chapter 3). Further studies combining the new trimline expression classification scheme with the use of environmental dating of trimline features are highly recommended to further examine the

links between trimline expression, formation, and preservation, particularly confirming which modes of trimline expression are most likely to be subglacial in origin. Development of dating methods or sampling strategies targeted specifically at glacial trimlines will be important for this research and could enable robust identification of invisible trimlines.

The use of trimlines to constrain basal shear stress, as demonstrated in the production of the 3D reconstruction of the LIA glaciers in central western Spitsbergen, will be most effective where trimlines exist in both the accumulation and ablation areas. However, where trimlines are present only in the ablation area of the palaeo glacier, this thesis has shown that basal shear stress values based on the modern ice surface in the accumulation area and values derived from the trimlines in the ablation area can produce successful reconstructions (e.g. Figure 7.1; Chapter 5). These methods will enable better constraint of basal shear stress in other historic settings, where both trimlines and modern glaciers are present. In Quaternary settings, constraining the basal shear stress with trimlines will be possible using the same methods but this may provide unrealistic ice thickness where trimlines are only present in the ablation area of the former ice mass. However, it is hypothesised that use of trimlines in conjunction with the C-values method of Ng *et al.* (2010) could enable improved constraint of basal shear stress in 3D reconstruction, with basal shear stress values constrained by the empirical trimline evidence in the ablation area and the C-value derived ice surface in the accumulation area.

Glacial trimlines are important landforms for reducing the need for interpolation and hence limiting uncertainty in ice margin reconstructions in rugged terrain. Discoveries made by this thesis about the links between trimline expression and glaciological variables, particularly glacier type, may allow future trimline research to provide more information about the behaviour of palaeo glaciers. The case study of central western Spitsbergen has additionally demonstrated the use of these features to help to identify the influence of valley-scale topography and palaeo-confluence on the response of individual glaciers to a given climate forcing. These findings should now be built upon to expand the usage of glacial trimlines in the production of palaeo ice margins and in the interpretation of the impact of local topography and palaeo-confluence on the fluctuations of glaciers.

Bibliography

Ackert, R. P., Mukhopadhyay, S., Parizek, B. R. & Borns, H. W. (2007). Ice Elevation near the West Antarctic Ice Sheet Divide during the Last Glaciation. *Geophysical Research Letters*, 34(21).

Ackert, R. P., Mukhopadhyay, S., Pollard, D., DeConto, R. M., Putnam, A. E. & Borns, H. W. (2011). West Antarctic Ice Sheet Elevations in the Ohio Range: Geologic Constraints and Ice Sheet Modeling prior to the Last Highstand. *Earth and Planetary Science Letters*, 307(1), 83–93.

Ahlmann, H. W. (1919). *Geomorphological Studies in Norway*. Svenska sällskapet för antropologi och geografi.

Anderson, F. W. & Dunham, K. C. (1966). *The Geology of Northern Skye: FW Anderson and KC Dunham*. HM Stationery Office.

Anderson, R. S. (2002). Modeling the Tor-Dotted Crests, Bedrock Edges, and Parabolic Profiles of High Alpine Surfaces of the Wind River Range, Wyoming. *Geomorphology*, 46(1), 35–58.

Anderson, R. S., Dühnforth, M., Colgan, W. & Anderson, L. (2012). Far-Flung Moraines: Exploring the Feedback of Glacial Erosion on the Evolution of Glacier Length. *Geomorphology*. 179, 269–285

Armienti, P. & Baroni, C. (1999). Cenozoic Climatic Change in Antarctica Recorded by Volcanic Activity and Landscape Evolution. *Geology*, 27(7), 617–620.

Aylsworth, J. M. & Shilts, W. (1989a). Glacial Features around the Keewatin Ice Divide: Districts of Mackenzie and Keewatin. Geological Survey of Canada Paper 88-24.

Aylsworth, J. & Shilts, W. (1989b). Bedforms of the Keewatin Ice Sheet, Canada. *Sedimentary Geology*, 62(2), 407–428.

Ballantyne, C. K. (1984). The Late Devensian Periglaciation of Upland Scotland. *Quaternary Science Reviews*, 3(4), 311–343.

Ballantyne, C. K. (1987). Wester Ross: Field Guide, in: Quaternary Research Association.

Ballantyne, C. K. (1989). The Loch Lomond Readvance on the Isle of Skye, Scotland: Glacier Reconstruction and Palaeoclimatic Implications. *Journal of Quaternary Science*, 4(2), 95–108.

Ballantyne, C. K. (1990). The Late Quaternary Glacial History of the Trotternish Escarpment, Isle of Skye, Scotland, and Its Implications for Ice-Sheet Reconstruction. *Proceedings of the Geologists' Association*, 101(3), 171–186.

Ballantyne, C. K. (1994b). Gibbsitic Soils on Former Nunataks: Implications for Ice Sheet Reconstruction. *Journal of Quaternary Science*, 9(1), 73–80.

Ballantyne, C. K. (1994a). Scottish Landform examples—10: The Tors of the Cairngorms. *The Scottish Geographical Magazine*, 110(1), 54–59.

Ballantyne, C. K. (1997). Periglacial Trimlines in the Scottish Highlands. *Quaternary International*, 38, 119–136.

Ballantyne, C. K. (1998). Age and Significance of Mountain-Top Detritus. *Permafrost and Periglacial Processes*, 9(4), 327–345.

Ballantyne, C. K. (1999b). A Late Devensian Nunatak on the Knoydart Peninsula, NW Scotland: Implications for Ice-Sheet Reconstruction. *The Scottish Geographical Magazine*, 115(4), 319–328.

Ballantyne, C. K. (1999a). An Teallach: A Late Devensian Nunatak in Wester Ross. *The Scottish Geographical Magazine*, 115(3), 249–259.

Ballantyne, C. K. (2002). The Loch Lomond Readvance on the Isle of Mull, Scotland: Glacier Reconstruction and Palaeoclimatic Implications. *Journal of Quaternary Science*, 17(8), 759–771.

Ballantyne, C. K. (2007). Loch Lomond Stadial Glaciers in North Harris, Outer Hebrides, North-West Scotland: Glacier Reconstruction and Palaeoclimatic Implications. *Quaternary Science Reviews*, 26(25), 3134–3149.

Ballantyne, C. K. (2010). Extent and Deglacial Chronology of the Last British-Irish Ice Sheet: Implications of Exposure Dating Using Cosmogenic Isotopes. *Journal of Quaternary Science*, 25(4), 515–534.

Ballantyne, C. K. & Hall, A. M. (2008). The Altitude of the Last Ice Sheet in Caithness and East Sutherland, Northern Scotland. *Scottish Journal of Geology*, 44(2), 169.

Ballantyne, C. K. & Hallam, G. E. (2001). Maximum Altitude of Late Devensian Glaciation on South Uist, Outer Hebrides, Scotland. *Proceedings of the Geologists' Association*, 112(2), 155–167.

Ballantyne, C. K. & McCarroll, D. (1997). Maximum Altitude of the Late Devensian Ice Sheet on the Isle of Rum. *Scottish Journal of Geology*, 33(2), 183–186.

Ballantyne, C. K., McCarroll, D., Nesje, A. & Dahl, S. O. (1997). Periglacial Trimlines, Former Nunataks and the Altitude of the Last Ice Sheet in Wester Ross, Northwest Scotland. *Journal of Quaternary Science*, 12(3), 225–238.

Ballantyne, C. K., McCarroll, D., Nesje, A., Dahl, S. O. & Stone, J. O. (1998). The Last Ice Sheet in North-West Scotland: Reconstruction and Implications. *Quaternary Science Reviews*, 17(12), 1149–1184.

Ballantyne, C. K., McCarroll, D., Nesje, A., Dahl, S. O., Stone, J. O. & Fifield, L. K. (1998). High-Resolution Reconstruction of the Last Ice Sheet in NW Scotland. *Terra Nova*, 10, 63–67.

Ballantyne, C. K., McCarroll, D. & Stone, J. O. (2006). Vertical Dimensions and Age of the Wicklow Mountains Ice Dome, Eastern Ireland, and Implications for the Extent of the Last Irish Ice Sheet. *Quaternary Science Reviews*, 25(17), 2048–2058.

Ballantyne, C. K., McCarroll, D. & Stone, J. O. (2007). The Donegal Ice Dome, Northwest Ireland: Dimensions and Chronology. *Journal of Quaternary Science*, 22(8), 773–783.

Ballantyne, C. K., McCarroll, D. & Stone, J. O. (2011). Periglacial Trimlines and the Extent of the Kerry-Cork Ice Cap, SW Ireland. *Quaternary Science Reviews*, 30(27), 3834–3845.

Ballantyne, C. K. & Stone, J. O. (2015). Trimlines, Blockfields and the Vertical Extent of the Last Ice Sheet in Southern Ireland. *Boreas*.

Ballantyne, C. K., Stone, J. O. & Fifield, L. K. (2009). Glaciation and Deglaciation of the SW Lake District, England: Implications of Cosmogenic 36Cl Exposure Dating. *Proceedings of the Geologists' Association*, 120(2), 139–144.

Ballantyne, C. K., Stone, J. O. & McCarroll, D. (2008). Dimensions and Chronology of the Last Ice Sheet in Western Ireland. *Quaternary Science Reviews*, 27(3), 185–200.

Bamber, J. L., Krabill, W., Raper, V., Dowdeswell, J. A. & Oerlemans, J. (2005). Elevation Changes Measured on Svalbard Glaciers and Ice Caps from Airborne Laser Data. *Annals of Glaciology*, 42(1), 202–208.

Baroni, C., Fasano, F., Giorgetti, G., Salvatore, M. C. & Ribecai, C. (2008). The Ricker Hills Tillite Provides Evidence of Oligocene Warm-Based Glaciation in Victoria Land, Antarctica. *Global and Planetary Change*, 60(3), 457–470.

Barr, I. D. & Lovell, H. (2014). A Review of Topographic Controls on Moraine Distribution. *Geomorphology*, 226, 44–64.

Barth, A.M., Clark, P.U., Clark, J., Marshall McCabe, A. & Caffee, M. (2016). Last Glacial Maximum cirque glaciation in Ireland and implications for reconstructions of the Irish Ice Sheet. *Quaternary Science Reviews*, 141, 85–93.

Beason, S. R. (2017). *Change in glacial extent at Mount Rainier National Park from 1896 to 2015*. Natural Resource Report NPS/MORA/NRR—2017/1472. National Park Service, Fort Collins, Colorado.

Van der Beek, P. & Bourbon, P. (2008). A Quantification of the Glacial Imprint on Relief Development in the French Western Alps. *Geomorphology*, 97(1), 52–72.

Benn, D. I. & Ballantyne, C. K. (2005). Palaeoclimatic Reconstruction from Loch Lomond Readvance Glaciers in the West Drumochter Hills, Scotland. *Journal of Quaternary Science*, 20(6), 577–592.

Benn, D. I. & Evans, D. J. (2010). *Glaciers and Glaciation.* Hodder Education.

Benn, D. I. & Hulton, N. R. (2010). An Excel TM Spreadsheet Program for Reconstructing the Surface Profile of Former Mountain Glaciers and Ice Caps. *Computers & Geosciences*, 36(5), 605–610.

Bennett, M. R. (1994). Morphological Evidence as a Guide to Deglaciation Following the Loch Lomond Readvance: A Review of Research Approaches and Models. *The Scottish Geographical Magazine*, 110(1), 24–32.

Bennett, M. R. (2001). The Morphology, Structural Evolution and Significance of Push Moraines. *Earth-Science Reviews*, 53(3), 197–236.

Bentley, M. J., Fogwill, C. J., Kubik, P. W. & Sugden, D. E. (2006). Geomorphological Evidence and Cosmogenic 10Be/26Al Exposure Ages for the Last Glacial Maximum and Deglaciation of the Antarctic Peninsula Ice Sheet. *Geological Society of America Bulletin*, 118(9-10), 1149–1159.

Bickerdike, H. L., Evans, D. J. A., Ó Cofaigh, C. & Stokes, C. R. (2016). The glacial geomorphology of the Loch Lomond Stadial in Britain: a map and geographic information system resource of published evidence. *Journal of Maps*, 12(5), 1178–1186.

Bierman, P. R., Davis, P. T., Corbett, L. B., Lifton, N. A. & Finkel, R. C. (2015). Cold-Based Laurentide Ice Covered New England's Highest Summits during the Last Glacial Maximum. *Geology*, 43(12), 1059–1062.

Bierman, P. R., Marsella, K. A., Patterson, C., Davis, P. T. & Caffee, M. (1999). Mid-Pleistocene Cosmogenic Minimum-Age Limits for Pre-Wisconsinan Glacial Surfaces in Southwestern Minnesota and Southern Baffin Island: A Multiple Nuclide Approach. *Geomorphology*, 27(1), 25–39.

Bingham, R. G., King, E. C., Smith, A. M. & Pritchard, H. D. (2010). Glacial Geomorphology: Towards a Convergence of Glaciology and Geomorphology. *Progress in Physical Geography*, 34(3), 327–355.

Blomdin, R., Heyman, J., Stroeven, A. P., Hättestrand, C., Harbor, J. M., Gribenski, N., Jansson, K. N., Petrakov, D. A., Ivanov, M. N., Alexander, O., Rudoy, A. N., & Walther, M. (2016). Glacial Geomorphology of the Altai and Western Sayan Mountains, Central Asia. *Journal of Maps*, 12(1), 123–136.

Blytt, A. (1876). Immigration of the Norwegian Flora. *Alb. Cammermeyer, Christiania*.

Boulton, G. & Hagdorn, M. (2006). Glaciology of the British Isles Ice Sheet during the Last Glacial Cycle: Form, Flow, Streams and Lobes. *Quaternary Science Reviews*, 25(23), 3359–3390.

Boulton, G. & Jones, A. (1979). Stability of Temperate Ice Caps and Ice Sheets Resting on Beds of Deformable Sediment. *Journal of Glaciology*, 24, 29–43.

Boulton, G., Jones, A., Clayton, K. & Kenning, M. (1977). A British Ice-Sheet Model and Patterns of Glacial Erosion and Deposition in Britain. *British Quaternary Studies*, 231–246.

Boulton, G., Peacock, J. & Sutherland, D. (1991). Quaternary. *Geology of Scotland*, 3, 503–543.

Bowen, D., Phillips, F., McCabe, A., Knutz, P. & Sykes, G. (2002). New Data for the Last Glacial Maximum in Great Britain and Ireland. *Quaternary Science Reviews*, 21(1), 89–101.

Bowen, D., Rose, J., McCabe, A. & Sutherland, D. (1986). Correlation of Quaternary Glaciations in England, Ireland, Scotland and Wales. *Quaternary Science Reviews*, 5, 299–340.

Boyer, S. J. & Pheasant, D. R. (1974). Delimitation of Weathering Zones in the Fiord Area of Eastern Baffin Island, Canada. *Geological Society of America Bulletin*, 85(5), 805–810.

Bradwell, T., Stoker, M. S., Golledge, N. R., Wilson, C. K., Merritt, J. W., Long, D., Everest, J. D., Hestvik, O. B., Stevenson, A. G., Hubbard, A. L., Finlayson, A. G., & Mathers, H. E. (2008). The Northern Sector of the Last British Ice Sheet: Maximum Extent and Demise. *Earth Science Reviews*, 88(3), 207–226.

Braithwaite, R.J. & Raper, S.C.B. (2007). Glaciological conditions in seven contrasting regions estimated with the degree-day model. *Annals of Glaciology,* 46(1), 297–302.

Braithwaite, R.J. & Raper, S.C.B., (2009). Estimating equilibrium-line altitude (ELA) from glacier inventory data. *Annals of Glaciology,* 50(53), 127–132.

Briner, J., Miller, G., Davis, P. T., Bierman, P. & Caffee, M. (2003). Last Glacial Maximum Ice Sheet Dynamics in Arctic Canada Inferred from Young Erratics Perched on Ancient Tors. *Quaternary Science Reviews*, 22(5), 437–444.

Briner, J. P., Gosse, J. C. & Bierman, P. R. (2006). Applications of Cosmogenic Nuclides to Laurentide Ice Sheet History and Dynamics. *Geological Society of America Special Papers*, 415, 29–41.

Briner, J. P., Miller, G. H., Davis, P. T. & Finkel, R. C. (2005). Cosmogenic Exposure Dating in Arctic Glacial Landscapes: Implications for the Glacial History of Northeastern Baffin Island, Arctic Canada. *Canadian Journal of Earth Sciences*, 42(1), 67–84.

Briner, J. P., Miller, G. H., Davis, P. T. & Finkel, R. C. (2006). Cosmogenic Radionuclides from Fiord Landscapes Support Differential Erosion by Overriding Ice Sheets. *Geological Society of America Bulletin*, 118(3-4), 406–420.

Briner, J. P. & Swanson, T. W. (1998). Using Inherited Cosmogenic 36Cl to Constrain Glacial Erosion Rates of the Cordilleran Ice Sheet. *Geology*, 26(1), 3–6.

Brook, E. J., Nesje, A., Lehman, S. J., Raisbeck, G. M. & Yiou, F. (1996). Cosmogenic Nuclide Exposure Ages along a Vertical Transect in Western Norway: Implications for the Height of the Fennoscandian Ice Sheet. *Geology*, 24(3), 207–210.

Brooks, A. J., Bradley, S. L., Edwards, R. J., Milne, G. A., Horton, B. & Shennan, I. (2008). Postglacial Relative Sea-Level Observations from Ireland and Their Role in Glacial Rebound Modelling. *Journal of Quaternary Science*, 23(2), 175–192.

Brown, V. H., Evans, D. J., Vieli, A. & Evans, I. S. (2013). The Younger Dryas in the English Lake District: Reconciling Geomorphological Evidence with Numerical Model Outputs. *Boreas*.

Bruno, L. A., Baur, H., Graf, T., Schlu, C., Signer, P., Wieler, R. (1997). Dating of Sirius Group Tillites in the Antarctic Dry Valleys with Cosmogenic 3 He and 21 Ne. *Earth and Planetary Science Letters*, 147(1), 37–54.

Brunsden, D. (1993). The Persistence of Landforms. *Zeitschrift für Geomorphologie*, 93, 13–28.

Brynjólfsson, S. S. A. & Ingólfsson, Ó. (2014). Geomorphology and the Little Ice Age Extent of the Drangajökull Ice Cap, NW Iceland, with Focus on Its Three Surge-Type Outlets. *Geomorphology*, 213, 292–304.

Bursik, M. (1991). Relative Dating of Moraines Based on Landform Degradation, Lee Vining Canyon, California. *Quaternary Research*, 35(3), 451–455.

Carisio, S. P. (2012). *Evaluating areal errors in Northern Cascade Glacier inventories*. M.S. Geography Thesis, University of Delaware.

Carr, S. J., Lukas, S. & Mills, S. C. (2010). Glacier Reconstruction and Mass-Balance Modelling as a Geomorphic and Palaeoclimatic Tool. *Earth Surface Processes and Landforms*, 35(9), 1103–1115.

Carrivick, J. L., Davies, B. J., Glasser, N. F., Nývlt, D. & Hambrey, M. J. (2012). Late-Holocene Changes in Character and Behaviour of Land-Terminating Glaciers on James Ross Island, Antarctica. *Journal of Glaciology*, 58(212), 1176–1190.

Charlesworth, J. K. (1921). *The Glacial Geology of the North-West of Ireland*, In: Proceedings of the Royal Irish Academy. Section B: Biological, Geological, and Chemical Science, 174–314.

Charlesworth, J. K. (1955). XIX.—The Late-Glacial History of the Highlands and Islands of Scotland. *Transactions of the Royal Society of Edinburgh*, 62(3), 769–928.

Chiverrell, R. C. & Thomas, G. S. (2010). Extent and Timing of the Last Glacial Maximum (LGM) in Britain and Ireland: A Review. *Journal of Quaternary Science*, 25(4), 535–549.

Christoffersen, P., Piotrowski, J.A. & Larsen, N.K. (2005). Basal processes beneath an Arctic glacier and their geomorphic imprint after a surge, Elisebreen, Svalbard. *Quaternary Research*, 64(2), 125–137.

Clarhäll, A. & Kleman, J. (1999). Distribution and Glaciological Implications of Relict Surfaces on the Ultevis Plateau, Northwestern Sweden. *Annals of Glaciology*, 28(1), 202–208.

Clark, C. D. (1993). Mega-Scale Glacial Lineations and Cross-Cutting Ice-Flow Landforms. *Earth Surface Processes and Landforms*, 18(1), 1–29.

Clark, C. D. (1997). Reconstructing the Evolutionary Dynamics of Former Ice Sheets Using Multi-Temporal Evidence, Remote Sensing and GIS. *Quaternary Science Reviews*, 16(9), 1067–1092.

Clark, C. D., Evans, D. J., Khatwa, A., Bradwell, T., Jordon, C. J., Marsh, S. H., Mitchell, W. A. & Bateman, M. D. (2004). Map and GIS Database of Glacial Landforms and Features Related to the Last British Ice Sheet. *Boreas*, 33(4), 359–375.

Clark, C. D., Hughes, A. L., Greenwood, S. L., Jordan, C. & Sejrup, H. P. (2012). Pattern and Timing of Retreat of the Last British-Irish Ice Sheet. *Quaternary Science Reviews*, 44, 112–146.

Clark, C. D., Ely, J. C., Greenwood, S. L., Hughes, A. L. C., Meehan, R., Barr, I. D., Bateman, M. D., Bradwell, T., Doole, J., Evans, D. J. A., Jordan, C. J., Monteys, X., Pellicer, X. M. & Sheehy, M. (2018). BRITICE Glacial Map, version 2: a map and GIS database of glacial landforms of the last British–Irish Ice Sheet. *Boreas*, 47, 11–27.

Clark, P. U. (1988). Glacial Geology of the Torngat Mountains, Labrador. *Canadian Journal of Earth Sciences*, 25(8), 1184–1198.

Clark, P. U. (1991). Landscapes of Glacial Erosion, Torngat Mountains, Northern Labrador/Ungava. *The Canadian Geographer/Le Géographe canadien*, 35(2), 208–213.

Clark, P. U., Brook, E. J., Raisbeck, G. M., Yiou, F. & Clark, J. (2003). Cosmogenic 10Be Ages of the Saglek Moraines, Torngat Mountains, Labrador. *Geology*, 31(7), 617–620.

Cockburn, H. A. & Summerfield, M. A. (2004). Geomorphological Applications of Cosmogenic Isotope Analysis. *Progress in Physical Geography*, 28(1), 1–42.

Cogley, J. G. & McIntyre, M. (2003). Hess Altitudes and Other Morphological Estimators of Glacier Equilibrium Lines. *Arctic, Antarctic, and Alpine Research*, 35(4), 482–488.

Csatho, B. M., Van Der Veen, C. J. & Tremper, C. M. (2005). Trimline Mapping from Multispectral Landsat ETM+ Imagery. *Géographie physique et Quaternaire*, 59(1), 49–62.

Csatho, B., Schenk, T., Van Der Veen, C. J. & Krabill, W. B. (2008). Intermittent Thinning of Jakobshavn Isbrae, West Greenland, since the Little Ice Age. *Journal of Glaciology*, 54(184), 131–144.

Cuffey, K.M. & Paterson, W.S.B., (2010). *The physics of glaciers*. Academic Press.

Dahl, E. (1948). Studier over Forvitringstyper I Strøket Nordfjord-Sunnmøre, Og Deres Relasjon Til Istidene. *Norsk Geologisk Tidsskrift*, 27, 242–244.

Dahl, E. (1955). Biographic and Geological Indications of Unglaciated Areas in Scandinavia during the Glacial Ages. *Bulletin of the Geological Society of America*, 66(12), 1499–1520.

Dahl, E. (1961). Refugieproblemet Og de Kvartaergeologiske Metodene. *Svensk Naturvetenskap*, 14, 81–96.

Dahl, E. (1987). The Nunatak Theory Reconsidered. *Ecological bulletins*, 77–94.

Dahl, E. (1992). Nunatakkteori: IV. Hvor Fantes Isfrie Områder Og Hva Slags Planter Kunne Leve På Dem. *Blyttia*, 50, 23–35.

Dahl, R. (1966b). Block Fields and Other Weathering Forms in the Narvik Mountains. *Geografiska Annaler. Series A, Physical Geography*, 48(4), 224–227.

Dahl, R. (1966a). Block Fields, Weathering Pits and Tor-like Forms in the Narvik Mountains, Nordland, Norway. *Geografiska Annaler. Series A. Physical Geography*, 55–85.

Dahl, S.-O., Ballantyne, C. K., McCarroll, D. & Nesje, A. (1996). Maximum Altitude of Devensian Glaciation on the Isle of Skye. *Scottish Journal of Geology*, 32, 107–116.

Dallmann W.K. (2015) (Ed.). *Geoscience Atlas of Svalbard.* Norwegian Polar Institute, Report 148, Tromsø.

Darvill, C.M., Bentley, M.J., Stokes, C.R. (2015). Geomorphology and weathering characteristics of erratic boulder trains on Tierra del Fuego, southernmost South America: Implications for dating of glacial deposits. *Geomorphology*, 228, 382–397.

Deswal, S., Sharma, M.C., Saini, R., Chand, P., Juyal, N., Singh, I., Srivastava, P., Ajai, & Bahuguna I.M. (2017). Late Holocene Glacier Dynamics in the Miyar Basin, Lahaul Himalaya, India. *Geosciences*, 7(3), 64.

Dowdeswell, J., Hamilton, G., & Hagen, J. (1991). The duration of the active phase on surge-type glaciers: Contrasts between Svalbard and other regions. *Journal of Glaciology,* 37(127), 388–400.

Dyke, A. S. (1979). Glacial and Sea-Level History of Southwestern Cumberland Peninsula, Baffin Island, N.W.T., Canada. *Arctic and Alpine Research,* 11(2), 179–202.

Dyke, A. S. & Prest, V. K. (1987). Late Wisconsinan and Holocene History of the Laurentide Ice Sheet. *Géographie physique et Quaternaire*, 41(2), 237–263.

Edwards, R., Gehrels, W. R., Brooks, A., Fyfe, R., Pullen, K., Kuchar, J. & Craven, K. (2017). Resolving discrepancies between field and modelled relative sea-level data: lessons from western Ireland. *Journal Quaternary Science*, 32, 957–975.

Egholm, D. L., Knudsen, M. F., Clark, C. D. & Lesemann, J. E. (2011). Modeling the flow of glaciers in steep terrains: The integrated second-order shallow ice approximation (iSOSIA), *Journal of Geophysical Research*, 116(F2).

Evans, D. J. A. (2016). Landscapes at the Periphery of Glacierization – Retrospect and Prospect, *Scottish Geographical Journal*, 132(2), 140–163.

Evans, D. J. A., Clark, C. D. & Mitchell, W. A. (2005). The Last British Ice Sheet: A Review of the Evidence Utilised in the Compilation of the Glacial Map of Britain. *Earth Science Reviews*, 70(3), 253–312.

Evans, D. J. A. & Rea, B. (2003). Glacial Landsystems, in: Evans, DJA (Ed.), (pp. 259–288). London: Arnold.

Fabel, D., Ballantyne, C. K. & Xu, S. (2012). Trimlines, Blockfields, Mountain-Top Erratics and the Vertical Dimensions of the Last British-Irish Ice Sheet in NW Scotland. *Quaternary Science Reviews*, 55, 91–102.

Fabel, D., Stroeven, A. P., Harbor, J., Kleman, J., Elmore, D. & Fink, D. (2002). Landscape Preservation under Fennoscandian Ice Sheets Determined from in Situ Produced 10 Be and 26 Al. *Earth and Planetary Science Letters*, 201(2), 397–406.

Farinotti, D., Huss, M., Bauder, A., Funk, M. & Truffer, M. (2009). A Method to Estimate the Ice Volume and Ice-Thickness Distribution of Alpine Glaciers. *Journal of Glaciology*, 55(191), 422–430.

Fiebig, M., Pacher, M. & Saemann, S. (2005). Trimlines and Fauna in the Eastern Alps during the Last Glacial Cycle. *Abhandlung Naturhistorische Gesellschaft Nuernberg*, 45, 105–109.

Fjellanger, J., Sørbel, L., Linge, H., Brook, E. J., Raisbeck, G. M. & Yiou, F. (2006). Glacial Survival of Blockfields on the Varanger Peninsula, Northern Norway. *Geomorphology*, 82(3), 255–272.

Flink, A. E., Noormets, R., Kirchner, N., Benn, D. I., Luckman, A. & Lovell, H. (2015). The Evolution of a Submarine Landform Record Following Recent and Multiple Surges of Tunabreen Glacier, Svalbard. *Quaternary Science Reviews*, 108, 37–50.

Florineth, D. (1998). Surface Geometry of the Last Glacial Maximum (LGM) in the Southeastern Swiss Alps (Graubünden) and Its Paleoclimatological Significance, *Quaternary Science Journal*, 48, 23–37.

Florineth, D. & Schluchter, C. (1998). Reconstructing the Last Glacial Maximum (LGM) Ice Surface Geometry and Flowlines in the Central Swiss Alps. *Eclogae Geologicae Helvetiae*, 91(3), 391–407.

Førland, E.J., I. Hanssen-Bauer and P.Ø. Nordli (1997). Climate statistics and longterm series of temperature and precipitation at Svalbard and Jan Mayen. *DNMI Rapp.* 21/97.

Forman, S. L., Marín, L., Veen, C., Tremper, C. & Csatho, B. (2007). Little Ice Age and Neoglacial Landforms at the Inland Ice Margin, Isunguata Sermia, Kangerlussuaq, West Greenland. *Boreas*, 36(4), 341–351.

Fowler, A., Murray, T., & Ng, F. (2001). Thermally controlled glacier surging. *Journal of Glaciology,* 47(159), 527–538.

French, H. & Guglielmin, M. (2002). Cryogenic Grooves on a Granite Nunatak, Northern Victoria Land, Antarctica. *Norsk Geografisk Tidsskrift-Norwegian Journal of Geography*, 56(2), 112–116.

Fretwell, P., Smith, D. & Harrison, S. (2008). The Last Glacial Maximum British-Irish Ice Sheet: A Reconstruction Using Digital Terrain Mapping. *Journal of Quaternary Science*, 23(3), 241–248.

Fu, P., Harbor, J. M., Stroeven, A. P., Hättestrand, C., Heyman, J. & Zhou, L. (2013). Glacial Geomorphology and Paleoglaciation Patterns in Shaluli Shan, the Southeastern Tibetan Plateau—Evidence for Polythermal Ice Cap Glaciation. *Geomorphology*, 182, 66–78.

Furbish, D. & Andrews, J. (1984). The Use of Hypsometry to Indicate Long-Term Stability and Response of Valley Glaciers to Changes in Mass Transfer. *Journal of Glaciology*, 30(105), 199–211.

Geikie, J. (1873). On the Glacial Phenomena of the Long Island or Outer Hebrides. First Paper. *Quarterly Journal of the Geological Society*, 29(1-2), 532–545.

Geikie, J. (1874). *The Great Ice Age and Its Relation to the Antiquity of Man*. New York: Appleton.

Geikie, J. (1878). On the Glacial Phenomena of the Long Island, or Outer Hebrides. Second Paper. *Quarterly Journal of the Geological Society*, 34(1-4), 819–870.

Gjærevoll, O. (1963). Survival of Plants on Nunataks in Norway during the Pleistocene Glaciation, in: Löve, Áskell and Löve, Doris (Ed.), *North Atlantic biota and their history*. Macmillian.

Gjærevoll, O. & Ryvarden, L. (1978). Botanical Investigations on JAD Jensens Nunatakker in Greenland. *Kong. Norske Vidensk. Selsk. Skr*, (4).

Gjessing, J. (1967). Norway's Paleic Surface. N*orsk Geografisk Tidsskrift*, 21(2). 69–132.

Glasser, N. F. (1995). Modelling the Effect of Topography on Ice Sheet Erosion, Scotland. *Geografiska Annaler. Series A. Physical Geography*, 67–82.

Glasser, N. F., Harrison, S., Jansson, K. N., Anderson, K. & Cowley, A. (2011). Global Sea-Level Contribution from the Patagonian Icefields since the Little Ice Age Maximum. *Nature Geoscience*, 4(5), 303–307.

Glasser, N. F., Hughes, P. D., Fenton, C., Schnabel, C. & Rother, H. (2012). 10Be and 26Al Exposure-Age Dating of Bedrock Surfaces on the Aran Ridge, Wales: Evidence for a Thick Welsh Ice Cap at the Last Glacial Maximum. *Journal of Quaternary Science*, 27(1), 97–104.

Glasser, N. F., Jansson, K. N., Harrison, S. & Kleman, J. (2008). The Glacial Geomorphology and Pleistocene History of South America between 38 S and 56 S. *Quaternary Science Reviews*, 27(3), 365–390.

Glasser, N. F., Jansson, K. N., Harrison, S. & Rivera, A. (2005). Geomorphological Evidence for Variations of the North Patagonian Icefield during the Holocene. *Geomorphology*, 71(3), 263–277.

Godard, A. (1965). *Recherches de Géomorphologie En Écosse Du Nord-Ouest*. Publications de la Faculté des lettres de l'Université de Strasbourg.

Goehring, B. M., Brook, E. J., Linge, H., Raisbeck, G. M. & Yiou, F. (2008). Beryllium-10 Exposure Ages of Erratic Boulders in Southern Norway and Implications for the History of the Fennoscandian Ice Sheet. *Quaternary Science Reviews*, 27(3), 320–336.

Golledge, N. R. (2010). Glaciation of Scotland during the Younger Dryas Stadial: A Review. *Journal of Quaternary Science*, 25(4), 550–566.

Goodfellow, B. (2007). Relict Non-Glacial Surfaces in Formerly Glaciated Landscapes. *Earth-Science Reviews*, 80(1), 47–73.

Gordon, J. E. (1979). Reconstructed Pleistocene Ice-Sheet Temperatures and Glacial Erosion in Northern Sotland. *Journal of Glaciology*, 22, 331–344.

Gosse, J., Bell, T., Gray, J., Klein, J., Yang, G. & Finkel, R. (2006). Using Cosmogenic Isotopes to Interpret the Landscape Record of Glaciation: Nunataks in Newfoundland? *Glacier science and environmental change*, 442–446.

Gourronc, M., Bourgeois, O., Mège, D., Pochat, S., Bultel, B., Massé, M., Le Deit, L., Le Mouélic, S. & Mercier, D. (2014). One million cubic kilometers of fossil ice in Valles Marineris: Relicts of a 3.5Gy old glacial landsystem along the Martian equator. *Geomorphology*, 204, 235–255.

Grant, D. R. (1977). Altitudinal Weathering Zones and Glacial Limits in Western Newfoundland, with Particular Reference to Gros Morne National Park. *Geological Survey of Canada Paper*, 77, 455–463.

Grønlie, A. (1953). Litt Om Trollheimen under Siste Istid. *Nor. Geol. Tidsskr*, 32, 168–190.

Hall, A. (1985). Cenozoic Weathering Covers in Buchan, Scotland and Their Significance. *Nature*, 315(6018), 392–395.

Hall, A. M. & Sugden, D. E. (1987). Limited Modification of Mid-Latitude Landscapes by Ice Sheets: The Case of Northeast Scotland. *Earth surface processes and landforms*, 12(5), 531–542.

Hannah, G., Hughes, P.D., & Gibbard, P.L. (2017). *Pleistocene plateau ice fields in the High Atlas, Morocco*. In: Hughes, P.D., Woodward, J.C. (Eds.), Quaternary glaciation in the Mediterranean Mountains. Geological Society of London Special Publications 433, 25-53.

Hannesdóttir, H., Björnsson, H., Pálsson, F., Aðalgeirsdóttir, G. & Guðmundsson, S. (2016). Variations of southeast vatnajökull ice cap (iceland) 1650–1900 and reconstruction of the glacier surface geometry at the little ice age maximum, *Geografiska Annaler. Series A Physical Geography*, 97(2), 237–264.

Hansen, S. (2003). From surge-type to non-surge-type glacier behaviour: Midre Lovénbreen, Svalbard. *Annals of Glaciology*, 36, 97–102.

Harrison, S., Winchester, V. & Glasser, N. (2007). The Timing and Nature of Recession of Outlet Glaciers of Hielo Patagónico Norte, Chile, from Their Neoglacial IV (Little Ice Age) Maximum Positions. *Global and Planetary Change*, 59(1), 67–78.

Hättestrand, C. & Stroeven, A. P. (2002). A Relict Landscape in the Centre of Fennoscandian Glaciation: Geomorphological Evidence of Minimal Quaternary Glacial Erosion. *Geomorphology*, 44(1), 127–143.

Hayes, R. J. (2014). *Mountain glacier health signatures stored in their three-dimensional ice surface geometry*. PhD Thesis, University of Sheffield.

Henriksen, M., Alexanderson, H., Landvik, J. Y., Linge, H. & Peterson, G. (2014). Dynamics and Retreat of the Late Weichselian Kongsfjorden Ice Stream, NW Svalbard. *Quaternary Science Reviews*, 92, 235–245.

Hess, H. (1904). *Die Gletscher*. F. Vieweg and Son, Brunswick, Germany.

Heusser, C. J., Schuster, R. L. & Gilkey, A. K. (1954). Geobotanical Studies on the Taku Glacier Anomaly. *Geographical Review*, 44(2), 224–239.

Hodgkins, R., Hagen, J., & Hamran, S. (1999). 20th century mass balance and thermal regime change at Scott Turnerbreen, Svalbard. *Annals of Glaciology*, 28, 216–220.

Hormes, A., Gjermundsen, E. F. & Rasmussen, T. L. (2013). From Mountain Top to the Deep Sea-Deglaciation in 4D of the Northwestern Barents Sea Ice Sheet. *Quaternary Science Reviews*, 75, 78–99.

Hormes, A., Ivy-Ochs, S., Kubik, P. W., Ferreli, L. & Michetti, A. M. (2008). 10 Be Exposure Ages of a Rock Avalanche and a Late Glacial Moraine in Alta Valtellina, Italian Alps. *Quaternary International*, 190(1), 136–145.

Hubbard, A., Bradwell, T., Golledge, N., Hall, A., Patton, H., Sugden, D., Cooper, R. & Stoker, M. (2009). Dynamic Cycles, Ice Streams and Their Impact on the Extent, Chronology and Deglaciation of the British-Irish Ice Sheet. *Quaternary Science Reviews*, 28(7), 758–776.

Hubbard, A., Sugden, D., Dugmore, A., Norddahl, H. & Pétursson, H. G. (2006). A Modelling Insight into the Icelandic Last Glacial Maximum Ice Sheet. *Quaternary Science Reviews*, 25(17), 2283–2296.

Huber, N. K. (1989). *The geologic story of Yosemite National Park*. Yosemite Association.

Hughes, P. D. (2002). Loch Lomond Stadial glaciers in the Aran and Arenig Mountains, North Wales, Great Britain. *Geological Journal*, 37, 9–15.

Hughes, P.D. (2009). Twenty-first Century Glaciers in the Prokletije Mountains, Albania. *Arctic, Antarctic and Alpine Research*, 41, 455-459.

Hughes, P.D. (2018). Little Ice Age glaciers and climate in the Mediterranean mountains: a new analysis. *Cuadernos de Investigación Geográfica*, 44(1), 15–45.

Hughes, P. D., Braithwaite, R., Fenton, C. R., & Schnabel, C. (2012). Two Younger Dryas glacier phases in the English Lake District: geomorphological evidence and preliminary 10Be exposure ages. *North West Geography*, 12(1), 10–19.

Hughes, A. L., Greenwood, S. L. & Clark, C. D. (2011). Dating Constraints on the Last British-Irish Ice Sheet: A Map and Database. *Journal of Maps*, 7(1), 156–184.

Huss, M. & Farinotti, D. (2012). Distributed Ice Thickness and Volume of All Glaciers around the Globe. *Journal of Geophysical Research*, 117, F04010.

Ingólfsson, Ó. (2011). Fingerprints of Quaternary Glaciations on Svalbard. *Geological Society, London, Special Publications*, 354(1), 15–31.

Ingólfsson, Ó. & Landvik, J. Y. (2013). The Svalbard-Barents Sea Ice-Sheet - Historical, Current and Future Perspectives. *Quaternary Science Reviews*, 64, 33–60.

IPCC (2014). *Climate Change 2014: Synthesis Report*. Contribution of Working Groups I, II and III to the Fifth Assessment Report of the Intergovernmental Panel on Climate Change [Core Writing Team, R.K. Pachauri and L.A. Meyer (Eds.)]. IPCC, Geneva, Switzerland.

Ives, J. (1957). Glaciation of the Torngat Mountains, Northern Labrador. *Arctic*, 10(2), 66–87.

Ives, J. (1958a). Glacial Geomorphology of the Torngat Mountains, Northern Labrador. *Geographical Bulletin*, 12, 47–75.

Ives, J. (1958b). Mountain-Top Detritus and the Extent of the Last Glaciation in Northeastern Labrador-Ungava. *The Canadian Geographer/Le Géographe canadien*, 3(12), 25–31.

Ives, J. (1974). Biological Refugia and the Nunatak Hypothesis. *Arctic and alpine environments*, 605–636.

Ives, J. D. (1975). Delimitation of Surface Weathering Zones in Eastern Baffin Island, Northern Labrador and Arctic Norway: A Discussion. *Geological Society of America Bulletin*, 86(8), 1096–1100.

Ives, J. D. (1976). The Saglek Moraines of Northern Labrador: A Commentary. *Arctic and Alpine Research*, 403–408.

Ives, J. D. (1977). Late- and Postglacial Glacier Fluctuations and Sea Level Changes in Arctic Canada. *Geografiska Annaler. Series A. Physical Geography*, 253–256.

Ives, J. D. (1978). The Maximum Extent of the Laurentide Ice Sheet along the East Coast of North America during the Last Glaciation. *Arctic*, 24–53.

Ives, J. D., Nichols, H. & Short, S. (1976). Glacial History and Palaeoecology of Northeastern Nouveau-Quebec and Northern Labrador. *Arctic*, 29(1), 48–52.

Jansson, K. N. (2005). Map of the Glacial Geomorphology of North-Central Québec-Labrador, Canada. *Journal of Maps*, 1(1), 46–55.

Jansson, K. N. & Glasser, N. F. (2005). Palaeoglaciology of the Welsh Sector of the British-Irish Ice Sheet. *Journal of the Geological Society*, 162(1), 25–37.

Johnson, M. D., Schomacker, A., Benediktsson, Í. Ö., Geiger, A. J., Ferguson, A. & Ingólfsson, Ó. (2010). Active Drumlin Field Revealed at the Margin of Múlajökull, Iceland: A Surge-Type Glacier. *Geology*, 38(10), 943–946.

Jonsson, S. A., Schomacker, A., Benediktsson, I. Ö., Ingolfsson, O., & Johnson, M. D. (2014). The drumlin field and the geomorphology of the Mulajokull surge-type glacier, central Iceland. *Geomorphology*, 207, 213–220.

Kaitanen, V. (1969). A Geographical Study of the Morphogenesis of Northern Lapland. *Fennia*, 99(5).

Kaplan, M., Miller, G. & Steig, E. (2001). Low-Gradient Outlet Glaciers (ice Streams?) Drained the Laurentide Ice Sheet. *Geology*, 29(4), 343–346.

Kelley, S. E., Briner, J. P., Young, N. E., Babonis, G. S. & Csatho, B. (2012). Maximum Late Holocene Extent of the Western Greenland Ice Sheet during the Late 20th Century. *Quaternary Science Reviews*, 56, 89–98.

Kelly, M. A., Buoncristiani, J.-F. & Schlüchter, C. (2004). A Reconstruction of the Last Glacial Maximum (LGM) Ice-Surface Geometry in the Western Swiss Alps and Contiguous Alpine Regions in Italy and France. *Eclogae Geologicae Helvetiae*, 97(1), 57–75.

Kelly, M., von Blanckenburg, F., Kubik, P. & Schlüchter, C. (2002). Surface Exposure Ages of High Elevation Glacial Erosion Forms: An Attempt to Date Deglaciation of the Last Glacial Maximum Ice Cap in the Western Swiss Alps, in: *Geochimica et cosmochimica acta*, A392–A392.

Kern, Z. & László, P. (2010). Size specific steady-state accumulation-area ratio: an improvement for equilibrium-line estimation of small palaeoglaciers. *Quaternary Science Reviews*, 29, 2781–2787.

Kirkbride, M. & Winkler, S. (2012). Correlation of Late Quaternary Moraines: Impact of Climate Variability, Glacier Response, and Chronological Resolution. *Quaternary Science Reviews*, 46, 1–29.

Kjeldsen, K. K., Korsgaard, N. J., Bjørk, A. A., Khan, S. A., Box, J. E., Funder, S., Larsen, N. K., Bamber, J. L., Colgan, W., van den Broeke, M., Siggaard-Andersen, M.-L., Nuth, C., Schomaker, A., Andresen, C. S., Willerslev, E., & Kjær, K. H. (2015). Spatial and Temporal Distribution of Mass Loss from the Greenland Ice Sheet since AD 1900. *Nature*, 528(7582), 396–400.

Kleman, J. (1992). The Palimpsest Glacial Landscape in Northwestern Sweden. Late Weichselian Deglaciation Landforms and Traces of Older West-Centered Ice Sheets. *Geografiska Annaler. Series A. Physical Geography*, 305–325.

Kleman, J. (1994). Preservation of Landforms under Ice Sheets and Ice Caps. *Geomorphology*, 9(1), 19–32.

Kleman, J. & Borgström, I. (1990). The Boulder Fields of Mt. Fulufjället, West-Central Sweden-Late Weichselian Boulder Blankets and Interstadial Periglacial Phenomena. *Geografiska Annaler. Series A. Physical Geography*, 63–78.

Kleman, J. & Borgström, I. (1996). Reconstruction of Palaeo-Ice Sheets: The Use of Geomorphological Data. *Earth surface processes and landforms*, 21(10), 893–909.

Kleman, J. & Glasser, N. F. (2007). The Subglacial Thermal Organisation (STO) of Ice Sheets. *Quaternary Science Reviews*, 26(5), 585–597.

Kleman, J., Hattestra, C. & Borgstrom, I. (1997). Fennoscandian Palaeoglaciology Reconstructed Using a Glacial Geological Inversion Model. *Journal of Glaciology*, 43(144).

Kleman, J., Hättestrand, C. & Clarhäll, A. (1999). Zooming in on Frozen-Bed Patches: Scale-Dependent Controls on Fennoscandian Ice Sheet Basal Thermal Zonation. *Annals of Glaciology*, 28(1), 189–194.

Kleman, J. & Stroeven, A. P. (1997). Preglacial Surface Remnants and Quaternary Glacial Regimes in Northwestern Sweden. *Geomorphology*, 19(1), 35–54.

Knight, P., Weaver, R. & Sugden, D. (1987). Technical Note. Using LANDSAT MSS Data for Measuring Ice Sheet Retreat. *International Journal of Remote Sensing*, 8(7), 1069–1074.

Koffman, T.N.B., Schaefer, J.M., Putnam, A.E., Denton, G.H., Barrell, D.J.A., Rowan, A.V., Finkel, R.C., Rood, D.H., Schwartz, R., Plummer, M.A., Brocklehurst, S.H. (2017). A beryllium-10 chronology of late-glacial moraines in the upper Rakaia valley, Southern Alps, New Zealand supports Southern-Hemisphere warming during the Younger Dryas. *Quaternary Science Reviews*, 170, 14–25.

Kohler, J., James, T., Murray, T., Nuth, C., Brandt, O., Barrand, N., Aas, H. & Luckman, A. (2007). Acceleration in Thinning Rate on Western Svalbard Glaciers. *Geophysical Research Letters*, 34(18).

König, M., Nuth, C., Kohler, J., Moholdt, G. & Pettersen, R. (2014*). A digital glacier database for Svalbard*. In: Kargel J., Leonard G., Bishop M., Kääb A., Raup B. (Eds) Global Land Ice Measurements from Space. Springer Praxis Books. Springer, Berlin, Heidelberg.

Kuchar, J., Milne, G., Hubbard, A., Patton, H., Bradley, S., Shennan, I. & Edwards, R. (2012). Evaluation of a Numerical Model of the British-Irish Ice Sheet Using Relative Sea-Level Data: Implications for the Interpretation of Trimline Observations. *Journal of Quaternary Science*, 27(6), 597–605.

Kurowski, L. (1891). Die Höhe der Schneegrenze mit besonderer Berücksichtigung der Finsteraarhorngruppe. *Geographische Abhandlungen*, 5(1), 115–160.

Kverndal, A.-I. & Sollid, J. L. (1993). Late Weichselian Glaciation and Deglaciation in Northeastern Troms, Northern Norway. *Norsk Geografisk Tidsskrift*, 47(3), 163-177.

Lagerbäck, R. (1988a). The Veiki Moraines in Northern Sweden-Widespread Evidence of an Early Weichselian Deglaciation. *Boreas*, 17(4), 469–486.

Lagerbäck, R. (1988b). Periglacial Phenomena in the Wooded Areas of Northern Sweden-Relicts from the Tärendö Interstadial. *Boreas*, 17(4), 487–499.

Lamb, A. L. & Ballantyne, C. K. (1998). Palaeonunataks and the Altitude of the Last Ice Sheet in the SW Lake District, England. *Proceedings of the Geologists' Association*, 109(4), 305–316.

Lambeck, K. (1993). Glacial Rebound of the British Isles—II. A High-Resolution, High-Precision Model. *Geophysical Journal International*, 115(3), 960–990.

Lambeck, K. (1995). Late Devensian and Holocene Shorelines of the British Isles and North Sea from Models of Glacio-Hydro-Isostatic Rebound. *Journal of the Geological Society*, 152(3), 437–448.

Landvik, J. Y., Bondevik, S., Elverhøi, A., Fjeldskaar, W., Mangerud, J., Salvigsen, O., Siegert, M. J., Svendsen, J.-I. & Vorren, T. O. (1998). The Last Glacial Maximum of Svalbard and the Barents Sea Area: Ice Sheet Extent and Configuration. *Quaternary Science Reviews*, 17(1), 43–75.

Larsen, N.K., Piotrowski, J.A., Christoffersen, P. & Menzies, J. (2006). Formation and deformation of basal till during a glacier surge; Elisebreen, Svalbard. *Geomorphology*, 81(1–2), 217–234.

Larsen, E., Fredin, O., Jensen, M., Kuznetsov, D., Lysså, A. & Subetto, D. (2014). Subglacial sediment, proglacial lake-level and topographic controls on ice extent and lobe geometries during the Last Glacial Maximum in NW Russia. *Quaternary Science Reviews*, 92, 369–387.

Lawrence, D. B. (1950b). Glacier Fluctuation for Six Centuries in Southeastern Alaska and Its Relation to Solar Activity. *Geographical Review*, 40(2), 191–223.

Lawrence, D. B. (1950a). Estimating Dates of Recent Glacier Advances and Recession Rates by Studying Tree Growth Layers. *Eos, Transactions American Geophysical Union*, 31(2), 243–248.

Lawson, T. (1990). Former Ice Movement in Assynt, Sutherland, as Shown by the Distribution of Glacial Erratics. *Scottish Journal of Geology*, 26(1), 25–32.

Leiber, O. M. (1861). *Geology of the coast of Labrador*. Appendix to: US Coast Survey Report for 1860, Government Printing Office, Washington.

Li, Y. & Li, Y. (2014). Topographic and Geometric Controls on Glacier Changes in the Central Tien Shan, China, since the Little Ice Age. *Annals of Glaciology*, 55(66), 177.

Lidmar-Bergström, K., Ollier, C. & Sulebak, J. (2000). Landforms and Uplift History of Southern Norway. *Global and Planetary Change*, 24(3), 211–231.

Linge, H., Brook, E. J., Nesje, A., Raisbeck, G. M., Yiou, F. & Clark, H. (2006). In Situ 10 Be Exposure Ages from Southeastern Norway: Implications for the Geometry of the Weichselian Scandinavian Ice Sheet. *Quaternary Science Reviews*, 25(9), 1097–1109.

Linton, D. L. (1949). Unglaciated Areas in Scandinavia and Great Britain. *Irish Geography*, 2(1), 25–33.

Linton, D. L. (1950). Unglaciated Enclaves in Glaciated Regions. *Journal of Glaciology*, 1, 451–452.

Linton, D. L. (1955). The Problem of Tors. *The Geographical Journal*, 121(4), 470–487.

Locke, W. W. (1995). Modelling of Icecap Glaciation of the Northern Rocky Mountains of Montana. *Geomorphology*, 14(2), 123–130.

Loibl, D., Lehmkuhl, F. & Grießinger, J. (2014). Reconstructing Glacier Retreat since the Little Ice Age in SE Tibet by Glacier Mapping. *Geomorphology*, 214, 22–39.

Løken, O. (1962). On the Vertical Extent of Glaciation in North-Eastern Labrador-Ungava. *The Canadian Geographer/Le Géographe canadien*, 6(3-4), 106–115.

Lønne, I. & Lysså, A. (2005). Deglaciation Dynamics Following the Little Ice Age on Svalbard: Implications for Shaping of Landscapes at High Latitudes. *Geomorphology*, 72(1), 300–319.

Lowe, J. J. & Walker, M. J. (1997). *Reconstructing Quaternary Environments*. Longman Londres.

Lukas, S. (2006). Morphostratigraphic Principles in Glacier Reconstruction-a Perspective from the British Younger Dryas. *Progress in physical geography*, 30(6), 719–736.

Lukas, S. (2012). Processes of Annual Moraine Formation at a Temperate Alpine Valley Glacier: Insights into Glacier Dynamics and Climatic Controls. *Boreas*, 41(3), 463–480.

Lukas, S. & Bradwell, T. (2010). Reconstruction of a Lateglacial (Younger Dryas) Mountain Ice Field in Sutherland, Northwestern Scotland, and Its Palaeoclimatic Implications. *Journal of Quaternary Science*, 25(4), 567–580.

Lukas, S., Graf, A., Coray, S. & Schlüchter, C. (2012). Genesis, Stability and Preservation Potential of Large Lateral Moraines of Alpine Valley Glaciers-towards a Unifying Theory Based on Findelengletscher, Switzerland. *Quaternary Science Reviews*, 38, 27–48.

McCarroll, D. (2016). Trimline Trauma: The Wider Implications of a Paradigm Shift in Recognising and Interpreting Glacial Limits, *Scottish Geographical Journal*, 132(2), 130–139.

McDougall, D. A. (1998). *Loch Lomond Stadial Plateau Icefields in the Lake District, Northwest England*. PhD Thesis, University of Glasgow.

Mackintosh, A., White, D., Fink, D., Gore, D. B., Pickard, J. & Fanning, P. C. (2007). Exposure Ages from Mountain Dipsticks in Mac. Robertson Land, East Antarctica, Indicate Little Change in Ice-Sheet Thickness since the Last Glacial Maximum. *Geology*, 35(6), 551–554.

Mahaney, W. (1987). Lichen Trimlines and Weathering Features as Indicators of Mass Balance Changes and Sucessive Retreat Stages of the Mer de Glace in the Western Alps. *Zeitschrift fur Geomorphologie*, 31(4), 411–418.

Mahaney, W. (1991). Holocene Glacial Sequence and Soils of Stratigraphic Important, Mer de Glace, Western Alps, France . *Zeitschrift fur Geomorphologie*, 35(2), 225–237.

Makos, M. & Nitychoruk, J. (2011). Last Glacial Maximum climatic conditions in the Polish part of the High Tatra Mountains (Western Carpathians). *Geological Quarterly,* 55(3), 253–268.

Makos, M., Nitychoruk, J. & Zreda, M. (2013). Deglaciation chronology and paleoclimate of the Pięciu Stawów Polskich/Roztoki Valley, high Tatra Mountains, Western Carpathians, since the Last Glacial Maximum, inferred from 36Cl exposure dating and glacier–climate modelling, *Quaternary International*, 293, 63–78.

Mangerud, J. (1973). Unglaciated refugia in Norway during the ice ages*, Norges Geologiske Undersokelse*, 297, 1–23.

Mangerud, J. & Landvik, J. Y. (2007). Younger Dryas Cirque Glaciers in Western Spitsbergen: Smaller than during the Little Ice Age. *Boreas*, 36(3), 278–285.

Mangerud, J., Larsen, E., Longva, O. & Sønstegaard, E. (1979). Glacial History of Western Norway 15,000-10,000 BP. *Boreas*, 8(2), 179–187.

Marquette, G. C., Gray, J. T., Gosse, J. C., Courchesne, F., Stockli, L., Macpherson, G. & Finkel, R. (2004). Felsenmeer Persistence under Non-Erosive Ice in the Torngat and Kaumajet Mountains, Quebec and Labrador, as Determined by Soil Weathering and Cosmogenic Nuclide Exposure Dating. *Canadian Journal of Earth Sciences*, 41(1), 19–38.

Mathews, W. (1951). Historic and Prehistoric Fluctuations of Alpine Glaciers in the Mount Garibaldi Map-Area, Southwestern British Columbia. *The Journal of Geology*, 357–380.

May, J.-H., Zech, J., Zech, R., Preusser, F., Argollo, J., Kubik, P. W. & Veit, H. (2011). Reconstruction of a Complex Late Quaternary Glacial Landscape in the Cordillera de Cochabamba (Bolivia) Based on a Morphostratigraphic and Multiple Dating Approach. *Quaternary Research*, 76(1), 106–118.

McCarroll, D. & Ballantyne, C. K. (2000). The Last Ice Sheet in Snowdonia. *Journal of Quaternary Science*, 15(8), 765–778.

McCarroll, D., Ballantyne, C. K., Nesje, A. & Dahl, S.-O. (1995). Nunataks of the Last Ice Sheet in Northwest Scotland. *Boreas*, 24(4), 305–323.

McCarroll, D. & Nesje, A. (1993). The Vertical Extent of Ice Sheets in Nordfjord, Western Norway: Measuring Degree of Rock Surface Weathering. *Boreas*, 22(3), 255–265.

McCormack, D. C., Brocklehurst, S. H., Irving, D. H. & Fabel, D. (2011). Cosmogenic 10Be Insights into the Extent and Chronology of the Last Deglaciation in Wester Ross, Northwest Scotland. *Journal of Quaternary Science*, 26(1), 97–108.

McDougall, D. (2013). Glaciation Style and the Geomorphological Record: Evidence for Younger Dryas Glaciers in the Eastern Lake District, Northwest England. *Quaternary Science Reviews*, 73, 48–58.

McKinzey, K. M., Lawson, W., Kelly, D. & Hubbard, A. (2004). A Revised Little Ice Age Chronology of the Franz Josef Glacier, Westland, New Zealand. *Journal of the Royal Society of New Zealand*, 34(4), 381–394.

Migoñ, P. & Goudie, A. (2001). Inherited Landscapes of Britain-Possible Reasons for Survival. *Zeitschrift für Geomorphologie*, 417–441.

Möller, P., Hjort, C., Björck, S., Rabassa, J. & Ponce, J. F. (2010). Late Quaternary Glaciation History of Isla de Los Estados, Southeasternmost South America. *Quaternary Research*, 73(3), 521–534.

Munroe, J. S. (2006). Investigating the Spatial Distribution of Summit Flats in the Uinta Mountains of Northeastern Utah, USA. *Geomorphology*, 75(3), 437–449.

Murray, T., Stuart, G. W., Miller, P. J., Woodward, J., Smith, A. M., Porter, P. R., & Jiskoot, H. (2000). Glacier surge propagation by thermal evolution at the bed. *Journal of Geophysical Research: Solid Earth*, 105(B6), 13491–13507.

Navarro, F., Glazovsky, A., Macheret, Y., Vasilenko, E., Corcuera, M., Cuadrado, M. (2005). Ice-Volume Changes (1936-1990) and Structure of Aldegondabreen, Spitsbergen. *Annals of Glaciology*, 42(1), 158–162.

Nesje, A. (1989). The Geographical and Altitudinal Distribution of Blockfields in Southern Norway and Its Significance to the Pleistocene Ice Sheets. *Zeitschrift für Geomorphologie*, 72, 41–53.

Nesje, A., Anda, E., Rye, N., Lien, R., Hole, P. & Blikra, L. H. (1987). The Vertical Extent of the Late Weichselian Ice Sheet in the Nordfjord-Møre Area, Western Norway. *Norsk Geologisk Tidsskrift*, 67(2), 125–141.

Nesje, A. & Dahl, S. O. (1990). Autochthonous Block Fields in Southern Norway: Implications for the Geometry, Thickness, and Isostatic Loading of the Late Weichselian Scandinavian Ice Sheet. *Journal of Quaternary Science*, 5(3), 225–234.

Nesje, A., Dahl, S. O., Linge, H., Ballantyne, C. K., McCarroll, D., Brook, E. J., Raisbeck, G. M. & Yiou, F. (2007). The Surface Geometry of the Last Glacial Maximum Ice Sheet in the Andøya-Skånland Region, Northern Norway, Constrained by Surface Exposure Dating and Clay Mineralogy. *Boreas*, 36(3), 227.

Nesje, A., Dahl, S.-O., Anda, E. & Rye, N. (1988). Block Fields in Southern Norway: Significance for the Late Weichselian Ice Sheet. *Norsk Geologisk Tidsskrift*, 68(3), 149–169.

Nesje, A., McCarroll, D. & Dahl, S. O. (1994). Degree of Rock Surface Weathering as an Indicator of Ice-Sheet Thickness along an East—west Transect across Southern Norway. *Journal of Quaternary Science*, 9(4), 337–347.

Nesje, A. & Sejrup, H. P. (1988). Late Weichselian/Devensian Ice Sheets in the North Sea and Adjacent Land Areas. *Boreas*, 17(3), 371–384.

Ng, F. S., Barr, I. D. & Clark, C. D. (2010). Using the Surface Profiles of Modern Ice Masses to Inform Palaeo-Glacier Reconstructions. *Quaternary Science Reviews*, 29(23), 3240–3255.

Nichols, R. L. & Miller, M. M. (1951). Glacial Geology of Ameghino Valley, Lago Argentino, Patagonia. *Geographical Review*, 41(2), 274–294.

Nixon, F. C. & England, J. H. (2014). Expanded Late Wisconsinan Ice Cap and Ice Sheet Margins in the Western Queen Elizabeth Islands, Arctic Canada. *Quaternary Science Reviews*, 91, 146–164.

Norddahl, H. (1983). Late Quaternary Stratigraphy of Fnjóskadalur, Central North Iceland: A Study of Sediments, Ice-Lake Strandlines, Glacial Isostasy and Ice-Free Areas. *Lunqua*, 12, 78.

Norddahl, H. (1991). *A review of the glaciation maximum concept and the deglaciation of Eyjafjörður, North Iceland*. In: Maizels, J.K., Caseldine, C. (Eds.), Environmental Change in Iceland: Past and Present. Kluwer Academic Publishers, Netherlands, 31–47.

Nordhagen, R. (1936). *Skandinavias Fjellflora Og Dens Relasjoner Til Den Siste Istid*.

Nordhagen, R. (1963). Recent Discoveries in the South Norwegian Flora and Their Significance for the Understanding of the History of the Scandinavian Mountain Flora during and after the Last Glaciation, in: Löve, Áskell and Löve, Doris (Ed.), *North Atlantic biota and their history*. Macmillian.

Nussbaumer, S. U., Zumbühl, H. J. & Steiner, D. (2007). *Fluctuations of the " Mer de Glace" (Mont Blanc Area, France) AD 1500-2050: An Interdisciplinary Approach Using New Historical Data and Neural Network Simulations*. Universitätsverlag Wagner.

Nuth, C., Kohler, J., Aas, H., Brandt, O. & Hagen, J. (2007). Glacier Geometry and Elevation Changes on Svalbard (1936-90): A Baseline Dataset. *Annals of Glaciology*, 46(1), 106–116.

Nuth, C., Moholdt, G., Kohler, J., Hagen, J. O. & Kääb, A. (2010). Svalbard Glacier Elevation Changes and Contribution to Sea Level Rise. *Journal of Geophysical Research: Earth Surface (2003-2012)*, 115(F1).

Ó Cofaigh, C., Evans, D. & England, J. (2003). Ice-Marginal Terrestrial Landsystems: Sub-Polar Glacier Margins of the Canadian and Greenland High Arctic. *Glacial Landsystems*, 45–64.

Oberholzer, P., Baroni, C., Salvatore, M., Baur, H. & Wieler, R. (2008). Dating Late Cenozoic Erosional Surfaces in Victoria Land, Antarctica, with Cosmogenic Neon in Pyroxenes. *Antarctic Science*, 20(01), 89–98.

Orombelli, G. B. C. & Denton, G. H. (1990). Late Cenozoic Glacial History of the Terra Nova Bay Region, Northern Victoria Land, Antarctica. *Geografia Fisica e Dinamica Quaternaria*, 139–163.

Ottesen, D., Dowdeswell, J., Benn, D., Kristensen, L., Christiansen, H., Christensen, O., Hansen, L., Lebesbye, E., Forwick, M. & Vorren, T. (2008). Submarine Landforms Characteristic of Glacier Surges in Two Spitsbergen Fjords. *Quaternary Science Reviews*, 27(15), 1583–1599.

Patton, H., Hubbard, A., Glasser, N. F., Bradwell, T. & Golledge, N. R. (2013a). The Last Welsh Ice Cap: Part 2-Dynamics of a Topographically Controlled Icecap. *Boreas*. 42(3), 491-510.

Patton, H., Hubbard, A., Glasser, N. F., Bradwell, T. & Golledge, N. R. (2013b). The Last Welsh Ice Cap: Part 1-Modelling Its Evolution, Sensitivity and Associated Climate. *Boreas*. 42(3), 471-490.

Pearce, D.M., Mair, D.W.F., Rea, B.R., Lea, J.M., Schofield, J.E., Kamenos, N. & Schoenrock, K. (2018). The glacial geomorphology of upper Godthåbsfjord (Nuup Kangerlua) in southwest Greenland. *Journal of Maps*, 14(2), 45–55.

Pellitero, R., Rea, B. R., Spagnolo, M., Bakke, J., Ivy-Ochs, S., Hughes, P., Lukas, S. & Ribolini, A. (2015). A GIS Tool for Automatic Calculation of Glacier Equilibrium-Line Altitudes. *Computers & Geosciences*, 82, 55-62.

Pellitero, R., Rea, B. R., Spagnolo, M., Bakke, J., Ivy-Ochs, S., Frew, C. R., Hughes, P., Ribolini, A., Lukas, S. & Renssen, H. (2016). Glare, a GIS Tool to Reconstruct the 3D Surface of Palaeoglaciers. *Computers & Geosciences*, 94, 77-85.

Phillips, W. M., Hall, A. M., Ballantyne, C. K., Binnie, S., Kubik, P. W. & Freeman, S. (2008). Extent of the Last Ice Sheet in Northern Scotland Tested with Cosmogenic 10Be Exposure Ages. *Journal of Quaternary Science*, 23(2), 101–107.

Phillips, W. M., Hall, A. M., Mottram, R., Fifield, L. K. & Sugden, D. E. (2006). Cosmogenic 10 Be and 26 Al Exposure Ages of Tors and Erratics, Cairngorm Mountains, Scotland: Timescales for the Development of a Classic Landscape of Selective Linear Glacial Erosion. *Geomorphology*, 73(3), 222–245.

Pierce, K. L. (1982). *History and Dynamics of Glaciation in the Northern Yellowstone National Park Area*. US Geological Survey Professional Paper 729-F.

Pfeffer, W. T., Arendt, A. A., Bliss, A., Bolch, T., Cogley, J. G., Gardner, A. S., Hagen, J.-O., Hock, R., Kaser, G., Kienholz, C., Miles, E. S., Moholdt, G., Mölg, N., Paul, F., Radić, V., Rastner, P., Raup, B. H., Rich, J. and Sharp, M. J. (2014). The Randolph Glacier Inventory: A globally complete inventory of glaciers. *Journal of Glaciology*, 60(221), 537–552.

Pollard, D. & DeConto, R. M. (2009). Modelling West Antarctic Ice Sheet Growth and Collapse through the Past Five Million Years. *Nature*, 458(7236), 329–332.

Post, A., D. Richardson, W. V. Tangburn, & F. L Rosselot (1971). *Inventory of glaciers in the North Cascades, Washington.* U.S. Geological Survey Professional Paper 705-A.

Rae, A. C., Harrison, S. , Mighall, T. and Dawson, A. G. (2004). Periglacial trimlines and nunataks of the Last Glacial Maximum: the Gap of Dunloe, southwest Ireland. *Journal of Quaternary Science*, 19, 87–97.

Ragg, J. & Bibby, J. (1966). Frost Weathering and Solifluction Products in Southern Scotland. *Geografiska Annaler. Series A, Physical Geography*, 48(1), 12–23.

Raper, S. C. & Braithwaite, R. J. (2009). Glacier Volume Response Time and Its Links to Climate and Topography Based on a Conceptual Model of Glacier Hypsometry. *The Cryosphere*, 3(2), 183–194.

Rea, B. R. (2009). Defining modern day area-altitude balance ratios (AABRs) and their use in glacierclimate reconstructions. *Quaternary Science Reviews,* 28(3–4), 237–248.

Rea, B. R., Whalley, W. B., Rainey, M. M. & Gordon, J. E. (1996). Blockfields, Old or New? Evidence and Implications from Some Plateaus in Northern Norway. *Geomorphology*, 15(2), 109–121.

Reed, W. J. (1989). *The Vertical Dimensions of the Last Ice Sheet and Late Quaternary Events in Northern Ross-Shire, Scotland*. PhD Thesis, University of St Andrews.

Riedel, J. L., & Larrabee, M. A. (2015). *Mount Rainier National Park glacier mass balance monitoring annual report, water year 2011: North Coast and Cascades Network*. Natural Resource Data Series NPS/NCCN/NRDS—2015/752. National Park Service, Fort Collins, Colorado.

Riedel, J. L., Wilson, S., Baccus, W., Larrabee, M.A. & Fudge, T. J. (2015). Glacier status and contribution to streamflow in the Olympic Mountains, USA. *Journal of Glaciology*, 61(225).

Reusch, H. (1901). Nogle Bidrag Til Forstaaelsen Af Hvorledes Norges Dale Og Fjelde Er Blevne Til. *Norges geologiske undersøkelse*, 32, 124–263.

Reuther, A., Geiger, C., Urdea, P., Niller, H. & Heine, K. (2004). Determining the Glacial Equilibrium Line Altitude (ELA) for the Northern Retezat Mountains, Southern Carpathians and Resulting Paleoclimatic Implications for the Last Glacial Cycle. *Analele UniversitâTii de Vest din Timiøeoara, Seria Geografie*, 14, 11–34.

Reuther, A. U., Urdea, P., Geiger, C., Ivy-Ochs, S., Niller, H.-P., Kubik, P. W. & Heine, K. (2007). Late Pleistocene Glacial Chronology of the Pietrele Valley, Retezat Mountains, Southern Carpathians Constrained by 10 Be Exposure Ages and Pedological Investigations. *Quaternary International*, 164, 151–169.

Roaldset, E., Pettersen, E., Longva, O. & Mangerud, J. (1982). Remnants of Preglacial Weathering in Western Norway. *Norsk geologisk tidsskrift*, 62(3), 169–178.

Romans, J., Stevens, J. & Robertson, L. (1966). Alpine Soils of North-East Scotland. *Journal of Soil Science*, 17(2), 184–199.

Rowan, A. V. (2012). Geomorphological Techniques (online Edition), in: Clarke, L. (Ed.). London, UK: British Society for Geomorphology.

Rye, N., Nesje, A., Lien, R. & Anda, E. (1987). The Late Weichselian Ice Sheet in the Nordfjord-Sunnmøre Area and Deglaciation Chronology for Nordfjord, Western Norway.

Saintenoy, A., Friedt, J.-M., Booth, A. D., Tolle, F., Bernard, E., Laffly, D., Marlin, C. & Griselin, M. (2013). Deriving Ice Thickness, Glacier Volume and Bedrock Morphology of the Austre LovénBreen (Svalbard) Using Ground-Penetrating Radar. *Near Surface Geophysics*, 11, 253–261.

Sejrup, H. P., Hjelstuen, B. O., Dahlgren, K. T., Haflidason, H., Kuijpers, A., Nygård, A., Praeg, D., Stoker, M. S. & Vorren, T. O. (2005). Pleistocene Glacial History of the NW European Continental Margin. *Marine and Petroleum Geology*, 22(9), 1111–1129.

Sernander, R. (1896). Några Ord Med Anledning Af Gunnar Andersson, Svenska Växtvärldens Historia. *Botaniska notiser*, 114–128.

Sevestre, H. (2015). *Surge-type glaciers: controls, processes and distribution*. PhD Thesis, The University Centre in Svalbard & University of Oslo.

Sevestre, H. & Benn, D. I. (2015). Climatic and Geometric Controls on the Global Distribution of Surge-Type Glaciers: Implications for a Unifying Model of Surging. *Journal of Glaciology*.

Sissons, J. (1974). A Late-Glacial Ice Cap in the Central Grampians, Scotland. *Transactions of the Institute of British Geographers*, 95–114.

Sissons, J. B. (1967). *The Evolution of Scotland's Scenery*. Archon Books.

Sitts, D. J., Fountain, A. G., & Hoffman, M. J. (2010). Twentieth century glacier change on Mount Adams, Washington, USA. *Northwest Science*, 84(4), 378–385.

Smith, M. & Pain, C. (2009). Applications of Remote Sensing in Geomorphology. *Progress in Physical Geography*, 33(4), 568–582.

Sollid, J. L. & Sørbel, L. (1979). Deglaciation of Western Central Norway. *Boreas*, 8(2), 233–239.

Sollid, J. & Reite, A. (1983). The Last Glaciation and Deglaciation of Central Norway, *Glacial deposits in north-west Europe*, 41–60.

Sørensen, N. (1949). Gjevilvasskammene-Nunatakker I Trollheimens Midte. *Naturen*, 73, 65–81.

Stevens, J. & Wilson, M. (1970). Alpine Podzol Soils on the Ben Lawers Massif Perthshire. *Journal of Soil Science*, 21(1), 85–95.

Stone, J. O. & Ballantyne, C. K. (2006). Dimensions and Deglacial Chronology of the Outer Hebrides Ice Cap, Northwest Scotland: Implications of Cosmic Ray Exposure Dating. *Journal of Quaternary Science*, 21(1), 75–84.

Stone, J. O., Ballantyne, C. K. & Fifield, L. K. (1998). Exposure Dating and Validation of Periglacial Weathering Limits, Northwest Scotland. *Geology*, 26(7), 587–590.

Stroeven, A. P., Fabel, D., Hättestrand, C. & Harbor, J. (2002). A Relict Landscape in the Centre of Fennoscandian Glaciation: Cosmogenic Radionuclide Evidence of Tors Preserved through Multiple Glacial Cycles. *Geomorphology*, 44(1), 145–154.

Stroeven, A. P. & Kleman, J. (1999). Age of Sirius Group on Mount Feather, McMurdo Dry Valleys, Antarctica, Based on Glaciological Inferences from the Overridden Mountain Range of Scandinavia. *Global and Planetary Change*, 23(1), 231–247.

Sugden, D. (1968). The Selectivity of Glacial Erosion in the Cairngorm Mountains, Scotland. *Transactions of the Institute of British Geographers*, 79–92.

Sugden, D. (1977). Reconstruction of the Morphology, Dynamics, and Thermal Characteristics of the Laurentide Ice Sheet at Its Maximum. *Arctic and Alpine Research*, 21–47.

Sugden, D. (1978). Glacial Erosion by the Laurentide Ice Sheet. *Journal of Glaciology*, 20(83), 367–391.

Sugden, D. (1989). Modification of Old Land Surfaces by Ice Sheets. *Zeitschrift fur Geomorphologie*, 72, 163–172.

Sugden, D. E. (1970). Landforms of Deglaciation in the Cairngorm Mountains, Scotland. *Transactions of the Institute of British Geographers*, 201–219.

Sugden, D. E. (1974). Landscapes of Glacial Erosion in Greenland and Their Relationship to Ice, Topographic and Bedrock Conditions. *Institute of British Geographers Special Publication*, 7, 177–195.

Sugden, D. E., Balco, G., Cowdery, S. G., Stone, J. O. & Sass, L. C. (2005). Selective Glacial Erosion and Weathering Zones in the Coastal Mountains of Marie Byrd Land, Antarctica. *Geomorphology*, 67(3), 317–334.

Sugden, D.E., Hein, A.S., Woodward, J., Marrero, S.M., Rodés, A.,Dunning, S.A, Stuart, F.M., Freeman, S.P.H.T., Winter, K. & Westoby, M.J. (2017). The million-year evolution of the glacial trimline in the southernmost Ellsworth Mountains, Antarctica, *Earth and Planetary Science Letters*, 469, 42–52.

Sugden, D. E. & John, B. S. (1976). *Glaciers and Landscape: A Geomorphological Approach*. Edward Arnold London.

Sugden, D. E. & Watts, S. (1977). Tors, Felsenmeer, and Glaciation in Northern Cumberland Peninsula, Baffin Island. *Canadian Journal of Earth Sciences*, 14(12), 2817–2823.

Thomsen, H. H. & Winding, O. (1988). *Margin of the Inland Ice North-East of Jakobshavn (Paakitsup Akuliarusersua 1985) Glacier Hydrological Map, 1:75 000*. The Geological Survey of Greenland.

Thorp, P. (1981). A Trimline Method for Defining the Upper Limit of Loch Lomond Advance Glaciers: Examples from the Loch Leven and Glen Coe Areas. *Scottish Journal of Geology*, 17(1), 49–64.

Thorp, P. W. (1986). A Mountain Icefield of Loch Lomond Stadial Age, Western Grampians, Scotland. *Boreas*, 15(1), 83–97.

Thorp, P. W. (1987). Late Devensian Ice Sheet in the Western Grampians, Scotland. *Journal of Quaternary Science*, 2(2), 103–112.

Traczyk, A. & Migoñ, P. (2003). Cold-Climate Landform Patterns in the Sudetes. Effects of Lithology, Relief and Glacial History. *Acta Universitatis Carolinae, Geographica*, 35, 185–210.

Van der Veen, C. J. & Csatho, B. M. (2005). Spectral Characteristics of Greenland Lichens. *Géographie physique et Quaternaire*, 59(1), 63–73.

Walden, J. & Ballantyne, C. K. (2002). Use of Environmental Magnetic Measurements to Validate the Vertical Extent of Ice Masses at the Last Glacial Maximum. *Journal of Quaternary Science*, 17(3), 193–200.

Way, R. G., Bell, T. & Barrand, N. E. (2015). Glacier Change from the Early Little Ice Age to 2005 in the Torngat Mountains, Northern Labrador, Canada. *Geomorphology*, 246, 558–569.

Weidick, A. (1968). Landscapes of Glacial Erosion in Greenland and Their Observations on Some Holocene Glacier Fluctuations in West Greenland Relationship to Ice, Topographic and Bedrock Conditions. *Bulletin Grønlands Geologiske Undersøgelse*.

Weidick, A. (1969). The Periglacial Environment: Past and Present, in: Péwé, Troy L. (Ed.), (pp. 249–262). Montreal: McGill–Queens University Press.

Weidick, A. (1995). Satellite Image Atlas of Glaciers of the World, in: Williams, Richard S and Ferrigno, Jane G (Ed.). US Government Printing Office.

Weidick, A., Bøggild, C. E. & Knudsen, N. (1992). *Glacier Inventory and Atlas of West Greenland*. Grønlands geologiske undersøgelse.

Whalley, W. B., Rea, B. R. & Rainey, M. M. (2004). Weathering, Blockfields, and Fracture Systems and the Implications for Long-Term Landscape Formation: Some Evidence from Lyngen and Oksfordjøkelen Areas in North Norway. *Polar Geography*, 28(2), 93–119.

Whalley, W. B., Rea, B. R., Rainey, M. M. & McAlister, J. J. (1997). Rock Weathering in Blockfields: Some Preliminary Data from Mountain Plateaus in North Norway. *Geological Society, London, Special Publications*, 120(1), 133–145.

White, D. A. & Fink, D. (2014). Late Quaternary Glacial History Constrains Glacio-Isostatic Rebound in Enderby Land, East Antarctica. *Journal of Geophysical Research: Earth Surface*, 119(3), 401–413.

Winkler, S. & Matthews, J. A. (2010). Holocene Glacier Chronologies: Are "high-Resolution"global and Inter-Hemispheric Comparisons Possible? *The Holocene*, 20(7), 1137–1147.

Winsborrow, M., Andreassen, K., Corner, G. D. & Laberg, J. S. (2010). Deglaciation of a Marine-Based Ice Sheet: Late Weichselian Palaeo-Ice Dynamics and Retreat in the Southern Barents Sea Reconstructed from Onshore and Offshore Glacial Geomorphology. *Quaternary Science Reviews*, 29(3), 424–442.

Wirsig, C., Zasadni, J., Ivy-Ochs, S., Christl, M., Kober, F. & Schlüchter, C. (2016a), A deglaciation model of the Oberhasli, Switzerland. *Journal of Quaternary Science*, 31, 46–59.

Wirsig, C., Zasadni, J., Christl, M., Akçar, N. & Ivy-Ochs, S. (2016b). Dating the onset of LGM ice surface lowering in the High Alps, *Quaternary Science Reviews*, 143, 37–50.

Wolken, G. J., England, J. H. & Dyke, A. S. (2005). Re-Evaluating the Relevance of Vegetation Trimlines in the Canadian Arctic as an Indicator of Little Ice Age Paleoenvironments. *Arctic*, 341–353.

Wråk, W. O. O. (1908). *Bidrag till Skandinaviens reliefkronologi, akademisk avhandling*. Central tryckeriet.

Zasadni, J. & Kłapyta, P. (2014). The Tatra Mountains during the Last Glacial Maximum. *Journal of Maps*, 10(3), 440–456.

Ziaja, W. (2005). Response of the Nordenskiöld Land (Spitsbergen) Glaciers Grumantbreen, Håbergbreen and Dryadbreen to the Climate Warming after the Little Ice Age. *Annals of Glaciology*, 42(1), 189–194.

Zumbühl, H., Steiner, D. & Nussbaumer, S. (2008). 19th Century Glacier Representations and Fluctuations in the Central and Western European Alps: An Interdisciplinary Approach. *Global and Planetary Change*, 60(1), 42–57.